Artificial Intelligence Advances

Volume 2 | Issue 1 | 2020 April | ISSN 2661-3220 (Online)

01

BILINGUAL PUBLISHING CO.
Pioneer of Global Academics Since 1984

Volume 2 Issue 1 • April 2020 • ISSN 2661-3220 (Online)

Artificial Intelligence Advances

Editor-in-Chief

Dr. Sergey Victorovich Ulyanov

BILINGUAL PUBLISHING CO.

Pioneer of Global Academics Since 1984

BILINGUAL PUBLISHING CO.
Pioneer of Global Academics Since 1984

Volume 2 | Issue 1 | April 2020 | Page 1-92
Artificial Intelligence Advances

Contents

Article

BILINGUAL PUBLISHING CO.
Pioneer of Global Academics Since 1984

Artificial Intelligence Advances
https://ojs.bilpublishing.com/index.php/aia

ARTICLE

Human Being Emotion in Cognitive Intelligent Robotic Control Pt I: Quantum / Soft Computing Approach

Alla A. Mamaeva Andrey V. Shevchenko Sergey V. Ulyanov*

Dubna State University, Universitetskaya Str.19, Dubna, Moscow Region, 141980, Russia
ISESYS LLC (EFKO GROUP), Naberezhnaya Ovchinnikovskaya Str.20 Bld.2, Moscow, Russia

ARTICLE INFO

Article history
Received: 21 October 2019
Accepted: 7 April 2020
Published Online: 15 April 2020

Keywords:
Neural interface
Computational intelligence toolkit
Intelligent control system
Deep machine learning
Emotions
Quantum soft computing optimizer

ABSTRACT

The article consists of two parts. Part I shows the possibility of quantum / soft computing optimizers of knowledge bases (QSCOptKB™) as the toolkit of quantum deep machine learning technology implementation in the solution's search of intelligent cognitive control tasks applied the cognitive helmet as neurointerface. In particular case, the aim of this part is to demonstrate the possibility of classifying the mental states of a human being operator in on line with knowledge extraction from electroencephalograms based on SCOptKB™ and QCOptKB™ sophisticated toolkit. Application of soft computing technologies to identify objective indicators of the psychophysiological state of an examined person described. The role and necessity of applying intelligent information technologies development based on computational intelligence toolkits in the task of objective estimation of a general psychophysical state of a human being operator shown. Developed information technology examined with special (difficult in diagnostic practice) examples emotion state estimation of autism children (ASD) and dementia and background of the knowledge bases design for intelligent robot of service use is it. Application of cognitive intelligent control in navigation of autonomous robot for avoidance of obstacles demonstrated.

1. Introduction

The state-of-the-art sensing and processing tools, health-monitoring technologies attract significant attention in research and industry in the last three decades [1, 2]. The inclusion of human being operator in the feedback loop of intelligent control systems (ICS) for decision-making in complex situations creates both an information resource that can improve the efficiency of the development and application of ICS. Unfortunately, it is often associated with an increasing in the information risk of hazard situations due to the presence of an unpredictable human health-monitoring and emotion state factors [2].

Thus, it is necessary to have quantitative and qualitative indicators that would not depend on the individual characteristics of the human being emotion operator and at the same time guaranteed objectivity of the obtained indicators. In that case, the developed ICS will be able to perceive, adapt and make decisions in difficult situations [3] due to the inclusion in the structure of these indicators as criteria for the quality of intelligent control.

1.1 Tasks of hybrid cognitive and intelligent control

A number of studies [4-7] showed the possibility of development a simplified mathematical model of emotions. But

**Corresponding Author:*
Sergey V. Ulyanov,
ISESYS LLC (EFKO GROUP), Naberezhnaya Ovchinnikovskaya Str.20 Bld.2, Moscow, Russia;
Email: ulyanovsv@mail.ru

 DOI: https://doi.org/10.30564/aia.v2i1.1323

due to physical limitations, the trade-off of informational boundaries on the applicability of the developed model also have a significant influence on the correctness of description and reliability of the extracted knowledge from the imperfect mathematical model. In ICS theory, one of the effective approaches to the risk decreasing of decision-making is the development of robust ICS structures with corresponding knowledge bases (KBs).

The problems of physical limitations and information boundaries solved by the possibility of forming KB with the required level of robustness in the design process of ICS by extracting knowledge and valuable information from the dynamic behavior of the model of the physical control object [8].

Figure 1 demonstrates general structure of hybrid cognitive intelligent control system. The structure based on fuzzy and cognitive controllers, includes quantum fuzzy inference with quantum genetic algorithm in Box "Quantum computing KB optimizer" and are the background of quantum cognitive self-organized controller (see, in details Part II).

The main problem of cognitive intelligent control system (presented in Fig. 1) is to design optimal robust control with minimal loss of value work and minimum of required initial information on external environments.

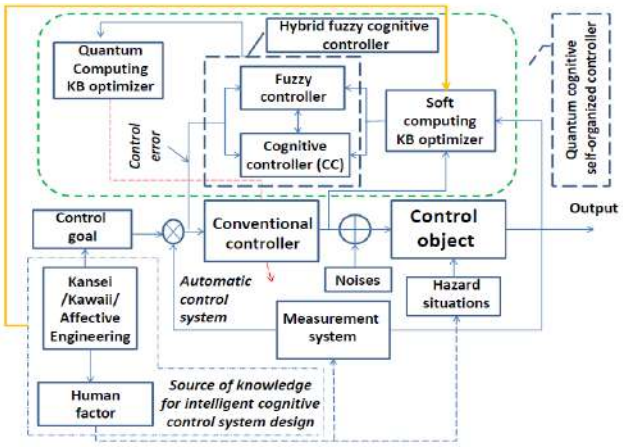

Figure 1. Structure of hybrid intelligent cognitive control system based on quantum soft computing.

Let us consider briefly the solution of this problem using information-thermodynamic approach.

1.2 Synergetic effect of information-thermodynamic trade-off interrelations between stability, controllability and robustness of robotic motion intelligent control

Consider the distribution equation of the trade-off control qualities of a dynamic system $\dot{q}_i=\varphi(q,t,S(t),u)$ as control object in the form:

$$\frac{dV}{dt}=\sum_{i=1}^{n} q_i\cdot\ \varphi\left(q,t,S(t),u\right)+\left(S_p-S_c\right)\cdot\left(\dot{S}_p-\dot{S}_c\right)\le 0 \quad (1)$$

where S_p is an entropy production of control object (plant), S_c is an entropy production of controller, $S=S_p-S_c$ is a generalized entropy production of dynamic control system.

Eq. (1) in analytical form relates such qualitative concepts of control theory as stability, controllability and robustness based on the concept of phenomenological thermodynamics entropy. An approach like this allows to design the necessary distribution between levels of stability, controllability and robustness, which allows achieving the control goal in emergencies with a minimum consumption of useful resource due to the application of the minimum generalized entropy production included in the right-hand side as a fitness function in the genetic algorithm.

Now let us look at Eq. (1), taking into account the connection between thermodynamic entropy and Shannon's information entropy. The definitions of thermodynamic entropy S and information entropy H related by the von Neumann relation in the form:

$$S=kH=-k\sum_i p_i\ln p_i \quad (2)$$

where $k\approx 1.38\cdot 10^{-23}J/K$ and is the Boltzmann constant.

In Eq. (1) replace S(t) with the Shannon's entropy:

$$\frac{dV}{dt}=\sum_{i=1}^{n} q_i\cdot\varphi\left(q,t,\left(H_p-H_c\right),u\right)+k\left(H_p-H_c\right)\cdot\left(\dot{H}_p-\dot{H}_c\right)\le 0 \quad (3)$$

Thus, Eq. (3) also relates stability, controllability and robustness, but already based on Shannon's information entropy, which also allows one to determine control for guaranteed achievement of the control goal in emergencies with a minimum required amount of information about the external environment and the state of the control object.

A generalization of Eqs (1) and (3) is the following system of equations:

$$\frac{dV}{dt}=\sum_{i=1}^{n} q_i\cdot\varphi\left(q,t,\left(S_p-\left(S_{Int}+S_{Cog}\right)\right),u\right)+\left(S_p-\left(S_{Int}+S_{Cog}\right)\right)\cdot\left(\dot{S}_p-\left(\dot{S}_{Int}+\dot{S}_{Cog}\right)\right)\le 0 \quad (4)$$

$$\frac{dV}{dt}=\sum_{i=1}^{n} q_i\cdot\varphi\left(q,t,k\left(H_p-\left(H_{Int}+H_{Cog}\right)\right),u\right)+k\left(H_p-\left(H_{Int}+H_{Cog}\right)\right)\cdot\left(\dot{H}_p-\left(\dot{H}_{Int}+\dot{H}_{Cog}\right)\right)\le 0 \quad (5)$$

DOI: https://doi.org/10.30564/aia.v2i1.1323

where $\left(S_{Int}+S_{Cog}\right)$ and $\left(H_{Int}+H_{Cog}\right)$ means total thermodynamic and information entropies of intelligent and cognitive controllers, respectively.

It follows from Eq. (4) that the robustness of an intelligent control system can increased by producing the minimum entropy (value information) of the cognitive controller, which reduces the loss of useful life (safety increasing), and Eq. (5) shows that the negentropy of the cognitive controller reduces the minimum requirements for the initial information to achieve robustness. Moreover, information action based on knowledge (in the knowledge base of the cognitive regulator) allows get an additional resource for useful work, which is equivalent to the appearance of a targeted action on the control object to ensure the guaranteed achievement of the control goal in uncertainty and information risk conditions.

Due to the synergetic effect, an additional information resource created, and the multi-agent system is able to solve complex dynamic tasks for performing mutual work. The given task may not be fulfilled by each element (agent) of the system separately in various environments without external management, control or coordination, however, exchange of knowledge and information allows perform useful mutual work to achieve the management goal under the conditions of uncertainty of the initial information and limited consumption of useful resources. In particular, it is known that for closed-loop control systems, the maximal amount of useful work W that extracted with information amount satisfies the inequality:

$$W_{max}\left(t\right)=k\int_0^t T_{min}\dot{I}_c dt' \le kTI \tag{6}$$

where k is the Boltzmann constant, $T_{\min}\left(t\right)$ is interpreted as the lowest achievable temperature by the system in time t for feedback control, assuming $T_{\min}\left(0\right)=T$ and I_c determines the amount of Shannon information (entropy transfer), extracted by the system from the measurement process [9, 10].

Figure 2 demonstrates logical interrelations of information role in process of work extraction and trade-off of control qualities.

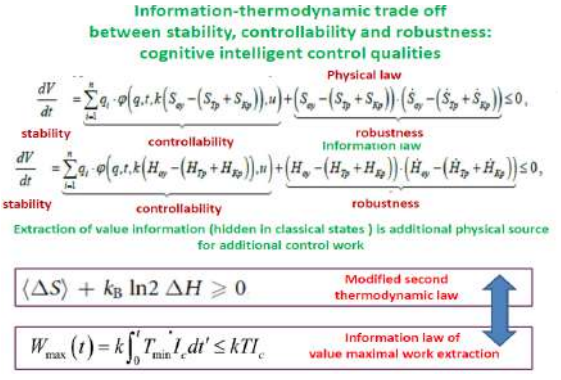

Figure 2. Interrelations between extracted work and information, and trade-off of control qualities.

Physically, the synergetic effect means self-organization of knowledge and creation of additional information that allows the multi-agent system to perform the most useful work with a minimum loss of useful resource and with a minimum of the required initial information, without destroying the lower executive level of the control system [9]. Together with the information-thermodynamic law of intelligent control (optimal distribution of the management qualities "stability - controllability - robustness"), an ICS is designed with multi-agent systems, ensuring the achievement of the management goal under the conditions of uncertain initial information and limited useful resource [9-13].

1.3 Extracted work and information

If microscopic degrees of freedom are accessible to the observer in the form of the Maxwell demon, then the second law of thermodynamics may violate (see Fig. 2). Szilard showed from an analysis of the Maxwell demon model that work is extracted from the thermodynamic cycle in the form as the amount, k*T*ln2. Moreover, in [12, 13] it is shown that the recoverable work W^S_{ext} from the system determined by the amount of information *I* (or quantum-classical mutual information) that measures the knowledge of the system when measuring. At the same time, such a ratio in the form of a lower boundary exists for the total cost of measuring and erasing information $W^S_{ext} \le -\Delta F^S + kTI$ and $W^M_{ext} \ge kTI$, where ΔF^S is determines the free energy of the system. Then it is easy to notice that the speed of the extracted work $\dot{W}_{ext}$ is limited by the value $\dot{W}_{ext} \le kT\dot{I}$, i.e., it is limited by the speed of the extracted information [13].

Let us consider a network of loosely coupled groups of robots working together to solve tasks that go beyond individual capabilities. Different nodes of such a system have a different intelligent level (knowledge, algorithms, and computational bases) and various information resources in designing. Each node should be able to modify its behavior depending on the circumstances, as well as to plan its communication and cooperation strategies with other nodes. Here the indicators of the level of cooperation are the nature of the distribution of tasks, the unification of various information resources and, of course, the possibility of solving a common problem in a given time.

1.4 Quantum algorithm of knowledge self-organization

A quantum algorithm (QA) model of ICS self-organization, proposed in [9], is based on the principles of mini-

 DOI: https://doi.org/10.30564/aia.v2i1.1323

mum information entropy (in the "intelligent" state of control signals) and a generalized thermodynamic measure of entropy production (in the system "control object + controller"). The main result of the application of the self-organization process is the acquisition of the necessary level of robustness and the flexibility (adaptability) of the reproducible structure. It is noted that the property of robustness (by its physical nature) acts as an integral part of self-organization, and the required level of robustness of ICS is achieved by fulfilling the principle of minimum production of generalized entropy, which was noted above.

The principle of minimum entropy production in control object and control system [14] serves as the physical principle of optimal functioning with a minimum consumption of useful work and underlies the development of robust ICS. This statement based on the fact that for the general case of controlling dynamic objects, the optimal solution is to the finite variation problem of determining the maximum of the useful work W is equivalent, according to [15], to the solution of the finite variation problem of finding the minimum of the entropy production S. Therefore, the developed QA model used principle of minimum informational entropy guarantees the necessary condition for self-organization — the minimum of the required initial information in the teaching signals; the thermodynamic criterion of the minimum of a new measure of generalized entropy production provides a sufficient condition for self-organization - the robustness of control processes with a minimum consumption of useful resource.

More significant is the fact that the average amount of work done by dissipation force $\frac{W_{diss}}{kT} = S_{KL}\left(P_F \,\|\, P_B\right)$, i.e., the work of dissipation forces is determined by the Kullback-Leibler divergence for probability distributions P_F ,P_B. Note that the left side of this relation represents physically thermal energy, and the right side defines purely information about the system. A similar relationship exists between the work produced by the forces of dissipation and the difference between generalized Renyi divergences [16].

Figure 3 illustrates the QA structure of self-organization (QASO) in design process of robust intelligent PID-controller with application of quantum fuzzy inference with quantum genetic algorithm for choice the optimal quantum correlation type between PID-controller coefficient gains in temporal schedule.

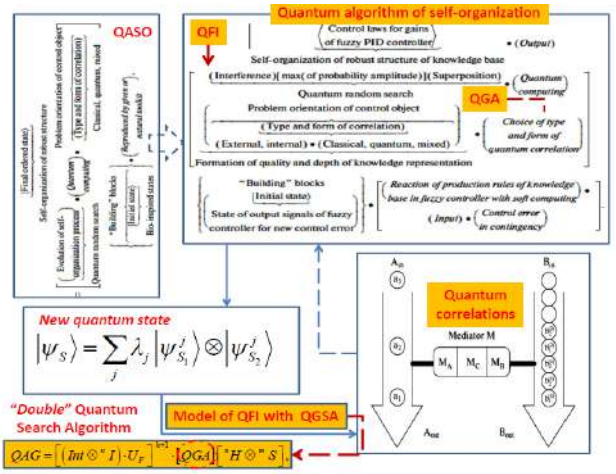

Figure 3. Quantum algorithm of self–organization based on quantum fuzzy inference and quantum genetic algorithm

Thus, substituting the relations between the information and the extracted free energy and work in (4) and (5), we obtain the conclusion that the robustness of the intelligent control system can increased by producing the entropy of the cognitive controller. The optimal cognitive controller reduces the loss of useful resource of the control object, and negentropy of the cognitive regulator reduces the requirements for minimum initial information to achieve robustness. Therefore, the extracted information, based on knowledge (in the knowledge base of the cognitive controller), allows to get an additional resource for useful work, which is equivalent to the appearance of a targeted action on the control object to guarantee the achievement of the control goal in unpredicted situations.

Let us consider briefly Brain Emotional Learning Based Intelligent Controller (BELBIC) structure [17] as the consequence of the intelligent cognitive control system in Fig. 3.

Example. In a biological system, emotional responses of human being operator are utilized for fast decision - making in complex environments or emergencies. It is thought that the amygdala and the orbitofrontal cortex are the most important parts of the brain involved in emotional responses and learning. The amygdala is a small structure in the medial temporal lobe of the brain that is thought to be responsible for the emotional evaluation of stimuli (see, Appendices 1 and 2). This evaluation is in turn used as a quantum basis for emotional states and responses and is used for attention signals and laying down long - term memories. The amygdala and the orbitofrontal cortex compute their outputs based on the emotional signal (the reinforcing signal) received from the environment. The final output (the emotional responses)

DOI: https://doi.org/10.30564/aia.v2i1.1323

calculated by subtracting the amygdala's output from the orbitofrontal cortex's (OFC) output (see Fig. 4).

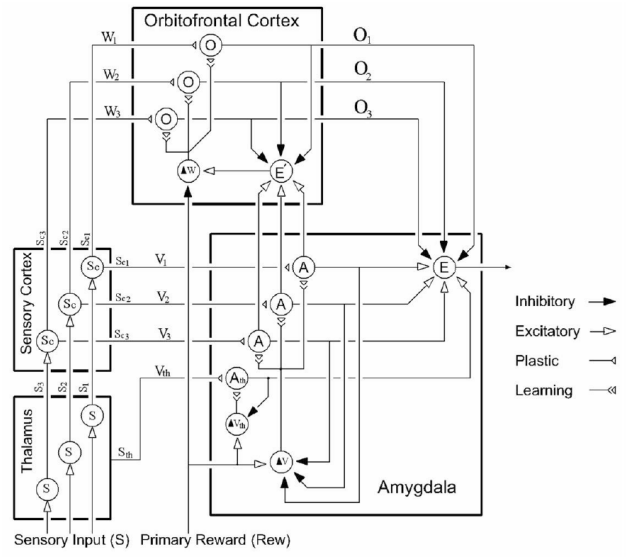

Figure 4. Graphical depiction of the developed computational model of brain

It should observe that it essentially converts two sets of inputs (sensory inputs and emotional cues or reinforcing signals) into the decision signal (the emotional responses) as its output. Closed loop configurations using this block (BELBIC) in the feed‑forward‑loop of the total system in an appropriate manner have implemented so that the input signals have the proper interpretations. The block implicitly implemented the critic, the learning algorithm and the action selection mechanism used in the functional implementations of emotionally based (or, generally, reinforcement learning‑based) controllers, all at the same time.

The policies design for PID‑based controller and the BELBIC controller are the same due to the equal number of states, which needed for the feedback. The structure of the control circuit using the direct‑adaptive control strategy illustrated in Fig. 5.

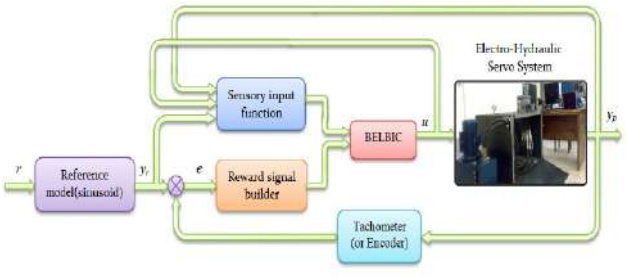

Figure 5. System configuration using brain emotional controller

The PID controller contains a constant steady‑state position error, yet in the BELBIC the steady‑state position error eventually decreases. Unlike the PID controller, learning the dynamics through online implementation causes the BELBIC to track the reference signal inaccurately at the beginning of the experiment (shown in [17]). Despite the fact that the initial weights are all set to zero, the BELBIC rapidly learns the dynamics of the plant without any offline training. During transient states, a slight overshoot observed in the control signal of the BELBIC since the servo‑valve draws more current; however, in the PID‑based controller no such change realized. As the BELBIC passes on to a steady state, the control signal becomes uniform and smooth, which is an important advantage in practical use, especially in high power systems such as EHS systems. The energy consumption of the BELBIC is about the same as the PID controller, whilst the BELBIC has less tracking error. The BELBIC tracks the reference signal with very low error in comparison with the PID controller. The BELBIC displays good robustness to a change in the dynamics of the system, an acceptable overshoot and a good tracking ability (compared to the PID [18]). A main advantage in the performance of the controlled EHS system is in the high degree of the adaptability of the control system and the robustness of the performance with respect to the initial error in relation to modeling and identification (even with a total lack of knowledge about the system model) [17, 18].

1.5 Problems in intelligent control systems design

Modern control objects are complex dynamic systems that characterized by information uncertainty of model structures and control goals, a high degree of freedom and essential nonlinearities, instability, distributed sensors and actuators, high level of noise, abrupt jump changes in structure and dynamics, and so on. It is the typical information resources of unpredicted control situations. The structure design of robust advanced control systems for unpredicted control situations is the corner stone of modern control theory and systems. The degree to which a control system deals successfully with above difficulties depends on the intelligent level of advanced control system.

In Step I of developed design technology, we focus the main attention on the description of particular results of KB design and simulating intelligent control systems with essentially nonlinear CO with a randomly time-dependent structure and control goals. In this case, the aim of this step is to determine the robustness levels of control processes that ensure the required reliability and accuracy indices under the conditions of uncertainty of the information employed in decision-making (learning situations).

For Step 2, the description of the strategy of robust

 DOI: https://doi.org/10.30564/aia.v2i1.1323

structure's design of an intelligent control system based on the technologies of quantum and soft computing given. The developed strategy allows one to improve the robustness level of fuzzy controllers under the specified unpredicted or weakly formalized factors for the sake of forming and using new types of self-organization processes in the robust KB with the help of the quantum computing methodology. A particular solution of a given problem obtained by introducing a generalization of decision-making strategies in models of fuzzy inference in the form of a new quantum fuzzy inference (QFI) on a finite set of fuzzy controllers designed in advance [19].

The basis for the development of control systems is the proportional-integral-differentiating controller, which used in 70% of industrial automation, but often does not cope with the control task and works very poorly in unforeseen situations. Fuzzy controllers allow to partially expand the scope of PID controllers by adding production logic rules and partially adapt the system. The combined use of genetic algorithms (GA) and a fuzzy neural network made it possible fully adapt the system, but it takes time to train such a system, which is critical in emergency and unforeseen situations. Modeling the optimal training signal makes it possible to create partial self-organization in the system due to the formation of optimal trajectories of the gain of the PID controller. The application of quantum computing and, as a particular example, quantum fuzzy inference (QFI) allows increasing robustness without spending a temporary resource in online.

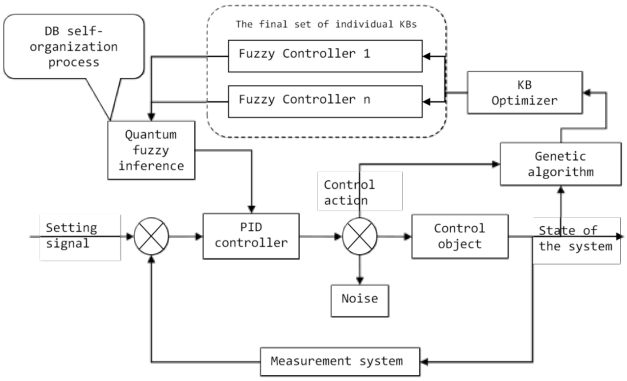

Figure 6. Intelligent control system including quantum fuzzy inference

The Fig. 6 shows the ICS structure with the combination of several fuzzy regulators and the quantum fuzzy controller. The main problem in the development and design of this structure that it is very difficult to design a globally good and robust control structure for all possible cases, especially when the system works in poorly predictable situations. One of the best solutions is the formation of a finite number of knowledge bases of a fuzzy controller for a variety of fixed control situations. The goal of a quantum regulator is to combine the knowledge bases obtained with the help of the soft computing optimizer knowledge base into self-organizing quantum fuzzy regulators. The QFI model uses private individual knowledge bases of the fuzzy controller, each of which designed using SCOptKB™ and QCOptKB™ toolkits.

Box "Kansei / Kawaii / Affective engineering" (Fig. 1) forming the knowledge about fillings of human being operator and concentrate the attention on control goal. KBs of fuzzy controllers and cognitive controllers designed with SCOptKBTM toolkit using objective information of control object response from measurement system in feedback loop and affective response and will of human being operator described with new type of computational intelligence technology. The main performance of Part I to show the description of emotion estimation in Box "Kansei / Kawaii / Affective engineering" and the introduction of physical interpretation of quantum interference in cognition as quantum models of patterns.

Example. In order to clarify the difference in the definition of emotions / feelings used in [20], Figure 7 illustrates concrete examples. In the Figure 7, there is stimulus A and a bodily state that evoke the "Fight" action, whereas a stimulus B and a bodily state activate the "Flight" action. In this case, the emotional state that stimulus A and the bodily sate cause is labeled as "anger," and the emotional state caused by the stimulus B and the bodily sate is labeled as "Fear." This definition directly connects emotions to the somatic marker hypothesis, which means that the emotion should generated by considering internal appraisal, external appraisal, and decision-making mechanisms.

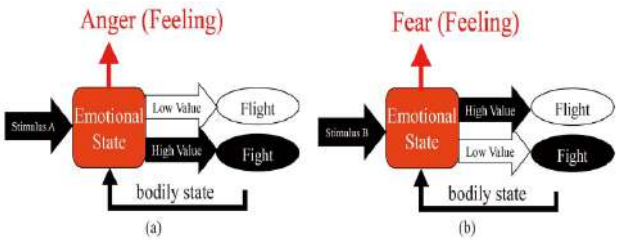

Figure 7. Illustration of "anger" and "fear", which highlights the difference: (a) emotional feeling of anger, and (b) emotional feeling of fear

However, the ICS structures do not have a specialized software module to describe and implement the processes of adaptation and learning of the control system to the qualitative characteristics of human being operator behavioral responses. Proven in a wide class of areas of soft computing (genetic algorithms, fuzzy logic and fuzzy neural networks) and computational technology in the form of intelligent tools (Computational Intelligence Toolkit),

DOI: https://doi.org/10.30564/aia.v2i1.1323

allows to design an intelligent cognitive control system that has the required qualities.

The cognitive processes of non-verbal communication in the human brain (see Fig. 8) modeling on such a level: they explain the correlation between what the human perceives from the clinician's communication, and what the human in turn communicates. The underlying condition of an observed human can then infer from the recorded interaction with the clinician.

Figure 8 describes general structure of intelligent cognitive robotic control with "brain-computer-robot-device" neurointerface and affect decoding controller based on Kansei / Affective Engineering and its cognitive computing technology.

Kansei / Affective Engineering technology and its cognitive computing toolkit include qualitative description of human being emotion, instinct and intuition that used effectively in design processes of smart / wise robotics and intelligent mechatronics as example robot for service use [11, 21] and robotic unicycle (see, for example below).

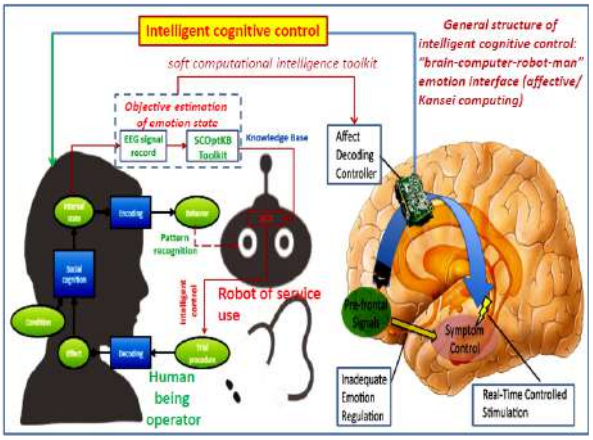

Figure 8. General structure of intelligent cognitive human-robotic interaction control

Remark. According to general definition Kansei Engineering (Japanese: 感性工学 kansei kougaku, emotional / affective engineering) aims at the development or improvement of products and services by translating the customer's psychological feelings and needs into the domain of product design (i.e. parameters). Mitsuo Nagamachi, Ph.D, Professor Emeritus of Hiroshima University founded it. Kansei Engineering parametrically links the customer's emotional responses (i.e. physical and psychological) to the properties and characteristics of a product or service. In consequence, products can design to bring forward the intended feeling. The main part the mammalian brain is responsible for emotional processes and called the limbic system. The computational models of the amygdala and orbitofrontal cortex are the main parts of the limbic system recently introduced for the first time. Therefore, Kansei result is a synthesis of sensory brain cognitive qualities. For example, it has argued that emotion, pain and cognitive control functionally segregated in distinct subdivisions of the cingulate cortex of brain (see, Appendix 1).

The processes depicted in Fig. 8 represent incredibly complex, non-smooth, and non-linear mappings and representations, which indicates that it will be suitable to use a deep neural network [4] approach. In this paper we concentrate our attention on description on the box "Objective estimation of emotion state" of Fig. 8 for design of knowledge base of robot for service use [11, 21]. Robots for service use can practically implemented into current education and therapy interventions for children ASD.

1.6 Social human-robot emotion interaction and application.

The Center for Disease Control (CDC), has recently announced that the incidence of autism is 1 in every 59 children. There has been a growth rate of 250% during the last 15 years. Autism is now emerging as a public health priority. ASD occurs in all racial, ethnic, and socio-economic groups. However, the incidence is five times more common among boys than among girls [22, 23]. In particular, according to the Centers for Disease Control and Prevention, one in every 68 children (1:42 boys, 1:189 girls) ASD [24]. Individuals with ASD exhibit impairments in three key areas: (a) communication, (b) social interaction, and (c) restricted interests and repetitive behaviors. The American Psychiatric Association recently redefined qualifiers for ASD, citing levels of severity, the impact deficits key areas have on the quality of life and the amount of support needed, beginning with Level I (less support, formerly included diagnosis of Asperger Syndrome, Pervasive Developmental Delay-Not Otherwise Specified), Level II (moderate support), and Level III (most support).

The schema at the Fig. 9 shows how the child-robot interaction loop and the software modules are used by the robot to interact with the child: The Robot Intelligent Module (RIM) and the Behavior Manager (BM).

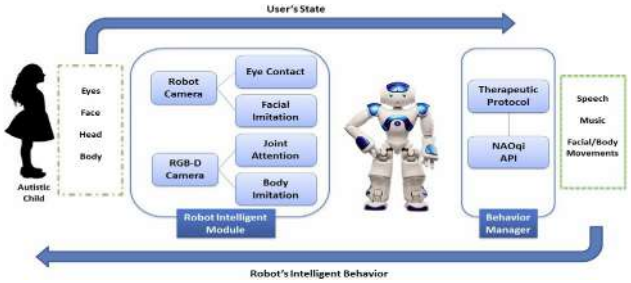

Figure 9. Artificial Intelligence System for Robot-Assisted Treatment of Autism

The RIM is composed of four components: head pose, body posture, eye contact, and facial expression. The BM consist of two components: the treatment protocol and the NAOqi API [25].

Although robot therapists are better than human therapists in these three areas, they are not yet perfect. The robots for the therapies come at a high cost. Robokind, the company that makes Milo, reports that its robot has an initial cost of $5,000 plus an additional cost of $4,500 every year after. This is lower than the $29,000 cost of human therapy, but Robokind's cost estimates are still too optimistic. A 2015 study found that parents have a preference that there is a human complementing the robot in autism therapy. If humans have to complement robots in robot-assisted therapy, the cost might even be higher than the human-led therapy cost of $29,000 per year.

As you can see at the Figs 10 and 11, robots used in autism therapy.

Figure 10. ROBOJJANG developed by Robocare Co., Ltd.

Interacting with robots can be particularly empowering for children with ASD, because it may overcome various barriers experienced in face-to-face interaction with humans. Moreover, robot assisted interventions can be tailored to the needs of the specific child and can be used in an identical manner as often as needed.

Figure 11. Robots used in autism therapy

Figure 11 shows the robots used in autism therapy all around the world:

a) Kaspar (courtesy of the Adaptive Systems Research Group, University of Hertfordshire, UK),

b) Tito (courtesy of F. Michaud),

c) Roball (courtesy of F. Michaud),

d) Muu (courtesy of M. Okada, Toyohashi University of Technology, Japan),

e) Pleo (courtesy of Innvo Labs Corporation),

f) Bubble blower (courtesy of D. Feil-Seifer),

g) Nao (courtesy of Aldebaran),

h) Robota (courtesy of A. Billard),

i) Infanoid (courtesy of H. Kozima),

j) Bandit (courtesy of M. Mataric, USC, USA),

k) Robojjang (courtesy of Robocare Co., Ltd.).

1.7 Therapy of the autism using the intelligent cognitive system

It is believed that effective therapy for autism is extremely expensive. It is not because it is complicated, but because the small number of the specialists who own behavioral techniques. There is a situation when the majority of families do not have access to the necessary treatment [26].

Remark. This work is a continuation of the development of a cognitive-intelligent system for the diagnosis, adaptation and training of autistic children (CISDAEAC). A more detailed description of the CISDAEAC may be found in [27-29].

The main part of this cognitive-intelligent system is the data processing module (see Fig. 12). It represents the structure of a child's interaction and training program through the application of fuzzy logic.

The data processing module is designed to extract the EEG based on a cognitive helmet, process and filter the received signal, create a cognitive process training program on the platform, diagnose problems with the child's work with the system and evaluate the operator's response to the tasks generated by the training module.

CISDAEAC is designed to extract process and formulate a learning program based on cognitive processes, in particular, EEG signals, adaptation of autistic children to society and training in basic household skills. One of the tasks of this work is the processing of the EEG signal, based on the recognition of emotions, and forming an encephalographic portrait of the child on the next step.

Before working with the system, a detailed assessment of the current level of social interaction of the child, revealing the difference between the difficulties in acquiring. Next creating a minimum training package to determine the starting point consisting of basic logical tasks. To receive feedback, the Emotiv EPOC+

DOI: https://doi.org/10.30564/aia.v2i1.1323

cognitive helmet used, which allows recording the brain activity signal and transferring it to the data processing module.

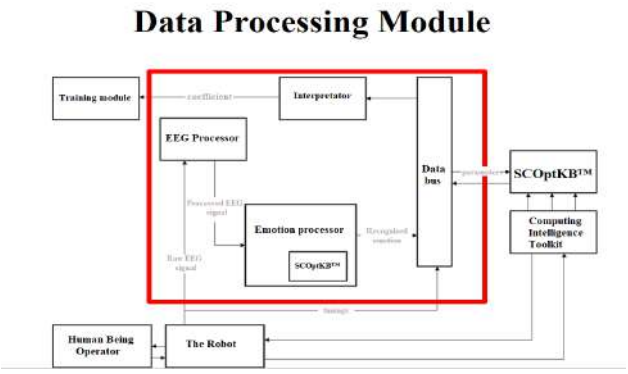

Figure 12. CISDAEAC Data processing module

Next, by the EEG signal, evaluating the child's reaction to the interaction with environment, and monitoring parameters for solving the tasks. Then forming the strategy of learning using the technology of soft computing. The signal from the EPOC signal recognition unit, the decision time, the correctness of the solution and the task identification number are using as the input data. After this, the system sets the appropriate coefficients for adjusting the training program.

2. EEG signal processing

2.1 Features of experimental EEG registration and informative parameters of the patient's condition

The electroencephalogram (EEG) of the human operator can be used as a biometric parameter, since the brain activity is individual. It is made unique by synchronized activity of groups of neurons that process the same signals to form metastable group. Signals corresponding to one external stimulus or cognitive event trigger synchronized activity of neurons grouped together. A certain level of synchronization is maintained at rest state. Synchronized neuronal activity is observed on the EEG.

Recording EEG signal is a contact and long-term procedure, since the electrical activity of the brain is a value extended in time, and the data cannot be recorded for a long time because of the nonlinear distortions of the EEG signal appear at large intervals. The nonlinearity of the signal can be solved by a series of short measurements, during which the signal can be considered linear. Emotiv EPOC+ cognitive helmet was used for recording the brain activity (see Fig. 13).

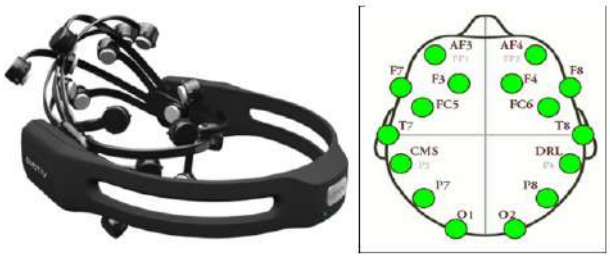

Figure 13. Emotiv EPOC+ cognitive helmet

EPOC has 14 electrodes, which are passive sensors that allow register electromagnetic signals. Sensors are attached to the surface of the skin (non-submersible, non-invasive interface). Figure 8 presents the structure of Emotiv EPOC+, consisting of channels AF3, F7, F3, FC5, T7, P7, O1, O2, P8, T8, FC6, F4, F8, AF4 and two reference sensors CMS/DRL, which purpose is to receive and filter bioelectric signals of muscle activity from the EEG signal.

Remark. In Fig. 14a, Hierarchical structure of studies and tasks. Dendrograms convey theoretical groupings of fMRI activity at levels of study (level 1: studies S1–S18), subdomain (level 2: thermal, visceral, mechanical, working memory (WM), response selection (RS), response conflict (RC), visual, social, and auditory), and domain (level 3: pain, cognitive control, and negative emotion). Colored regions illustrate model-based partitioning of neural similarity into components that generalize across subjects (unique to a study, top 18 squares), studies (unique to a subdomain, middle nine squares), and subdomains (unique to a domain, bottom three regions). b, Decomposing multivariate pattern similarity into study-, subdomain-, and domain-specific components.

The matrix in the left panel shows the dissimilarity of fMRI patterns across all subjects (n = 270) in the entire medial frontal cortex. Each row represents one individual participant and each element the dissimilarity (1–Pearson′ s correlation coefficient) in brain activity patterns for two individuals. Colored bars to the left indicate corresponding levels in the functional hierarchy. The right panel shows how the observed neural dissimilarity across pairs of images from the 18 studies is modeled as a weighted summation of theoretical dissimilarity matrices constructed according to study (18 parameters), subdomain (9 parameters), and domain (3 parameters) membership, in addition to a constant term (not shown).

 DOI: https://doi.org/10.30564/aia.v2i1.1323

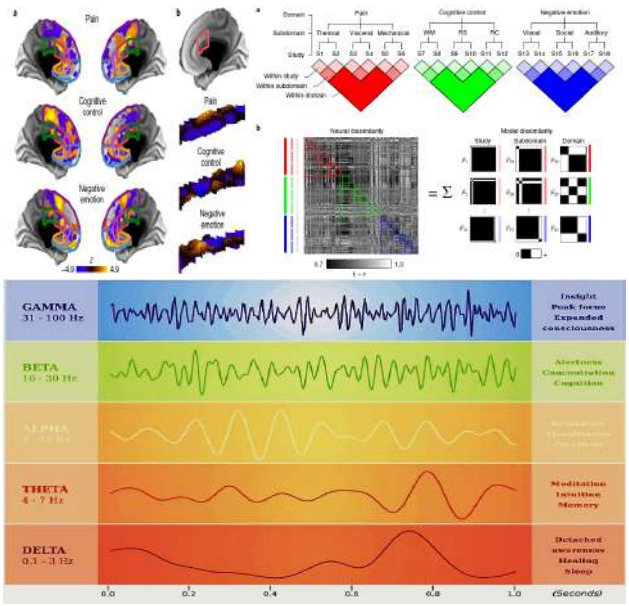

Figure 14. Hierarchical structure of studies and tasks

The supplied software allows in online to receive, recognize and register the EEG signal from the helmet [31]. As part of the solution of the problem it is necessary to obtain the most informative fragments of the signal. Frequency rhythms of EEG are distinguished for the analysis. The concept of frequency rhythm determines the type of electrical activity corresponding to a certain state of the brain which boundaries of the frequency range are determined (see Fig. 15).

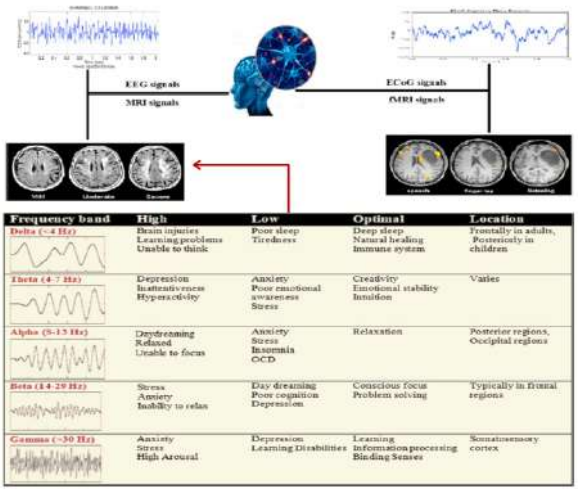

Figure 15. EEG frequency rhythms

This involves the decomposition of the EEG signal into frequency components, which is achieved by fast Fourier transforms (FFT), which returns for each frequency buffer a complex number containing the amplitude and phase.

$$X_k = \sum_{n=0}^{N-1} x_n \cdot e^{-i2\pi kn/N} \quad , \tag{6}$$

where N is the number of time samples, k = 0, N-1 is the current frequency, n = 0..., N-1 is the current sample, xn-input samples in the time domain, xk-output samples in the frequency domain.

2.2 Definition of emotional arousal

A well-known marker of cognitive processes is the restructuring of brain rhythms which occurs in the superficially recorded human EEG. Strong emotional experience, as a form of cognitive activity, can lead to inhibition of other mental processes, realization of behavioral appropriate reactions, violation of conscious control over actions, as a result of which uncontrolled actions can be committed [32]. States arise against the will, conscious control over their actions is not possible. The occurrence of such situations can lead to a critical error in the control loop [33].

Therefore, the first task was to determine the level of emotional arousal of the human being operator.

Figure 16 identifying latent brain representations that predict the occurrence of distinct functional domains in each region of interest:

a) searchlight maps display where local patterns of brain activity are consistent with domain-specific representation of pain (red), cognitive control (green), and negative emotion (blue; n = 270 participants).

b) Additive conjunction of searchlight maps, with each domain mapped onto orthogonal dimensions in the red–green–blue (RGB) color space. Overlap between pain and cognitive control is depicted in yellow; overlap between pain and negative emotion is colored magenta. Maps are thresholded at P < 0.05, two-tailed, uncorrected cutoff to highlight any possible overlap.

c) Brain maps of Bayes factors indicating relative evidence against overlap among the three domains at each voxel. Smaller values indicate evidence against overlap; values less than 0.1 are considered strong evidence (n = 270 participants).

d) River plots depict the similarity between searchlight maps and anatomical parcellation of MFC (left) and functional parcellation of cortical regions from resting-state data48 (right). Line thickness indicates the degree of correspondence between sets.

DOI: https://doi.org/10.30564/aia.v2i1.1323

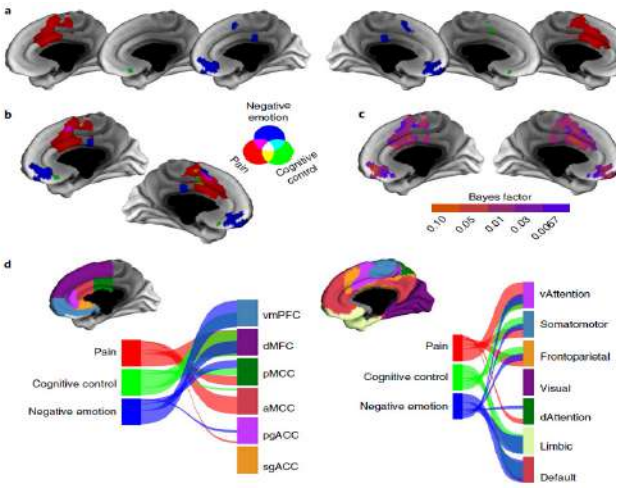

Figure 16. Representational mapping of pain, cognitive control, and negative emotion in MFC

2.3 Experimental results

During the study, the operator's EEG signal was recorded while in a calm state and in a state of stress. The source signal of each sensor, with a sampling frequency of 128Hz, is decomposed into frequency rhythms using a discrete Fourier transform.

For visual assessment of differences in emotional states, graphs of the spectral power of signals from AF3, AF4, F7, F3, F4, F8, FC5, FC6, T7, T8, O1, O2 sensors were constructed in the range of significant frequencies from 1 to 50 Hz. (see Fig. 17).

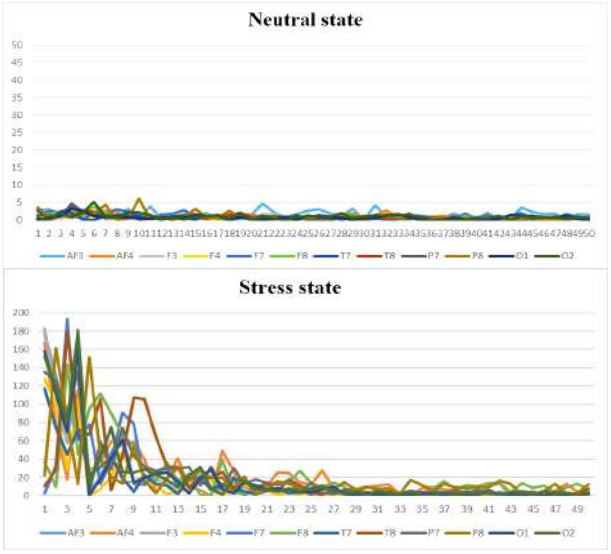

Figure 17. A graph of the spectral power density of the EEG signal obtained by discrete Fourier transform for the state and stress of rest

A comparative analysis of the spectral power of various emotional states for the frontal, temporal, and occipital-parietal lobes of the cerebral cortex has been carried out (see Figs 18, 19 and 20).

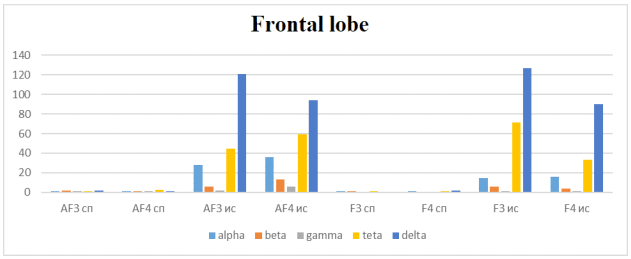

Figure 18. The level of spectral power of the EEG signal for sensors AF3, AF4, A3, A4 for each of the frequencies for two emotional states: calm and fright

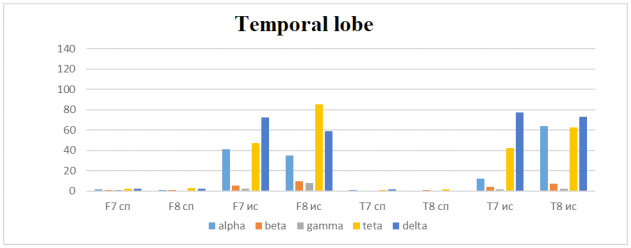

Figure 19. The level of spectral power of the EEG signal for sensors P7, P8, O1, O2 for each of the frequencies for two emotional states: calm and fright

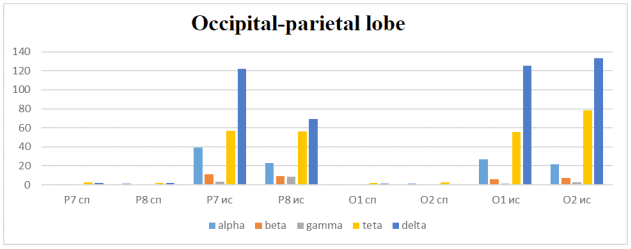

Figure 20. The level of spectral power of the EEG signal for sensors F7, F8, T7, T8 for each of the frequencies for two emotional states: calm and fright

Based on the assessment of the total tonic activity, as well as the values of the total spectral power of the frequency ranges, it was concluded that it is possible to estimate the emotional background of a human being operator.

Figure 21 shows the graphs of signal activation integral accumulation for various emotional states.

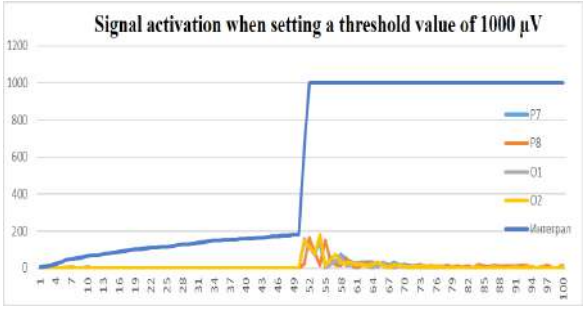

DOI: https://doi.org/10.30564/aia.v2i1.1323

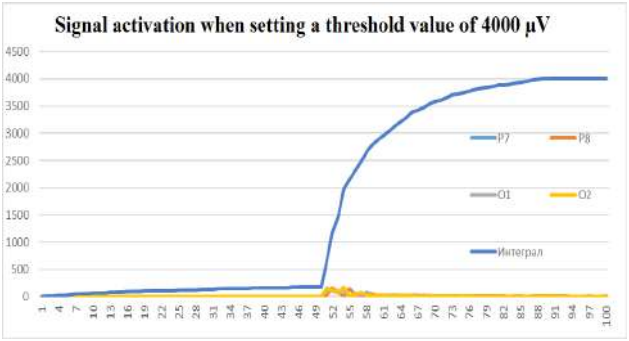

Figure 21. The accumulation of signal activation when setting a threshold value of 1000 and 4000 µV

At calm state, the signal integral does not exceed 200 µV, while in a state of emotional arousal a threshold value of 1000 µV achieved by one iteration, and for 4000 µV in 38 iterations.

The EEG signal registered by the software product using the knowledge base returns the coefficient determining the level of emotional arousal. Based on this coefficient a warning about the level of emotional arousal is displayed on the screen through expert judgment (see Fig. 22).

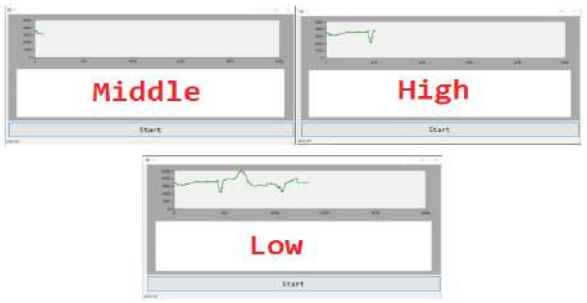

Figure 22. UI of the warning about the level of emotional arousal

3. Detecting the mental state of a human operator

First of all, we investigate the fear emotion — the marker of valence measurement of emotional states. Fear is realized more clearly, unlike other emotions, and finding its causes is much easier. In the case of autistic children, the emotion of fear is most critical to recognition.

Figure 23 shows a graph of the EEG signal taken by the sensors F3, F4, FC5, FC6 in two emotional states: on the left is fear, on the right is a neutral state.

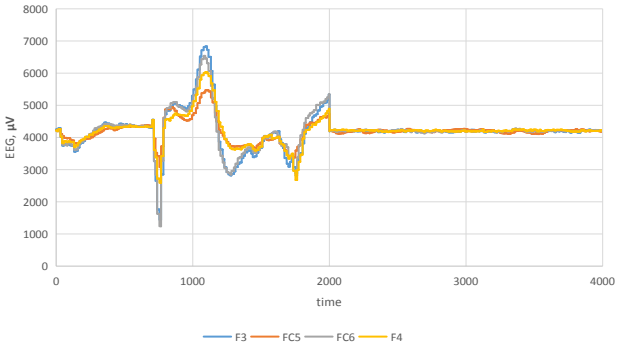

Figure 23. The value of the EEG signal of different emotional states

On the example of the data of the EEG signal values, the implementation of the visual display of the signal is considered, and also these data were used to form the knowledge base. This requires a transition from the representation of the EEG signal as a function of time, to the representation of the signal in the spatial frequency domain. This transition is carried out by decomposing the signal into harmonic components using the Fourier transform. Figure 24 shows a graph of the spectral power density of the EEG signal taken by the AF3 sensor in two emotional states: on the left is fear, on the right is a neutral state.

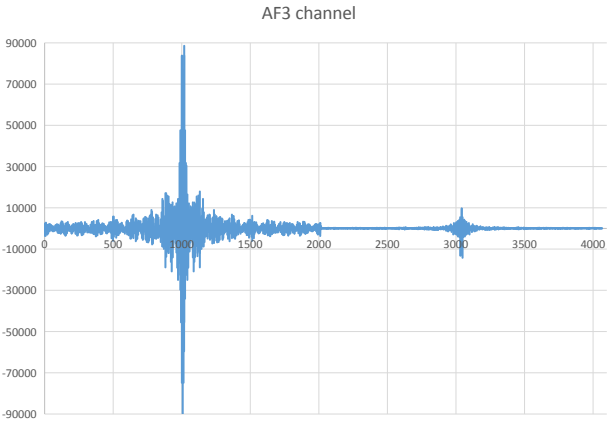

Figure 24. The value of the total spectral power density of the EEG signal for various emotional states

This approach reduces the amount of processed data for visual assessment, makes it possible to quickly classify electroencephalograms. Regardless of emotions sign, it can be generated in both hemispheres of the brain, but a number of studies focuses the attention of the anterior sections of the brain in the generation of emotions (see Fig. 25).

DOI: https://doi.org/10.30564/aia.v2i1.1323

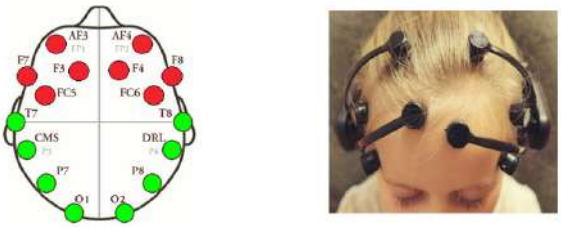

Figure 25. The location of the electrodes used in the experiment

The combination of simultaneously present rhythms forms a specific spatial-frequency EEG pattern. Patterns are typical for different types of cognitive activity and are highly individually specific. The ability of an individual to establish rhythmic EEG patterns when performing certain cognitive tasks called "encephalographic" portrait of personality [29].

During the experiment an EEG signal was recorded with a sampling frequency of 128 Hz for various emotional states: calm (neutral), positive emotions and negative emotions. There was no state of strong emotional arousal. The source signal of each sensor is decomposed into frequency rhythms using a discrete Fourier transform. Figure 26 shows a graph of the average spectral power of the frequency bands in 6 secs for the AF3 sensor in various emotional states.

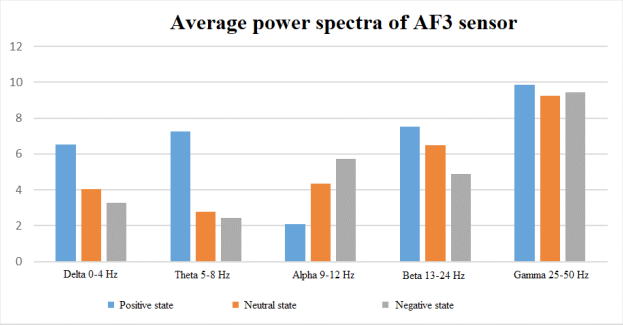

Figure 26. Average power spectra of AF3 sensor

Determining the sign of an emotion is a classic classification task. To solve it, it is necessary to determine the sign of the emotion at a specific point in time by analyzing the EEG signal. If we consider the state of rest as 0, positive emotion as +1, negative as –1, the definition of the sign of the emotion can be considered as a deviation from the neutral state.

A number of studies shows [34] that in determining the sign of an emotional reaction, it is necessary to rely on changes in the power of the alpha rhythm and beta rhythm in the frontal and temporal lobes. With positive emotions, there is a strong depression of the alpha rhythm in comparison with the neutral condition, as well as an increase in the power of the beta rhythm (see tab. 1).

Table 1. Frequency rhythms with different emotional signs

Frequency rhythm	Positive emotions	Negative emotions
Alpha rhythm	More pronounced depression of the alpha rhythm in comparison with the neutral condition in the frontal and temporal lobes.	The power of the alpha rhythm is greater than or equal to the power of the alpha rhythm with a neutral condition in the frontal and temporal lobes.
Beta rhythm	Increase of beta rhythm power compared to neutral condition in frontal and temporal leads.	Decrease in amplitude in comparison with a neutral condition in frontal assignments.
Theta rhythm	The change in the power of theta rhythm in the frontal and temporal leads in comparison with the neutral condition depending on the gender.	The change in the power of the theta rhythm in the frontal and temporal leads in comparison with the neutral condition depending on the gender.

The coefficients are placed in accordance with the significance of the spectral power, they also reflecting the weight of the frequency rhythm to determine the sign of emotional activity.

4. Description of the software platform

As a software platform for processing the EEG signal, the Python programming language version 3.7 was chosen. The NumPy package was chosen as a library for mathematical operations. NumPy is a fundamental package for scientific computing in Python, providing:

- powerful N-dimensional array object;
- complex (broadcast) functions;
- tools for integrating C / C ++ and Fortran code;
- algorithms linear algebra, Fourier transform and extended possibilities of random numbers.

In addition to obvious scientific applications, NumPy can also be used as an effective multidimensional container of common data. The ability to define arbitrary data types allows you to easily and quickly integrate with a wide range of databases.

4.1 Using the deep machine learning in the task of classifying an emotional sign

TensorFlow was used as a library for machine learning. It is a neural network that learns how to solve problems by positive amplification and processes data at various levels (nodes), which helps to find the desired correct result with a given level of the training signal approximation error. This kind of machine learning is very well adapted for research purposes. The library was developed by the Google Brain team for a variety of tasks, including searching for images and improving speech recognition algorithms. As a starting point for the use of machine learning technolo-

DOI: https://doi.org/10.30564/aia.v2i1.1323

gies (and later - soft computing), for recognizing emotions through the EEG signal, the TensorFlow library makes it easy to integrate into the applications self-learning elements and functions of artificial intelligence designed for speech recognition, computer vision or natural language processing.

The principle of working with TensorFlow involves the compilation of a graph of operations, data transfer and the work of calculations. The graphs allow define the calculation process, where the vertices perform operations, and the edges describe the connection between them. Thus, when adding two numbers, it is necessary to define a vertex with two inputs (numbers for addition), some calculations (addition function of two numbers) and an output (result).

Deep learning is a subset of machine learning. Usually, when people use the term deep learning, they are referring to deep artificial neural networks, and somewhat less frequently to deep reinforcement learning. Deep artificial neural networks are a set of algorithms that have set new records in accuracy for many important problems, such as image recognition, sound recognition, recommender systems, natural language processing etc. We are using it to identify the sign of emotion.

It was decided to implement a classifier based on a convolutional neural network in order to be able to assign features in the original data set. This feature is especially useful in the problem under study, since it is practically impossible to select significant features in the initial data set in manual mode in accordance with desired output. This significantly limits the possibility of using other types of classifiers. The training of the classification algorithm for EEG signals was based on data from four channels AF3, T7, F71 and F8. As an activation function, a rectified linear unit, specified by the expression, was used:

$$f(x) = \max(0,\ x) \tag{7}$$

where x is the input to a neuron.

In order for TensorFlow to train the model, it is necessary to set the loss function. As the loss function cross entropy was used. Cross entropy is extremely important for modern systems, because it makes it possible to create highly accurate forecasts, even for alternative indicators. Into the learning algorithm, the power values of the spectra are fed to the input for each of the frequencies (alpha, beta, gamma, theta, delta). The task of recognizing an emotion is the task of classification, so the loss function will return:

- Neutral state — 0;
- Negative state — - 1;
- Positive state — +1.

Figures 27 and 28 show the visualization of data to the input of the neural network.

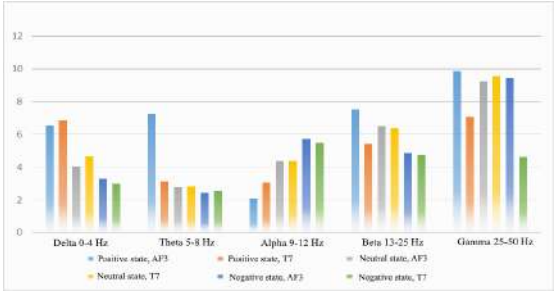

Figure 27. AF3 and T7 sensor power spectra for positive, negative emotions and a calm state

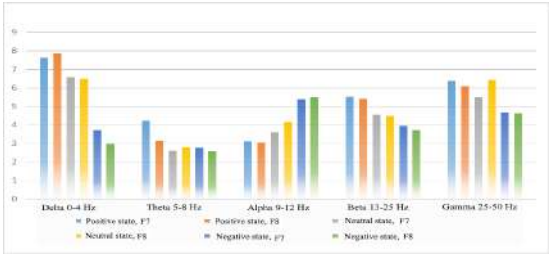

Figure 28. Power ratings of the F7 and F8 sensor spectra for positive, negative emotions and a calm state

Figure 27 reflects the total tonic activity of the spectra of emotions of a different sign for sensors located in the same hemisphere of the brain, and Figure 28 show sensors symmetrically located on opposite points of the two hemispheres of the brain.

4.2 Soft Computing Optimizer

Figure 29 shows the result of the neural network processing: the coefficient of deviation from the neutral state, obtained after processing the EEG signal, decomposed into frequency bands.

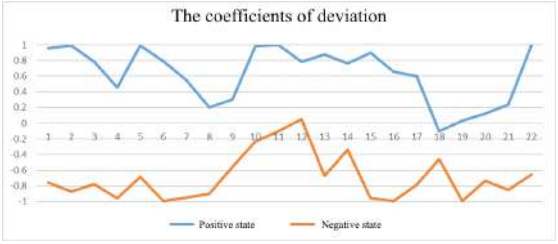

Figure 29. The coefficients of deviation from the neutral state of emotions of a different sign

As a part of the task, machine learning is used to determine the sign of the emotion at a particular point in time. For a correct description of the general psychophysical state of the operator, it is necessary to use the soft computing optimizer. Since emotions are characterized by clearly pronounced intensity, limited duration, awareness of the reasons for its appearance; connection with a specific ob-

DOI: https://doi.org/10.30564/aia.v2i1.1323

ject, circumstance; polarity, an approximation of the coefficient of deviation from the neutral state is necessary.

Remark. SCOptimizer software is used to create sophisticated knowledge bases. Soft Computing Optimizer of knowledge base (SCOptKB™) is a software toolkit for creating automatic fuzzy models and solves the universal approximator design problem of ill-defined control objects. The SCO uses sets of values of the input-output vector to create and optimize a fuzzy model. To perform various optimization algorithms, a learning signal is needed, which represents samples of input values and corresponding output values. Training signal files can be created using the SCO or taken from other sources. Text files are processed based on regional settings that define characters for the decimal point, the thousands separator, and so on. The default values for these parameters are set in Windows. If the settings do not match the signal format, they can be changed at any time. After the change, the parameters are saved in the model and will be used for further data processing. Regional settings affect the reading and writing of text data and model files.

The first step of model optimization is the definition of shape of membership functions of fuzzy sets of input and (if used by the model) of output variables. SCOptimizer supports two modes of MF's shape definition: using uniform distribution method or with GA1 optimization algorithm.

Uniform distribution method distributes fuzzy sets on signal change interval according to signal probability distribution and user selected shape of membership functions.

GA1 algorithm tries to find best possible combination of number of fuzzy sets per variable, membership function shape and overlap coefficient between neighbor fuzzy sets. For each combination it performs uniform distribution algorithm and tries to maximize the mutual possibility of the fuzzy sets of each variable.

The main part of the model is a rule database. It stores data, which shows which output should be activated for given input. SCOptimizer supports two types of rule database: complete database and LBRW database.

Rules of complete database present all possible combinations of fuzzy sets of input variables. Number of rules in complete database equals to product of numbers of fuzzy sets of input variables. This will result in extremely large database and very slow optimization speed if you will try to use it with more than one-two variables. LBRW database store not all the rules, but only a number of rules selected with "Let the Best Rule Win" algorithm. LBRW algorithm selects those rules, which contribute the most noticeable part of the output. Reducing number of rules with LBRW algorithm provides faster optimization speed without loss of model precision.

After the database was created it should be filled with actual rule data. This is accomplished on the final step of model creation – rule database optimization. SCOptimizer uses genetic optimization algorithm (GA2) to tune database parameters.

Quality of the model created during previous steps may still be inadequate. In order to improve model quality GA3 algorithm is used. It alters shapes of membership functions and optimizes model output with fixed number of membership functions and database structure. Error back propagation algorithm can be used to improve model output but fine-tuning database parameters using classical gradient optimization method.

SCOptKB™ supports model export in a C program. The code in these files is written with minimal use of functions from the standard C language library and can be compiled by any C compiler, including those oriented to embedded systems and microcontrollers [8]. To approximate the training signal, the knowledge optimizer is used with the selected model of fuzzy inference (Sugeno 0 order). The coefficient of deviation from the neutral state and the identification value of the corresponding emotion are used. At the next stage of designing a knowledge base for fuzzy inference, a full knowledge base is automatically generated, and the right parts of the rules are further optimized (see Fig. 30).

The first layer is a layer of input variables: the spectral density of the signal power and expert evaluation. The second layer is fuzzy term-sets of input variables. The third layer corresponds to the rules of the knowledge base with the corresponding rule number in the rule base. The last layer is the output layer, which displays the numeric parameters of the rule.

The optimizer of knowledge bases on soft computing automatically forms the optimal structure of the neural network, allows from the point of view of computational mathematics to approximate the training signal with the required (given) approximation error, and from the point of view of the theory of artificial intelligence implements a deep machine learning algorithm.

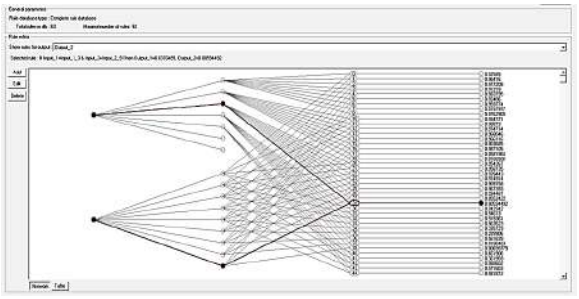

Figure 30. The rule base is in the form of a network with four layers

 DOI: https://doi.org/10.30564/aia.v2i1.1323

In Figure 31, the first graph shows the training signal and the model of the output variable.

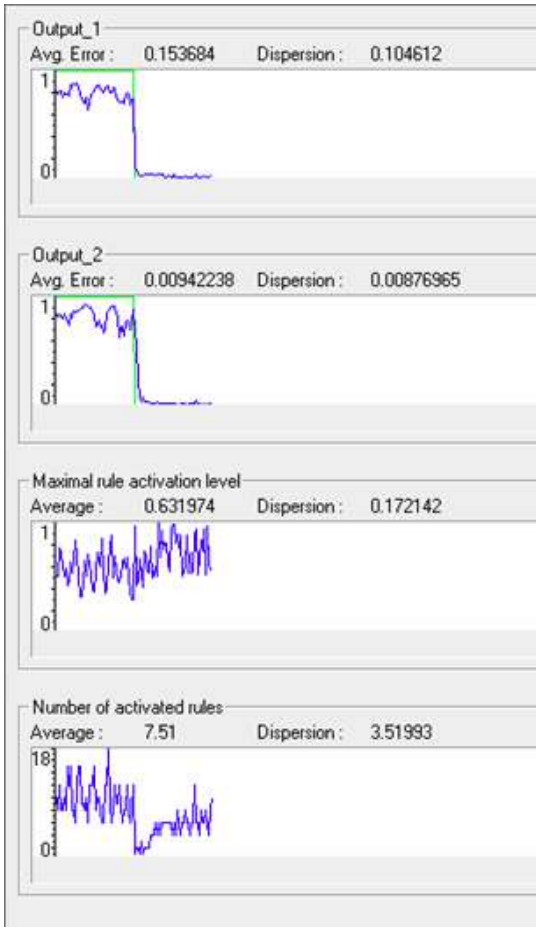

Figure 31. The result of the model is the output variable

The green line displays the training signal and the blue line shows the model output. On the second and third graphs presented the maximum level of activations of the rules and the number of activated rules.

5. Examples of solutions

In 1995 the robotic unicycle [35-37] and in 1994 robot for service use [11] was developed with the biomechanical mechanism description of emotion, instinct and intuition as corresponding look-up tables based on expert estimation of finite number of production rules and linguistic variables with fuzzy logic inference. In addition to design of look-up table in [35] in the structure of intelligent control system (for the feeling support of comfort car passenger) "friendly ship" bio-inspired frequency filter was introduced; robust control of passenger comfort feelings based on quantum soft computing technology is achieved [36]. In this article applied SCOptKB™ toolkit [37] extract information from EEG signal, design optimal structure of fuzzy neural network and create the universal approximator of deep machine learning processes with optimal finite number of production rules, choice optimal type and parameters of linguistic variables for fixed model of fuzzy logic inference. The learning architecture and the associated unsupervised learning algorithm of recurrent quantum neural network [38] have been modified to take into account the complex nature of EEG signal. The basic approach is to ensure that the statistical behavior of input signal is properly transferred to the wave packet associated with the response of quantum dynamics of the network. EEG signals can be considered a realization of a random or stochastic process. When an accurate description of the system is unavailable, a stochastic filter [39] can be designed on the basis of probabilistic measures cooperated with fuzzy modeling. This approach for Social Robotics design with successful emotion state recognition of ASD children and for detecting early signs of dementia [40] based on quantum deep machine learning with smart quantum computational intelligence toolkit [42] can be applied.

5.1 Cognitive intelligent control in navigation of autonomous robot

Usually, a regulator is installed at the facility as a control system, which, depending on the mental commands of the operator, generates a control action for the actuators. Such a controller can be a simple relay controller, where the same control actions are generated for a finite set of output commands (forward, backward, left, right). In this work, we tested a proportional controller, a proportional-integral (PI) controller with a fuzzy output unit, and a proportional-integral derivative (PID) controller with various gain factors.

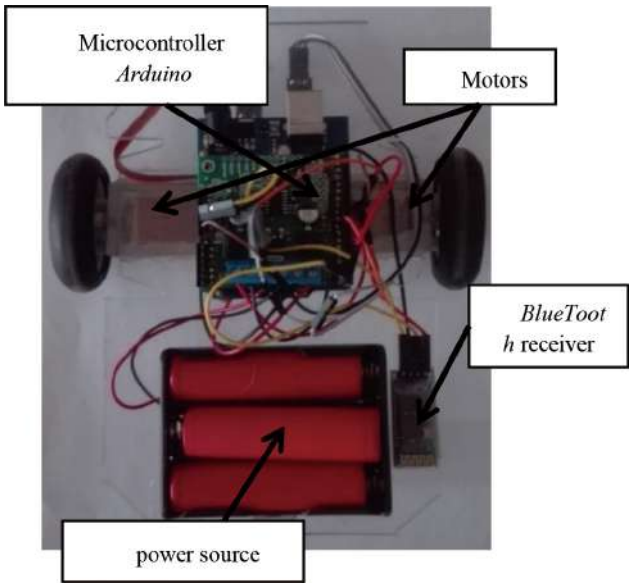

Figure 32. Control Unit

DOI: https://doi.org/10.30564/aia.v2i1.1323

For the experiment was been select the object of control — mobile robot in the form of three-wheel vehicle with Bluetooth-control showed in Figure 32. The control device as a control processor used the Arduino Uno, together with the engine drive Pololu Dual MC33926, Motor- DC 9V Motor Bluetooth module HC-05 and with the power supply serves 3 3.7V Li-On battery.

Figure 33. Activating the commands in the proportional controller

The first and easiest implementation regulator for vehicle is a proportional controller. Such a regulator sends a proportional value of motors cars depending on which team has the greatest affinity to recorded in advance mental command (see Fig. 33 and 34).

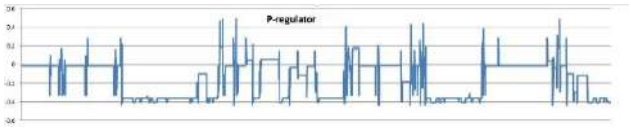

Figure 34. Control impact produced p-controller while moving back and forth

For example, activation command associated in pairs of movement forward and backward was made according to the difference of activation levels for these commands.

Next, let us look at the process of design PI regulator using SCO. To do this, in the first phase the expert generates a training signal, driving based on proportional regulator machine. During system operation, recording the signals received from the block recognizer. Coming from this signal by adding formed integral component (see Fig. 35). Then the expert put the respective control impact based on previous experience with the system.

To approximate the teaching signal (see Fig. 36) applied the developed SCO with selected the model of fuzzy inference (Sugeno type models). As teaching signal used the signal from the block signal recognition EPOC, as well as the integral value of the signal.

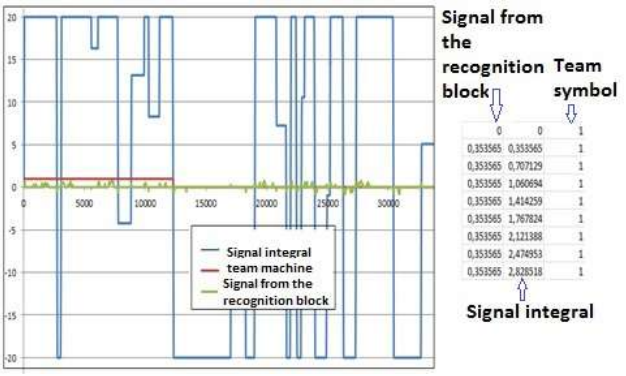

Figure 35. The training signal

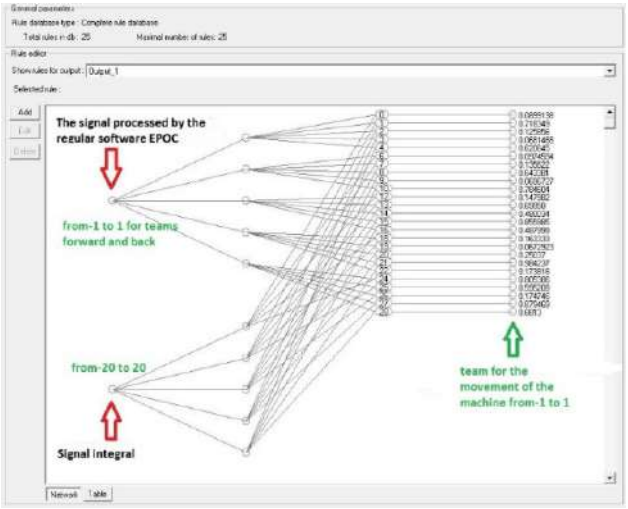

Figure 36. Neural network fuzzy inference

At the next stage of design for fuzzy knowledge base withdrawal is carried out in automatic mode formation full knowledge base and further optimization of right-hand sides (see Fig.37).

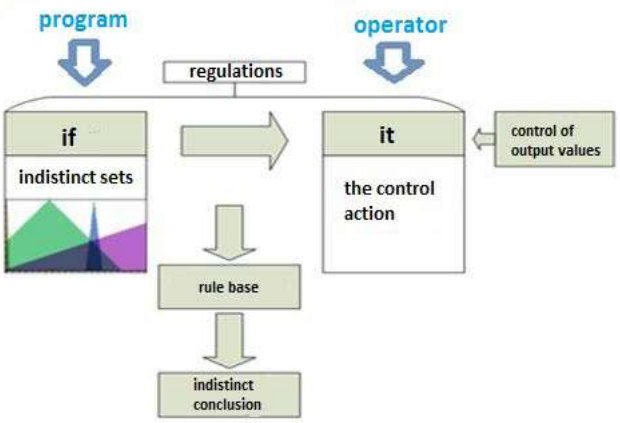

Figure 37. Block diagram the formation rules in the knowledge base

In other words, at the entrance to the neural net receives commands from the software module signal recog-

 DOI: https://doi.org/10.30564/aia.v2i1.1323

nition (forward, backward, left and right) the output value is the commands then receives vehicle.

The knowledge base is applied in conjunction with PI controller. Using soft computing need to build more "soft" structure to control. For this purpose, created linguistic variables (LV) for each of the commands recorded in the system, was formed a complete knowledge base (see Fig. 38). The right side of the regulator contains appropriate values for control action using PI controller. Thus, the activation level of rules in base corresponds to the activation level of the control action.

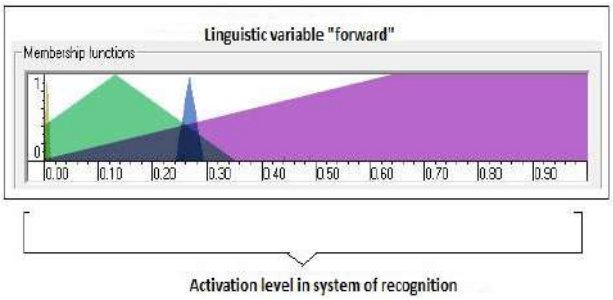

Figure 38. An example of the linguistic variable for the team forward

Figure 39 shows the result of cognitive motion control of mobile robot in maze based on the PI-regulator.

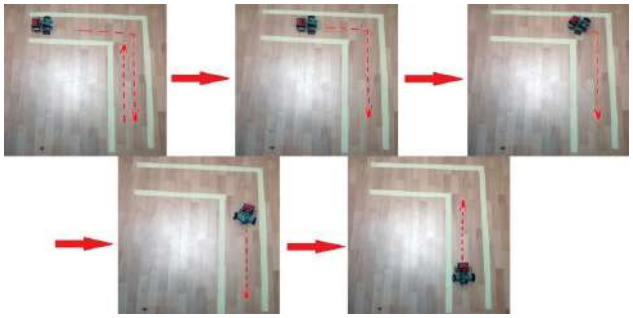

Figure 39. Controlling the trajectory of mobile robot based on the PI-regulator

The following verified regulator to control machines was PID controller with constant coefficients. The coefficients of the regulators were PID 1 [1 0.1 1] and for PID 2 [3 0.1 10].

In Figs 40 and 41 shown the commands of control systems to manage control object. The first chart, green introduced the target signal, which corresponds to a movement back and forth, and the rest of the colors allocated to the activation levels and PI controller with knowledge base.

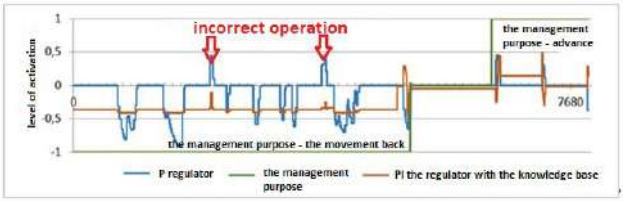

Figure 40. Controlling actions produced by standard signal and PI regulator. Forward and backward

As can be seen from the graphs in Fig. 40, when the motion task is the moving the vehicle back, and the operator's concentration of the thinking process focuses on that command, recognition block is not always correctly identifying the control command. Vehicle goes in spurts or even to the other side (false positives motions). PI control can compensate this, and additional add-in as an integral component in the knowledge base, allows a smooth sequence of commands and reduce errors in reaching the goal. Moreover, the system becomes adaptive and learnable, because the basis of the base is the software tool SCO.

In Fig. 41, move to right corresponds to 1, and the movement to the left corresponds to -1.

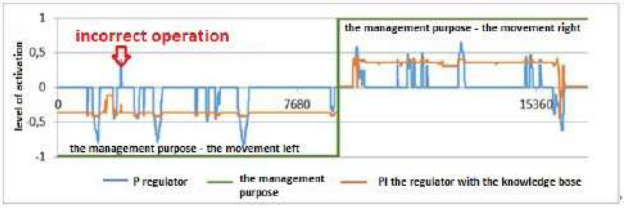

Figure 41. Control actions produced by relay and PI adjuster when moving left and right

Additionally, there was decry the problem of the motion using control system with PID regulator.

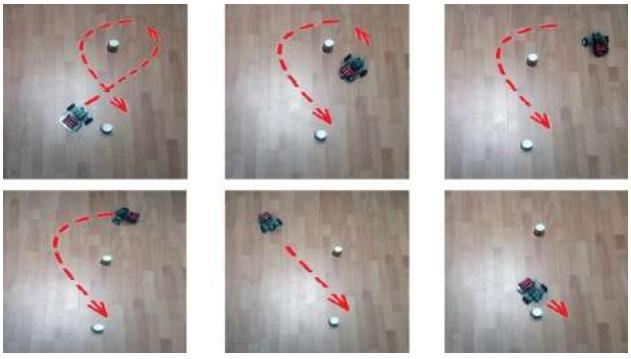

Figure 42. Detour obstacles control system with PID regulator

Figure 42 presents the results of an experiment using PID controllers with different coefficients of gain control action. The odds were set in manual mode. Differential component in PID controller associated with the speed of

DOI: https://doi.org/10.30564/aia.v2i1.1323

the operator activates the mental command.

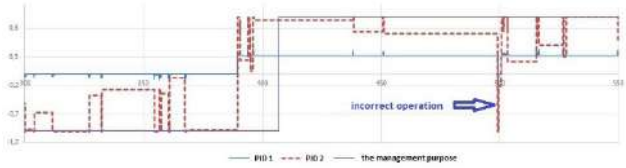

Figure 43. Control actions produced PID regulators when driving forward

The choice of gain factors naturally influences on the computation the action of controller and the operation of the system as a whole. However, establishing the optimal values of coefficients for each point in time is relevant and very interesting task. When incorrect (false) installation values the same way there has been an incorrect actuation, control object moves in spurts.

To compare the results obtained in the experiments used value is the mean deviation from the desired result. As can be seen from table 2 and Fig. 44, using a more complex controller, the deviation has reduced. However, the wrong setting of the gain increases the deviation of the system from the intended target.

Table 2. Compare mean deviation of different controllers

/	P	PI	PID1	PID2
Mean deviation	0,846	0,853	0,860	0,505

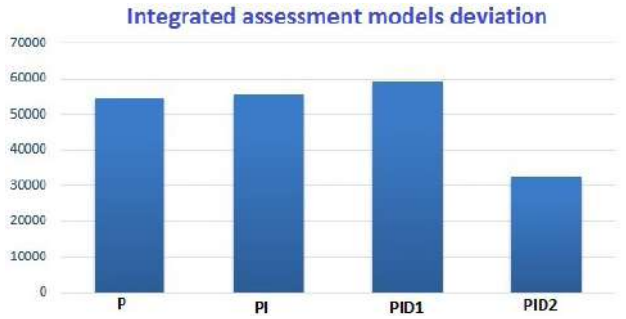

Figure 44. Cumulative score deviation module

Analysis of results of experiments showed that quality control is greatly improved when more complex control schemes.

5.2 Robotic unicycle

We attempted in the present work the emulation of human riding a unicycle by a robot. It is well known that the unicycle system is an inherently unstable system and both longitudinal and lateral stability control are simultaneously needed to maintain the unicycle's postural stability. It is an unstable problem in three dimensions (3D). However, a rider can achieve postural stability on a unicycle, keep the wheel speed constant and change the unicycle's posture in the yaw direction at will by using his flexible body, good sensory systems, skill and intelligent computational abilities.

Investigating this phenomenon and emulating the system by a robot, we aim to construct a biomechanical model of human motion dynamics, and also evaluate the new methods for the stability control and analysis of an unstable system. We developed a new biomechanical model with two closed link mechanism and one turntable to emulate a human riding a unicycle by a robot. This study of rider's postural stability control on a unicycle began from the observation of a human riding on a unicycle with vestibular model as intelligent biomechanical model including instinct and intuition mechanisms.

We consider the dynamic behavior of the biomechanical model from the standpoint of mechanics, decision-making process, action logic, and information processing with distributed knowledge base levels. The physical and mathematical background for the description of the biomechanical model is introduced. In this paper a thermodynamic approach is used for the investigation of an optimal control process and for the estimation of an artificial life of mobile robots [36, 37].

A new physical measure (the minimum entropy production) for the description of the intelligent dynamic behavior and thermodynamic stability condition of a biomechanical model with an AI control system for the robot unicycle is introduced. This measure is used as a fitness function in a GA for the computer simulation of the intuition mechanism as a global searching measure for the decision-making process to ensure optimal control of the global stability on the robot unicycle throughout the full space of possible solutions. The simulation of an instinct mechanism based on FNN is considered as a local active adaptation process with the minimum entropy production in the learning process of the vestibular system by teaching the control signal accordingly to the model representation results of [35]. Computer simulations in this study are carried out by the usage of thermodynamic equations for the motion of the robot unicycle. Entropy production and entropy measures for the robot unicycle motion and the control system are calculated directly from the proposed thermodynamic equations of motion.

Figure 45. Robotic unicycle model

 DOI: https://doi.org/10.30564/aia.v2i1.1323

In particular, Fig. 45 shows the main idea of robotic unicycle design using Kansei and System of System Engineering approaches. With genetic algorithm the intuition of solution search is developed based on bio-inspired model of unicycle rider behavior. Instinct and emotion are introduced based on fuzzy neural network and corresponding look-up tables.

Fuzzy simulation and soft computing, based on GA and FNN, it is obvious that the intelligent behavior controllability and postural stability of the robot are largely improved by two fuzzy gain schedule PD-controllers in comparison to those controlled only by a conventional PD and a fuzzy gain schedule PD-controller As a result of this investigation the look-up tables for fuzzy robust controllers of the robotic unicycle are formed with minimum production entropy in intelligent controllers and the robotic unicycle model uses this approach. The FNN controller offers a more flexible structure of controllers with a smaller torque, and the learning process produces less entropy. FNN controller gives a more flexible structure to controllers with smaller torque and the learning process produces less entropy than GA.

Thus, an instinct mechanism produces less entropy than an intuition mechanism. However, the necessary time for achieving an optimal control with the learning process on FNN (instinct) is larger than that with the global search on GA (intuition). The general approach for forming a look-up-table with GA and the fuzzy classifier system based on FNN. Intuition and instinct mechanisms are considered as global and local search mechanisms of the optimal solution domains for an intelligent behavior and can be realized by GA and FNN accordingly. For the fitness function of the GA, a new physical measure as the minimum entropy production for a description of the intelligent behavior in a biological model is introduced.

Thus, the posture stability and driving control of a human riding-type unicycle have been realized. The robot unicycle is considered as a biomechanical system using an internal world representation with a description of emotion, instinct and intuition mechanisms. We introduced intelligent control methods based on soft computing and confirmed that such an intelligent control and biological instinct as well as intuition together with a fuzzy inference is very important for emulating human behaviors or actions.

Intuition and instinct mechanisms are considered as global and local search mechanisms of the optimal solution domains for an intelligent behavior and can be realized by genetic algorithms (GA) and fuzzy neural networks (FNN) accordingly. For the fitness function of the GA, a new physical measure as the minimum entropy production for a description of the intelligent behavior in a biological model is introduced. The calculation of robustness and controllability of the robot unicycle is presented. This report provides a general measure to estimate the mechanical controllability qualitatively and quantitatively, even if any control scheme is applied.

The measure can be computed using a Lyapunov function coupled with the thermodynamic entropy change. Described above interrelation between Lyapunov function (stability condition) and entropy production of motion (controllability condition) in an internal biomechanical model is a mathematical background for the design of soft computing algorithms for the intelligent control of the robotic unicycle.

Fuzzy simulation and experimental results of a robust intelligent control motion for the robot unicycle are discussed. Robotic unicycle is a new Benchmark [25] of non-linear mechatronics and intelligent smart control. It is confirmed that the proposed fuzzy gain schedule PD-controller is very effective for the handling of the system's nonlinearity dealing with the robot's posture stability controls. Furthermore, an important result is that the minimum entropy production gives a quantitative measure concerning the controllability and also qualitative explanations.

Thus, we provide a new benchmark of Kansei engineering for the controllability of unstable nonlinear nonholonomic dynamic systems by means of intelligent tools based on a new physical concept of robust control: the minimum entropy production in control systems and in control object motion in general.

6. Quantum computing approach – quantum deep learning and quantum neural network

The work carried out showed that it is possible (in principle) to classify the mental states of a human being operator, demonstrates the optimal deep machine learning ability of the system, the ability to create knowledge bases based on the recorded EEG signal and use the results to recognize emotions.

Since emotions are characterized by clearly pronounced intensity, limited duration, awareness of the reasons for its appearance; connection with a specific object, circumstance; polarity, the use of machine learning and intelligent superstructure in the form of SCO, based on fuzzy controllers, is the best tool for correctly describing the general psychophysical state of the human being operator in Affective / Kansei Engineering approach [41, 42].

The ICS robustness, obtained on the basis of such an approach, requires a minimum of initial information, both on the behavior of the control object, and on external disturbances.

DOI: https://doi.org/10.30564/aia.v2i1.1323

An assessment of the accumulation of integral error (without using intellectual tools) can only evaluate the tonic activity of the brain, which shows a strong surge in the emotional background. Fuzzy controls allow you to slightly expand the ability to recognize the emotional background by adding production logic rules.

The combined use of an artificial neural network and soft computing optimizer on fuzzy controller allows to fully adapt the system, but it takes a long time to learn. This is critical in emergency and unforeseen situations for a system of intelligent robust control. The percentage of successful classification of the emotional sign in a human operator when working with quantum neural networks is much higher than that of classical neural networks. This leads to an increase in the reliability of the system as a whole, and allows the formation of more robust knowledge bases.

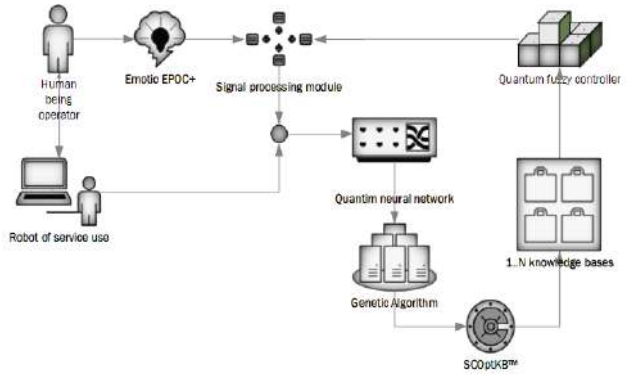

Figure 46. Intelligent control system with the integration of several fuzzy regulators

The Figure 46 shows the system with the integration of several fuzzy regulators and quantum fuzzy inference, contributing to the creation of a new quality of management: self-organization of knowledge bases online apply quantum neural network.

6.1 Quantum neural network application

Classic neural networks have some attractive features: parallel processing, error tolerance, the ability to learn and generalize the knowledge gained. The generalization property is understood as the ability of the neutral network to generate the correct outputs for input signals that were not taken into account during the learning. However, artificial neutral networks also face many difficulties: lack of rules for deterministic optimal architectures, limited memory capacity, time-consuming learning, etc. But there are quantum neural networks that solve these problems.

Remark. The idea of a quantum neural network was first described in [43]. It is a combination of the concept of a conventional neural network and the paradigm of quantum computing. In 1997, A. Vlasov proposed a hypothetical model of a quantum neural network using optical interference [42]. The first systematic review of artificial quantum neural networks is given in the dissertation of T. Menner [44]. The main advantage of quantum computing over classical is quantum parallelism, which allows to work with all valid states at the same time.

There are various prototypes of quantum neural networks. Some of them are very similar to their classical counterparts, while others use quantum operators that do not have classical equivalents, for example, phase shifts. Distinguish a wide range of different structures of the quantum neural networks. It is important to note that the efficiency of using neural networks is associated with massive parallel distributed processing of information and the nonlinearity of the transformation of input vectors by neurons. In addition, quantum systems have a much more powerful quantum parallelism, expressed by the principle of superposition.

The idea of creating an artificial quantum neural network consists in replacing the classical signals arriving at the input of a neuron with quantum states with amplitude and phase. At the same time, a quantum state, depending on the linear superposition of the incoming states, should also be formed at the output of the neuron. The weights in the case of a quantum neural network (QNN) are complex numbers (which change during the training of the network (see, Fig. 47)), so that each input quantum state is not only weighted in amplitude, but also shifted in phase.

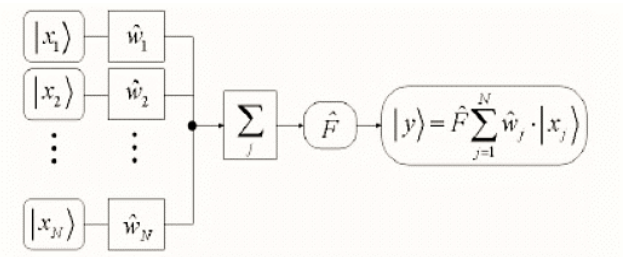

Figure 47. The mathematical model of a quantum neuron

The device maps inputs - a tuple of quantum and classical data - to outputs that may also contain quantum and classical parts, i.e., $\left(|x\rangle, \vec{x}\right) \mapsto \left(|y\rangle, \vec{y}\right)$. Supervised training of the QNN uses input-output pairs as training data (e.g., the x and $y = f\left(x\right)$ values from a nonlinear function) or quantum channel (e.g., a unitary quantum circuit or dissipative evolution), and attempts to optimize the QNN's parameters to make the QNN's outputs for each input match the training set. In addition to depending on the QNN architecture (the layout of the QNN and its trainable parameters), C and W also depend on the execution and training protocols (which include, e.g., the input data encoding and learning method). Applies universally, regardless of whether the learning machine and / or training

 DOI: https://doi.org/10.30564/aia.v2i1.1323

involves quantum, classical, or hybrid operations, whether the trained parameters are classical or quantum, how many uses of the QNN (or repeats of the input data) occur per input, or how the data is encoded.

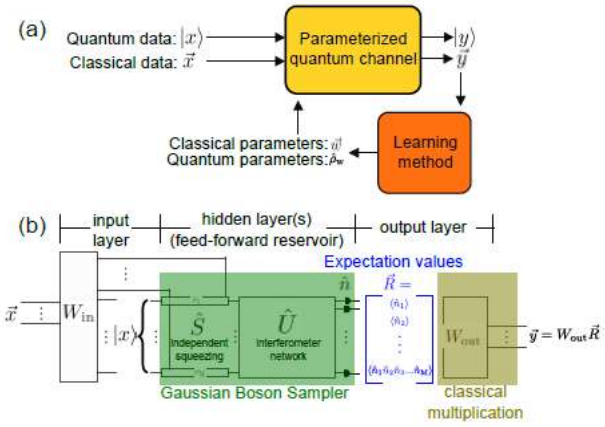

Figure 48. Schema of a general feed-forward QNN

Fig. 48a shows schema of a general feed-forward QNN, a parameterized quantum channel (which could include unitary and/or dissipative quantum evolutions, classical data processing, ancillary parameter states, etc.) which is trained in a supervised fashion to optimize the classical and quantum parameters $\vec{\omega}$ and / or ρ_ω so that the QNN best approximates the transformation implied by the training data. Fig. 48b shows the schematic of a feed-forward quantum reservoir computer based on a Gaussian Boson Sampler. For classical tasks considered here, $|x\rangle = |0\rangle$ and data is then encoded through the squeezing parameters, and for all tasks we take Win to be the identify matrix [44].

Quantum tasks, such as preparing states or learning a quantum circuit, are unitary approximation tasks.

6.2 EEG Data processing based on QNN

EEG signals can be considered a realization of a random or stochastic process [8]. When an accurate description of the system is unavailable, a stochastic filter can be designed on the basis of probabilistic measures. Every solution to a stochastic filtering problem involves the computation of a time-varying probability density function (pdf) on the state–space of the observed system. The architecture of recurrent quantum neural network RQNN model is based on the principles of QM with the Schrodinger wave equation (SWE) playing a major part. This approach enables the online estimation of a time-varying pdf that allows estimating and removing the noise from the raw EEG signal.

Fig. 49 shows a basic architecture of RQNN model in which each neuron mediates a spatio-temporal field with a unified quantum activation function in the form of Gaussian that aggregates pdf information from the observed noisy input signal. Thus, the solution of SWE (which is complex valued and whose modulus square is the pdf that localizes the position of quantum object in the vector space) gives the activation function. From a mathematical point of view, the time-dependent single-dimension nonlinear SWE is a partial differential equation describing the dynamics of wave packet (modulus-square of this wave is the pdf) in the presence of a potential field (or function) (which is the force field in which the particles defined by the wave function are forced to move). Thus, the RQNN model is based on novel concept that a quantum object mediates the collective response of a neural lattice (a spatial structure of an array of neurons where each neuron is a simple computational unit.

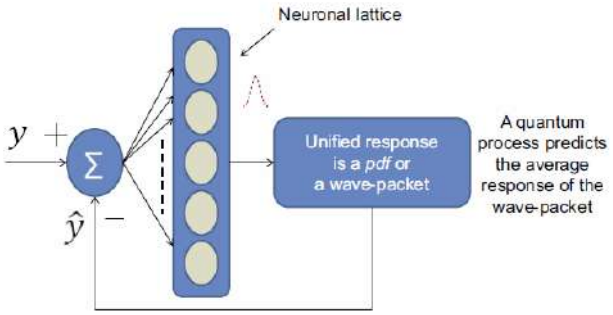

Figure 49. Conceptual framework of RQNN model

Such RQNN filter used for stochastic filtering is able to reduce noise, because of its stability being highly sensitive to model parameters, in case of imperfect tuning, the system may fail to track the signal and its output may saturate to absurd values. In the architecture used in Fig. 53, the spatial neurons are excited by the input signal y(t). The difference between the output of spatial neuronal network and the pdf feedback |ψ(x, t)|2 is weighted by a weight vector W(x) to get the potential energy V(x). The model can thus be seen as a Gaussian mixture model estimator of potential energy with fixed centers and variances, and only the weights are variable. These weights can be trained using any learning rule.

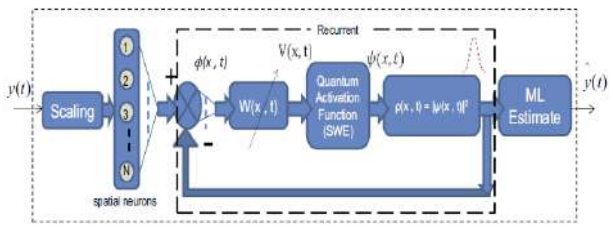

Figure 50. Signal estimation using RQNN model

In the RQNN architecture (see Fig. 50) makes the assumption that the average behavior of neural lattice that estimates the signal is a time-varying pdf which is mediated

DOI: https://doi.org/10.30564/aia.v2i1.1323

by a quantum object placed in the potential field V(x) and modulated by the input signal so as to transfer he information about pdf. SWE to recurrently track this pdf because it is a well-known fact that the square of the modulus of ψ function, the solution of the wave equation, is also a pdf.

$$\phi(x,t)=\exp\left(-\frac{\left(y(t)-x\right)^2}{2\sigma^2}\right)-\left|\psi(x,t)\right|^2 \qquad (7)$$

The potential energy is calculated as $V(x)=\varsigma W(x,t)\phi(x,t)$, where and $y(t)$ is the input signal and the synapses are represented by the time-varying synaptic weights W(x, t). The variable ζ represents the scaling factor to actuate the spatial potential energy V (x, t), and σ is the width of the neurons in the lattice (taken here as unity). This potential energy modulates the nonlinear SWE described by:

$$i\hbar\frac{\partial\psi(x,t)}{\partial t}=-\frac{\hbar^2}{2m}\nabla^2\psi(x,t)+V(x,t)\psi(x,t)\ , \qquad (8)$$

where ψ(x, t) represents the quantum state, ∇ is the Laplacian operator and V (x, t) is the potential energy.

The neuronal lattice sets up the spatial potential energy V(x). A quantum process described by the quantum state ψ which mediates the collective response of neuronal lattice, evolves in this spatial potential V (x) according to (2). As V (x) sets up the evolution path of the wave function, any desired response can be obtained by properly modulating the potential energy. Such RQNN filter used for stochastic filtering. Although this filter is able to reduce noise, because of its stability being highly sensitive to model parameters, in case of imperfect tuning, the system may fail to track the signal and its output may saturate to absurd values.

In the architecture used in this paper (Fig. 50), the spatial neurons are excited by the input signal y(t). The difference between the output of spatial neuronal network and the pdf. The filtered estimate is calculated using MLE as $\hat{y}(t)=E\left[\left|\psi(x,t)\right|^2\right]=\int x\left|\psi(x,t)\right|^2 dx$, where x represents the different possible values which may be taken up by the random process y. The variable x can be interpreted as the discrete version of quantum space with the resolution within this discrete space being referred to as δx (taken as 0.1). Thus, all the possible values of x will construct the number of spatial neurons N for RQNN model.

On the basis of MLE, the weights are updated and a new potential V (x, t) is established for the next time evolution. It is expected that the synaptic weights W(x, t) evolve in such a manner so as to drive the ψ function to carry the exact information of pdf of the filtered signal $\hat{y}(t)$. To achieve this goal, the weights are updated using the following learning rule:

$$\frac{\partial W(x,t)}{\partial t}=-\beta_d W(x,t)+\beta\phi(x,t)\left(1+\vartheta(t)^2\right)\ , \qquad (9)$$

where β is the learning rate, and βd is the delearning rate. Delearning is used to forget the previous information, as the input signal is not stationary, rather quasistationary in nature.

The second right-hand side term in the above equation maybe purely positive and so in the absence of delearning term, the value of synaptic weights W may keep growing indefinitely. Delearning thus prevents unbounded increase in the values of the synaptic weights W and does not let the system become unstable. The variable v(t) in the second term is the difference between the noisy input signal and the estimated filtered signal, thereby representing the embedded noise as $\vartheta(t)=y(t)-\hat{y}(t)$. If the statistical mean of the noise is zero, then this error correcting signal v(t) has less impact on weights, and it is the actual signal content in input y(t) that influences the movement of wave packet along the desired direction which results in helping the goal of achieving signal filtering.

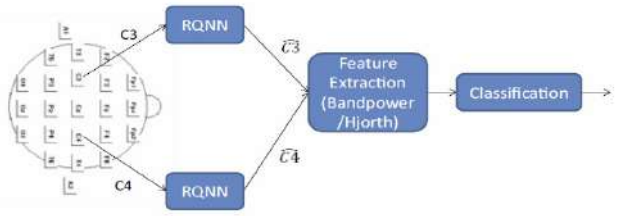

Figure 51. RQNN model framework for EEG signal enhancement

Figure 51 shows the position of RQNN model within the BCI system. The raw EEG signal is fed one sample at a time and an enhanced signal is obtained as a result of filtering process. The raw EEG is first scaled in the range 0–2 before it is fed to the RQNN model. During the off-line classifier training process, all the trials from a particular channel of EEG are available. Therefore, the complete EEG is scaled using the maximum of amplitude value from that specific channel. During the online process, the EEG signal is approximately scaled in the range 0–2 using the maximum of amplitude value obtained from the off-line training data of that specific channel. The net effect is that the input signal during the online process is also maintained approximately in the region 0–2, and this enables the tracking of sample using a reduced range of the movement of wave packet. In addition, the number of spatial neurons has also been reduced along the x-axis from an earlier value of 401 to 612 in the present case. The primary assumption in

 DOI: https://doi.org/10.30564/aia.v2i1.1323

doing this is that the unknown nonstationary and evolving EEG signal during the evaluation stage will stay within the bound of the range of 61 spatial neurons which can cover the input signal range up to three. If the scaling of the input signal is not implemented, then the number of neurons required to cover the input signal range will be larger thereby leading to an increased computational expense [45, 46].

7. Conclusion

One of the important tasks of the intelligent robust control systems is a control in unforeseen / unsharp situations. Modern solutions to this problem already make it possible to achieve good results, but such systems cannot be trained in online. Thus, the set of response methods to events is extremely limited. With the quantum computing and, in particular, the fuzzy quantum algorithm, it is possible to solve such problems by increasing the speed of deep machine learning. The use of quantum fuzzy inference can increase robustness without the expense of a time. One of the most optimal solutions in the design of intelligent robust control systems is the formation of knowledge bases for a variety of fixed control situations. The goal of a quantum regulator is to combine the knowledge bases obtained using the SCO into self-organizing quantum fuzzy regulators. Quantum deep machine learning on quantum artificial network and optimization on quantum genetic algorithm are perspective and applied examples in cognitive intelligent robotics in Part II considered.

Appendix 1: Emotion, pain and cognitive control and cingulate cortex [50].

It has been argued that emotion, pain and cognitive control are functionally segregated in distinct subdivisions of the cingulate cortex. However, recent observations encourage a fundamentally different view. In humans and other primates, the cingulate — a thick belt of cortex encircling the corpus callosum — is one of the most prominent features on the mesial surface of the brain (Fig. A1.1a). Early research suggested that the rostral cingulate cortex (Brodmann's 'precingulate'; architectonic areas) plays a key part in affect and motivation (Fig. A1.1b). More recent research has enlarged the breadth of functions ascribed to this region; in addition to emotion, the rostral cingulate cortex has a central role in contemporary models of pain and cognitive control. Work in these three basic domains has, in turn, strongly influenced prominent models of social behavior, psychopathology and neurological disorders. The most basic question is whether emotion, pain and cognitive control are segregated into distinct subdivisions of the rostral cingulate or are instead integrated in a common region. There is a growing recognition that aMCC might implement a domain-general process that is integral to negative affect, pain and cognitive control.

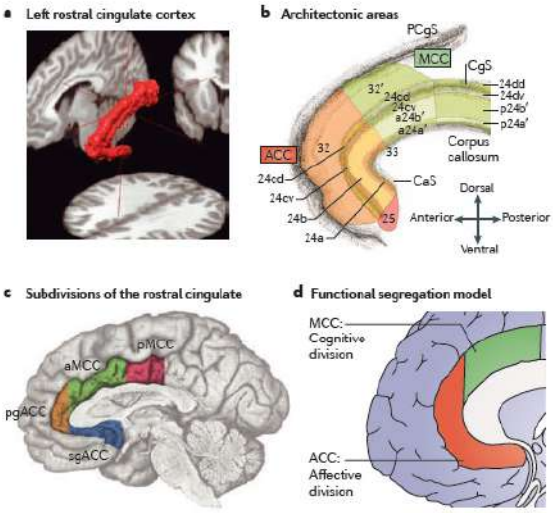

Figure A1.1 Divisions of the human rostral cingulate cortex

Figure A1.1 shows the divisions of the human rostral cingulate cortex (The rostral cingulate has been partitioned on physiological and anatomical grounds at spatial scales ranging from the macroscopic to the molecular).

The map depicts the results of a coordinate-based meta-analysis (CBMA) of 380 activation foci derived from 192 experiments and involving more than 3,000 participants. The uppermost panel shows the spatially normalized foci for each domain. The next panel shows thresholded activation likelihood estimate (ALE) 38,214 maps for each domain considered in isolation. The two lowest panels depict the region of overlap across the three domains.

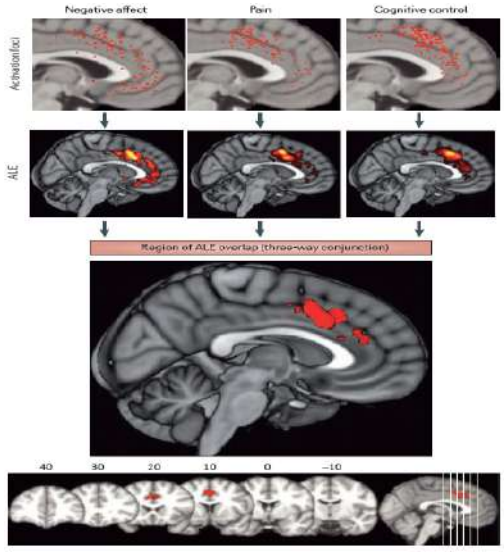

Figure A1.2. Negative affect, pain and cognitive control activate a common region

DOI: https://doi.org/10.30564/aia.v2i1.1323

Recent imaging data (see. Fig. A1.2) implicate the anterior cingulate cortex (ACC) and the midcingulate cortex (MCC) in the regulation of autonomic activity and the perception and production of emotion.

Similarly, neuronal recordings demonstrate that MCC is responsive to emotionally charged words in humans. Especially robust links have been forged between activity in the anterior subdivision of the MCC (aMCC; Fig. A1.1c) and the experience of more intense states of negative affect, as with the anticipation and delivery of pain and other kinds of aversive stimuli.

Importantly, meta-analyses that have examined imaging studies of negative affect, pain or cognitive control in isolation suggest that each of these domains consistently activate aMCC. Therefore, based on such observations, there is a growing recognition that aMCC might implement a domain-general process that is integral to negative affect, pain and cognitive control. Collectively, these observations refute claims that cognition and emotion are strictly segregated into different divisions of the rostral cingulate cortex — claims that were heavily based on an early meta-analysis of imaging studies. Instead, these observations show that aMCC is consistently activated by the elicitation of negative affect, pain and cognitive control. of course, these results do not preclude the possibility that this region contributes to other psychological processes, such as reward motivated behavior. Furthermore, they do not address whether segregation is present at finer levels of analysis — for example, in individual participants or neurons.

Similarly, segregation may be present on a finer timescale than that resolved by conventional imaging techniques. Nevertheless, what these results do demonstrate is that conventional functional imaging studies of negative affect, pain and cognitive control all consistently report activation in this subdivision of rostral cingulate cortex. We refer to the cluster of activation overlap obtained in our meta-analysis as aMCC (Fig. A1.2). Nevertheless, the relatively dorsal position of the cluster within aMCC (approximately corresponding to architectonic areas; Fig A1.1b) is consistent with the provisional location of the rostral cingulate zone (RCZ). This suggests that it is specifically RCZ that is commonly activated by imaging studies of negative affect, pain and cognitive control.

Appendix 2. Quantum models of cognition and of EEG data processing

Two of the most surprising properties of quantum systems are state superposition and entanglement. Superposition is the coexistence of different state values of the same particle at the same time. Superposed states are reduced to a single one by the act of measurement or by other kinds of interaction with the macro-environment, which are called decoherence. Entanglement is a strong state correlation between spatially separated particles.

Example A2.1. In quantum mechanics a quantum state A described by wave function and probability amplitude $\psi_A(x)$. According to Born rule probability of macro state A is defined as $|\psi_A(x)|^2$. For two quantum states A and B probability amplitude is defined as

$$|\psi_A(x)+\psi_B(x)|^2 = |\psi_A(x)|^2 + |\psi_B(x)|^2 + 2\psi_A(x)\psi_B(x)\cos\theta, \quad (1)$$

where θ is the quantum phase difference at (A; B).

Let us consider two slit experiment. Suppose the experiment is carried out with only one slit opened, say Slit 1. The particles target the detecting screen and the experimental outcome is represented by a curve $P_1(x)$ in a way that $P_1(x)$ and $\delta(x)$ represents the probability of a particle landing in the range (x, x + δx). If this slit cover and open the other, we will obtain a curve $P_1(x)$ similar to $P_1(x)$. This is of course exactly what we expect when performing such experiment at a macroscopic level. Finally, admit that both slits are opened. We would then observe that the particles would sometimes come through Slit 1 and sometimes through Slit 2, varying between the two possibilities in a random way. This will produce two piles behind each slit which constitute the sum of the results that would be observed with one or the other slit opened. Consequently, we should have $P_{12}(x) = P_1(x) + P_2(x)$. Instead, according to quantum mechanics, as mentioned above, $P_{12}(x) = P_1(x) + P_2(x) + 2\sqrt{P_1(x)P_2(x)}\cos\theta \neq P_1(x) + P_2(x)$.

We obtain what it is called a typical quantum interference pattern where a new term is given by $2\sqrt{P_1(x)P_2(x)}\cos\theta$. Mental events cause neural events analogously to the manner in which probability fields of quantum mechanics are causatively responsible for physical events. Probabilistic brain feature to do conscious predictions does not relate rules of classical probability but instead quantum probabilistic rules.

Experiment [47]. Forty healthy children with ages between 6 and 11 years (mean age 8 ± 1.7) were randomly recruited in a commercial area, after voluntary acceptance to participate in the experiment and written signature of parent's agreement. They were then randomly allocated into two subgroups-each composed of 10 subjects of each sex-identified as groups A and B. The first group was shown a picture displayed on a tablet screen (Figure A2.1), and then asked if they felt more prompt to attack the represented element or to withdraw from it.

 DOI: https://doi.org/10.30564/aia.v2i1.1323

Figure A2.1 Presented picture in experiment.

The same picture shown to group B however, before submitting them to the precedent task, asked them to first identify the evoked feelings through the question "does this picture scare you or make you angry?".

In this manner, in such group B objectively marked more integration of emotion and cognition respect to group A. With this experiment, it was intention to demonstrate a quantum interference effect. Therefore, in Group A introduced a dichotomous variable A, taking the possible two values, +1 or −1. The probabilities $P(A=+1)$ and $P(A=-1)$ were then estimated. To Group B introduced a new variable B, with possible values B = +1 or B = −1, before submitting them to the task already proposed to Group A. In this case the following probabilities were estimated

$$P(B=+1), P(B=-1), P(A=+1|B=+1),$$
$$P(A=+1|B=-1), P(A=-1|B=+1)$$

and $P(A=-1|B=-1)$. If, during the perception and cognition effort of the subjects submitted to the tasks, quantum mechanics did not apply, classical Bayes's theorem should hold and we should obtain,

$$P(A=+1)\,(\text{Group A}) = P(B=+1)P(A=+1|B=+1) + P(B=-1)P(A=+1|B=-1)\,(\text{Group B})$$

and a similarly expression for $P(A=-1)$. If instead the superposition principle and quantum interference were to be manifested in this experiment - thus confirming a role for quantum mechanics during the perception and the cognition of children, should have

$$P(A=+1) = P(B=+1)P(A=+1|B=+1) + P(B=-1)P(A=+1|B=-1) + 2\sqrt{P(B=+1)P(A=+1|B=+1)P(A=-1|B=+1)}\cos\theta \quad (2)$$

Implying the presence of the quantum interference term

$$2\sqrt{P(B=+1)P(A=+1|B=+1)P(A=-1|B=+1)}\cos\theta.$$

The following results are obtained:

Group A	Group B	
Variable A	Variable B	Variable B/A
$P(+1)=0.15$	$P(+1)=2/20=0.1$	$P(A=+1/B=+1)=0.5,\ P(A=+1/B=-1)=0.167$
$P(-1)=0.85$	$P(-1)=0.9$	$P(A=-1/B=+1)=0.5,\ P(A=-1/B=-1)=0.833$

Using the formula previously outlined, a value $\cos\theta_+ = -0.29011, \theta_+ = 1.865146$. for $P(A=+1)$ obtained.

Thus, children's perceptive-cognitive performance is subject to quantum interference. This conclusion, already achieved with adult subjects, strengthens the role of quantum cognition in the study of human cognitive operations, eventually leading to the development of a more complete grounded theory of the mind which can help better understand not only human personality, but also mental disorders.

Example A2.2. Let us now explicitly construct a quantum mechanical model in complex Hilbert space for the pair of concepts Fruit and Vegetable and their disjunction "Fruit or Vegetable", and show that quantum interference models the experimental data gathered [48]. In Fig. A2.2 the data for "Fruits or Vegetables" are graphically represented.

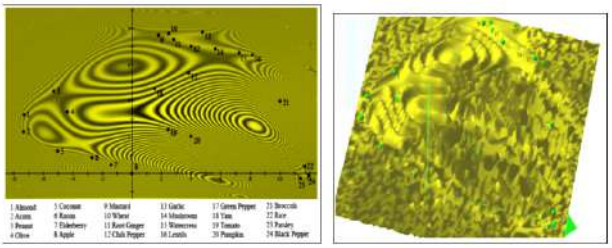

Figure A2.2 The probabilities of a person choosing the exemplar k as an example of `Fruits or Vegetables' [2]

Figure A2.2 shows the probabilities $\rho(A \text{ or } B)_k$ of a person choosing the exemplar k as an example of `Fruits or Vegetables' are fitted into the two-dimensional quantum wave function $\frac{1}{\sqrt{2}}(\psi_A(x,y)+\psi_B(x,y))$, which is the normalized superposition of the wave functions (a); and A three-dimensional representation of the interference landscape of the concept `Fruits or Vegetables' as shown in Fig. A2.2 a (b).

This is just a normalized sum of the Gaussians,

DOI: https://doi.org/10.30564/aia.v2i1.1323

since it is the probability distribution corresponding to $\frac{1}{\sqrt{2}}\left(\psi_A(x,y)+\psi_B(x,y)\right)$, which is the normalized superposition of the wave functions. The numbers are placed at the locations of the different exemplars with respect to the probability distribution

$$\frac{1}{2}\left|\psi_A(x,y)+\psi_B(x,y)\right|^2=\frac{1}{2}\left|\left|\psi_A(x,y)\right|^2+\left|\psi_B(x,y)\right|^2\right| + \left|\psi_A(x,y)\psi_B(x,y)\right|\cos\phi(x,y)$$

where $\phi(x,y)$ is the quantum phase difference at (x; y). The values of $\phi(x,y)$ are given for the locations of the different exemplars in [2].

The interference pattern shown in Fig. A2.2 is very similar to well-known interference patterns of light passing through an elastic material under stress. In considered case it is the interference pattern corresponding to "Fruits or Vegetables" The interference pattern is clearly visible. The model shows how "interference of concepts" explains the effects of under extension and overextension when two concepts combine to the disjunction of these two concepts.

This result supports hypothesis that human thought has a superposed two-layered structure, one layer consisting of classical logical thought and a superposed layer consisting of quantum conceptual thought. Possible connections with recent findings of a grid-structure for the brain are analyzed, and influences on the mind / brain relation, and consequences on applied disciplines, such as artificial intelligence and quantum computing [49].

Example A2.3. The presence of typically quantum effects, namely superposition and interference, in what happens when human concepts are combined, and provide a quantum model in complex Hilbert space that represents faithfully experimental data measuring the situation of combining concepts. Left panel on the Fig. A2.3 portrays major characteristic substrate (e.g., receptors, organelles, etc.) involved in Ca2+ -mediated response regulation of arbitrary glutamatergic neurons, including, but not limited to, substrate critical for synaptic plasticity, cellular energetics, immune protection, homeostasis, gene expression, biosynthesis, molecular trafficking, cytoskeletal organization, and cell fate.

Similar mechanisms affect both pre- and post-synaptic neurons, but, for descriptive purposes, post-synaptic cell activity is emphasized. Ca2+ entry into the post-synaptic neuron through voltage-gated receptor (VGC), ligand-gated receptor (LGC), and transient potential receptor (TRP) channels and stimulated inositol 1,4,5-trisphosphate (IP3) production by activated G-protein coupled receptors (GCR) help initiate cytosolic CICRs from integral IP3 receptors (IP3 R) located along the endoplasmic reticulum (ER) membrane. CICRs may cause traveling waves of varying velocities and patterns which emulate search routines capable of eliciting/suppressing appropriate response regulation from different cellular compartments. Lower right panel illustrates CICR saltatory and continuous waves. Saltatory Ca2+ waves and the information they carry conduct at velocities (V) proportional to the classical Ca2+ diffusion coefficient (D).

Whereas, faster continuous Ca2+ waves and the information they transmit move at velocities proportional to the square-root of the classical Ca2+ diffusion coefficient. Coefficient D of continuous waves for either intercluster or intracluster diffusion is assumed to be up to orders of magnitude greater than that for saltatory waves. The quadratic disparity in the velocities of saltatory and continuous waves corresponds to the root-rate increase of information processing by Grover's quantum algorithm over classical algorithms.

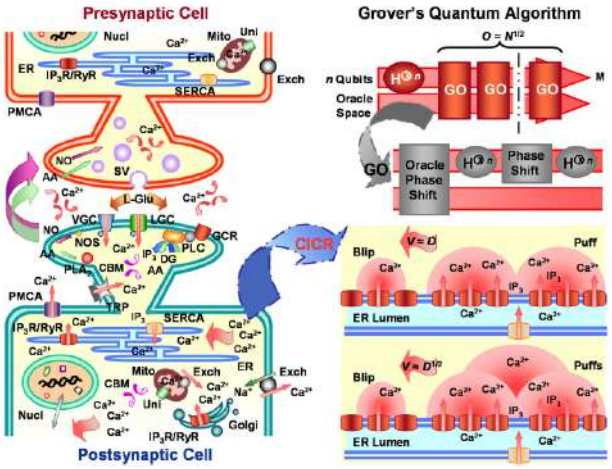

Figure A2.3. Calcium-induced calcium reactions (CICRs) emulate Grover quantum search algorithm [49]

Upper right panel in Fig. A2.3 shows schematic of Grover's quantum algorithm. The algorithm takes as input n qubits, upon which it performs Hadamard transformations ($H^{\otimes n}$) and Grover's operation (GO) to find a target m of M solutions stored in database N. Regardless of whether one or more consultations of the Oracle are needed, Grover's quantum algorithm finds the target solution within $O\left(\sqrt{N}\right)$ algorithmic steps or operations O. Additional abbreviations: arachidonic acid (AA), Ca2+ binding molecule (CBM), Ca2+ uniporter (Uni), diacylglycerol (DG), Golgi apparatus (Golgi), L-glutamate (L-Glu), nucleus (Nucl), mitochondria (Mito), nitric oxide (NO), nitric oxide synthase (NOS), phospholipase A2 (PLA2), phospholipase C (PLC), plasma-membrane Ca2+ ATPase (PMCA), ryanodine receptor (RyR), sarcoplasmic-endo-

 DOI: https://doi.org/10.30564/aia.v2i1.1323

plasmic-reticulum Ca2+ ATPase (SERCA), Na+ / Ca2+ exchanger (Exch), synaptic vesicle (SV).

References

[1] Petrov, B, Ulanov, G., Ulyanov S. and Hazen E. Information semantic problems in organization control [M]. Nauka, 1977, pp. 452.

[2] Ozer, E. and Feng, M. Structural reliability estimation with participatory sensing and mobile cyber-physical structural health monitoring systems [J]. Appl. Sci. 9, 2019, pp. 2840.

[3] Noor A. Potential of cognitive computing and cognitive systems [J]. Open Eng, 5, 2015, pp. 75-88.

[4] Chie H., Takato H. and Takayuki N. Deep Emotion: A Computational Model of Emotion Using Deep Neural Networks [J]. CoRR, 2018, available at: http://arxiv.org/abs/1808.08447.

[5] Rozaliev V. Postroenie matematicheskoj modeli emocij: Integrirovannye modeli i myagkie vychisleniya v iskusstvennom intellekte [R]. V Mezhdunarodnaya nauchno-prakticheskaya konferenciya "Integrirovannye modeli i myagkie vychisleniya v iskusstvennom intellekte" Sbornik nauchnyh trudov, 2009, pp. 950-957.

[6] Bazgir O., Mohammadi Z. and Habibi S. Emotion recognition with machine learning using EEG signals [R]. 25th National and 3rd International Iranian Conference on Biomedical Engineering (ICBME), 2018, pp. 1-5.

[7] Xie H., Pan J. and Wen Z. An EEG-based brain computer interface for emotion recognition and its application in patients with disorder of consciousness [J]. IEEE Transactions on Affective Computing, 2019, pp. 1.

[8] Ulyanov S. and Litvintceva L. Intelligent robust control: soft computing technology [M]. VNIIgeosistem, 2011, pp. 406.

[9] Ulyanov S.V. (inventor) Self-organizing quantum robust control methods and systems for situations with uncertainty and risk // Patent US 8788450 B2. – Date Publ. July 22, 2014.

[10] Sandberg H, et al. Maximum work extraction and implementation costs for nonequilibrium Maxwell's demon [J] // Physical Review E. 2014. No 4. pp. 042119.

[11] Ulyanov S., Yamafuji K., Gradetsky V. and Fukuda T. Development of intelligent mobile robots for service use and mobile automation systems including wall climbing robots: Pt. 1. Fundamental design principles and motion models [J]. International Journal of Intelligent Mechatronics: Design and Production. 1, 3, 1997, pp. 111-143.

[12] Sagawa T, Ueda M. Minimal Energy Cost for Thermodynamic Information Processing: Measurement and Information Erasure [J]. Phys. Rev. Lett. 102, 25. pp. 250602.

[13] Horowitz J. M., Sandberg H. Second-law-like inequalities with information and their interpretations [J]. New Journal of Physics. 16, 2014, pp. 125007.

[14] Ulyanov S.V., Litvintseva L.V., Kurawaki I. et al. Principle of minimum entropy production in applied soft computing for advanced intelligent robotics and mechatronics [J]. Soft Computing. 4, 3, 2000, pp. 141–146.

[15] Sieniutycz S., et all. Framework for optimal control in multistage energy systems [J]. Physics Reports, 326, 2, 2000.

[16] Ulyanov S.V. Quantum relativistic informatics [J]. LAP LAMBERT Academic Publishing, OmniScriptum GmbH & Co. KG, 2015.

[17] Sadeghieh A., Roshanian J., Najafari F. Implementation of an intelligent adaptive controller for an electrohydravlic servo system based on a brain mechanism of emotional learning [J]. Intern. J. of Advanced Robotic Systems (INTECH). 9, 2012, pp. 1–12.

[18] E. Daryabeigi, A. Zarchi, Gh. R. Arab Markadeh, M. A. Rahman. Implementation of Emotional Controller (BELBIC) for Synchronous Reluctance Motor Drive Proc [R]. IEEE Intern. Electric Machines & Drivers Conf. (IEMDC), 2011, pp. 1066-1093.

[19] L. V. Litvintseva, I.S. Ulyanov, S. V. Ulyanov and S. S. Ulyanov. Quantum fuzzy inference for knowledge base design in robust intelligent controllers [J]. J. of Computer and Systems Sciences Intern., 46, 9, 2007, pp. 908 – 961.

[20] Ulyanov, S. V Intelligent Robust Control System Based on Quantum KB-Self-organization: Quantum Soft Computing and Kansei / Affective Engineering Technologies [J]. Springer International Publishing, 2014, pp. 37-48.

[21] Takayuki T., Junji O., Litvintseva L., Kazuo Y. and Ulyanov S. Intelligent control of a mobile robot for service use in office buildings and its soft computing algorithms [J]. Journal of Robotics and Mechatronics, 8, 1996, pp. 538-554.

[22] Dawson G. and Toth K. Autism spectrum disorders. In D. Cicchetti & D. J. Cohen (Eds.). [J]. Developmental psychopathology: Risk, disorder, and adaptation, 2006, pp. 317-357.

[23] Stanton C., Kahn P. Jr., Severson R., Ruckert J. and Gill B. Robotic Animals Might Aid in the Social Development of Children with Autism [R]. 3rd ACM/IEEE International Conference on Human-Robot Interaction, 2008.

DOI: https://doi.org/10.30564/aia.v2i1.1323

[24] Wei C., Wenxu S., Xinge L., Sixiao Zh., Ge Zh., Yanting W., Sailing H., Huilin Zh. and Jiajia Ch. Could Interaction with Social Robots Facilitate Joint Attention of Children with Autism Spectrum Disorder? [J]. Computers in Human Behavior, 2019, pp. 98.

[25] Palestra, G., Carolis, B.D., & Esposito, F. Artificial Intelligence for Robot-Assisted Treatment of Autism [J]. WAIAH@AI*IA, 2017.

[26] Cho, S.J. and Ahn, D. Socially Assistive Robotics in Autism Spectrum Disorder [J]. Hanyang Medical Reviews, 36, 2016, pp. 17.

[27] Rudovic O., Lee J., DaiM., Schuller B. and Picard R. W. Personalized Machine Learning for Robot Perception of Affect and Engagement in Autism Therapy [J]. Science. 3, 2018.

[28] Ulyanov S., Mamaeva A. and Shevchenko A. Programmnaya realizaciya modulya obrabotki dannyh dlya kognitivno-intellektual'noj sistemy dlya detej-autistov [R]. «Sbornik dokladov XXV Mezhdunarodnoj konferencii «MATEMATIKA. KOMPYUTER. OBRAZOVANIE» 25, 2018, pp. 398.

[29] Ulyanov S., Mamaeva A. and Shevchenko A. Kognitivno-intellektual'naya sistema diagnostiki, obucheniya i adaptacii detej-autistov. Chast. 1 [J]. Sistemnyj analiz v nauke i obrazovanii, 5, 2016, available at: http:/www.sanse.ru/archive/42.

[30] Ulyanov S., Mamaeva A. and Shevchenko A. Kognitivno-intellektual'naya sistema diagnostiki, obucheniya i adaptacii detej-autistov. Chast 2. Opredelenie emocij [J]. Programmnye produkty i sistemy: elektron. nauch. zhurnal. 4, 2017, available at: http://swsys-web.ru/cognitive-intellectual-system-for-diagnosis-and-education-of-autistic- children-2.html.

[31] Nikolaev A. Spektral'nye harakteristiki EEG na pervom etape resheniya razlichnyh prostranstvennyh zadach [J]. Psihologicheskij zhurnal, 15, 6, 1994, pp. 100-106.

[32] Lapshina T. Psihofiziologicheskaya diagnostika emocij cheloveka po pokazatelyam EEG [R]. Materialy Mezhdunarodnoj nauchno-prakticheskoj konferencii "Razvitie nauchnogo naslediya Borisa Mihajlovicha Teplova v otechestvennoj i mirovoj nauke" Nauchnyj sbornik. Moskva: BF "Tverdislov". Moskva, 2006, pp. 160-165.

[33] Fretska E., Bauer H., Leodolter M. and Leodolter U. Loss of control and negative emotions: a cortical slow potential topography study [J]. International Journal of Psychophysiology. 33, 1999, pp. 127-141.

[34] Ulyanov S., Reshetnikov A. and Mamaeva A. Gibridnye kognitivnye nechetkie sistemy upravleniya avtonomnym robotom na osnove nejrointerfejsa i tekhnologii myagkih vychislenij [J]. Programmnye produkty i sistemy / Software & Systems, 30, 3, 2017, pp. 420–424.

[35] Ulyanov S.V., Yamafuji K. Fuzzy intelligent emotion and instinct control of a robotic unicycle [R]. In Proc. 4th Intern. Workshop on Advanced Motion Control. 18-21 Mar., 1996, Mie, Japan, 1, 1996, pp. 127-132.

[36] Ulyanov S.V., Watanabe S., Yamafuji K. A new physical measure for mechanical controllability of a robotic unicycle on basis of intuition, instinct and emotion computing [R]. In Proc. 2nd Intern. Conf. on Application of Fuzzy Systems and Soft Computing. June 25-27, 1996, pp. 78-92.

[37] Ulyanov V.S., Ohkura T., Yamafuji K., Ulyanov S.V. Intelligent control of an extension-less robotic unicycle: A study of mechanical controllability via minimum entropy criteria [J]. Lecture Notes in Control and Information Sciences: Progress in System and Robot Analysis and Control Design, 243, 1999, pp. 559-570.

[38] Hagiwara T., Ulyanov S.V., Takahashi K., Diamante O. An application of a smart control suspension system for a passenger car based on soft computing [R]. Yamaha Motor Technical Report, 2003.01.15.

[39] EU PCT Patent WO 2004/012139 A2 (PCT/US2003/023727), "Intelligent mechatronic control suspension system based on quantum soft computing" (Inventor: S. V. Ulyanov). [P], International publication Date: 5 February 2004 (US Patent US 2004/0024750 A1. Publ. Date: Feb. 5, 2004).

[40] US Patent No 2006,0218 A1, "System for soft computing simulation" (Inventor: S. V. Ulyanov). [P], Date of patent: Sept. 2006, 2006.

[41] Ulyanov S. Intelligent self-organized robust control design based on quantum / soft computing technologies and Kansei engineering [J]. Computer Science Journal of Moldova, 21, 62, 2013, pp. 242-279.

[42] Ulyanov S.V., Yamafuji K. Intelligent self-organized cognitive controllers. Pt. 1: Kansei / affective engineering and quantum / soft computing technologies [J]. System Analysis in Science and Education, 4, 2014, available at: http:/www.sanse.ru/archive/48.

[43] Kak S. On Quantum Neural Computing [J]. Inf. Sci, 83, 1995 pp 143-160.

[44] Menner T. Quantum Artificial Neural Networks [D]. Univ. of Exeter, UK, 1998.

[45] Gandhi V., Prasad G., Coyle D. et al. Quantum neural network-based EEG filtering for a brain-computer interface [J]. IEEE Trans. on Neural Network and Learning Systems, 25, 2, 2014, pp. 278-288.

[46] Ulyanov S.V., Feng M., Ulyanov V.S., Yamafuji K., Fukuda T., Arai F. Stochastic analysis of

 DOI: https://doi.org/10.30564/aia.v2i1.1323

time-variant nonlinear dynamic systems. Part 1: the Fokker-Planck-Kolmogorov equation approach in stochastic mechanics [J]. Prob. Engng. Mech., 13, 3, 1998, pp. 183-203.

[47] Elio Conte, Rui Freire Lucas. First Time Demonstration of the Quantum Interference Effect during Integration of Cognition and Emotion in Children [J]. World Journal of Neuroscience, 2015, 5, pp. 91-98.

[48] Diederik Aerts and Sandro Sozzo Quantum Interference in Cognition: Structural Aspects of the Brain [J}. arXiv:1204.4914v1 [cs.AI] 22 Apr 2012

[49] Clark K. Basis for a neuronal version of Grover's quantum algorithm [J]. Frontiers in Molecular Neuroscience. 2014, doi: 10.3389/fnmol.2014.0002 http://community.frontiersin.org/people/u/52068

[50] Alexander J. Shackman, Tim V. Salomons, Heleen A. Slagter, Andrew S. Fox, Jameel J. Winter and Richard J. Davidson. The integration of negative affect, pain and cognitive control in the cingulate cortex [J]. Nature, 12, 2011.

DOI: https://doi.org/10.30564/aia.v2i1.1323

BILINGUAL PUBLISHING CO.
Pioneer of Global Academics Since 1984

Artificial Intelligence Advances
https://ojs.bilpublishing.com/index.php/aia

ARTICLE

Intelligent Robust Control of Redundant Smart Robotic Arm Pt I: Soft Computing KB Optimizer - Deep Machine Learning IT

Alena V. Nikolaeva Sergey V. Ulyanov*

Dubna State University, Universitetskaya Str.19, Dubna, Moscow Region, 141980, Russia
ISESYS LLC (EFKO GROUP), Naberezhnaya Ovchinnikovskaya Str.20 Bld.2, Moscow, Russia

ARTICLE INFO

Article history
Received: 29 October 2019
Accepted: 8 April 2020
Published Online: 15 April 2020

Keywords:
Intelligent control system
Knowledge base
Soft computing technology
Decomposition
Redundant robotic manipulator

ABSTRACT

Redundant robotic arm models as a control object discussed. Background of computational intelligence IT on soft computing optimizer of knowledge base in smart robotic manipulators introduced. Soft computing optimizer is the sophisticated computational intelligence toolkit of deep machine learning SW platform with optimal fuzzy neural network structure. The methods for development and design technology of control systems based on soft computing introduced in this Part 1 allow one to implement the principle of design an optimal intelligent control systems with a maximum reliability and controllability level of a complex control object under conditions of uncertainty in the source data, and in the presence of stochastic noises of various physical and statistical characters. The knowledge bases formed with the application of soft computing optimizer produce robust control laws for the schedule of time dependent coefficient gains of conventional PID controllers for a wide range of external perturbations and are maximally insensitive to random variations of the structure of control object. The robustness is achieved by application a vector fitness function for genetic algorithm, whose one component describes the physical principle of minimum production of generalized entropy both in the control object and the control system, and the other components describe conventional control objective functionals such as minimum control error, etc. The application of soft computing technologies (Part I) for the development a robust intelligent control system that solving the problem of precision positioning redundant (3DOF and 7 DOF) manipulators considered. Application of quantum soft computing in robust intelligent control of smart manipulators in Part II described.

1. Introduction

The approach based on Soft Computing Optimizer (SCO) for design intelligent control systems (ICS) allows one to design an optimal ICS with a maximum reliability and controllability level for the set of dynamic systems under the presence of uncertainty in the source data; to reduce the number of sensors both in the control channel and in the Measurement System (MS) without loss of precision control quality and accuracy. The robust ICS based on this approach requires minimum source data on both the behavior of the Control Object (CO) and the external perturbations. SCO is the SW toolkit of deep machine learning platform with optimal struc-

**Corresponding Author:*
Sergey V. Ulyanov,
ISESYS LLC (EFKO GROUP), Naberezhnaya Ovchinnikovskaya Str.20 Bld.2, Moscow, Russia;
Email: ulyanovsv@mail.ru

 DOI: https://doi.org/10.30564/aia.v2i1.1339

ture of fuzzy neural network (FNN).

Let us consider the design features of the ICS IT structure and the SCO of knowledge base (SCOptKBTM). Analysis of the simulation results made it possible to establish that the application of the FNN-based technique does not guarantee the required accuracy achievement of the Teaching Signal (TS) approximation. As a result, the level of sensitivity of CO increases, and the reliability of ICS decreases. SCO based on soft computing techniques increases the level of ICS reliability. Consider an SCO structure containing the optimal FNN configuration. The main features of SCO, the design of reliable Knowledge Bases (KB) of Fuzzy Controllers (FC) are described in the Appendix. The methodology of fuzzy and joint stochastic modeling of control system based on SCO is discussed to assess the stability and limitations of ICS. The effectiveness of SCO-based control processes using specific typical examples (standards) of COs such as a robotic manipulator is demonstrated under conditions of incomplete information about the CO structure and unpredicted control situations.

1.1. Background of physical laws ICS design

Figures 1 and 2 demonstrate typical criteria for control quality, their interrelations with different types of computations and simulation types, as well as the hierarchy of levels of control quality depending on the required level of intelligence of the Automatic Control System (ACS).

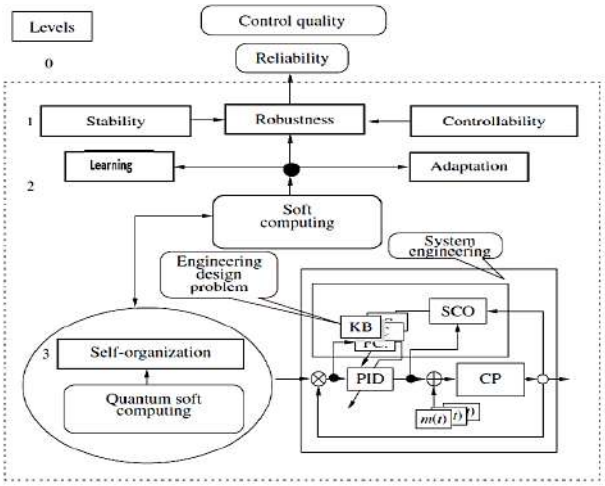

Figure 1. The interrelation between the types and hierarchical levels of control quality criteria

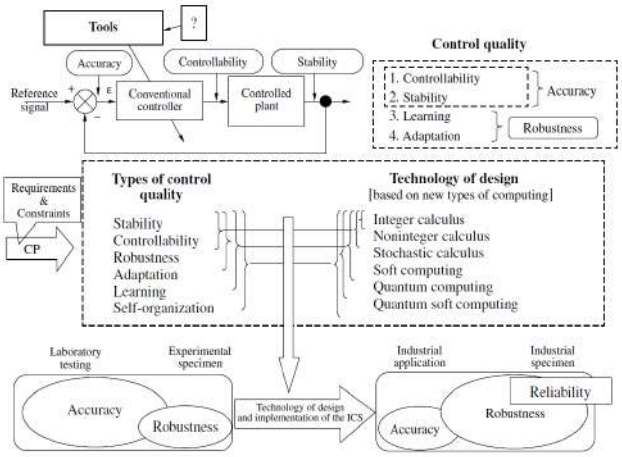

Figure 2. The interrelation between the control quality criteria, types of intelligent computing, and simulation in designing robust KBs of the FC

The key point of this design IT is the use of the method of eliciting objective knowledge about the control process irrespective of the subjective experience of experts and the design of objective KBs of a FCs which is principal component of a robust ICS.

Figure 3 presents the main components and their interrelations in the information design technology based on new types of computing (soft and quantum computational intelligence).

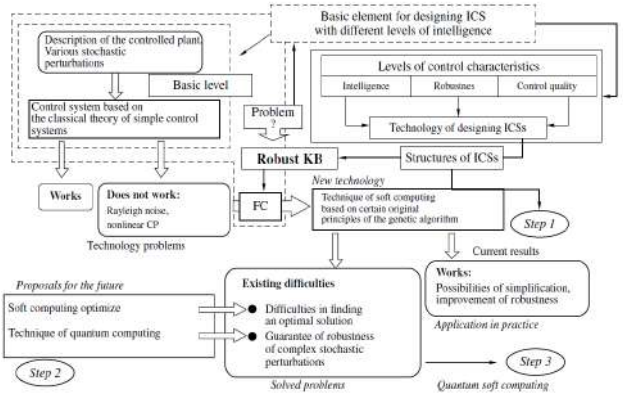

Figure 3. The process of development and creation of information technology for design an integrated ICS

A robust KB of the FC is the result of application considered technology. We can change the property of the system without changing the intrinsic passive property using the generalized canonical transformation. Indeed, if a given system fails to satisfy the stabilizable conditions by the feedback: positive definiteness of the Hamiltonian function and zero-state detectability, then still we may be able to transform the system into an appropriate Hamiltonian system which can be stabilized by the intelligent feedback.

DOI: https://doi.org/10.30564/aia.v2i1.1339

Figure 4 shows the role of thermodynamic trade-off in robust control design.

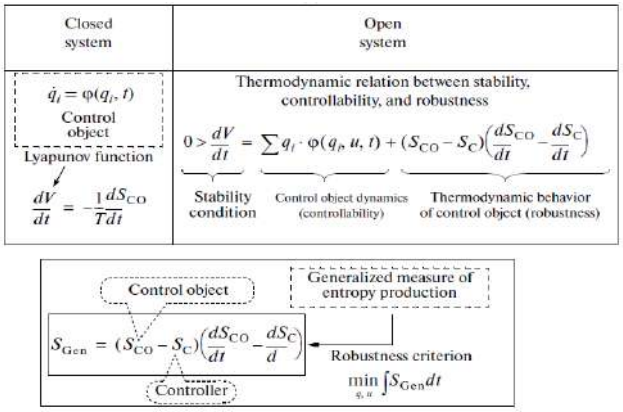

Figure 4. Physical law of intelligent control as background of ICS design technology

Remark. This approach was firstly presented in [1]. It was introduced the new physical measure of control quality to complex non-linear controlled objects described as non-linear dissipative models. This physical measure of control quality is based on the physical law of minimum entropy production rate in ICS and in dynamic behavior of complex object. The problem of the minimum entropy is equivalent with the associated problem of the maximum released mechanical work as the optimal solutions of corresponding Hamilton-Jacobi-Bellman equations. It has shown that the variational fixed-end problem of the maximum work W is equivalent to the variational fixed-end problem of the minimum entropy production. In this case both optimal solutions are equivalent for the dynamic control of complex systems and the principle of minimum of entropy production guarantee the maximal released mechanical work with *intelligent* operations. This new physical measure of control quality applied as fitness function of Genetic Algorithm (GA) in optimal control system design. The introduction of physical criteria (the minimum entropy) can guarantee the stability and robustness of control. This method differs from aforesaid design method in that a new intelligent global feedback in control system introduced. The interrelation between the stability of CO (the Lyapunov function) and controllability is used. The basic peculiarity of the given method is the necessity of model investigation for CO and the computing of entropy production rate through the parameters of the developed model. The integration of joint systems of equations (the equations of mechanical model motion and the equations of entropy production rate) enable to use the result as the fitness function in GA as a new type of CI. Acceleration method of integration for these equations is described in [2].

A continuous-time system in the feedback interconnection with the resetting controller is considering in [3]. Every time the emulated energy of the controller reaches its maximum, the states of the controller reset in such a way that the controller's emulated energy becomes zero. Alternatively, the controller states can be made reset every time the emulated energy is equal to the actual energy of the plant, enforcing the second law of thermodynamics that ensures that the energy flows from the more energetic system (the plant) to the less energetic system (the controller). The proof of asymptotic stability of the closed-loop system in this case requires the non-trivial extension of the hybrid invariance principle, which in turn is a very recent extension of the classical Barbashin-Krasovskii invariant set theorem. The subtlety here is that the resetting set is not a closed set and as such a new transversality condition involving higher-order Lie derivatives is needed. A system theoretic foundation for thermodynamics is developed in [4].

Main goal of robust intelligent control is support of optimal trade-off between stability, controllability and robustness with thermodynamic relation as thermodynamically stabilizing compensator (see Figure 4). The hybrid energy dissipating controller provides effectively one-way energy transfer between the CO and the controller [4].

The hybrid controller with resetting set is a thermodynamically stabilizing compensator. Analogous thermodynamically stabilizing compensators can be constructed for lossless dynamical systems. Detail description of interrelations between energy-based and thermodynamic-based controller design is given in [4, 5].

On Figure 4 joint in analytic form different measures of control quality such as stability, controllability, and robustness supporting the required level of reliability and accuracy. Consequently, the interrelation between the Lyapunov stability and robustness is the main physical law for designing ACS. This law provides the background for an applied technique of robust ICS's (with different levels of intelligence designing KB's) based on the application based of soft computing technologies.

2. The structure of ICS design IT

The general hierarchical structure and stages of execution of information technology embedded in the process of design of integrated fuzzy ICS for autonomous and interconnected COs with different physical nature (so called port-controlled Hamiltonian systems) is shown in Figure 5.

 DOI: https://doi.org/10.30564/aia.v2i1.1339

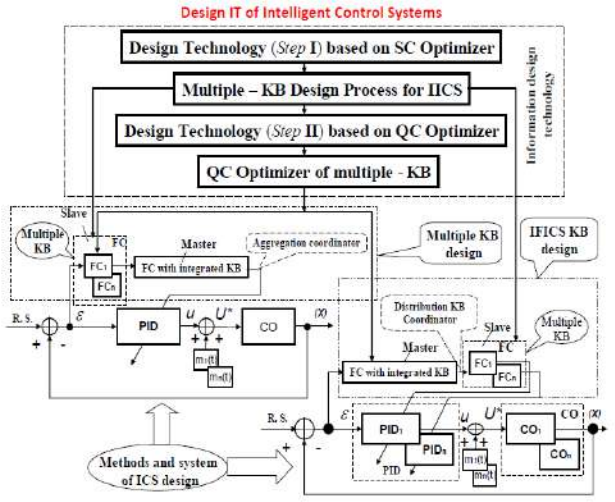

Figure 5. General hierarchical structure of information design technology of robust KBs for integrated fuzzy ICS

This technology uses computational intelligence toolkit for design of KBs in the FC of the lower executive level. The main role in the structure of this technology is played by the development of robust KBs based on corresponding optimizers (see the block "Information design technology" labeled by dashed lines). Note some structural and functional specific features of design stages in Figure 5.

At the *first* stage the technology of design of optimizer KBs with soft computing SCOptKB™ forms robust KBs for fixed learning control situation. At the *second* stage quantum optimizer QCOptKB™ used to realize the process of design of the generalized robust KB of hybrid fuzzy PID controllers operating in contingency control situations.

Thus, the process of design of robust KBs consists of two interconnected stages based on soft and quantum computing, respectively. Functionally, at the first design stage (see Figure 5) individual KBs for two (or more) FCs for particular control situations (learning situations) are formed. Optimizer of KBs are used with the technology of soft computing and fuzzy stochastic simulation. The optimizer of KB SCOptKB™ was developed in [6, 7] as the new toolkit of computational intelligence based on the technology of soft computing (first design stage), including the GAs and FNNs for realization of optimization and learning procedures (universal robust approximation) of production rules in KBs, respectively. The toolkit was used for extraction of objective knowledge from the dynamic behavior of weakly structured models of complex COs and design of robust KBs in FC with deep knowledge representation (see Figure 6).

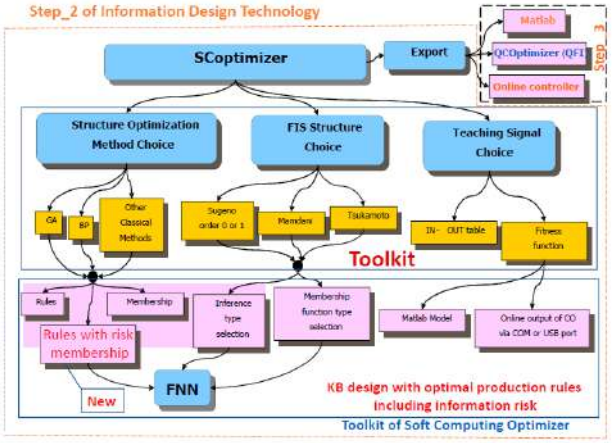

Figure 6. Structure of computational intelligence toolkit of design IT

It should be underlined that the toolkit of Knowledge Base Optimizer (KBO) realizes in the stochastic fuzzy simulation *global intelligent feedback* (new type of feedback [8]), which makes it possible to objectively extract and compress valuable information from the dynamic behavior of the CO and applied controller type. For guaranteed achieving the required robustness level and control quality in the form of fitness functions of GA information and physical criteria are introduced (information- thermodynamic criterion of optimal distribution of physically achievable levels of stability, controllability, and robustness in ICSs [6, 8]). The optimization of control processes with required quality and robustness levels is achieved for fixed search space and type of fitness functions of the GA. The developed new toolkit of computational intelligence is the generalization of methodology and methods in [5, 9-11].

The application of the self-organization principle based on quantum computing is the algorithmic essence of the second stage for increasing the robustness of the KB. The block diagram of design of robust KBs based on the principle of self-organization of ICSs (using quantum effects) and the structure of information flows in the design technology are shown in Figure 7; in this figure the main objectives and content of stages of design technology (Figure 5) are explained.

The structure and software support of quantum KBO QCOptKB™ are considered below in Part II. Let us elucidate some specific features and technical details of realization of technologies of intelligent computing in processes of design of robust KBs shown in Figures 5 and 6.

Studies performed in [6, 12] demonstrated the existence of a rather broad domain of preservation of robustness of individual KBs designed at the first stage based on optimizer KBs. The introduction of the technology of soft computing (whose kernel is comprised of GAs and FNNs)

DOI: https://doi.org/10.30564/aia.v2i1.1339

extended the domains of efficient application of FCs due to the addition of new functions in the form of learning and adaptation. Multiple results of simulation and practical application showed [6, 13, 14] that for random events and control situations with known perturbation probability distribution density functions optimizer KBs with soft computing can be used to design robust KBs in FCs, which do not lose the robustness property in many contingency control situations.

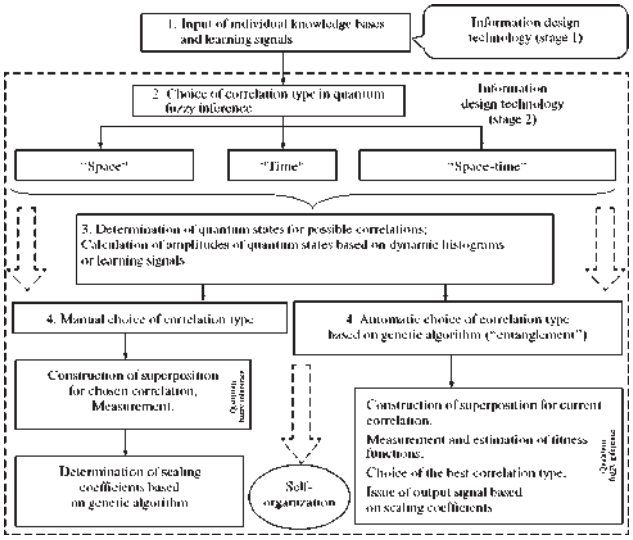

Figure 7. Block diagram of design of robust KBs and structure of information flows in technology of design of robust KBs based on the principle of self-organization of ICS

The SCO is a new, efficient software tool for KBs design of robust ICSs based on soft computing with the use of new optimization criteria (in the form of new fitness functions of Gas; see in details Appendix). As these criteria, we take the thermodynamic and information-entropy criteria represented in Table 1.

Table 1. The types and the role of the fitness function of the GA in the SCO

Type of GA	Criteria	Fitness function (FF)	Role of the FF
GA_1: Optimization of linguistic variables	Maximum joint information entropy and minimum information about signals separately	$H^j_{X_i} = -p^j_{X_i}\log(p^j_{X_i}) = -p(x_i \mid x_i = \mu^j_{X_i})\log[p(x_i \mid x_i = \mu^j_{X_i})] = -\frac{1}{N}\sum_{t=1}^{N}\mu^j_{X_i}(x_i(t))\log[\mu^j_{X_i}(x_i(t))]$	Elimination of redundancy of the TS Choice of an optimal cardinality of term-sets of linguistic variables of the components of the TS
		$H^{(j,l)}_{X_i} = H\left(x_j\right)_{x_i = \mu^j_{X_i} x_k = \mu^l_{X_k}} = -\frac{1}{N}\sum_{t=1}^{N}[\mu^j_{X_i}(x_i(t)) * \mu^l_{X_k}(x_k(t))]\cdot \log[\mu^j_{X_i}(x_i(t)) * \mu^l_{X_k}(x_k(t))]$, where * is the chosen operation of fuzzy AND	
GA_2: Optimization of rule base	Minimum approximation error	$E = \sum_p E^p$, where $E^p = 1/2(F(x^p_1, x^p_2, \ldots, x^p_n) - d^p)^2$	Choice of optimal parameters of the right sides of rules
GA_3: Adjustment of the KB	Minimum approximation error or maximum joint information entropy	$E = \sum_p E^p$	Fine adjustment of the parameters of membership functions
		$H^j_{X_i}$	

The structure of the SCO for design robust ICSs is presented in Figure 8.

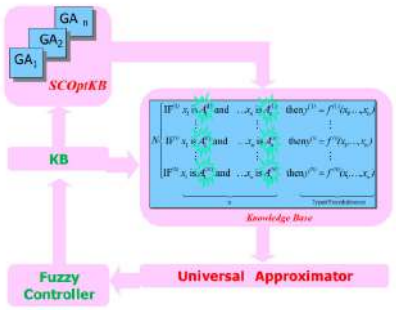

Figure 8. Structure of SCO of knowledge base SCOptKB^{TM}

The SCO consists of interrelated GA1, GA2, GA3, which optimize particular components of KB.

The input of the SCO is TS, which can be obtained either at the stage of stochastic simulation of the behavior of the controlled plant (with the use of its mathematical model) or experimentally, i.e., directly from the measurement of the parameters of the physical model of the controlled plant.

Figure 9 also presents the successive implementation of the stages of designing the SCO.

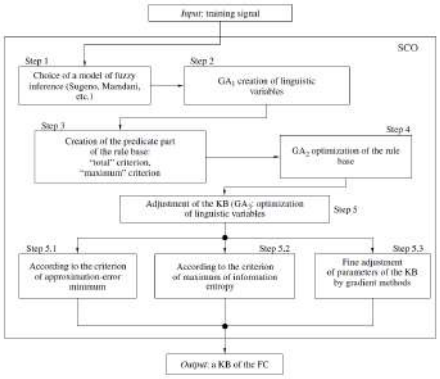

Figure 9. The algorithm of interaction of operations in the SCO

Let us specify the steps of the optimization algorithm.

Step 1. *Choice of the model of fuzzy inference*. The user specifies the particular type of model of fuzzy inference (Sugeno, Mamdani, etc.) and the number of input and output variables.

Step 2. *Creation of linguistic variables*. With the application of GA_1, an optimal number of membership functions (MF) is determined for each input linguistic variable, and an optimal form for the representation of its MFs (triangular, Gaussian, etc.) is chosen.

Step 3. *Design of the rule base*. At this stage, a special algorithm for selection of the most robust rules is used in accordance with the following two criteria:

1) "total" criterion: choose only the rules that satisfy

 DOI: https://doi.org/10.30564/aia.v2i1.1339

the following condition: $R^l_{total\_fs} \geq TL$, where TL (threshold level) is a given (manually or chosen automatically) level of rule activation, and $R^l_{total\_fs} = \sum_{k=1}^{N} R^l_{fs}(t_k)$, and

$$R^l_{fs}(t_k) = \prod[\mu^l_{j1}((x_1(t_k)), \mu^l_{j2}((x_2(t_k)), ..., \mu^l_{jn}((x_n(t_k))],$$

where t_k are time instants, $k = 1, ..., N$, and N is equal to the number of points in the control signal; $\mu^l_{jk}(x_k)$, $k = 1, ..., n$ are membership functions of input variables, l is the index of the rule in the KB; and symbol "Π" means the operation of fuzzy conjunction (in particular, it may be interpreted as a product);

2) "maximum" criterion: choose only the rules that satisfy the condition $\max_t R^l_{fs}(t) \geq TL$.

Step 4. *Optimization of base rules*. With the help of GA_2, the right sides of rules of the KB defined at Step 3 are optimized. At this stage, a solution that is close to the global optimum is found (minimum TS approximation error). With the application of the next step, this solution can be improved locally.

Step 5. *Adjustment of the base of rules*. With the help of GA_3, the left and right sides of the rules of the KB are optimized; i.e., optimal parameters of the MFs of the input/output variables are chosen (from the viewpoint of a given fitness function of the GA). In this optimization process, three different fitness functions chosen by the user (steps 5.1 and 5.2 in Figure 9) are used. In addition, there is also the opportunity to adjust the KB with the help of conventional error-back-propagation method (step 5.3 in Figure 9).

Verification (testing) of the designed knowledge base. Constructed at stages 4, 5.1, 5.2, and 5.3 on Figure 9 KBs of the ICS are tested from the viewpoint of robustness and control quality. For further use, the best functionally KB is chosen, which is tested in the functional mode in online.

Examples of KBs simulation on the basis of efficient application of the SCO below on redundant robotic manipulators considered.

2.1. Software implementation of the soft computing optimizer

The SCO was implemented as a software system [9, 15-17]. As a programming language, C++ (Microsoft Visual Studio.net) was chosen. The algorithmic part devoted to the implementation of the main stages of optimization algorithms was implemented as a platform-independent tool (see, Appendix). The graphical interface presented in Figure 10 was developed for operating systems of the Win32 family and was tested on personal computers with different versions of the Windows operating system. The main menu of the optimizer was divided into several sections (Figure 10) devoted to execution of the main functions and visualization of the results of algorithm operation.

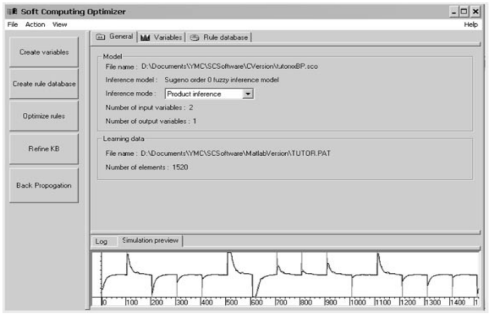

Figure 10. The main menu of the SCO

In the *left section* of the main menu, a group of buttons is located. These buttons run different optimizing components such as following:

- creation of linguistic variables (Create variables) with the help of GA_1;
- algorithm of generation of the predicate part of fuzzy rules (Create rule base);
- GA_2 for optimization of the consequence part of fuzzy rules (Optimize rules);
- GA_3, which represent the algorithm of readjustment of the parameters of linguistic variables for a more accurate approximation of TS by the obtained rules (Refine KB). The error-back-propagation algorithm is also included (Back propagation), which guarantees a given accuracy of the approximation of TS of the designed KB.

In the *central section* of the main menu of the optimizer, the basic information about the designed fuzzy system is located, such as the type, address of the main file of the KB, the number of input and output variables, as well as generic information about the TS. Here, can also find the *editor of linguistic variables* and the editor of rules.

Figure 11 presents the editor of linguistic variables. The membership functions of fuzzy variables can be edited both manually, by dragging the corresponding values, and by manual input of parameters.

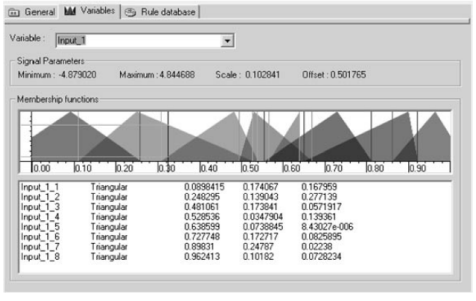

Figure 11. The editor of linguistic variables

DOI: https://doi.org/10.30564/aia.v2i1.1339

Figure 12 presents the *editor of the base of fuzzy rules*. The fuzzy rules are structurally represented in the form of FNN. The number of neurons of the first layer corresponds to the number of input signals, while the number of neurons of the second layer corresponds to the total number of MFs involved in the linguistic variables describing the corresponding input signals.

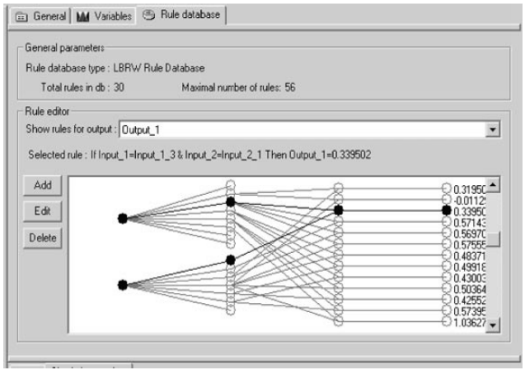

Figure 12. The editor of the base of fuzzy rules

The number of neurons of the third layer is given by the set of fuzzy rules involved in a given KB. To choose a particular rule, it is necessary to choose the corresponding neuron of the third layer. The chosen rule can be further changed and appended.

In the bottom part of the main menu of the optimizer, the window for the output of system messages is located, in which the parameters of algorithms and all actions made by the user are copied. The constantly updated result of fuzzy inference is output together with the approximating TS. Any actions aimed at a change of parameters of the designed KB results in updating the approximation results. Thus, the user can visually control the effect of modification of parameters of the KB on the result of the approximation.

In the design of this system, it was initially planned to use it together with Matlab, which allows one to flexibly compute the values of the fitness functions of GA. Note that, together with the TS, it is possible to apply the results of numerical integration of models of the controlled plant executed in the Simulink environment controlled by FC with the synthesized SCO. An approach that allows one to compute the fitness function in Matlab with the subsequent transfer of the results to the GA of the optimizer was developed [18]. For this purpose, the corresponding library of units of the Simulink environment was designed. This library supports the loading of the KB and fuzzy inference (in the simulation mode), as well as the communication with the optimizer (in the optimization mode). The unit of fuzzy inference for Simulink was written in C++, in the form of the corresponding S -function of Simulink. To simulate fuzzy inference (without using Simulink models), the corresponding *.mex file was prepared, which allows one to obtain the results of fuzzy inference with the help of the command line and executed scripts of Matlab. The program is compatible with Matlab 6.1 and subsequent versions.

Since the main chain in the technology for designing ICSs is the stage of designing the corresponding KB, the design of robust KBs under the types of unpredicted control situations specified above allows one to establish in a general the accordance between the conditions of functioning of the controlled plant and the robustness level required for the ICS. Consider the results of simulation of robust structures of ICSs with efficient application of the SCO.

Remark. We are described a methodology for designing robust KBs and the corresponding software tools in the form of SCO based on soft computing, which allows one to solve the problem posed within the framework of processes of learning and adaptation. In what follows, we consider particular examples of application of the SCO in the problems of testing and evaluating the levels of structural robustness of the designed ICS based on the joint technique of stochastic and fuzzy simulation. As simulation objects, we chose benchmarks that allow us to demonstrate clearly the efficiency and advantage of the developed tools for designing the SCO.

The employed models of the controlled plant possess both local and global dynamic instabilities, high sensitivity to variation of the initial conditions, parameters of the CO structure, and random parametric, internal, and external perturbations. We present the results of simulation and practical recommendations for using them in the problems of designing robust ICS. The methodology of stochastic simulation is described in short below.

2.2. A system of stochastic fuzzy simulation of robust intelligent control systems

Fuzzy simulation of robust KBs with the SCO is based on the process of extraction of valuable information by simulation and investigation of individual (statistically represented) informative trajectories describing the behavior of the controlled plant and a conventional PID controller under the effect of stochastic processes. Within the scope of correlation theory, stochastic processes, which are different in their statistical nature (i.e., having different density functions of probability distribution), can be indistinguishable in their correlation properties. The density function of probability distribution is the complete statistical characteristics of stochastic processes. Therefore, the output process of the forming filter simulating the external

 DOI: https://doi.org/10.30564/aia.v2i1.1339

environment must be represented by the informatively significant selective trajectory of the stochastic process that allows one to investigate individual parameters of dynamic fuzzy systems. Selective trajectories should meet these requirements if their density function of the probability distribution is known. Stochastic processes with a required density function of probability distribution are simulated by the method of nonlinear forming filters.

In this section, we use the methodology of designing the structures of ICSs functioning in the external environment under the presence of stochastic processes having the same autocorrelation function and different distribution functions of the probability density. The method of nonlinear forming filters for describing stochastic processes with a required density function for the probability distribution based on the Fokker-Planck-Kolmogorov equations is described in [17]. This approach allows us to develop a generalized methodology for investigating the robustness of ICSs based on stochastic fuzzy simulation.

Figure 13 presents the generalized structure of the system of stochastic fuzzy simulation, which was applied for evaluating the robustness and limiting capabilities of the structures of ICSs with specifying the main factors that affect the sensitivity and reliability of control.

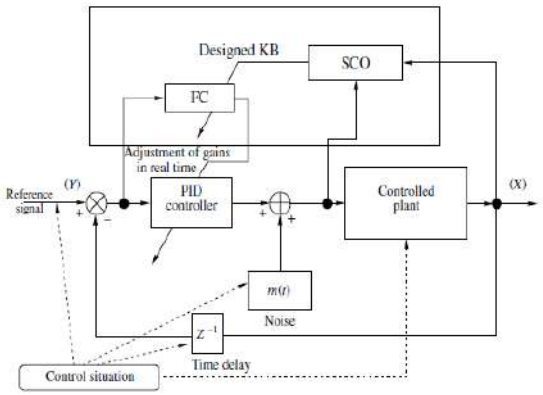

Figure 13. The block diagram of stochastic fuzzy simulation with unpredicted control situations

The efficiency of application of the SCO is demonstrated by particular typical examples of models of controlled plants, the so-called benchmarks of redundant robotic manipulators. In particular, the investigated models of physical controlled plants and their functioning environment are characterized by the following specific features typical of real dynamic controlled plants:

• they have local and global dynamic instability with respect to the generalized coordinates;

• they have essentially nonlinear cross constraints (stochastic nonlinearities) in the generalized dynamic coordinates, which mutually affect (antagonistically) the dynamic, stability, and controllability of the controlled plant;

• they operate under unpredicted control situations.

As unpredicted control situations, we consider four control models under the conditions of uncertainty of the source information: (1) with statistical information about the external and parametric random time dependent perturbations (selective trajectories of stochastic processes with density functions of probability distribution depending on time); (2) with uncertainty of information about the variation of parameters of the structure of the controlled plant; (3) under the presence of random delay time in the loops of control and measurement systems; and (4) when the control (reference signal) goals are changed.

The developed model of the ICS and controlled plant was simulated in the Matlab/Simulink system presented in Figure 14.

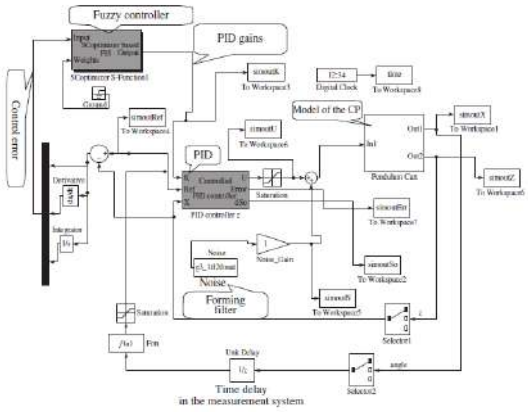

Figure 14. A Matlab/Simulink Model of the control system

As typical random noise, three types of stochastic processes with the corresponding density functions of probability distribution were simulated.

Figure 15 presents the form of the density functions of probability distribution and the simulation results of the output stochastic processes from the corresponding forming filters.

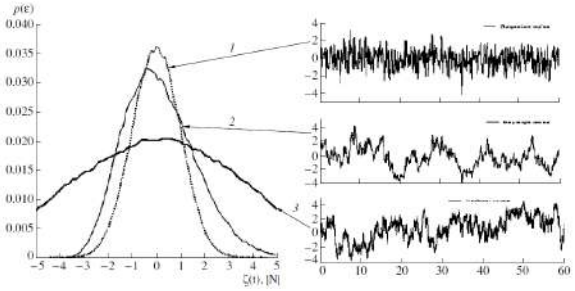

Figure 15. The form of the density function of the probability distribution and the results of simulation of output stochastic processes from the corresponding forming filters: (1) Gaussian; (2) Rayleigh; (3) uniformly distributed

DOI: https://doi.org/10.30564/aia.v2i1.1339

Varying the structure of the forming filters, the parameters in the models of the controlled plant, the delay time in the channel for measuring the control error, and the form of the reference signal (control goal), we can simulate unpredicted control situations and evaluate the sensitivity and the robustness level of the designed ICS.

In this section, we present the results of simulating the robust control laws for intelligent fuzzy PID controllers by complex essentially nonlinear dynamic controlled plants as robotic redundant manipulators To demonstrate the capabilities of simulation of the processes of intelligent control of a dynamic controlled plant and the conditions of functioning, the results of simulation of the following three typical controlled plants (benchmarks) are considered: (1) a nonlinear oscillator with essential dissipation and local dynamic instability; (2) an inverted pendulum mounted on a moving cart (so-called "cart-pole" system) and with global dynamic instability; and (3) an essentially nonlinear oscillator with local and global dynamic instability in cross constraints of the generalized coordinates of the controlled plant.

These oscillators are of independent interest for problems in robotics and mechanics (e.g., a stroboscopic manipulator robot with complex behavior dynamics and considerable dissipation) and allow one to compare our results with the results obtained by methods based on FNN[19].

Remark 6. In view of the large amount of the simulation results, we consider the first version of an oscillator containing all the qualitative specific features of the two types of oscillators listed above.

3. Control System of 7DOF Manipulator

Redundant manipulators have a greater number of Degrees of Freedom (DOF) than is necessary for the task solution more than the dimension of the workspace. Redundancy DOF allows the structure of the manipulator to adapt under conditions of insufficient information about an external changing environment, as well as in conditions of changing parameters of the manipulator (for example, an obsolescence or unit failure). Redundancy DOF also allow to specify the behavior of the robot manipulator with a minimum consumption of useful resource. The control tasks for redundant robot manipulator (positioning of the end effector, trajectory describing, solving the inverse dynamics problem, etc.), with increasing CO complexity, increasing performance requirements in unexpected situations, are being solved applying computational intelligence technologies GA[20, 21], neural and fuzzy neural networks[22, 23], fuzzy logic[24, 25]. The application of soft computing technologies [26] to build a robust ICS for solving the problem of precision positioning redundant (3DOF and 7 DOF) manipulators considered.

The control system is a combination of one or more COs and a control system. In general, a control system consists of a control link, an CO, and a Measuring System (MS) in a feedback circuit. To provide the given dynamic indicators in control systems, any types of controllers are used. Widespread is Proportional Differential Integral (PID) controller. The integral component of the controller allows eliminating the static error in the system, and the differential component allows improving the dynamic performance, and forcing the overshoot process.

3.1. Control systems with constant controller parameters

In the general case, it is necessary to find the coefficients $K_P, K_D, K_I, i = \overline{1,7}$ of the PID controller.

Initial knowledge of the control system and of CO[27, 28] are necessary for determining the coefficients by analytical methods, correct determination of PID controller coefficients K_P, K_D, K_I is possible with the help of an expert.

The inclusion of elements of intelligent computing in the control system may allow us to describe the requirements for the control system in terms of quality criteria.

For example, we can define control parameters using GA. It is necessary to correctly determine the fitness function of the GA, for example as follows:

$$fitness = (PTS = 1) \cap (I_T \to 0),$$

where *PTS* (Position Task Solution) is the solution to the positioning problem by the manipulator, and I_T is the ICS performance.

Based on the fitness function, the choice of coefficients $K_P, K_D, K_I, i = \overline{1,7}$ is determined on the basis of providing a guaranteed solution to the positioning problem with maximum performance.

An intelligent GA superstructure without destroying the lower executive level allows to operate with qualitative criteria of the system.

The block diagram of the ICS based on GA is shown in Figure 16, where Q_{ref} is the master reference signal, Q' is the measured variable, $K = [K_{P1}\ K_{D1}\ K_{I1}; \ldots; K_{P7}\ K_{D7}\ K_{I7}]$ is the coefficient matrix of the PID controller, $s(t)$ is the limitation of the control action, $d(t)$ is the delay in the MS, $m(t)$ is the external influence.

 DOI: https://doi.org/10.30564/aia.v2i1.1339

The selection of the PID controller coefficients in the control system based on GA is made once for one or a number of cases (regular control situations) and remain unchanged during operation. As a result, control system based on GA gets a good result with the task of accurately positioning the manipulator in standard situations. However, control system does not provide guaranteed control in unexpected control situations, which will be demonstrated below.

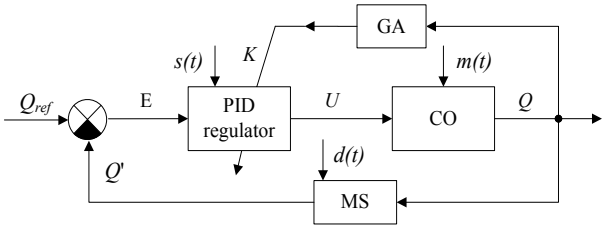

Figure 16. The block diagram of the control system based on GA

The use of the control system based on GA is limited by the requirement for a description of the constant environmental conditions and known structures of the control unit and CO.

Expanding the scope of the control system is possible by increasing the intelligence of the control system: using dynamic tuning of the PID controller coefficients, which is possible with the elements of soft computing technology.

3.2. Designing an intelligent control system based on Soft Computing Optimizer

FC is the main element of the ICS based on soft computing technologies[28], FC manages the gain of the PID controller due to the integrated KB, which includes data on the form and parameters of MFs of input and output fuzzy variables, and fuzzy production rules.

KBs are created using the intelligent tools the KBO based on soft computing [29] in the following sequence:

1) creating TS: determining a typical control situation (for example, a standard situation), generating a table of PID controller coefficients and control errors using a GA;

2) organization of a fuzzy inference model: determining of the type of fuzzy model, interpreting fuzzy operations, the number of input and output variables;

3) creating linguistic variables for input values;

4) creating a rule base;

5) setting up the rule base;

6) optimization of the left and right parts of the rules of the KB.

ICS based on KBO on soft calculations may contain one or more FC depending on the complexity of the system and CO. In the case of a simple CO, it is possible to implement one FC, respectively, with a single KB (Figure 17). However, with the increasing complexity of the CO, the time of creating the KB increases, the requirements for the computing resources of the processor on which the KB is created and the amount of memory of the system in which the KB is located increase.

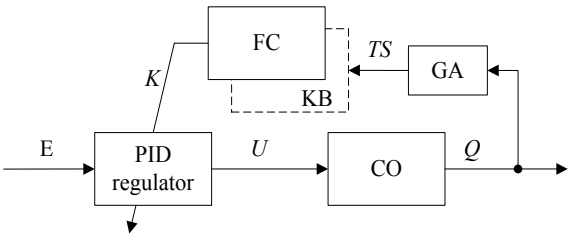

Figure 17. ICS based on KBO on soft computing with one FC

When the complexity of implementing a single KB is high, several KBs are created that are located in different FCs (Figure 18).

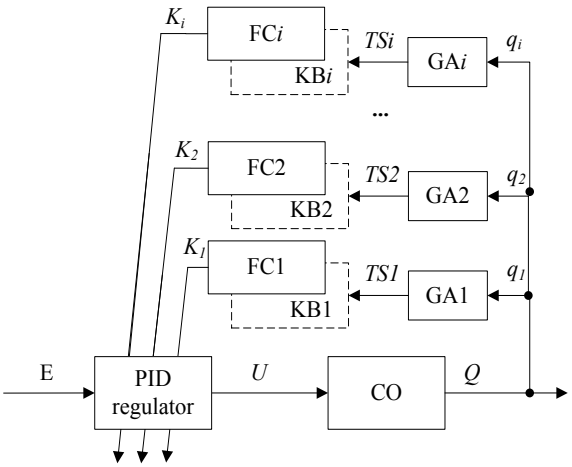

Figure 18. ICS based on KBO on soft computing with shared control

Separation of management somewhat reduces the quality of the system. However, the creation of several FCs is often the only way to organize intellectual management of complex CO.

Let us consider in more detail the process of creating a KB for ICS based on KBO on soft computing for a robot manipulator with 7 DOF.

Due to the complexity of the CO under consideration, the implementation of a single KB is impossible, therefore, we will initially organize a divided link management (one FC controls one link, as shown in Figure 19).

DOI: https://doi.org/10.30564/aia.v2i1.1339

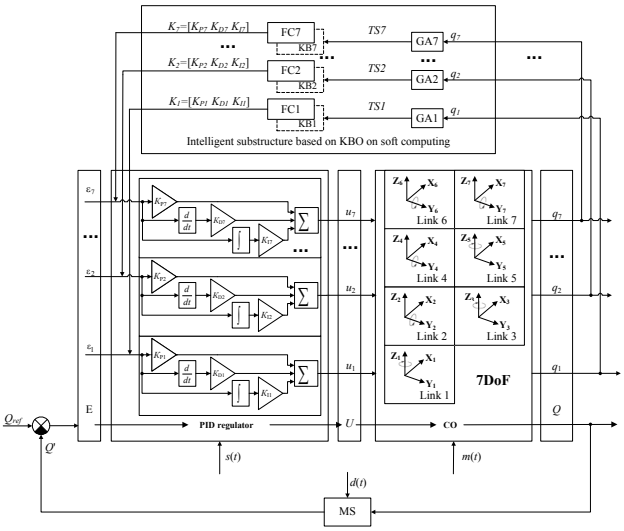

Figure 19. ICS 7DOF manipulator based on KBO on soft computing

In Figure 19: Q_{ref} is the reference signal, Q' is the measured variable, $E = [\varepsilon_1\ \varepsilon_2\ ...\ \varepsilon_7]$ is the control error, K is the matrix of proportional, differential and integral coefficients of the PID controller K_{Pi}, K_{Di}, K_{Ii}, $i = \overline{1,7}$, where i is the number of the corresponding link of the robot manipulator, $s(t)$ is the limitation of the control action, $U = [u_1\ u_2\ ...\ u_7]$ is the control action, $d(t)$ is delay in the Measuring System (MS), TS_i, $i = \overline{1,7}$ isTS of the corresponding FC, $m(t)$ is external environmental impact, $Q = [q_1\ q_2\ ...\ q_7]$ is adjustable value [30, 31].

The modeling of 7DOF manipulator control systems was carried out to study the quality of the considered control systems in the environment of MatLab/Simulink.

3.3. The model of Control Object

A formalized model of the 7DOF manipulator was built under the assumption that the links of the robot of the manipulator can rotate in the range of (-70 +70) degrees. The degree of freedom configuration corresponds to:

1 link) vertical axis of rotation α_{Z1};
2 link) transverse α_{Y2};
3 link) vertical α_{Z3};
4 link) transverse α_{Y4};
5 link) vertical α_{Z5};
6 link) transverse α_{Y6};
7 link) transverse α_{Y7}.

The CO model and formulas for determining the coordinates of the links of the manipulator were available in earlier works[32].

Creating a real CO model allowed accelerating the identification of the CO model, obtaining acceptable control parameters for different types of control systems and with a different level of intelligence.

To demonstrate the advantages and disadvantages of the considered types of control systems as applied to 7DOF manipulator, a series of experiments for MatLab/Simulink models was performed in this work.

Consider the test procedure order.

3.4. Test Procedure

A series of experiments is necessary to identify the advantages of various types of control systems of the 7DOF manipulator in both standard and unexpected control situations.

To test the robustness of control system models, a series of experiments is carried out, consisting of two stages: 1) work in standard control situations; 2) work in unexpected management situations.

As standard control situations, thirteen experiments are performed in accordance with the group of test points of the working space (Figure 20). The configuration is taken as the initial position of the manipulator: $Q = [q_1\ q_2\ q_3\ q_4\ q_5\ q_6\ q_7] = [0000000]\text{deg}$.

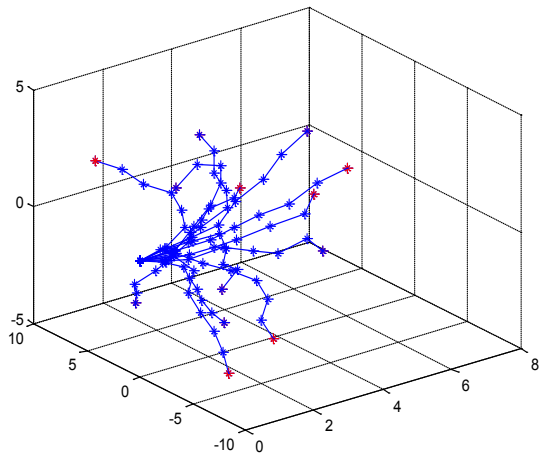

Figure 20. Test workspace

Unexpected situations are divided into external and internal. External unexpected situations:

1) forced change in the position of the links (Figure 21):

- the first link to a value of -30 degrees at the 25th iteration and to a value of 30 degrees at the 75th iteration;
- the second link to a value of -30 degrees at the 50th iteration and to a value of 30 degrees at the 100th iteration;
- the third link to a value of -30 degrees at the 50th iteration and to a value of 30 degrees at the 100th iteration;
- the fourth link to a value of -30 degrees at the 50th iteration and to a value of 30 degrees at the 100th iteration;
- the fifth link to a value of -30 degrees at the 50th iteration and to a value of 30 degrees at the 100th iteration;

 DOI: https://doi.org/10.30564/aia.v2i1.1339

- the sixth link to a value of -30 degrees at the 50th iteration and to a value of 30 degrees at the 100th iteration;
- the seventh link to a value of -30 degrees at the 50th iteration and to a value of 30 degrees at the 100th iteration;

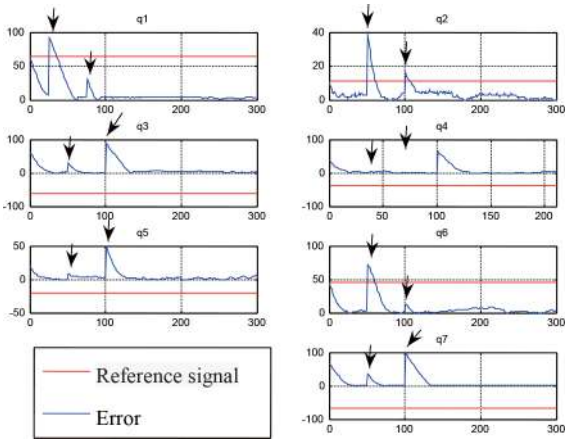

Figure 21. Forced change of links position

2) the initial conditions are changed

$$Q = [q_1; q_2; q_3; q_4; q_5; q_6; q_7] = [-30; -30; -30; -30; -30; -30; -30] \text{degrees};$$

3) at the same time a forced change in the positions of the links and a change in the initial conditions are carried out.

Each of the three external unexpected situations is tested at thirteen points of the test space; thus, 39 experiments are conducted for external contingency management situations.

Internal unexpected situations:

1) reduction of restrictions of control actions;

2) an increase in the limitations of control actions;

3) introduction of noise in the control channels (Figure 22);

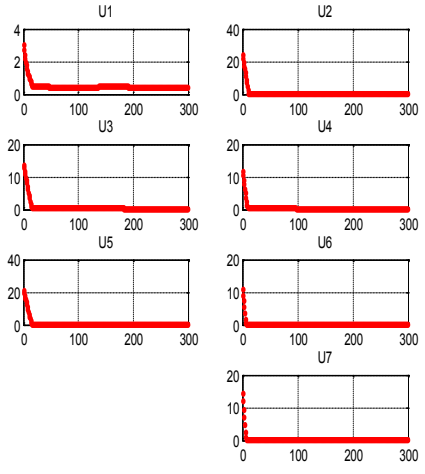

(a)

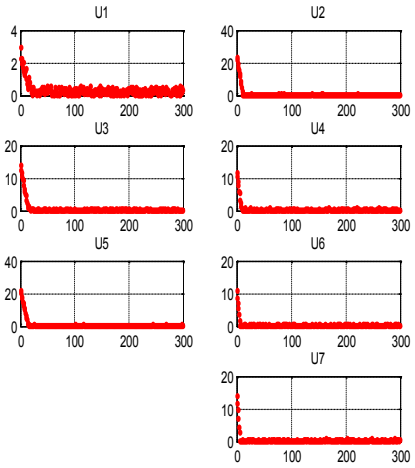

(b)

Figure 22. Control actions: initial (a); after making noise (b)

4) the introduction of errors in the MS (±1,5 degrees).

Each internal unexpected situation is tested at thirteen points of test space; thus, 52 experiments are conducted for internal unexpected control situations.

3.5. Definition of quality criteria

We introduce a system of quality criteria that takes into account methods of the theory of automatic control[28] to evaluate and compare the results of tests of control systems with constant PID regulator coefficients and ICS based on KBO on soft calculations.

These methods have been adapted for a specific CO 7DOF manipulator in the following form:

1. Position Task Solution in known control situations PTS_{KCS}.

The positioning problem is considered to be solved if, upon completion of a given number of iterations I_{max} = 300, the condition is satisfied:

$$\begin{cases} PTS = 1, if \left|q_{1ref} - q_1\right| + \left|q_{2ref} - q_2\right| + ... + \left|q_{7ref} - q_7\right| \le 2 \deg \\ PTS = 0, else \end{cases},$$

where $q_{1ref}, q_{2ref}, \dots, q_{7ref}$ are the desired positions of the links, $q_1, q_2, \dots, q_7$ are the current positions of links

$$PTS \text{ implementation} \equiv \frac{\sum_{i=1}^{N} PTS}{N},$$

where N is the number of experiments.

2. Position Task Solution in the external above considered control situations PTS_{ACCS1}.

3. Position Task Solution in the internal above consid-

DOI: https://doi.org/10.30564/aia.v2i1.1339

ered control situations PTS_{ACCS2}.

4. Performance I_T

The number of iterations from the beginning of the impact during which each of the links is positioned with an allowable error $2\Delta < 1\deg$:

$$I_T = I\Big|_{\left(\left|q_{1ref}-q_1\right|<1\deg\right)\cap\left(\left|q_{2ref}-q_2\right|<1\deg\right)\cap\ldots\cap\left(\left|q_{7ref}-q_7\right|<1\deg\right)},$$

$$I_T \text{ implementation} \equiv 1-\frac{\sum_{i=1}^{N} I_T}{NI_{\max}}.$$

5. Relative overshoot value σ

The ratio of the maximum deviation of the current position of the link from the steady-state value to the steady-state value:

$$\sigma = \max\left[\max\left|\frac{q_{1ref}-q_1}{q_{1ref}}\right| \max\left|\frac{q_{2ref}-q_2}{q_{2ref}}\right| \ldots \max\left|\frac{q_{7ref}-q_7}{q_{7ref}}\right|\right],$$

$$\sigma \text{ implementation} \equiv 1-\frac{\sum_{i=1}^{N}\sigma}{N}.$$

6. Relative error in link positioning after completion of a given number of iterations ε

$$\begin{cases} \text{å}=\left|\frac{q_{1ref}-q_1}{q_{1ref}}\right|, f\ \left(\left|q_{1ref}-q_1\right|>\left|q_{2ref}-q_2\right|\right)\cap\left(\left|q_{1ref}-q_1\right|>\left|q_{3ref}-q_3\right|\right)\cap\ldots\cap\left(\left|q_{1ref}-q_1\right|>\left|q_{7ref}-q_7\right|\right) \\ \text{å}=\left|\frac{q_{2ref}-q_2}{q_{2ref}}\right|, f\ \left(\left|q_{2ref}-q_2\right|>\left|q_{1ref}-q_1\right|\right)\cap\left(\left|q_{2ref}-q_2\right|>\left|q_{3ref}-q_3\right|\right)\cap\ldots\cap\left(\left|q_{2ref}-q_2\right|>\left|q_{7ref}-q_7\right|\right) \\ \ldots \\ \text{å}=\left|\frac{q_{7ref}-q_7}{q_{7ref}}\right|, f\ \left(\left|q_{7ref}-q_7\right|>\left|q_{1ref}-q_1\right|\right)\cap\left(\left|q_{7ref}-q_7\right|>\left|q_{2ref}-q_2\right|\right)\cap\ldots\cap\left(\left|q_{7ref}-q_7\right|>\left|q_{6ref}-q_6\right|\right) \end{cases},$$

$$\varepsilon \text{ implementation} \equiv 1-\frac{\sum_{i=1}^{N}\varepsilon}{N}.$$

7. One iteration time t

Execution time of one iteration I:

$$t \text{ implementation} \equiv 1-\frac{t}{t_{const}}, t < t_{const}.$$

8. Implementation complexity P

Evaluation of changes in control coefficients:

$$P \text{ implementation} \equiv 1-\frac{\sqrt{\frac{1}{N}\int_{i=1}^{N}\left(\frac{dK}{dt}\right)^2 dt}}{\max(K)}.$$

9. Full Control Behavior FCB

$$FCB \equiv w_1\cdot P\left[PTS_{KCS}\right]+w_2\cdot P\left[PTS_{ACCS1}\right]+w_3\cdot P\left[PTS_{ACCS2}\right]+w_4\cdot P\left[I_T\right]+ \\ +w_5\cdot P[\sigma]+w_6\cdot P[\varepsilon]+w_7\cdot P[t]+w_8\cdot P,$$

where $w=[0{,}1\ \ 0{,}2\ \ 0{,}2\ \ 0{,}2\ \ 0{,}05\ \ 0{,}1\ \ 0{,}1\ \ 0{,}05]$ are weights.

3.6. PID Constant Control Systems

The control task is reduced to finding the coefficients of the PID controller $K_P, K_D, K_I, i=\overline{1,7}$, which ensures the desired nature of the movement of the manipulator. In this section, we consider two types of control systems with constant coefficients: a control system on a PID controller and based on GA.

A comparison of the operation of 7DOF manipulator ACS based on the PID controller and based on GA in accordance with the introduced system of quality criteria is given in Table 2, and in Figure 23.

Table 2. Comparison of the operation of control systems with constant coefficient

Quality Criteria		based on PID	based on GA
1	PTS_{KCS}.	0,000	0,615
2	PTS_{ACCS1}.	0,000	0,256
3	PTS_{ACCS2}.	0,058	0,308
4	I_T	0,000	0,008
5	σ	0,892	0,956
6	ε	0,379	0,657
7	t	0,998	0,998
8	P	1,000	1,000
9	FCB	0,244	0,439

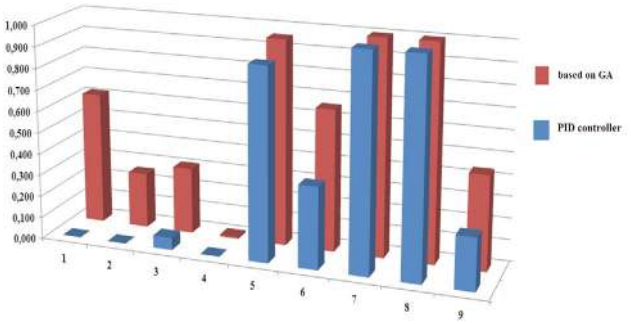

Figure 23. Comparison of the results of MatLab/Simulink control systems models based on the PID controller and with the use of GA

From the results of comparing control systems on PID controller and using the GA, we conclude:

1) applying the control system based on PID controller,

 DOI: https://doi.org/10.30564/aia.v2i1.1339

the positioning task was not solved in normal situations and external unexpected control situations, insignificant positive results (3/52 experiments) were obtained for internal unexpected control situations;

2) some improvement is achieved by using a control system based on GA: the positioning problem is solved in standard control situations in most experiments, but in unexpected control situations (external and internal), the solution is achieved in less than a third of the experiments;

3) both systems with constant PID controller coefficients have low speed;

4) applying the control system based on the GA, the relative values of overshoot and positioning errors are significantly improved compared to the control system on the PID controller;

5) applying the control system based on the GA, the Full Control Behavior in comparison with the control system on the PID controller improves.

In Figure 24 demonstrates the operation of the manipulator when using control systems on the PID controller and using the GA in the conditions of the third external unexpected control situation (the initial position has been changed and the links are forced to move at different times). In this experiment, the control system based on GA solves the control problem, unlike to the control system on the PID controller.

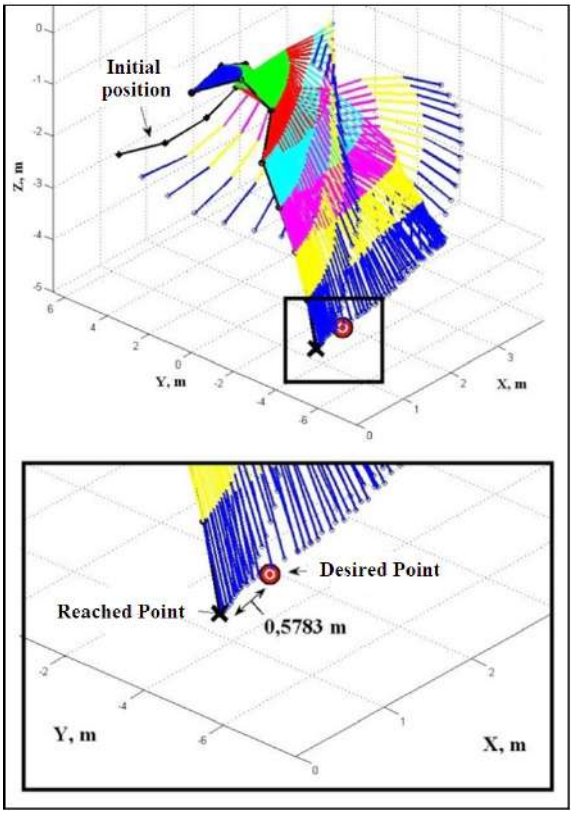

(a)

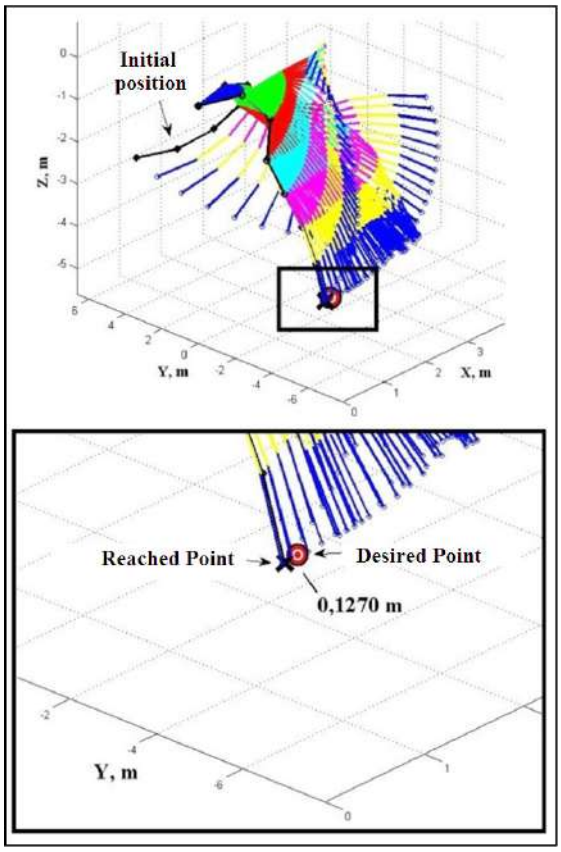

(b)

Figure 24. The movement of the manipulator in an external unexpected situation: ACS based on PID controller (a); GA control systems (b)

Despite the fact that the control system on the GA significantly improves the assessment of quality criteria compared to the ACS on the PID controller, the overall quality of control provided by the control system on the GA is rather low.

In the process of control, the PID controller coefficients for the considered structures do not change. This simplifies the control system design, but at the same time deprives the control system of the possibility of rebuilding and adaptation.

Next, we consider a structure with dynamic adaptation of the PID controller coefficients, implemented on the basis of soft computing technologies.

3.7. Quality of Control System based on Soft Computing Technologies

Testing of the obtained KB1 - KB7, respectively, FC1 - FC7 is carried out as part of the ICS based on soft computing.

The results of ICS based on soft computing tests and control systems with constant coefficients (based on the PID controller and using GA) in accordance with the introduced quality criteria are shown in Table 3 and in Figure 25.

DOI: https://doi.org/10.30564/aia.v2i1.1339

Table 3. Results comparison of the of control systems with constant coefficients and ICS based on KBO on soft computing

Quality Criteria		ICS based on soft computing	based on GA	based on PID
1	PTS_{KCS}.	0,923	0,615	0,000
2	PTS_{ACCS1}.	0,744	0,256	0,000
3	PTS_{ACCS2}.	0,923	0,308	0,058
4	I_T	0,092	0,008	0,000
5	σ	0,969	0,956	0,892
6	ε	0,911	0,657	0,379
7	t	0,973	0,998	0,998
8	P	0,946	1,000	1,000
9	FCB	0,728	0,439	0,244

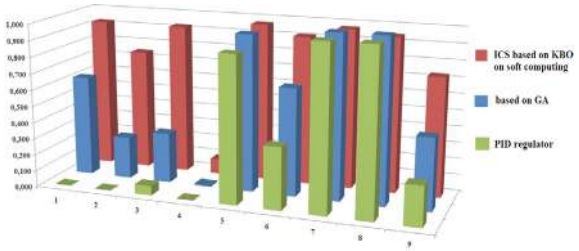

Figure 25. Comparison of the work of MatLab/Simulink ICS models based on KBO on soft computing and control systems with constant coefficients

From the results of the comparison of control systems (ICS based on soft computing, based on the PID controller and using GA) we conclude that when using the ICS based on soft computing:

1) the quality criterion position task solution in known control situations has increased compared to control systems with constant coefficients (based on the PID and using GA), the solution is positive in 12 out of 13 experiments;

2) the position task solution in the unexpected considered control situations has increased significantly compared to control systems with constant coefficients: 2,9 times for external unexpected situations and 3 times for internal unexpected situations (in comparison with the ICS based on GA);

3) the performance has increased significantly: more than 10 times in comparison with the ICS based on GA; however, as before, the performance is rather low;

4) the quality criterions relative overshoot value and relative error in link positioning improved compared to control systems with constant coefficients; but criterions one iteration time and implementation complexity have deteriorated somewhat;

5) the full control behavior is improved 1,7 times compared with the control system using GA and 3 times compared with the PID controller based control system.

In Figure 26 demonstrates the operation of the manipulator when using a control system based on GA and ICS based on KBO on soft computing in the conditions of the first external unexpected control situation (the links are forced to move at different points in time).

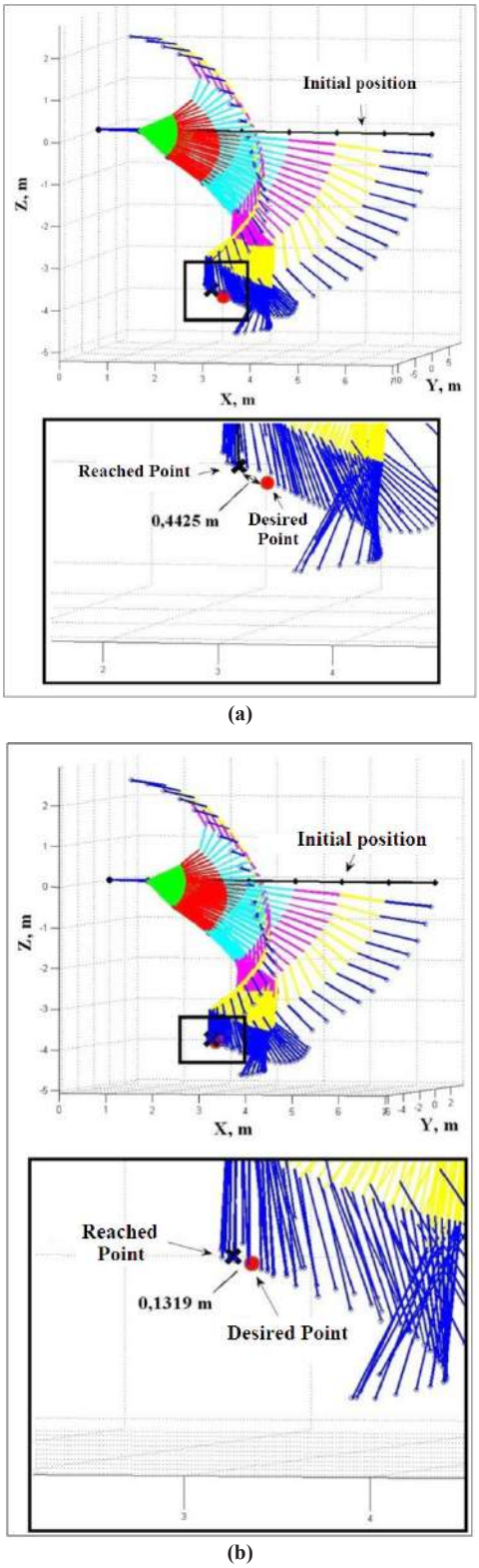

Figure 26. The movement of the manipulator in an external unexpected situation: the result of the control system based on the GA (a); ICS based on KBO on soft computing (b)

 DOI: https://doi.org/10.30564/aia.v2i1.1339

In Figure 27 shows the operation of the manipulator when using a control system based on GA and ICS based on KBO on soft computing in the conditions of the fourth internal unexpected control situation (introducing errors into the MS).

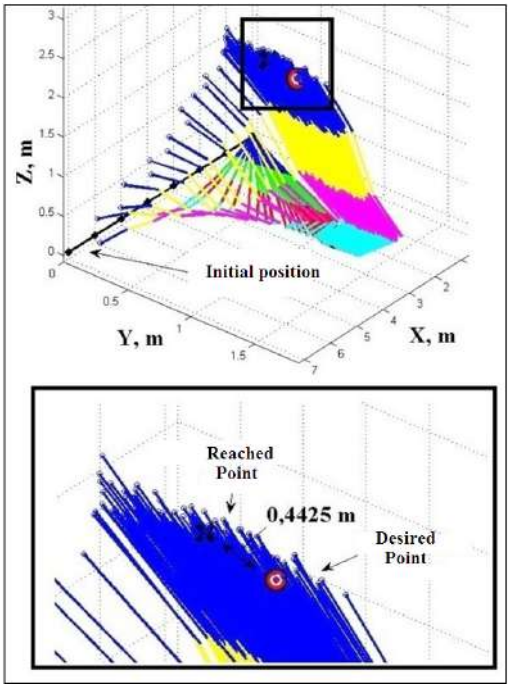

(a)

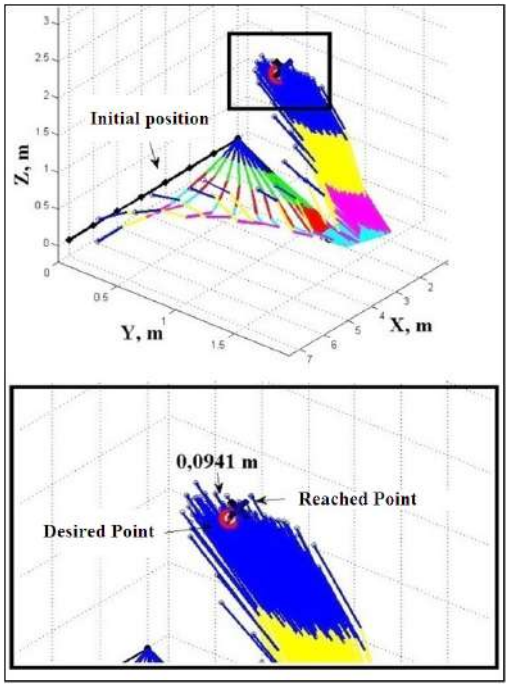

(b)

Figure 27. The movement of the manipulator in an internal unexpected situation: the result of the control system based on the GA (a); ICS based on KBO on soft computing (b)

In Figure 28 shows a comparison of phase portraits when using a control system based on GA and ICS on KBO on soft computing for the considered control situation.

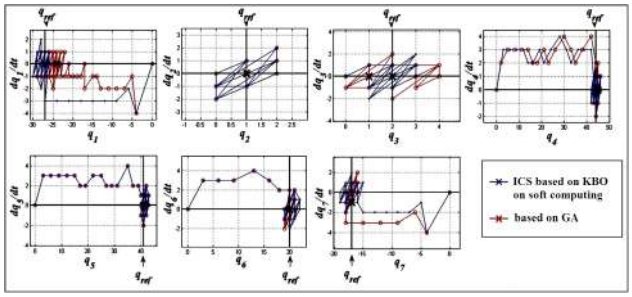

Figure 28. Changing the position of the links of the manipulator in the conditions of an internal unexpected situation: control systems based on GA and ICS based on KBO on soft computing.

The ICS by the 7DOF manipulator based on KBO on soft computing significantly improves the quality of control compared to control systems with constant coefficients (based on the PID controller and using the GA), however, the performance indicator remains at a fairly low level.

The ICS based on KBO on soft computing was organized with a separation of control: each link of the manipulator corresponds to one independent FC due to the fact that the CO is complex. Decomposition of control leads to a mismatch of work and some decrease in the quality of management.

It is possible to organize coordination control without significantly increasing the complexity of the system by introducing additional generalizing superstructure, the implementation of which is possible using quantum computing technologies, which will be discussed in the next part of the article.

Next, we consider a simpler example of an CO: this is a 3DOF robot manipulator, often used both in industry and in training.

4. 3DOF Manipulator control systems

The robot control systems for the 3DOF manipulator will be considered both at the simulation level and at the physical level. To demonstrate the quality of control systems, a test bench of 3DOF robot manipulator was developed.

4.1. Description of the 3DOF Manipulator Test Bench

In Figure 29 shows the test bench used to test control systems.

DOI: https://doi.org/10.30564/aia.v2i1.1339

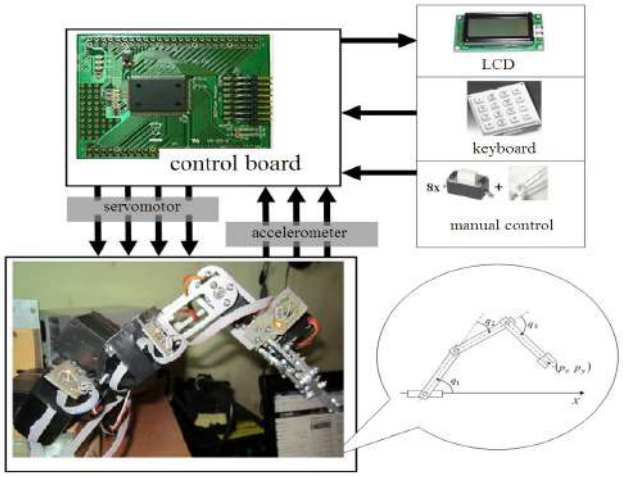

Figure 29. The manipulator test bench

As the MS (accelerometer on Figure 14), the board uses three boards with accelerometer installed on them with 3DOF ADXL335. The Renesas microcontroller is the core of the system (control board on Figure 14). Information about the current positions of the links and the characteristics of the quality of control is displayed on the LCD and serial interface. Both automatic and manual control modes are supported (the ability to move each of the 3 links and the manipulator's grip device using the manual control buttons). In robotics, as a rule, a mathematical model of the manipulator is built, simulation of the CO, identification of the parameters of the mathematical model, and then comparison of the simulation results on the mathematical model of the CO and a test bench robot manipulator are performed[27, 28]. In contrast to the traditional approach, in this case, the behavior of the links of the robot test bench was formalized by the correspondence tables "width of the servo drive control pulse ~ angle of movement", which allowed us to describe the behavior of the test bench in the MatLab/Simulink environment. The manipulator test bench was created without involving the mathematical model.

The creation of a formalized manipulator model allowed accelerating the identification of the CO model and obtaining acceptable control parameters.

4.2. Management Tasks

We examine the direct circuit of the control loop by the 3DOF manipulator to explain the operation of the PID controller.

In Figure 30: $E = [\varepsilon_1\ \varepsilon_2\ \varepsilon_3]$ is a control error, $K_{Pi}, K_{Di}, K_{Ii},\ i = \overline{1,3}$ is the proportional, differential and integral coefficients of the PID controller, i is the number of the corresponding link of the robot manipulator, $U = [u_1\ u_2\ u_3]$ is the control action, $Q = [q_1\ q_2\ q_3]$ is an adjustable value[30].

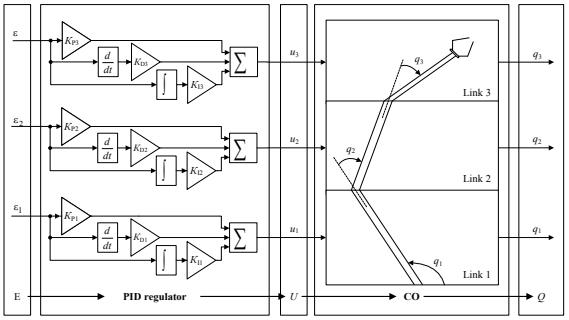

Figure 30. Direct circuit of control system with PID controller

The control task is reduced to finding the coefficients of the PID controller $K_{Pi}, K_{Di}, K_{Ii},\ i = \overline{1,3}$, which ensures the desired movement.

4.3. Test Procedure

A series of experiments is carried out for each of the considered types of control systems: based on GA, ICS based on KBO on soft computing with one FC and ICS based on soft computing with separated control.

A series of experiments is carried out in standard and unexpectedcontrol situations and is evaluated according to the quality criteria introduced above. As standard control situations, ten experiments are performed in accordance with a group of workspace test points (Figure 31).

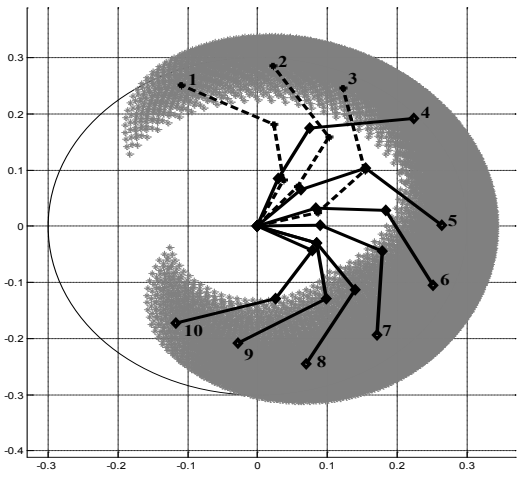

Figure 31. Test points

Configuration $Q = [q_1; q_2; q_3] = [60;\ 0;\ 0]$ degrees taken as the initial position of the manipulator.

Three cases act as unexpected control situations:

1) the position of the second link is changed to a value $q_2 = 45$ degrees at the 11th iteration;

2) initial conditions are changed

 DOI: https://doi.org/10.30564/aia.v2i1.1339

$Q = [q_1; q_2; q_3] = [60;\ 45;\ -43]$ degrees;

3) the initial conditions are changed $Q = [q_1; q_2; q_3] = [60;\ 45;\ -43]$ degrees: and the position of the second link is changed to the value $q_2 = 45$ degrees at the 11th iteration.

Three unexpected situations are tested at ten points in the test space. Thus, 30 experiments are conducted for unexpected control situations.

Consider the features of the design of ICS based on KBO on soft computing for 3DOF robot manipulator.

4.4. ICS based on SCOptKB™

FC with a built-in KB that controls the gain of the PID controller is the main elements of the ICS based on soft computing technologies. Implementation of the ICS based on KBO on soft computing for a 3DOF robot manipulator is possible both with one FC and with separated control.

Let us consider the process of creating KB for ICS based on KBO on soft computing.

1. Creating TS. Define a typical control situation. As typical control situations, we will consider standard control situations.

Three of the standard experiments were used to create TS1, TS2 and TS3, for which control situations in which the parameters of the PID controller were determined using GA were reproduced using MatLab/Simulink models.

The considered TS1-TS3 are tables where columns 1-9 are input values [errP1, errD1, errI1, errP2, errD2, errI2, errP3, errD3, errI3], and columns 10-18 are output values [KP1, KD1, KI1, KP2, KD2, KI2, KP3, KD3, KI3].

Input values are vectors of input variables of proportional, differential and integral errors of the first, second and third links of the manipulator. The output values are the vectors of the output of certain GA variables of proportional, differential and integral coefficients of the PID controller of the first, second and third links of the manipulator.

The final TS used to obtain the KB consists of sequentially connected TS1, TS2 and TS3.

2. Definition of a fuzzy inference model.

The following parameters must be defined:

1) type of fuzzy model: Sugeno 0 (zero order);

2) interpretation of fuzzy operations: fuzzy conjunction as a product;

3) the number of input and output variables: 9 and 9.

3. Creating linguistic variables for input values.

The optimal number and form of MFs are determined using the GA from the KBO software.

At the first stage of creating the KB, we set the task of creating five MFs for each of the nine input variables, i.e. the vector [n1 n2 n3 n4 n5 n6 n7 n8 n9] = [5 5 5 5 5 5 5 5 5], which would lead to the creation of n1 × n2 × n3 × n4 × n5 × n6 × n7 × n8 × n9 = 1953125 fuzzy rules. At the second stage, as a result of the GA operation, the vector [n1 n2 n3 n4 n5 n6 n7 n8 n9] took the value [4 4 4 4 3 4 4 3 3], and the maximum number of fuzzy rules was 110592.

4. Creating a rule base.

As a result of the work, the algorithm for selecting rules (passing the specified activation threshold) selected 33 of the most robust rules out of 110592.

5. Setting up the rule base and optimization of the left and right parts of the rules of the KB.

The traditional method of error back propagating is used at this stage.

In the considered example, the maximum number of fuzzy rules for 3-4 MFs was 110592 rules. We calculate the maximum number of fuzzy rules for 3,4,5,6 and 7 MFs for each input variable. Then the dependence of the maximum number of fuzzy rules on the number of degrees of freedom of the manipulator has the form shown in Figure 32.

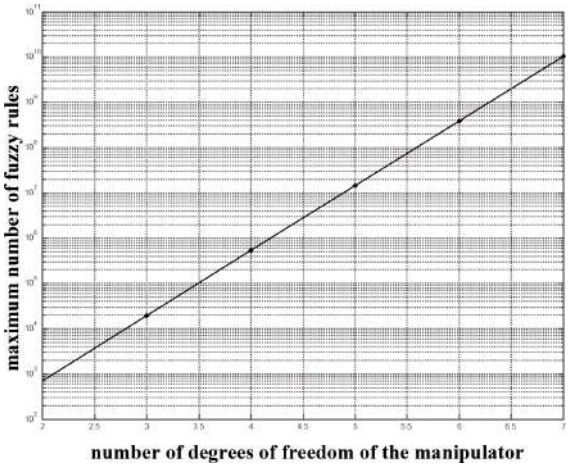

Figure 32. The dependence of the maximum number of fuzzy rules on the number of degrees of freedom of the manipulator

The introduction of additional links, the expansion of the functions of existing units, or the addition of other devices requiring coordination control will increase the maximum number of fuzzy rules by more than one and a half orders of magnitude. As a result, the complexity and time of creating KB will increase, the requirements for the computing resources of the processor and the memory capacity of the system in which the KB is located will also increase.

If it is difficult to implement a single KB, we will divide the KB into several, and use several FCs.

Consider the separation of control, in which one FC controls one link of the manipulator.

It is necessary to create 3 KBs for 3 FC respectively. The number of input and output variables for each of the KBs will decrease 3 times, and the maximum number of

DOI: https://doi.org/10.30564/aia.v2i1.1339

fuzzy rules will decrease.

Let us consider the process of creating KB

1. Creating TS.

We created 3 TSs for 3 KBs. Each of the TS, consists of two TSs based on two different experiments.

TS1, TS 2 and TS 3 for creating 3 independent KSs contain a vector of input variables in the left columns, and vectors of output variables of certain GAs in the right columns. Input variables are proportional, differential and integral errors ([errP1, errD1, errI1], [errP2, errD2, errI2] and [errP3, errD3, errI3] for the first, second and third links of the manipulator. Output variables are proportional, differential and integral coefficients of the PID controller [KP1, KD1, KI1], [KP2, KD2, KI2] and [KP3, KD3, KI3] for the first, second and third links of the manipulator.

2. Definition of a fuzzy inference model.

The following parameters must be defined for each of KB:

1) type of fuzzy model: Sugeno 0;

2) interpretation of fuzzy operations: fuzzy conjunction as a product;

3) the number of input and output variables: 3 and 3.

3. Creating linguistic variables for input values.

The optimal number and form of MFs are determined using the GA1 from the KBO software.

The number of functions during the creation of KB1, KB 2 and KB 3 and optimization of GA1 was [3 3 5], [5 5 9] and [7 7 8], the number of fuzzy rules corresponds to 45, 225 and 392.

4. Creating a rule base.

18 out of 45 rules were selected for KB1, 26 out of 225 rules were selected for KB2, 48 out of 392 rules were selected for KB3.

The maximum number of fuzzy rules when creating single KB with one FC was 110592, of which 33 most robust ones were selected. The maximum number of rules in the case of separated control is 392 for KB3, which significantly reduces the time for selecting the most robust rules.

However, the total number of selected rules 18 + 26 + 48 = 92 is more than 2 times higher than the number of selected rules when using one FC.

Consequently, the placement of the final KBs when using the ICS based on soft computing with separate control will require a larger amount of memory of the final device in which the control system is located.

5. Setting up the rule base and optimization of the left and right parts of the rules of the KB.

The traditional method of error back propagating is used at this stage.

4.5. Modeling and test bench: control quality

In Figure 33 and Figure 34 show a comparison of control quality criteria for a control system based on GA, ICS based on KBO on soft computing with one FC and ICS based on soft computing with separated control for MatLab/Simulink models and the robot manipulator test bench.

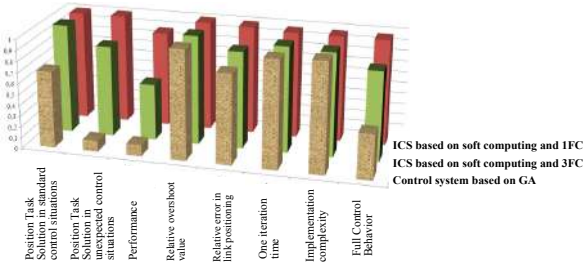

Figure 33. Comparison of quality criteria for a control system based on GA, ICS based on KBO on soft computing with one FC and ICS based on soft computing with separated control for MatLab/Simulink models

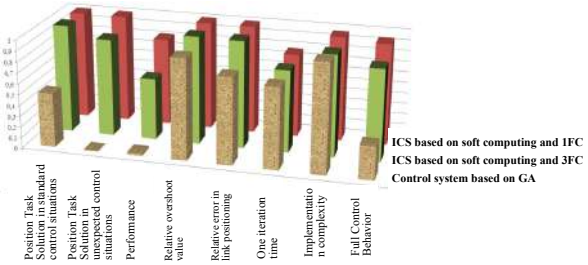

Figure 34. Comparison of quality criteria for a control system based on GA, ICS based on KBO on soft computing with one FC and ICS based on soft computing with separated control for the robot manipulator test bench

It can be seen from the comparison results that the use of the control system based on GA solves the problem of accurate positioning in half of the standard situations. The control system based on GA does not provide guaranteed control in unexpected control situations (as shown in Figure 35). The full control behavior is rather low. In Figure 35 shows the movement of the manipulator in an external unexpected situation.

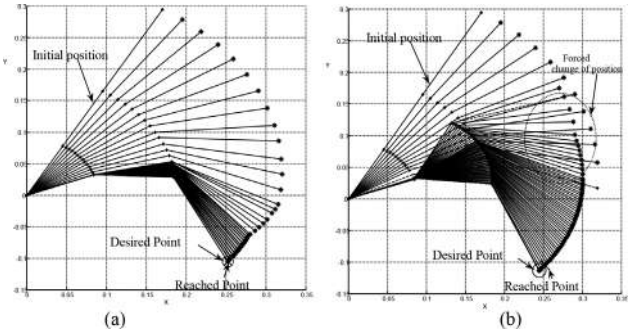

Figure 35. The operation of the control system based on GA: in a standard control situation (a); in an unexpected control situation (b)

 DOI: https://doi.org/10.30564/aia.v2i1.1339

The coefficients of the PID controller in the control system based on GA do not change. This facilitates the design of the control system, but deprives the control system of the possibility of rebuilding and adaptation.

In Figure 36 shows the work of the ICS based on KBO on soft computing with one FC and separated control in an unexpected control situation, previously proposed for a control system based on GA (Figure 35).

From Figure 35 and Figure 36, we conclude that both of ICS based on the KBO using soft computing technologies, in contrast to the control system based on GA, solve the problem of accurate positioning. ICS using a single KB provides a solution for fewer iterations than the structure of ICS with separated control.

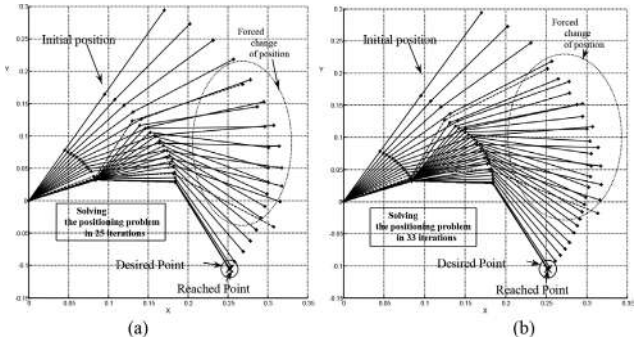

Figure 36. The operation of the ICS based on KBO on soft computing with one FC in an unexpected control situation (a); ICS based on soft computing with separated control (b)

The use of ICS based on KBO on soft computing with one FC allows:

1) to obtain maximum of quality criteria position task solution in standard and unexpected control situations;

2) to improve all quality criteria, except for the one iteration time and the implementation complexity, because dynamic adjustment of coefficients requires additional calculations;

ICS based on KBO on soft computing with one FC allows you to collect in a single KB information on the mutual behavior of 3 links of the robot manipulator at the same time, however, the high complexity of the implemented KB requires significant computational resources to create and placement.

Dividing of the control link into 3 independent FCs (one KB controls one link) allows, due to a certain decrease in the quality of management, to significantly simplify the processes of creating, optimizing and placing the KB.

It can be seen from the comparison results that when using the ICS based on KBO on soft computing with divided control with 3 FCs, all quality indicators are somewhat deteriorated, which occurs as a result of the mismatch of the work of the separated independent KBs.

4.6. Control actions

Consider the control actions generated by the considered types of control systems. In Figure 37 shows the control actions generated by the control system based on GA, ICS based on KBO on soft computing with one FC and ICS on soft computing with separated control. In Figure 37 *GA* is the signal generated by the control system based on the GA, FC is the signal generated by the ICS based on KBO on soft computing with one FC, *FC Decomposition* is the signal formed by the ICS on soft computing with separated control.

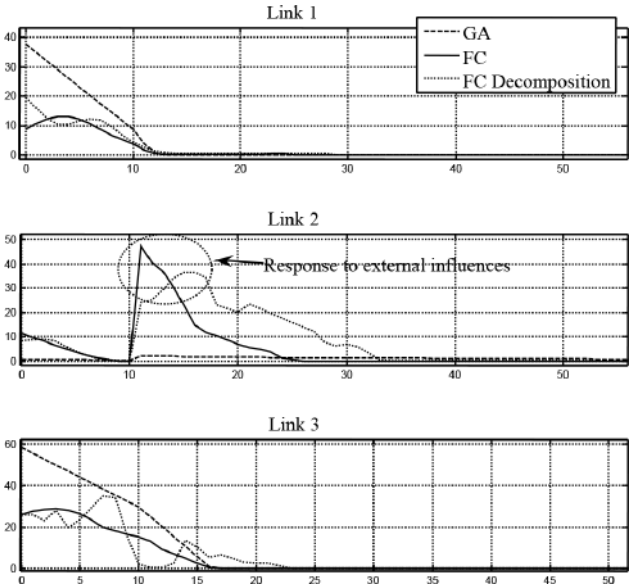

Figure 37. Control signals generated by the control system based on GA, ICS based on KBO on soft computing with one FC and ICS on soft computing with separated control

From Figure 37 it can be seen that the control signals generated by the control system based on the GA for the first and third links have a large amplitude compared to similar control signals generated by the ICS based on KBS on soft computing. For the second link in the control signal, formed by the control system based on GA, the reaction to external influence is not sufficiently reflected, as a result of which the task of precise positioning is not solved. The control signals generated by ICS based on KBO on soft computing with separate control, compared with ICS on KBO on soft computing with one FC, with a comparable amplitude, have greater overshoot.

Thus, the minimum consumption of useful resource in the formation of control signals is ensured when using the ICS based on KBO on soft computing with one FC.

DOI: https://doi.org/10.30564/aia.v2i1.1339

5. Conclusion

To control robots with manipulators of varying complexity, the following were considered:

1) control systems with constant coefficients of the PID controller;

2) control systems with adjustable PID controller coefficients depending on the situation.

It has been shown that:

1. Control systems with constant coefficients based on GA are attractive because of the simplicity of implementation, however, due to the constancy of control parameters, the solution of the problem of accurate positioning is possible only for regular situations.

2. The unified KB of the ICS based on KBO on soft computing with one FC contains the most complete information about the behavior of all links, which allows the ICS to work both in standard and unexpected control situations. However, the creation of a single KB is a complex and long temporal process that requires significant computing resources. So, the implementation of a single KB for the complex CO 7DOF robot manipulator is not possible.

3. The decomposition of the control in the structure of the ICS based on KBS on soft computing with separate control, due to a slight decrease in the quality of control due to the mismatch of the behavior of the links as a result of the independence of the creation and functioning of the KBs, can significantly simplify the processes of creating and placing the KB.

4. Computational intelligence toolkit SCOptKB™ realized deep machine learning with optimal structure of FNN and reduce redundant information in production logical rules of robust KB.

In the next Part II, to eliminate the mismatch of the work of the separated independent KBs, the method of organizing coordination control using quantum computing technologies to create robust ICS 3DOF and 7DOF manipulators will be considered [33].

Appendix: Soft Computing Optimizer toolkit

ICS based on new types of computation (soft and quantum computing) have the following advantages:

• maintain basic advantages of conventional, classical, control systems such as controllability and stability;

• have optimal (from a given criteria of control quality) KB;

• guarantee the achievement of the given control quality on the base of designed KB;

• have the property of robustness. It means that ISC allows to maintain the given control quality in the case of unexpected control situations.

A1. Peculiarities of the information technology for intelligent control system design based on Soft Computing Optimizer toolkit

For design of robust KBs of FC we developed the new program toolkit called *Soft Computing Optimizer* based on soft computing. SCO allows to design smart control systems with needed level of robustness.

Discuss the peculiarities of SCO and developed information technology.

We use *Genetic Algorithms* (GA) to find an optimal control signal and construct *teaching control signal* (TS). By using different GA fitness functions describing information-thermodynamic and control criteria and mathematical (or physical) model of CO we extract objective knowledge about control laws independent from human-expert. Processing of obtained TS is based on SCO with new types of computing. It allows us to design KB FC with a needed level of intelligence that supplies the needed level of robustness. Main components of SCO are the different GA structures with different constrains and fitness functions. Mutual actions of these components supply extraction, processing and design of KB, that is the main problem of Artificial Intelligence.

As summary list main factors of the information technology for ICS design: if we want to add to the known criteria stability and controllability a new one, we must use new types of computing.

New criterion of control quality *robustness* is introduced:

• Combined principle of control (*global negative back relation principle + global intelligent back relation principle*) allows us don't destroy the lowest control level (PID) and use the high level of control with the corresponding level of intelligence.

Introduction of *global intelligent back relation principle* allows realizing three steps of knowledge processing: extract information from dynamic behavior CO with PID control; use GA to construct *teaching control signal*; use a set of GA to design KB and optimize it.

By SCO we can design the given level of intelligence of control system and, hence, the given level of robustness.

A2. Main steps of the information technology for intelligent control system design based on Soft Computing Optimizer toolkit

Main steps of the information technology for ICS design based on SCO toolkit are shown on Figure A1.

 DOI: https://doi.org/10.30564/aia.v2i1.1339

Remark. Step 4 on Figure A1 is not considered in this Appendix. It is realized by SCO on quantum computing.

A2.1 Extraction, processing and design of objective knowledge based on stochastic simulation and soft computing

Describe main steps of developed KB FC design technology. At first consider briefly steps 1 - 3 (Figure A1), and then consider one example of KB FC design for the chosen dynamic CO.

The KB design process can be realized by the following steps.

Step 0. In this step one or a few typical *teaching situations* are defined. Here the following factors are described: parameters of the mathematical (or physical) model of CO; initial conditions; reference signal (a goal of control); external stochastic noise; presence/absence of time delay in the channel of CO state measurement and so on.

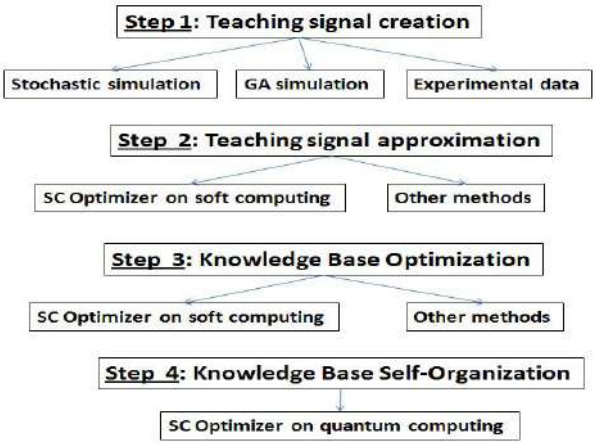

Figure A1. Main steps of the information technology for ICS design

Step1. Stochastic simulation system for teaching control signal design

For robust KBs design we will use *stochastic simulation system* in order to find robust teaching control signal.

Stochastic simulation is based on information extraction process by investigation of individual trajectories of dynamic object behavior under influence of stochastic noises acting on the object.

Stochastic noises simulation is considered as a random noises simulation with needed probability density function. Random noises simulation is realized by the method of forming filter on the base of Fokker-Planck-Kolmogorov equations[17] (see Appendix 2 to this Chapter 1).

S*tochastic simulation system* uses CO model with simulated stochastic noises and GA with a chosen fitness function. By using GA, we obtain a set of optimal control values, which minimize the selected physical characteristics of the stochastic model of CO. One of the characteristics can be control error, or the minimum entropy production rate of the control system and of the CO. In some complicated cases, the fitness function may include a weighted sum of different motion characteristics of the CO like accelerations, velocities, spectral characteristics. Thus, the resulted motion under control will tend to reduce all of them simultaneously. At this stage of simulation, we conduct simulation with the following aims:

• investigation free motion of CO in order to determine type of dynamic behavior, stable or locally/globally unstable motion,

• investigation an influence of different types of stochastic excitations on dynamic behavior and control laws,

• investigation an influence of type of traditional controllers (PID, PD, P) on type of control laws in a fuzzy control,

• investigation an influence of different GA fitness functions on type of control laws,

• comparison control quality of traditional PID control with *constant* gains and GA-PID control with *variable* gains obtained by GA,

• choice the best GA solution and designing a *teaching control signal* (TS) for the next steps of technology.

The general structure of stochastic simulation system is shown on Figure A2. On the figure the main factors that influent on the control accuracy are shown. They are: a presence of stochastic noises (as external and internal), a presence of time delay in the channel of CO state measurement, a presence of stochastic noises in the channel of CO state measurement. Moreover, we must consider also such factors as incompleteness of CO model, incorrectness of model parameters and so on.

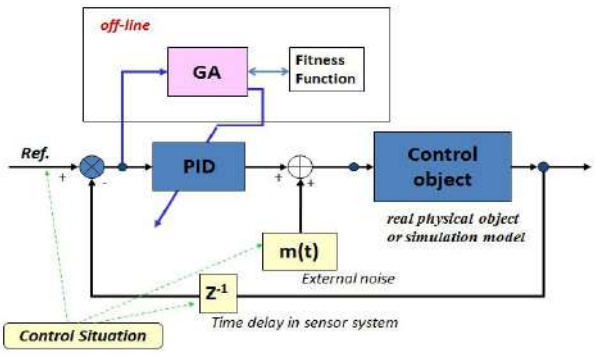

Figure A2. The general structure of stochastic simulation system

At the stage of GA based TS creation, we find a solution $\{K_p(t), K_d(t), K_i(t)\}$ close to a global optimum. The output of GA is TS (or training patterns) representing a table of 'in-out' patterns as fol-

DOI: https://doi.org/10.30564/aia.v2i1.1339

lows: $\{E(t_i)\}$, $\{K(t_i)\}$, $i=1,...,n$, where $E(t_i)=\{e(t_i),\ \dot{e}(t_i),\ \int e(t_i)dt_i\}$ is vector, containing control error, its derivative and integral parts correspondingly, and $K(t_i)=\{K_P(t_i),\ K_D(t_i),\ K_I(t_i)\}$ are PID gains at time moments t_i.

SC Optimizer has tools to create TS using genetic optimization and Matlab model of control system (or physical model). This step is realized by the button "create signal". On Figure A3 the main menu SCO and GA parameters window is shown.

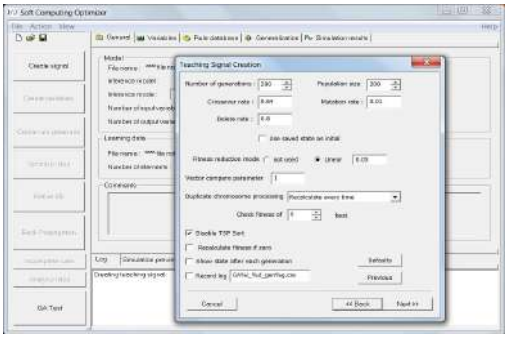

Figure A3. Main menu SCO and GA parameters window

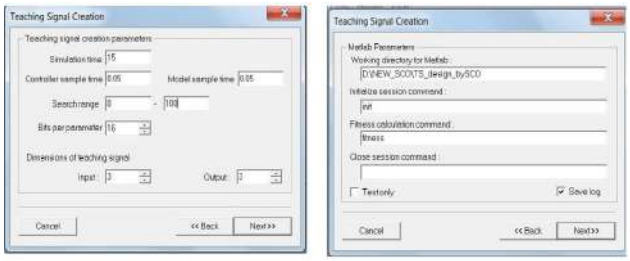

Figure A4. Windows of TS creation

By button "next" we go to the next windows shown on Figure A4. In the left window (Figure A4) signal creation parameters should be entered:

- Simulation time: time of simulation used to create TS.
- Controller sample time: sample time of control system.
- Model sample time: sample time of simulation.
- Search range: control signal search range.
- Bits per parameter: number of bits in GA chromosome per each control signal parameter. Greater values increase precision and optimization time.

Dimensions of TS: number of components in input and output parts of TS.

In the right window (Figure A4) the path to Matlab-model, initiation commands and fitness function are given. In the end of the given session, designed TS is saved in the «name».pat format as shown in Figure A5.

Figure A5. Window of saving TS

A3. Robust Knowledge Base Design based on SC Optimizer

Designed TS will be approximated by a fuzzy model chosen by a user.

Remark. TS also may be obtained experimentally from measurements of dynamic parameters of physical objects.

A3.1. Short general description

SCO uses the chain of GAs (GA_1, GA_2, GA_3) and approximates measured or simulated data (TS) about the modeled system with desired accuracy. GA_1 solves optimization problem connected with the optimal choice of number of MFs and their shapes. GA_2 searches optimal KB with given level of rules activation. Introduction of activation level of rules (LA) allows us to sort fuzzy rules in accordance with value information and design robust KB. GA_3 refines KB by using two criteria (see below). Figure A6 shows the flow chart of SCO operations on macro level and combines several stages.

Stage 1: *Fuzzy Inference System* (FIS) Selection. The user makes the selection of fuzzy inference model with the featuring of the initial parameters.

Stage 2: *Create linguistic values*. GA optimizes linguistic variable parameters, using the initial parameters, and TS, obtained from the in-out patterns, or from dynamic response of CO (real or simulated in Matlab).

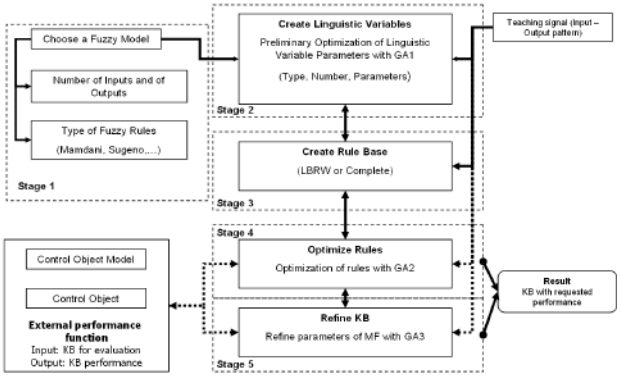

Figure A6. Flow chart of SC Optimizer

Stage 3: *Rule base creation*. At first, we use the rule rating algorithm (LBRW) for selection of the certain number of rules. The "Level of activation" (*LA*) criteria is a parameter given by a user. At this stage the *total firing strength of each rule* ($R^i_{total} = \sum_t R^i(t)$, where t is a time, i is a rule index) is calculated. Then the "*Sum of firing strength*" and "*Max of firing strength*" criterias are used for design KB[17]. Output of this stage is the rule base designed according to the chosen criteria and activation level.

Stage 4: *Rule base optimization*. GA_2 optimizes the rule base (Stage 3), using the fuzzy model (Stage 1), optimal linguistic variable parameters (Stage 2), and TS. If you are still not satisfied with model quality you can use *Error Back Propagation* algorithm.

Stage 5: *Refine KB*. On this stage, the structure of KB is already specified and close to global optimum. In order to reach the optimal structure, two criteria can be used. First criterion is based on the minimum error, and in this case KB refining is similar to classical derivative based optimization procedures (like error back propagation algorithm for FNN tuning). Second criterion is based on the maximum of mutual information entropy [17]. The result of the Stage 4 is a specification of fuzzy inference structure, optimal for solution of a current problem. In order to have robust solution, Stage IV can be bypassed, and the robust structure obtained with GAs of stages 2 - 3 can be used.

A4. Description of steps in SC Optimizer toolkit

Designed TS is used on the next step of technology (step 2 on the Figure A1). At first, we must create a new sco-project.

A4.1 *New Project creation* SCO allows to create a new model or load previously created model from file.

If you choose to create a new model the system will prompt you about model parameters, including inference model, number of input and output variables, number of fuzzy sets for each variable and so on. New model creation window is called by buttons «*File*», «*New*» in main menu. The window is shown on Figure A7 (a). Then following the button "next" we go to the window for TS input shown on Figure A7 (b).

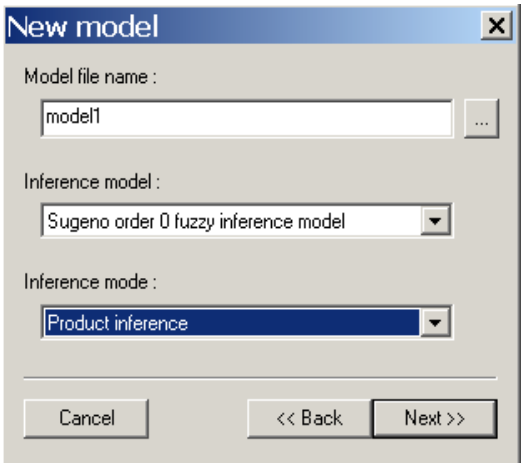

(a)

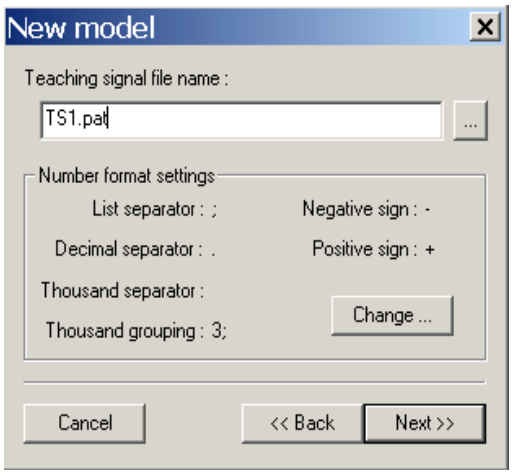

(b)

Figure A7. New model creation windows

After TS is inputted, it must be adopted for SCO data processing format. For that purpose there is the window (Figure A7 (b)) where you must push the button «Change».

Created model is saved into file «name.sco», for example, «Pcart_TS1.sco». After the model was created or loaded you will be presented with main program menu, allowing you to view model parameters, start different optimization algorithms or edit model manually.

After new model is created go to the next step create variables.

A4.2. Membership functions creation and its optimization

First step is GA_1 which solves optimization problem connected with the optimal choice of number of MFs and their shapes. This process is called by button «Create variables» and then you go forward according to menu.

When working with GA_1 algorithm you can run signal filtering algorithm which will remove redundant signal

DOI: https://doi.org/10.30564/aia.v2i1.1339

lines. This can improve quality of fuzzy sets created by GA_1 algorithm. If you wish to use this mode select Filter Signal checkbox on the first page of the dialog and enter desired filter threshold level (see Figure A8).

Next window will be the window with GA parameters. Fill it and press NEXT>> to switch to the next page. Select variables, which should be optimized, by holding CONTROL key and clicking items in the list. If you are running this algorithm for the first time it is recommended to leave all variables selected. Use this feature in order to improve quality of some variables later.

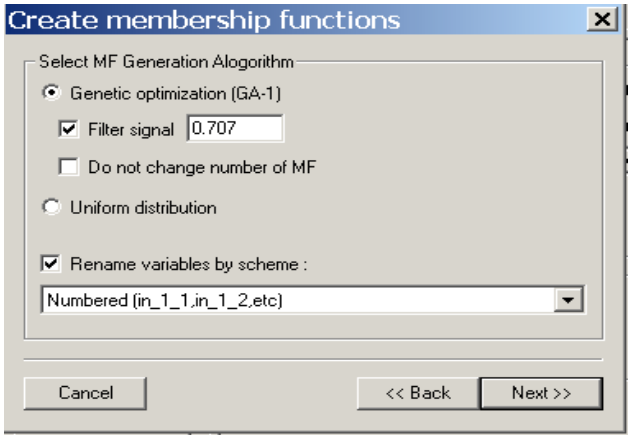

Figure A8. Create MFs window

SCO supplies two ways of MFs determining: creating variables *with uniform distribution algorithm* and creating variables *with* GA_1 that finds best (from the fitness function view) combination of fuzzy sets for each input variable. Also, GA_1 finds optimal form (type) of MFs and optimal value of intersection between neighbor fuzzy sets

On Figure A9 one example of designed MFs is shown. As shown in this figure, for «Input_3» values description GA_1 finds seven fuzzy sets (membership functions).

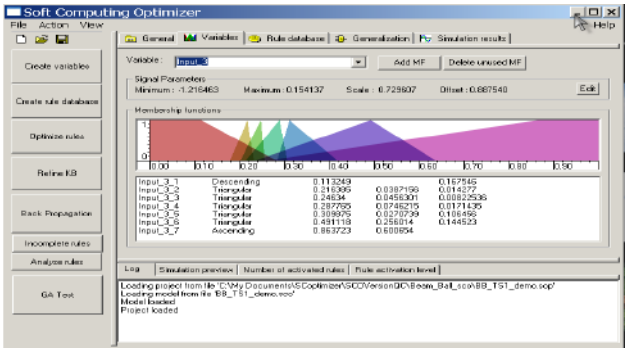

Figure A9. Example of designed MFs

A5. Rule database creation

After you have created variables and MFs you can create rule database. You can do this by pressing Create rule database command button or with Action/Create rule database menu. After pressing «Create rule database» the following window is shown (Figure A10).

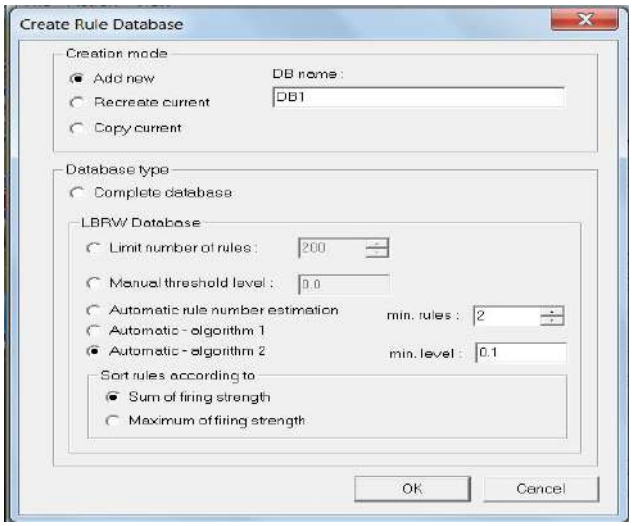

Figure A10. Create rules window

SCO support two types of rules database (RD): complete database and LBRW database (LBRW from "Let the Best Rule Win"). Complete database consists of all possible combinations of fuzzy sets describing input variables. The number of rules in complete RD equals the product of numbers of fuzzy sets for each input variables. If in the model there are more than three input variables then the complete RD has a large number of rules. Usually such kind of RD contains redundant information, and control with this RD is not effective.

LBRW algorithm chooses only valuable (robust) rules. Decreasing number of rules gives greater velocity of RD optimization without loss of accuracy. When creating LBRW database you can specify exact number of rules or minimal level of firing strength (threshold level). In the latter case created database will include all rules with firing strength greater than or equal to one you specify.

On Figure A11 an example of designed rules database is shown. As you can see, complete database contains 486 rules, but designed LBRW database consists only of 26 rules.

Next window will be the window with GA parameters. Fill it and press NEXT>> to switch to the next page. Select variables, which should be optimized, by holding CONTROL key and clicking items in the list. If you are running this algorithm for the first time it is recommended to leave all variables selected. Use this feature in order to improve quality of some variables later.

 DOI: https://doi.org/10.30564/aia.v2i1.1339

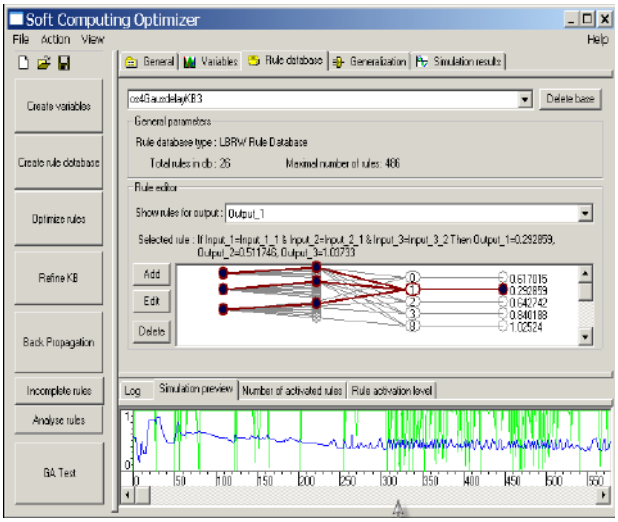

Figure A11. Example of designed rules database

On Figure A11 in the line named «Selected rule» a chosen rule (red bolt line on the FNN structure; order number of the chosen rule = 1) is shown in symbolic form:

« If Input_1 = Input_1_1 & Input_2 = Input_2_1 & Input_3 = Input_3_2 Then Output_1 = 0.292859, Output_2 = 0.511746, Output_3 = 1.03733»

In the low part of the window (Figure A11) the result of TS approximation is shown. Green line represents a TS, blue line represents approximation of TS by chosen fuzzy system with designed rule database with 26 rules.

A6. Rule database optimization

After rule database is created, proceed to their optimization by GA_2. Press «Optimize rules» and the window shown on Figure A12 is opened.

There are three possibilities:

- RD optimization with complete TS,
- RD optimization with optimized TS,
- RD optimization by Matlab simulation.

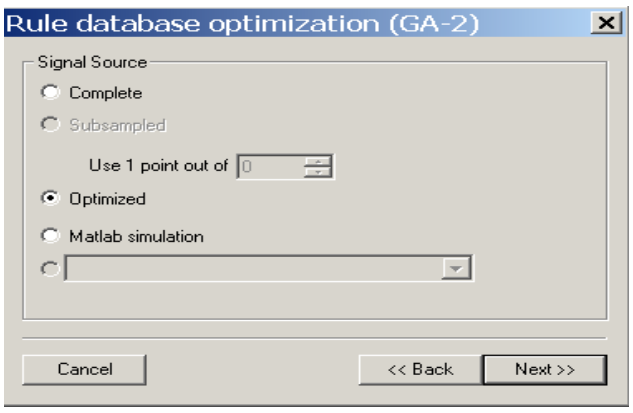

Figure A12. Rule database optimization window

Choose one way, press NEXT>> and the following windows are opened (see Figure A13).

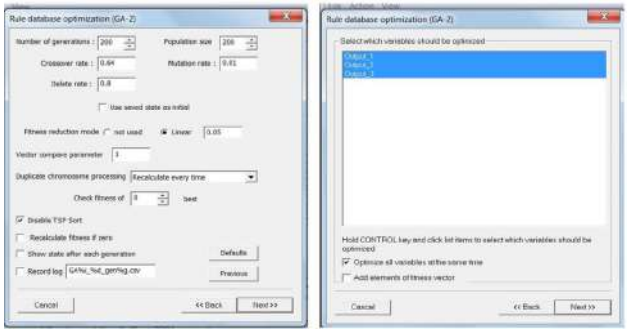

Figure A13. Choice of GA parameters and selecting variables

You should select output variables for which database should be optimized. By default, optimization is selected for all variables and you shouldn't change it when starting algorithm for the first time.

During optimization a progress window will appear (see Figure A14). It displays variables currently optimized, number of current generation and achieved level of evaluation function.

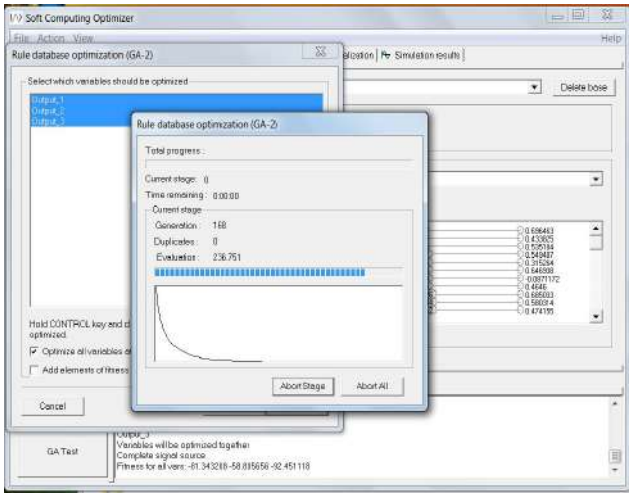

Figure A14. Progress window of optimization process

You can press Abort Stage button if you want to stop optimization for the current stage. The state of the variables will be set to the best state found before abort button was pressed and the optimization will switch to the next variable. Press Abort All to stop optimization process and return to SCO.

So, as result of GA_2 optimization we obtain optimal values of right parts of fuzzy rules.

Remark. GA_2 optimization is based on TS. If TS is not optimal (from the control quality criterion) GA_2 optimization may be not optimal too. For that case in SCO toolkit there is an effective way - RD optimization by Matlab simulation.

DOI: https://doi.org/10.30564/aia.v2i1.1339

A7. Rule database optimization with Matlab simulation

For RD optimization by Matlab simulation choose option «*Matlab simulation*» in window on Figure A12 (see above) and press NEXT>>. After two windows as shown on Figure A13 (see above) is fulfilled, by pressing again NEXT>> we get into the window shown on Figure A15.

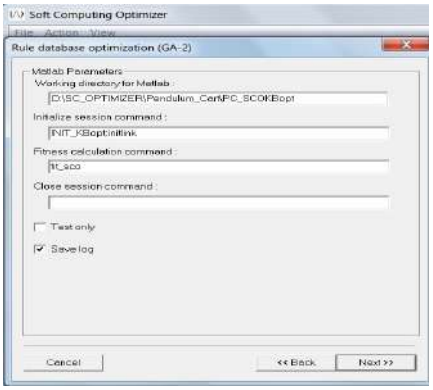

Figure A15. Window for connection to Matlab/Simulink model

In this window the path to Matlab model, initiation commands and fitness function are given.

A8. Fine tuning of the model

When rule database is optimized you can further improve model quality by returning to MFs optimization. This is accomplished by the last optimization step model refinement (known as GA_3 algorithm). You can start model refinement by clicking Refine KB command button or selecting Action/Refine KB menu item.

After you activate the command wizard dialog will appear. It will first prompt you which fitness function you would like to use. Three choices are available:

• Maximization of mutual information entropy: Tells SCO to minimize mutual information entropy between MF fuzzy sets. This is the same function used in GA_1 algorithm, but unlike GA_1, GA_3 won't change number of MF's per variable, only MF parameters will be changed.

• Minimization of output error: Minimize output error.

• Matlab simulation: Use Matlab/Simulink to calculate fitness function.

Select one of the variants and press NEXT>>. Enter genetic algorithm parameters on the second page and press NEXT>> to switch to the next page.

Now you should select input variables, which should be optimized. By default, optimization is selected for all variables. You can change selection by holding CTRL and clicking left mouse button on the list items. You also have an option to optimize all variables at the same time (if you check "optimize all the variables at the same time" check box). If you leave this checkbox unchecked program will optimize variables one after another. If you check Add elements of the fitness vector box then elements of the resulting fitness vector will be added together. Otherwise vector fitness function will be used. Press NEXT>> to start optimization.

While GA_3 algorithm operates the progress dialog will be shown. It will display number of current generation and achieved level of evaluation function. You can press Abort Stage button if you want to stop optimization for the current stage. The state of the variables will be set to the best state found before abort button was pressed and the optimization will switch to the next variable. Press Abort All to stop optimization process and return to SCO.

If you are still not satisfied with model quality you can run rule database optimization (GA_2) again or use Error Back Propagation algorithm. Error Back Propagation algorithm implements classical gradient optimization method, which provides an effective way to further improve model output after genetic optimization. You can start Back Propagation algorithm by clicking Back Propagation command button or selecting Action/Back Propagation menu item.

References

[1] Ulyanov, S. V. Self-organized Control System [P] US patent, No. 6, 411, 944, 1997.

[2] Aliev, R. A., Ulyanov, S. V. Fuzzy Models of Control Processes and Systems [J] Itog. Nauk. Tekh. (VINITI), Ser. Eng. Cybern., 29 (1990); 32 (1991).

[3] Haddad, W. M., Chellaboina, V., Nersesov, S. G. Energy-and entropy-based stabilization for lossless dynamical systems via hybrid controllers [J] IEEE Transactions on Automatic Control, Vol. 52, No 9, 2007: 1604-1614 pp.

[4] Haddad, W. M., Chellaboina, V., Nersesov, S. G. Thermodynamics: A Dynamical Systems Approach, Princeton Series in Applied Mathematics Princeton [M] NJ: Princeton University Press, 2005.

[5] Haddad, W. M.,Chellaboina, V., Nersesov, S. G. Impulsive and Hybrid Dynamical Systems: Stability, Dissipativity, and Control, Princeton Series in Applied Mathematics [M] Princeton, NJ: Princeton University Press, 2006.

[6] Ulyanov, S. V., Yamafuji, K., Kurawaki, I. et al. Computational Intelligence for Robust Control Algorithms of Complex Dynamic Systems with Minimum Entropy Production [J] Advanced Comput. Intelligence and Intelligent Informatic, Vol. 3, No 2, 1999.

[7] Bologna, M., Grigoloni, P., Karagiorgios, M. et al. Trajectory Versus Probability Density Entropy [J] Phys.

 DOI: https://doi.org/10.30564/aia.v2i1.1339

Rev. 64E (1), 2001.

[8] Petrov, B. N., Gol'denblat, I. I., Ulanov, G. M., Ul'yanov, S. V. The Theory of Models in Control Processes: Information Thermodynamic Aspects [M] Nauka, Moscow, 1978 [in Russian].

[9] Litvintseva, L. V., Takahashi, K., Ulyanov, S.V., et al. Intelligent Robust Control Design Based on New Types of Computations [J] Note del Polo Ricerca. Milano: Universitadegli Studidi Milano Publ., Vol. 60, 2004.

[10] Petrov, B. N., Ulanov, G. M., Ul'yanov, S. V. et al. Control Problems for Relativistic and Quantum Dynamic Systems [M], Nauka, Moscow, 1982 [in Russian].

[11] Petrov, B N., Pugachev, V. S., Ulyanov, S. V. et al. Informational Foundations of Qualitative Theory of Control Systems [J] in Proceedings of 7th IFAC Congress, Helsinki, Finland, Vol. 3, 1978.

[12] Granichin, O. N., Polyak, B. T. Randomized Estimation and Optimization Algorithms under Almost Arbitrary Noise [M] Nauka, Moscow, 2003 [in Russian].

[13] Polyak, B. T., Shcherbakov, P. S. Robust Stability and Control [M] Nauka, Moscow, 2002 [in Russian].

[14] Perroud, M., Saucier, A. Thermodynamics of Dissipative Systems [J] Helvetica Physica 60 (8), 1987.

[15] Ulyanov, S. V., Hagiwara, T. Intelligent Mechatronic Control Suspension System Based on Soft Computing [P] US patent, No. 6,701,236, 2001.

[16] Panfilov, S. A., Litvintseva, L. V., Ul'yanov, S. S. et al. Software Support of the Processes of Generation, Eliciting, and Design of Knowledge Bases of Robust Intelligent Control Systems [J] Program. Prod. Syst., No. 2, 2004.

[17] Fujii, S., Watanabe, H., Panfilov, S. A. et al. Intelligent Robust Control System for Motorcycle Using Soft Computing Optimizer [P] US patent, No. 20050197994, 2005.

[18] Ulyanov, S. V. et al. System and method for stochastic simulation of nonlinear dynamic systems with a high degree of freedom for soft computing applications [P] Patent US 2004/0039555 A1. Pub. Date: Feb. 26, 2004.

[19] Kurawaki, I, Litvintseva, L. V., Takakhashi, K. et al. Design of Robust Knowledge Bases of Fuzzy Controllers for Intelligent Control of Substantially Nonlinear Dynamic Systems, I. Application of Soft Computing [J] Izv. Ross. Akad. Nauk, Teor. Sist. Upr., No. 4, 2004 [Comp. Syst. Sci. Intern., Vol. 43, No 3, 2004: 615-632 pp.].

[20] Khoogar, A. R. et al. Obstacle Avoidance for Redundant Manipulators Using a Genetic Algorithm [J]. Southeastcon´91 Conference, Williamsburg, VA, 7-10 Apr., Vol. 1, 1991: 317–320.

[21] Secara, C., Vladareanu, L. Iterative genetic algorithm-based strategy for obstacles avoidance of a redundant manipulator [J] Wseas Transaction on Mathematics, Vol. 9, No 3, 2010: 211–221.

[22] Yu, W., Rosen, J. Neural PID Control of Robot Manipulators with Application to an Upper Limb Exoskeleton [J] Cybernetics, IEEE Transactions, Vol. 43, No 2, 2013: 673–684.

[23] Jasour, A. M, Farrokhi, M. Path Tracking and Obstacle Avoidance for Redundant Robotic Arms Using Fuzzy NMPC [J] American Control Conference, Hyatt Regency Riverfront, St. Louis, MO, USA, 10-12 June, 2009: 1353–1358.

[24] Meza, J. L. et al. Fuzzy Self-Tuning PID Semiglobal Regulator for Robot Manipulators [J] Industrial Electronics, IEEE Transactions, Vol. 59, No 6, 2012: 2709–2717.

[25] Salas, F. G., Santibanez, V., Llama, M. A. Variable Gains PD Tracking Control of Robot Manipulators: Stability Analysis and Simulations [J] World Automation Congress (WAC), Puerto Vallarta, Mexico, 24-28 June, 2012: 1–6.

[26] Ulyanov, S. V. et al. Intelligent robust control: soft computing technologies [M] M.: VNIIgeosystem, 2011: 408 p [in Russian].

[27] Panda, R. C. Introduction to PID Controllers - Theory, Tuning and Application to Frontier Areas [J] Rijeka, Croatia: InTech, 2012: 258 p.

[28] Mikhailov, V. S. Control Theory [M] K: Higher School, 1988: 312 p [in Russian].

[29] Ulyanov, S. V., Litvintseva, L. V., Mishin, A.A., Sorokin, S. V. Certificate of state registration of computer programs No. 2011619257. Optimizer of robust knowledge bases for the design of intelligent control systems on soft computing: [P] Application No. 2011617532 dated 11.10.2011 RF Registered in the Register of computer programs on December 1, 2011 [in Russian].

[30] Phillips, C., Harbor, R. Control systems with feedback [M] M.: Laboratory of Basic Knowledge, 2001: 616 p.

[31] Ulyanov, S. V. Soft Computing Optimizer of Intelligent Control System Structures [P]: US patent, No. 20,050,119,986, 2005.

[32] Nikolaeva, A. V., Ulyanov, S. V. Design of an intelligent control system for an excess robot with a manipulator with seven degrees of freedom. Part 1: Soft Computing Technologies [J] System analysis in science and education: a network scientific publication, No 4, 2013. Access mode: http://www.sanse.ru/download/193 [in Russian].

[33] Ulyanov, S. V. Self-organized robust intelligent control [M] Saarbrücken: LAP Lambert Academic Publishing, 2015: 412 p.

DOI: https://doi.org/10.30564/aia.v2i1.1339

BILINGUAL PUBLISHING CO.
Pioneer of Global Academics Since 1984

Artificial Intelligence Advances
https://ojs.bilpublishing.com/index.php/aia

ARTICLE

Robust PID Controller Design on Quantum Fuzzy Inference: Imperfect KB Quantum Self-Organization Effect-Quantum Supremacy Effect

L.V. Litvintseva[1] V.S. Ulyanov[1] Sergey V. Ulyanov[1,2*]

1. INESYS LLC (EFKO GROUP), Russia
2. Dubna State University, Universitetskaya Str.19, Dubna, Moscow Region, 141980, Russia

ARTICLE INFO

Article history
Received: 11 November 2019
Accepted: 8 April 2020
Published Online: 15 April 2020

Keywords:
PID controller tuning
Quantum fuzzy inference
Intelligent control
Quantum self-organization of imperfect KB
Quantum supremacy

ABSTRACT

The new method of robust self-organized PID controller design based on a quantum fuzzy inference algorithm is proposed. The structure and mechanism of a quantum PID controller (QPID) based on a quantum decision-making logic by using two K-gains of classical PID (with constant K-gains) controllers are investigated. Computational intelligence toolkit as a soft computing technology in learning situations is applied. Benchmark's simulation results of intelligent robust control are demonstrated and analyzed. Quantum supremacy demonstrated.

1. Introduction

A PID controller applied as the instrument in many industrial control applications last 70 years. PID controllers realize a control loop feedback mechanism to control object or plant process variables [1]. They perform an accurate and optimal control in many cases. But PID controllers do not guarantee an optimal and robust control in the case of complex, essentially non-linear and ill-defined structures of controlled objects and in the presence of different stochastic noises.

To improve robustness and control quality capabilities of traditional PID control systems design we have proposed a new approach based on soft and quantum computing toolkit [2].

In our approach a robustness of PID controllers depends on a presence of time dependent PID coefficient's gains, which computed applying Knowledge Bases and a fuzzy inference mechanism. Moreover, in unpredicted situations the robustness of PID controllers depends on a presence of a mechanism of Knowledge Bases self-organization [3]. This mechanism is described as a logical algorithmic process of a value information extraction from hidden layers (possibilities) in classical control laws using quantum decision-making logic [3,4]. The quantum operators, such as superposition, entanglement and interference, give rise to the quantum logic used in quantum computing.

In this article a quantum approach to the design of robust conventional PID controllers is demonstrated. We use a simplified method of a quantum fuzzy inference

**Corresponding Author:*
Sergey V. Ulyanov,
ISESYS LLC (EFKO GROUP), Naberezhnaya Ovchinnikovskaya Str.20 Bld.2, Moscow, Russia;
Email: ulyanovsv@mail.ru

 DOI: https://doi.org/10.30564/aia.v2i1.1401

algorithm, where instead of Knowledge Bases we use disturbed values of K-gains of classical PID controllers. We propose a new mechanism of a quantum PID controller (QPID) design based on a quantum decision-making logic by using two K-gains of classical PID. While in this case membership functions are singletons further instead of naming "quantum fuzzy inference" we will call our method as a "quantum inference" that the particular case of quantum fuzzy inference in [3,4].

Quantum supremacy on Benchmark's simulation results of QPID based robust control for a cart-pole system in unpredicted control situations demonstrated and analyzed.

2. General structure and main ideas of QPID controller design

On Fig. 1, the general structure of control system with quantum PID controller in the presence of external stochastic noise, sensor's time delay and noise in sensor system is shown.

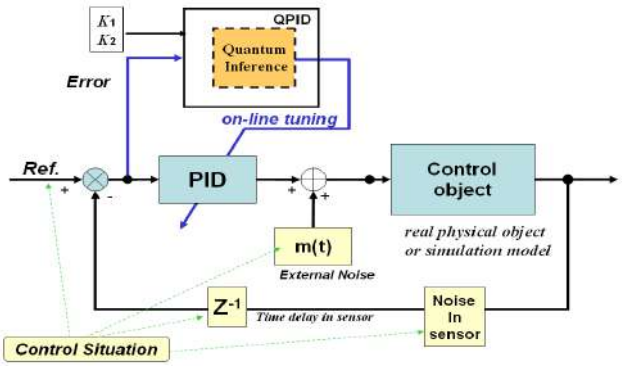

Figure 1. General structure of QPID based on two K-gains of conventional PID and quantum inference.

Consider main ideas of Quantum Inference (QI) [3] based on two PID coefficient gains schedule. We have the following computing steps.

First of all, for two teaching conditions (learning situations) we will design two K-gains, K_1 and K_2, by using genetic algorithm (GA) (so called PID tuning based on GA): $K_1 = \left[k_P^1\ k_D^1\ k_I^1\right]$ and $K_2 = \left[k_P^2\ k_D^2\ k_I^2\right]$.

Remark. See an example of fitness function for GA tuning in the section with simulation results.

By using an artificial stochastic noise disturb obtained K-gains as follows

$$K_{1,2}(t) = \begin{bmatrix} k_P + G_P \cdot \xi(t) \\ k_D + G_D \cdot \xi(t) \\ k_I + G_I \cdot \xi(t)] \end{bmatrix}, \text{where } \xi(t) - \textit{stochastic} \text{ noise with maximal amplitude} = 1 \tag{1}$$

and G_P, G_D, G_I are increasing / decreasing coefficients that can be chosen manually. In two learning situations, simulate a control object motion with new disturbed K-gains and design two probability distributions of K-signals for design of states $|0\rangle$ and $|1\rangle$ in QFI. (See an example of these states preparation in the section with simulation results.)

Realize QFI process based on two K(t)-gains by following steps.

Step 1: Coding. The preparation of all normalized states $|0\rangle$ and $|1\rangle$ for current values of disturbed control signals K_1 and K_2 including:

- a calculation of probability amplitudes α_0, α_1 of states $|0\rangle$ and $|1\rangle$ from histograms;
- a calculation of normalized value of state $|1\rangle$ by using α_1.

Step 2: Choose quantum correlation type for preparation of entangled state. Consider the following quantum correlation (spatial):

$$e_1 e_2 k_P^{1,2} k_D^{1,2} \to k_P^{new} \cdot gain_P;\ \ \dot{e}_1\, \dot{e}_2\, k_D^{1,2} k_I^{1,2} \to k_D^{new} \cdot gain_D;\ \ \ Ie_1\, Ie_2\, k_I^{1,2} k_P^{1,2} \to k_I^{new} \cdot gain_I;$$

where $e, \dot{e}, Ie$ – are control error, derivative and integral of control error correspondingly and $gain_{P(D,I)}$ – are QI scaling factors that can be obtained by GA.

So, a quantum state

$|a_1 a_2 a_3 a_4 a_5 a_6\rangle = |e_1 e_2 k_P^1(t) k_D^1(t) k_P^2(t)\ k_D^2(t)\rangle$ is considered as the entangled state.

Remark. The type of an entangled state is chosen from the list of entangled states types. This list is constructed manually (empirically) and checked by simulation.

Step 3: Superposition and Entanglement. According to the chosen quantum correlation type construct superposition of entangled states. (see an example in the section with simulation results)

Step 4: Interference and measurement. Choose a quantum state

$$|a_1 a_2 a_3 a_4 a_5 a_6\rangle = |e_1(t) e_2(t) k_P^1(t) k_D^1(t) k_P^2(t)\ k_D^2(t)\rangle$$

with the maximum amplitude of probability

$A = \sqrt{P_{e_1}} \cdot \sqrt{P_{e_2}} \cdot \sqrt{P_{k_P^1}} \cdot \sqrt{P_{k_D^1}} \cdot \sqrt{P_{k_P^2}} \cdot \sqrt{P_{k_D^2}}$. Choose subvector $|k_P^1(t) k_D^1(t) k_P^2(t)\ k_D^2(t)\rangle$.

Step 5: Decoding.

Calculate normalized output as a norm of subvector of the chosen quantum state as follows:

$$k_P^{new}(t) = \frac{1}{\sqrt{2^{n-2}}} \sqrt{\langle a_3 \ldots a_n | a_3 \ldots a_n \rangle} = \frac{1}{\sqrt{2^{n-2}}} \sqrt{\sum_{i=3}^{n} (a_i)^2},\ \ n = 6 \tag{2}$$

DOI: https://doi.org/10.30564/aia.v2i1.1401

Step 6: Denormalization.

Calculate final (denormalized) output result as follows:

$$k_P^{output} = k_P^{new}(t) \cdot gain_P, \quad k_D^{output} = k_D^{new}(t) \cdot gain_D, \quad k_I^{output} = k_I^{new}(t) \cdot gain_I. \tag{3}$$

Step 7: Find robust QI scaling gains $\{gain_P, gain_D, gain_I\}$ based on GA and a chosen fitness function. (See a fitness function example in the section with simulation results).

Let us consider the Benchmark of control object and investigate robustness and self-organization properties of proposed QPID controller based on developed QI algorithm.

3. Quantum PID based smart control design: example of Benchmark simulation results

Consider a QPID controller design for a typical benchmark of globally unstable dynamic system (a so called «cart-pole» system). The geometrical model of the «cart-pole» dynamic system is shown on Fig. 2.

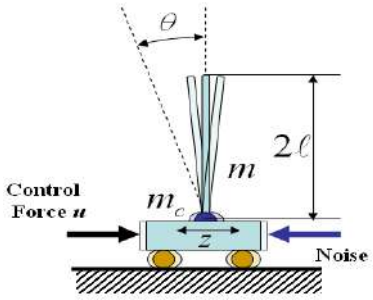

Figure 2. Geometrical model of cart-pole system

Control problem: acting by a control force on the cart, keep the Pole motion vertical and stable (pendulum angle $\theta = 0$) in spite of different environment conditions.

Our control goal is to balance the pole with limited cart's position and velocity, with limited control force and in the presence of stochastic noises and sensor's delay time.

These conditions and constraints in the search of optimal solutions are intractable task for conventional control system theory.

The inverted pendulum (called also a pole) problem control is described by second-order differential equations system for computing control force that to be used for moving the cart:

$$\ddot{\theta} = \frac{g\sin\theta + \cos\theta\left(\frac{+(u+\xi(t)) + \{+a_1\dot{z} + a_2 z\} - ml\dot{\theta}^2\sin\theta}{m_c + m}\right) - k\dot{\theta}}{l\left(\frac{4}{3} - \frac{m\cos^2\theta}{m_c + m}\right)} \tag{4}$$

$$\ddot{z} = \frac{u + \xi(t) + \{-a_1\dot{z} - a_2 z\} + ml(\dot{\theta}^2\sin\theta - \ddot{\theta}\cos\theta)}{m_c + m}, \tag{5}$$

where z and θ are generalized coordinate; g is the acceleration due to gravity (usually $9.8\ m/\sec^2$), m_c is the mass of the cart, m is the mass of inverted pendulum (called also as a pole), l is the half-length of the pendulum, k and a_1 are friction coefficients in z and θ correspondingly, a_2 is a spring force that bounded the cart motion, $\xi(t)$ is external stochastic noise and u is the applied control force in Newton's.

According to the control system structure (shown in Fig.1) we have at the low level one PID controller which controls a cart motion so that the Pole doesn't fail down.

For the pole stabilization ($\theta = 0$) we introduce a reference signal for z as following:

z_{ref} is a projection on axis z of the center of gravity of the pole. It must be equal 0 for stabilization the pole motion.

We can represent z_{ref} as $z_{ref} = -w \cdot l \cdot \sin\theta$, where *w* is some scaling parameter. If $\theta \to 0; z_{ref} \to 0$.

We also introduce constraints on the center of gravity projection: $|z_{ref}| \le 1$ and on applied control force: $\lfloor u \rfloor \le 5\,(N)$. We also consider a presence of a time delay in a measurement system.

Thus, one PID controller through cart motion (first DOF) controls a position of the inverted pendulum (second DOF), i.e. one PID controller control 2DOF control object through energy transfer phenomena from one DOF to another applying non-linear interrelations in Eqs (1) and (2).

3.1 Teaching conditions for PID tuning

In Table 1 model parameters for the chosen control object are described.

Table 1. Cart-Pole System: Model Parameters

m_C [kg]	m [kg]	l [m]	Damping in ɵ, k	Damping in z, a_2	Spring force coefficient in dz, a_1
1.0	0.1	0.5	0.4	0.1	5.0

We also take the following Cart-Pole initial conditions: the pole angle $\theta = {}^{[10\ ;\ 0.1]}$ in degrees; cart position z = $^{[0;\ 0]}$ in m.

Constraints: a cart position: -1.0 < z < 1.0 [m]; control force: -5.0 < u < 5.0 [N].

Sensor's delay time = 0.001 sec.

We will use two stochastic external noises (shown on Fig. 3) for two teaching conditions with different prob-

 DOI: https://doi.org/10.30564/aia.v2i1.1401

ability distribution density functions: Gaussian noise (symmetric probability distribution density function) and Rayleign noise (with nonsymmetrical probability distribution density function).

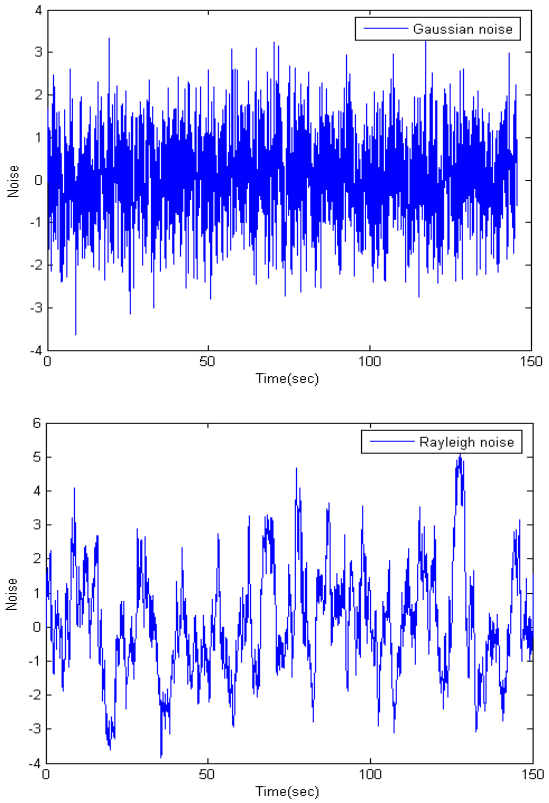

Figure 3. External stochastic noises in teaching control situations.

According to the step's description of QI algorithm above at first stage let us find for two teaching conditions two K-gains K_1 and K_2 by using GA. We have worked with a mathematical model of the cart-pole system represented in Matlab / Simulink.

3.2 PID tuning based on GA. Design time dependent K-gains for QPID

Teaching conditions 1 with Gaussian noise (named as TS1).

In order to apply GA, we must define a fitness function and a search space for GA. Search space for PID gains K = [100 100 100] is defined from preliminary simulations with PID control. We define the following Fitness Function (y) for GA tuning: $y = -\sum_t \theta^2 - \sum_t \dot{\theta}^2$. In Matlab toolkit, this fitness function is represented as following:

$$y = -sum(\text{simoutX}(:,1).\text{^}2)/\text{Norm} - sum(\text{simoutX}(:,2).\text{^}2)/\text{Norm}$$

where simoutX(:,1) is a vector of angle (ϴ) values; simoutX(:,2) is a vector of angular velocity values and Norm is a length of these vectors.

As result of GA tuning, we obtained the following value K_1 = [82.7 13.6 9.4]. We will call PID with K_1 as PID_1.

Now according to (1) we disturb K_1 gains as shown in Matlab model represented on Fig. 4 (a). (see right block).

QI process in QPID block in Matlab model on Fig. 4 (b) demonstrated.

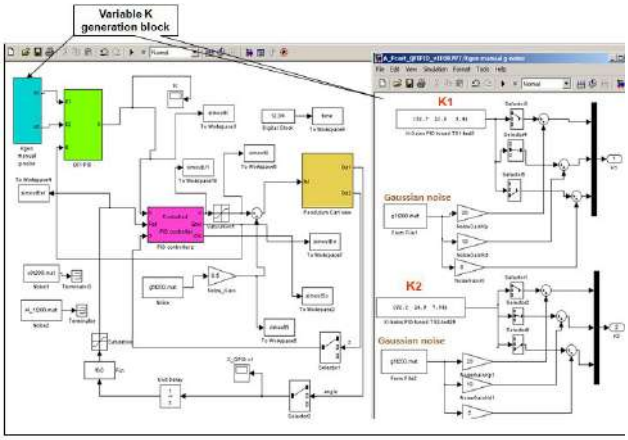

Figure 4 (a). The Matlab structure of QPID based control system.

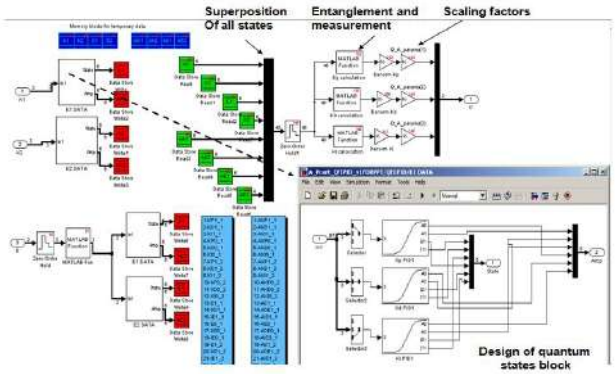

Figure 4 (b). QI process in QPID block in Matlab model.

By the Matlab simulation we define manually (it is easy to do) increasing noise coefficients G_P, G_D, G_I so that $K_1(t)$ and $K_2(t)$ give robust control (the Pole doesn't fall down).

If the Pole fails down, we take smaller G_P, G_D, G_I and check again robustness. Finally, we choose bigger G_P, G_D, G_I that give $K_1(t)$ and $K_2(t)$ with robust control (The Pole doesn't fall down).

Finally, we have the following time dependent $K_1(t)$ for our QPID.

1. TS1 control situation

DOI: https://doi.org/10.30564/aia.v2i1.1401

$$K_1(t) = \begin{bmatrix} k_p + gain_p \cdot \xi(t) \\ k_d + gain_d \cdot \xi(t) \\ k_i + gain_i \cdot \xi(t)] \end{bmatrix} = \begin{bmatrix} 82.7 + 20 \cdot \xi(t) \\ 13.6 + 10 \cdot \xi(t) \\ 9.4 + 5 \cdot \xi(t)] \end{bmatrix},$$

where $\xi(t)$ – Gaussian noise with maximal amplitude = 1.

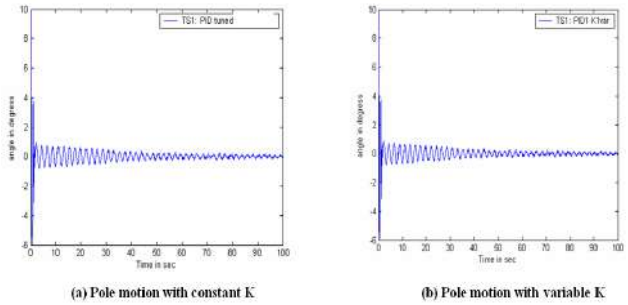

Figure 5. Teaching conditions 1: Pole motion with constant and disturbed K-gains of PID_1

Now let us see on the motion of our control object under constant and variable (time dependent) K_1-gains as shown on Fig. 5. We see that the pole motion is stable in both cases.

On Fig. 6 the disturbed K-gains of PID_1 (called as control laws) are shown.

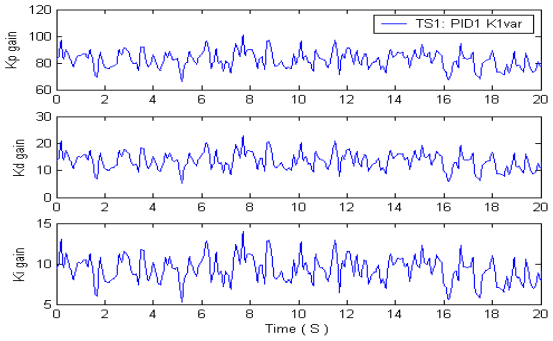

Figure 6. Teaching conditions 1: Control laws.

Teaching conditions 2 with Rayleigh noise (named as TS2). As result of GA tuning, we obtained K_2 = [92.2 14.9 7.84]. We will call PID with K_2 as PID_2. Analogically we obtain the following time depending $K_2(t)$.

$$K_2(t) = \begin{bmatrix} k_p + gain_p \cdot \xi(t) \\ k_d + gain_d \cdot \xi(t) \\ k_i + gain_i \cdot \xi(t)] \end{bmatrix} = \begin{bmatrix} 92.2 + 20 \cdot \xi(t) \\ 14.9 + 10 \cdot \xi(t) \\ 7.84 + 5 \cdot \xi(t)] \end{bmatrix},$$

where $\xi(t)$ – gaussian noise with maximal amplitude = 1.

Simulation results on Fig. 6 show the pole motion.

Remark. On Fig. 7 and all others below, we will denote pole angle θ as x.

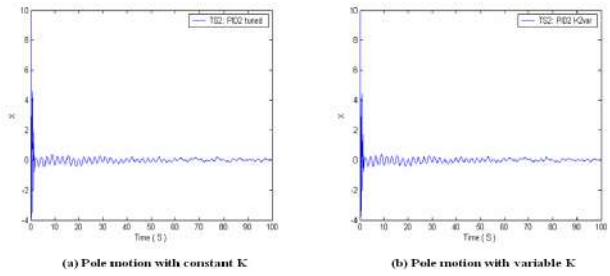

Figure 7. Teaching conditions 2: Pole motion with constant and disturbed K-gains of PID_2

In this case also simulation results show that the pole motion is stable in both cases.

On Fig. 8 the disturbed K-gains of PID_2 (called as control laws) are shown.

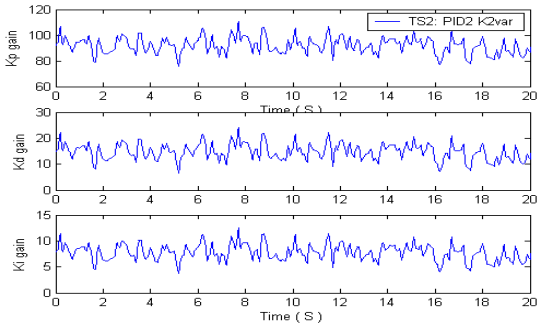

Figure 8. Teaching conditions 2: Control laws.

Conclusion: The simulation results (Figs. 5-8) show that the pole motion is stable in both cases (with constant K_1 and K_2 and with time-depending K_1 and K_2) . It means that we can use disturbed K-values for further calculations in QPID.

QPID controller based on a new type of computing

We developed special tools for Quantum Fuzzy and Quantum PID inference based on QC optimizer ($QCOptKB^{TM}$) [4,6].

$QCOptKB^{TM}$ toolkit allows to control as a physical system and a mathematical model of a control object as shown on Fig. 9.

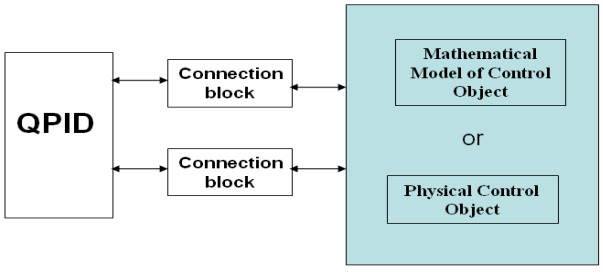

Figure 9. QPID controller connected with a control object.

We will work with mathematical model of control ob-

ject represented in Matlab / Simulink. Control loop with QPID is shown on Fig. 10.

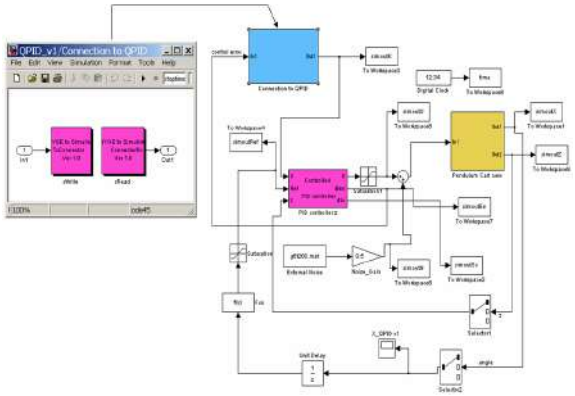

Figure 10. Matlab / Simulink model of control object with control loop based on QPID.

Calculations corresponding to QI based on two K-gains are realized in the block QPID by applying QC Optimizer toolkit.

3.3 QPID in terms of QC optimizer tool

On Figs 11a and 11b, internal structure of QPID in terms of our toolkit is shown.

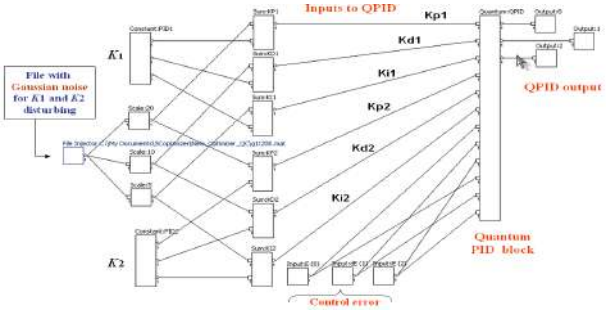

Figure 11a. QPID structure in terms of QC Optimizer tools

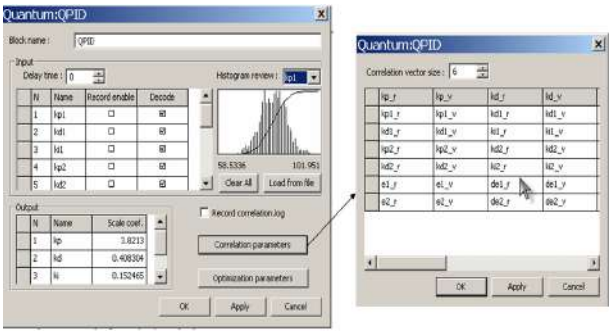

Figure 11b. QPID structure. Internal layer in terms of QC Optimizer tool.

On Fig. 11b internal structure of QPID block is shown. In this block the following items are described:

- names of input variables $k_{P(D,I)}^{1,2}$, where indexes 1, 2 denotes PID_1 and PID_2 (or K_1 and K_2);
- names of output variables $k_{P(D,I)}$;
- histograms for each input variable representing probability distribution of the given input;
- QI scaling coefficients for calculation output values (that is founded by GA for teaching conditions and then used for all control situations);
- knob «correlation parameters» is used for the choice of quantum correlation type description.

For example, let us use the following quantum correlations (spatial):

$$e_1 e_2 k_P^{1,2} k_D^{1,2} \to k_P^{new}; \quad e_1 \dot{e}_2 k_D^{1,2} k_I^{1,2} \to k_D^{new}; \quad Ie_1 Ie_2 k_I^{1,2} k_P^{1,2} \to k_I^{new}.$$

By using GA and chosen quantum correlation we obtained the following QI scaling coefficients: Q_A_params = 2.4200 0.3320 0.1000.

Remark. A fitness function is the same as in PID tuning. Only search space is different. In the case of GA for QI scaling gains search space is as the formula bar displays the contents.

Now investigate robustness properties of designed QPID based on QI with the given correlations in different control situations.

3.4 Investigation of self-organization capability of Quantum PID Control based on two PID controllers

We will consider the following controllers:

o PID_1 controller with constant gains K_1 = [82.7 13.6 9.4];

o PID_2 controller with constant gains K_2 = [92.2 14.9 7.84];

o QPID controller based on QI with K_1 and K_2.

Consider now behavior of control object in teaching and modeled unpredicted control situations and investigate robustness property of designed controllers.

Investigation of different types of quantum correlations: Spatial correlations.

TS1: Comparison of QPID, PID_1 and PID_2 control performances.

Figures 12-14 demonstrate simulation results in the first teaching control situation.

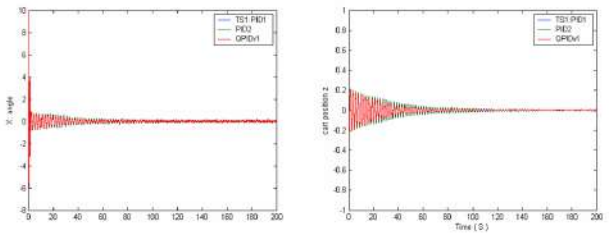

Figure 12. The Pole motion (left) and cart motion (right) comparison.

DOI: https://doi.org/10.30564/aia.v2i1.1401

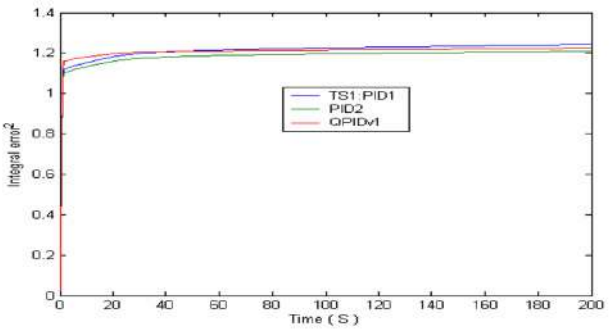

Figure 13. The integral control errors.

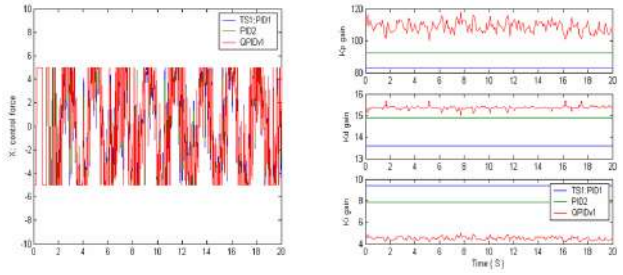

Figure 14. The control force and control laws

Conclusion: all considered controllers are successful to balance the Pole in TS1 situation.

TS2: Comparison of QPID, PID_1 and PID_2 control performance.

On Figs 15 – 17, a behavior of the Cart-Pole system in the teaching conditions TS2 is shown.

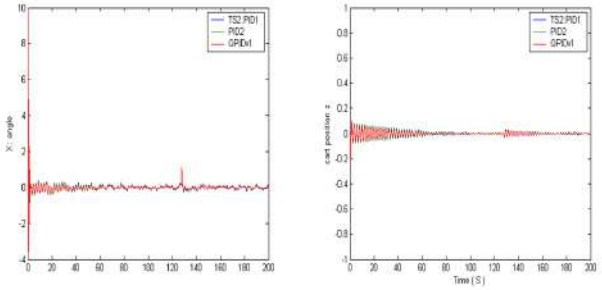

Figure 15. The Pole motion (left) and cart motion (right) comparison in TS2 situation

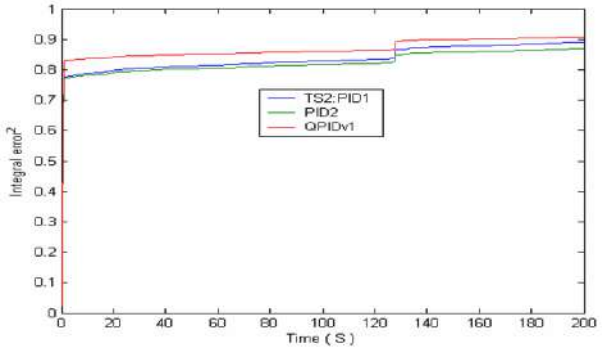

Figure 16. The Integral control errors.

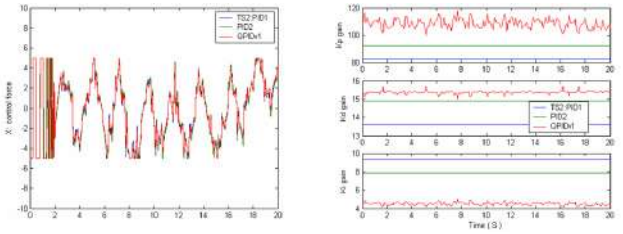

Figure 17. The control force and control laws in TS2 situation

Conclusion: all considered controllers are successful to balance the Pole in TS2 situation.

3.5 Investigation of self-organization capability of chosen QFI

In the Table 2 modeled unpredicted control situations (Class 1) are shown.

Table 2. Class 1 of modeled unpredicted control situations

New 1 control situation (in legend **S**1)	**New 2 control situation** (in legend **S**1a)	**New 3 control situation** (in legend **S**1b)
External noise: *Rayleigh* (TS2 teaching noise); New sensor's time delay = 0.005 sec; Internal sensor noise: Gaussian noise with amplitude = 0.015; TS model parameters	External noise: *Rayleigh* (TS2 teaching noise); New sensor's time delay = 0.005 sec; Internal sensor noise: Gaussian noise with amplitude = 0.015; *New model parameter a*2 = 8	External noise: *Rayleigh* (TS2 teaching noise); Sensor's time delay = 0.001 sec; Internal sensor noise: Gaussian noise with amplitude = 0.01; *New model parameter a*2 = 6

Let us investigate a robustness of the proposed QPID model in a new control environment (Table 2).

New 1 control situation. Figures 18 – 20 show the simulation results in unpredicted control situation Remark. In a plot presentation below "New1" is denoted as S1. See the Table 2.

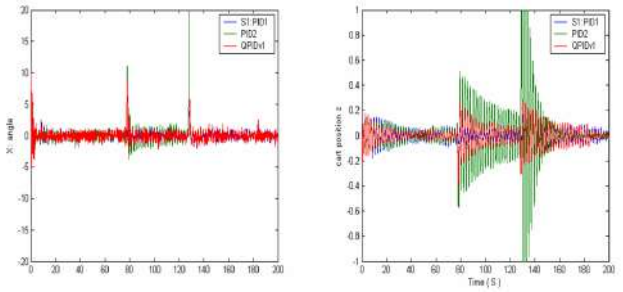

Figure 18. The Pole motion (left) and the cart motion (right) comparison in New 1 situation.

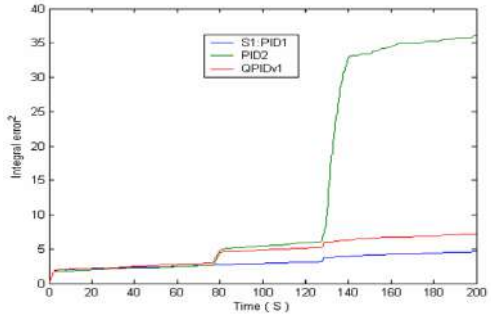

Figure 19. The Integral control error in New 1 situation.

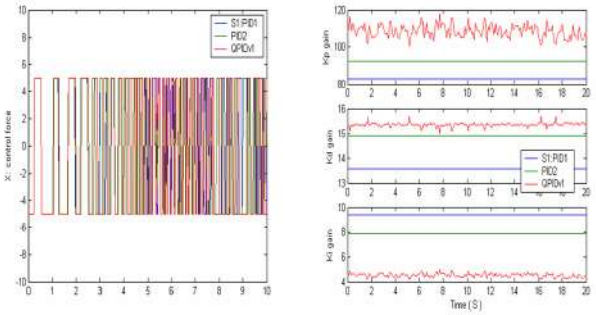

Figure 20. The control force and control laws in New 1 situation.

The presentation of control laws and control forces in a point where the Pole falls down.

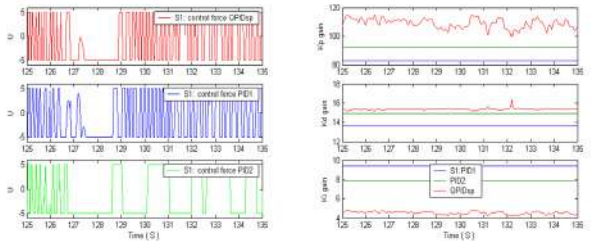

Figure 21. The control force and control laws in New 1 situation

Conclusion: QPID and PID_1 controllers are successful to balance the Pole in New 1 situation. PID_2 controller is unsuccessful to balance the Pole in New 1 situation.

New 2 control situation. Figures 22 – 25 show the simulation results of the cart-pole motion in New2 unpredicted situation.

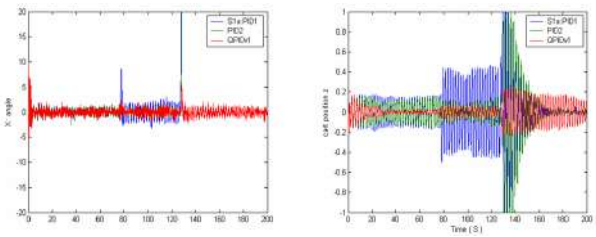

Figure 22. The Pole motion (left) and cart motion (right) comparison in New 2 situation.

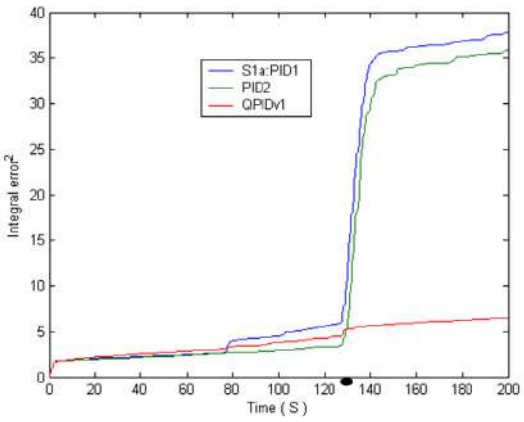

Figure 23. Integral control error in New 2 situation.

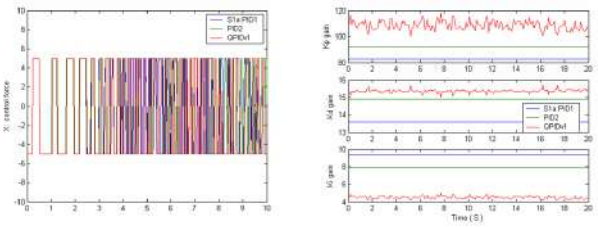

Figure 24. The control force and control laws in New 2 situation

The representation of control laws and control forces in a point where the Pole falls down.

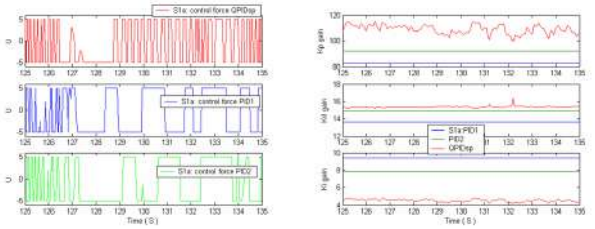

Figure 25. The control force and control laws in New 2 situation

Conclusion: QPID controller is successful to balance the Pole in New 2 situation. PID_1 and PID_2 controllers are unsuccessful to balance the Pole in New 2 situation.

New 3 control situation. Figures 26 – 28 show the simulation results of the cart-pole motion in New3 unpredicted situation.

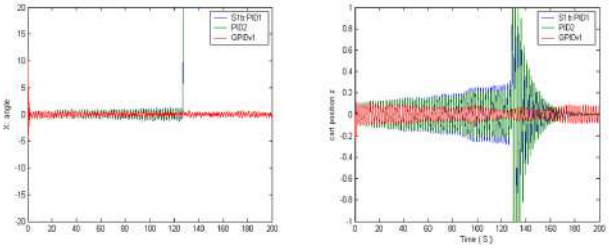

Figure 26. The Pole motion (left) and cart motion (right) comparison in New 3 situation.

DOI: https://doi.org/10.30564/aia.v2i1.1401

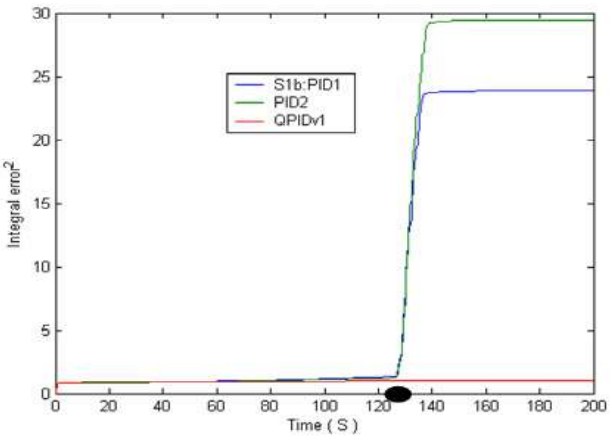

Figure 27. The integral control error in New 3 situation

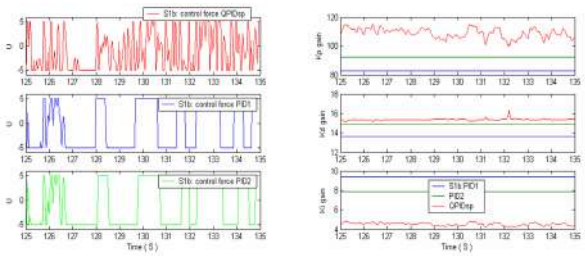

Figure 28. Control forces and control laws in New 3 situation

Conclusion: QPID controller is successful to balance the Pole in New 3 situation. PID_1 and PID_2 controllers are unsuccessful to balance the Pole in New 3 situation.

Final conclusions:

- QPID controller is robust in all situations of class1;
- PID_1 controller is robust in New 1 situation only;
- PID_2 controller is not robust in class 1 situations;
- QPID based on new type of calculations increases robustness of designed PID controllers.

3.6 Investigation of different types of quantum correlations: Temporal correlations

Investigate now a robustness of temporal quantum correlations and compare with the spatial type of QI for the given control object. Let us consider QI with the following temporal quantum correlations as follows:

$$e_1 e_2 k_P^{1,2}(t) k_P^{1,2}(t-\Delta t) \to k_P^{new}(t) \cdot gain_P; \quad \dot{e}_1 \dot{e}_2 k_D^{1,2}(t) k_D^{1,2}(t-\Delta t) \to k_D^{new}(t) \cdot gain_D;$$
$$Ie_1 Ie_2 k_I^{1,2}(t) k_I^{1,2}(t-\Delta t) \to k_I^{new}(t) \cdot gain_I.$$

On Fig. 29, a cart-pole dynamic motion in TS1 situation is shown for different values of time correlation parameter Δt = 0.25 sec and 0.05 sec.

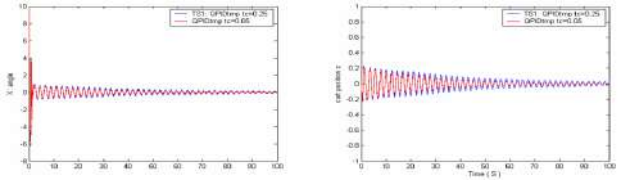

Figure 29. The Pole motion (left) and cart motion (right) comparison in TS1 situation – Temporal quantum correlations.

Check now a robustness of temporal correlations.

On Figs. 30 -31 the cart-pole dynamic motion in New 1 control situation (in legend S1) is shown for different values of time correlation parameter Δt = 0.25 sec and 0.05 sec. You can see that the Pole falls down.

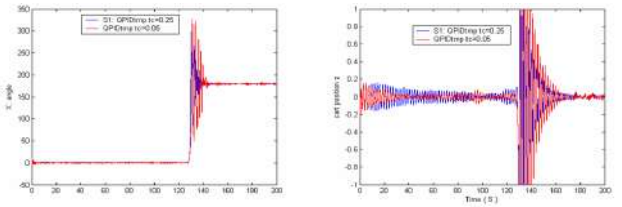

Figure 27. Pole motion (left) and cart motion (right) comparison in New 1 situation: Temporal quantum correlations. Pole falls down

3.7 Comparison QPID control performance under spatial and temporal correlations

Consider dynamic motion and control laws comparison (around the point, where the Pole falls down).

Figures 30 and 31 show results of the comparison.

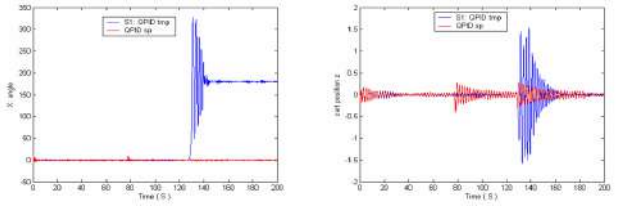

Figure 30. Pole motion (left) and cart motion (right) comparison.

Conclusion: QPID with temporal correlations is not robust in New 1 situation. So, choose the QI based on spatial quantum correlation as a best candidate the for robust QPID realization.

Consider now a new class of modeled unpredicted control situations (Class 2) shown in Table 3. For the new control situations (New 6 and New 7) the external uniform noise is used (Fig. 31).

 DOI: https://doi.org/10.30564/aia.v2i1.1401

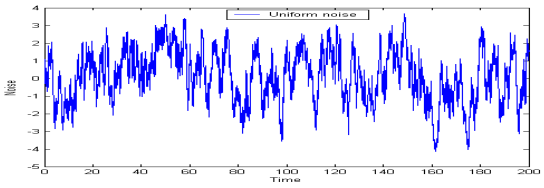

Figure 31. External Uniform noise applied in New 6 and New 7 control situations.

Table 3. Class 2 of modeled unpredicted control situations

New 4 control situation (in legend **S2**) External noise: *Gaussian* (TS1 teaching noise); New sensor's time delay = 0.004 sec; Internal sensor noise: Gaussian noise with amplitude = 0.015; TS model parameters	**New 5 control situation** (in legend **S2a**) External noise: *Gaussian* (TS1 teaching noise); New sensor's time delay = 0.004 sec; Internal sensor noise: Gaussian noise with amplitude = 0.015; *New model parameter a*2 = 8
New 6 control situation (in legend **S3**) New external noise: *Uniform* (Fig.13.32); New sensor's time delay = 0.005 sec; Internal sensor noise: Gaussian noise with amplitude = 0.015; TS model parameters	**New 7 control situation** (in legend **S3b**) New external noise: *Uniform* (Fig.13.32); New sensor's time delay = 0.005 sec; Internal sensor noise: Gaussian noise with amplitude = 0.015; *New model parameter a*2 = 8

New 4 control situation.

Figures 32 – 34 show the simulation results of the cart-pole motion in the New4 unpredicted situation.

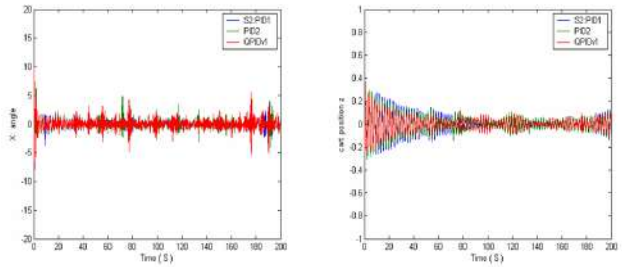

Figure 32. Pole motion (left) and cart motion (right) comparison in New 4 situation.

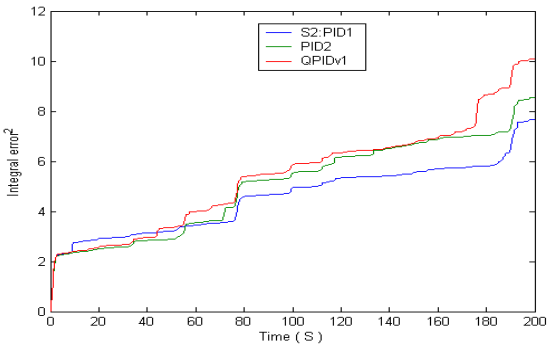

Figure 33. The Integral control error in New 4 situation.

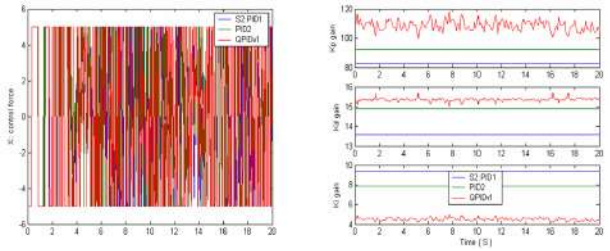

Figure 34. Control force and control laws in New 4 situation.

Conclusion: all controllers are successful to balance the Pole in New 4 situation.

New 5 control situation.

Figures 35 – 37 show the simulation results of the cart-pole motion in the New5 unpredicted situation.

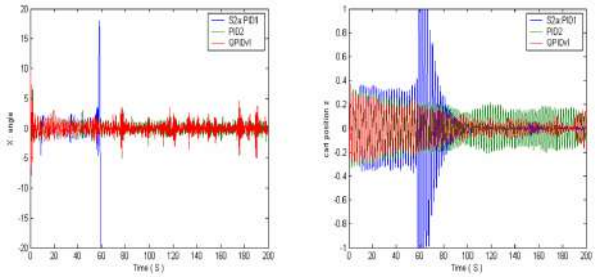

Figure 35. The Pole motion (left) and cart motion (right) comparison in New 5 situation.

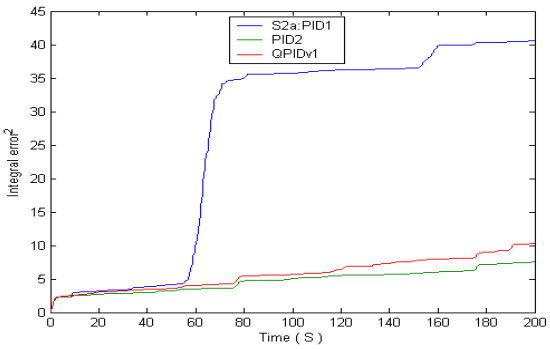

Figure 36. Integral control error in New 5 situation.

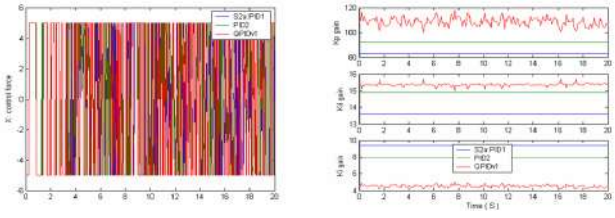

Figure 37. Control force and control laws in New 5 situation.

Conclusion: QPID controller and PID_2 controllers are successful to balance the Pole in New 5 situation. PID_1 controller is unsuccessful to balance the Pole in New 5 situation.

DOI: https://doi.org/10.30564/aia.v2i1.1401

New 6 control situation.

Figures 38 – 40 show the simulation results of the cart-pole motion in the New6 unpredicted situation where a new type of external noise is - Uniform (Fig.31);

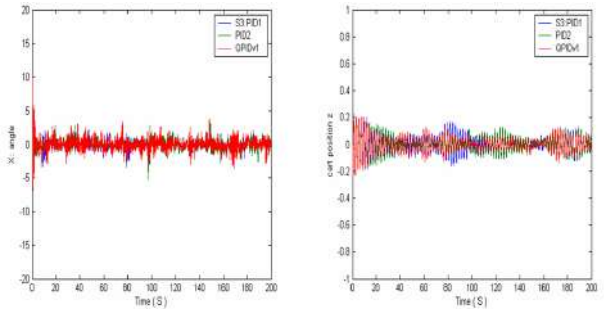

Figure 40. The Pole motion (left) and cart motion (right) comparison in New 6 situation.

Conclusion: All considered controllers are successful to balance the Pole in New 6 situation.

New 7 control situation

The cart-pole motion in the New6 unpredicted situation is shown on Fig.41.

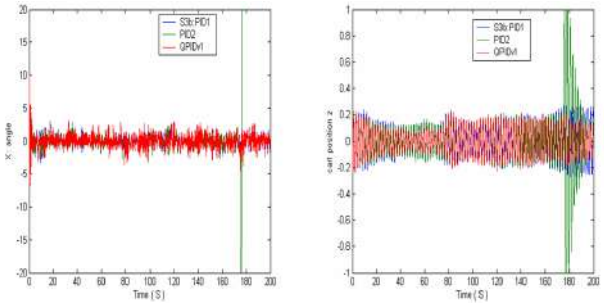

Figure 41. Pole motion (left) and cart motion (right) comparison in New 7 situation.

Conclusion: QPID and PID_1 controllers are successful to balance the Pole in New 7 situation. PID2 controller is unsuccessful to balance the Pole in New 7 situation.

Some important remarks

As shown on Fig. 42 and Fig. 43 below, control laws of QPID in teaching conditions and in new control situations are similar.

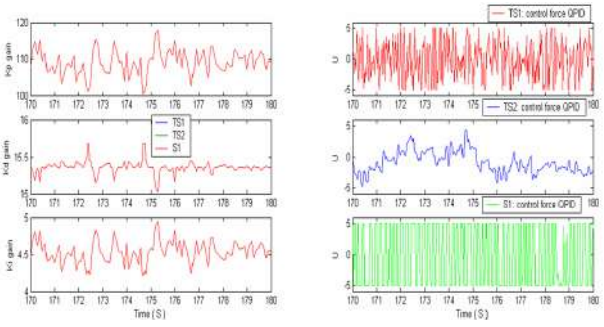

Figure 42. Control laws and control forces in teaching conditions (TS1 and TS2) and in New 1 situation

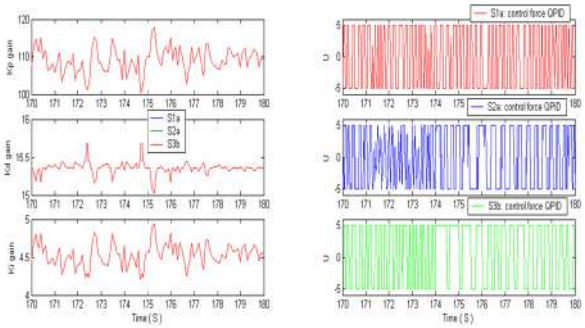

Figure 43. Control laws and control forces in New 2, New 5, New 7 situations

Thus, we have used constant values K_1 and K_2 of classical PID in order to obtain variable K-gains of QPID. Constant K_1 and K_2 of classical PID are not changed when control situation is changed, variable QPID K-gains also is not changed when control situation is changed. If so, let us take average values from obtained QPID K-gains. By this way we can receive new PID that we will call as PID-average.

If we take $K = \max_t K_{QPID}$, then we obtain new controller named as PID-max.

Let us testing robustness of new obtained controllers in chosen control situation (New 2 or in legend S1a). On Fig. 44 comparison of cart-pole motion under three types of control:

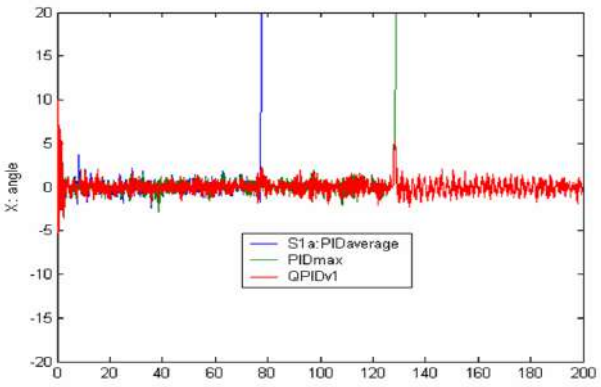

Figure 44. Pole motion under three types of control

- QPID with variable (time dependent) K-gains obtained by on-line QFI process;

- PID-average with constant gains K= [108.8507 15.3634 4.5209];

- PID-max with constant gains K= [119.2325 16.3510 5.1046].

Simulation results show that PID-average and PID-max controllers with constant gains are incapable to balance a Pole in the chosen control situation.

We have seen that constant K-gains obtained from

 DOI: https://doi.org/10.30564/aia.v2i1.1401

quantum inference cannot control pendulum motion in the new situation. But variable K-gains can do it. Thus, we have principally new computing process.

4. Conclusions

Main ideas, algorithm and simulation results of QPID controller are described.

o By applying the typical benchmark of a globally unstable control object (as a "cart-pole" system) a comparison of two types of PID control have been considered: 1) PID with constant coefficients gains; and 2) QPID with time dependent coefficients gains computed on the base of a proposed quantum inference algorithm.

o Simulation results allow us to make the following conclusion: control systems with constant coefficients gains are attractive for many conventional control situations. However due to the constancy of control parameters, standard PID controllers do not guarantee a robust control in unpredicted control situations.

o For practical applications, when we have deal only with PID controllers, we may increase a robustness of control system by using the quantum inference model.

o For achievement the robustness of QPID controller only two sets of PID constant K-gains are needed.

o Simulation results show good robustness properties of QPID based on quantum inference block.

Further investigations of different QPID models are considered as useful and important [7].

References

[1] R. E. Bellman, Adaptive Control Processes: A Guided Tour. Princeton University Press. 2015. ISBN 9781400874668.

[2] L. V. Litvintseva, S. V. Ulyanov, V. S. Ulyanov, Design of robust knowledge bases of fuzzy controllers for intelligent control of substantially nonlinear dynamic systems: II. A soft computing optimizer and robustness of intelligent control systems. J. of Computer and Systems Sci. Intern. 2006. (45) 5. 744-771 DOI: 10.1134/S106423070605008X.

[3] L. V. Litvintseva, S. V. Ulyanov, Intelligent control systems. I. Quantum computing and self-organization algorithm. J. of Computer and Systems Sci. Intern. 2009. (48) 6. 946-984 DOI: 10.1134/S1064230709060112.

[4] L. V. Litvintseva, S. V. Ulyanov, Intelligent control systems. II. Design of self-organized robust knowledge bases in contingency control situations. J. of Computer and Systems Sci. Intern. 2011. (50) 2. 250-292 DOI: 10.1134/S1064230710061036.

[5] S.V. Ulyanov, M. Feng, K. Yamafuji, T. Fukuda, Stochastic analysis of time-invariant non-linear dynamic systems. Pt 1: the Fokker-Planck-Kolmogorov equation approach in stochastic mechanic. Prob. Eng. Mech., 1998, Vol. 13, № 3, Pts 1&2. p. 183 – 203; 205-226.

[6] S.V. Ulyanov, Self-organization quantum robust control methods and systems for situations with uncertainty and risk. US Patent No 8, 0345 874. – 2014.

[7] S.V. Ulyanov, Quantum fast algorithm computational intelligence Pt I: SW / HW smart toolkit. Artificial Intelligence Advances. 2019. Vol. 1. No 1. Pp. 18-43 (URL: https://doi.org/10.30564/aia.v1i1.619).

DOI: https://doi.org/10.30564/aia.v2i1.1401

BILINGUAL PUBLISHING CO.
Pioneer of Global Academics Since 1984

Artificial Intelligence Advances
https://ojs.bilpublishing.com/index.php/aia

ARTICLE

Robotic Unicycle Intelligent Robust Control Pt I: Soft Computational Intelligence Toolkit

Ulyanov Sergey[1,2,3*] Ulyanov Viktor[2,3] Yamafuji Kazuo[4]

1. Dubna State University, Institute of system analysis and management, Dubna, Moscow, 141980, Russia
2. INESYS LLC (EFKO GROUP), Ovchinnikovskaya naberezhnaya 20, Bld 1, Business Centre "Central City Tower", Moscow, 115035, Russia
3. NUST MISIS IYS Lab, Leninskiy prospekt 4, Moscow, 119049, Russia
4. Dept. of Mechanical and Intelligent Control Eng., University of Electro-Communications, 1-5-1 Chofu, Chofugaoka, 182 Tokyo, Japan

ARTICLE INFO

Article history
Received: 12 December 2019
Accepted: 16 April 2020
Published Online: 30 April 2020

Keywords:
Robotics unicycle
Intelligent control systems
Essentially nonlinear model
Globally unstable model
Stochastic simulation
Soft computing

ABSTRACT

The concept of an intelligent control system for a complex nonlinear bio-mechanical system of an extension cableless robotic unicycle discussed. A thermodynamic approach to study optimal control processes in complex nonlinear dynamic systems applied. The results of stochastic simulation of a fuzzy intelligent control system for various types of external / internal excitations for a dynamic, globally unstable control object - extension cableless robotic unicycle based on Soft Computing (Computational Intelligence Toolkit - SCOptKB™) technology presented. A new approach to design an intelligent control system based on the principle of the minimum entropy production (minimum of useful resource losses) determination in the movement of the control object and the control system is developed. This determination as a fitness function in the genetic algorithm is used to achieve robust control of a robotic unicycle. An algorithm for entropy production computing and representation of their relationship with the Lyapunov function (a measure of stochastic robust stability) described.

1. Introduction: Intelligent Mechatronics as an Implementation Background of a New Types of Nonlinear Mechanical Systems Motion

The extraction of knowledge from a new movement types of real physical control objects is based on benchmarks mathematical models' simulation. The robotic unicycle motion is one of such type of "benchmark movements" (benchmark model of nonlinear mechanics [1-5]), described as nonlinear nonholonomic, global unstable dynamic system. Related research of such dynamic systems is interesting for nonlinear mechanics (to develop a new method of nonlinear effects research) and for modern control theory (to deve1op a new intelligent control algorithms).

Modern methods and algorithms of intelligent control development

**Corresponding Author:*
Ulyanov Sergey,
Dubna State University, Institute of system analysis and management, Universitetskaya str., 19, Dubna, Moscow, 141980, Russia; INESYS LLC (EFKO GROUP), Ovchinnikovskaya naberezhnaya 20, Bld 1, Business Centre "Central City Tower", Moscow, 115035, Russia; NUST MISIS IYS Lab, Leninskiy prospekt 4, Moscow, 119049, Russia;
Email: ulyanovsv@mail.ru

 DOI: https://doi.org/10.30564/aia.v2i1.1556

The development of an algorithm and control system for robotic unicycle benchmark requires a new technology of unconventional computing - computational intelligence toolkit. The physical feature of robotic-unicycle is that the real unicycle bike's control is realized by skillful human being operator only. This leads to the studying of the robotic unicycle as a biomechanical system includes new approaches to the control system, such as intuition, instinct and emotions inherent to the human-operator (rider) and allowing to study the possibility of cognitive control by including the "human factor" in the control loop. The control of the robotic unicycle motion is based on the coordination of the complex movement components (pedaling and movement of the rider's torso). Changing the components coordination type generates new types of movement (rectilinear movement, slalom, dance, jumping, etc.). From nonlinear mechanics view point it is 3D synergetic effects of energy transfer from one generalized coordinate to others apply nonlinear relationships between generalized coordinates described by system of nonlinear equations.

Related works. Previous studies conducted in the field of different unicycle robot mechanical models controlling (see, Table 1) considered the system only from the point of view of a mechanical model using classical control methods and / or a simplified, hybrid fuzzy proportional-differential controller (FPD) with empirical tables of fuzzy decision making (production) rules (look - up Tables) [1-4]. However, this become an algorithmically intractable problem for traditional control methods in the task solution of robust (stable) motion of the object and led to appearing of new approaches to solve this issue.

The concept of this research and development of robotic unicycle intelligent control system becomes the structure shown in Figure 1.

To solve the problem of this object controlling a cyber-physical model called as "Conceptual Logical Structure of the Distributed Knowledge Representation (Information Levels) in the Artificial Life of the Robotic Unicycle" (Figure 1 a, b) as a biomechanical model of movement and control was developed and proposed.

The main research objective is studying the control problem of the robotic unicycle nonlinear biomechanical model, as well as the creation and "training" of a control system by means of available soft computing methods and algorithms.

To assess the quality of control, a new physical principle: the minimum entropy production rate in the object's movement and in the control system [2-5,7-13]. The physical measure of entropy production rate is applied as a fitness function in the genetic algorithm (GA).

Table. 1 Models of unicycle robot

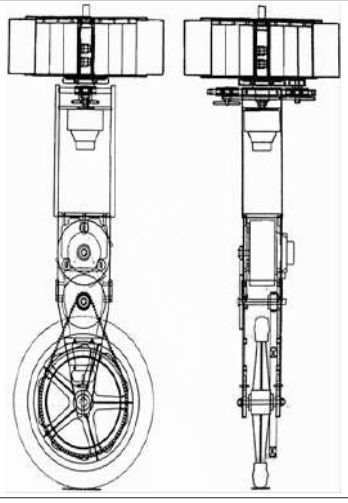

Schoonwinkel model 1987[1]

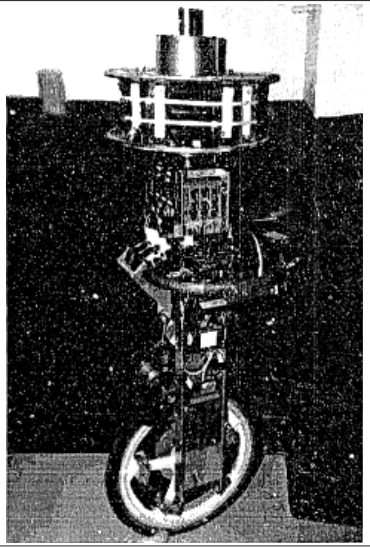

D.W. Vos model
1992 [2]

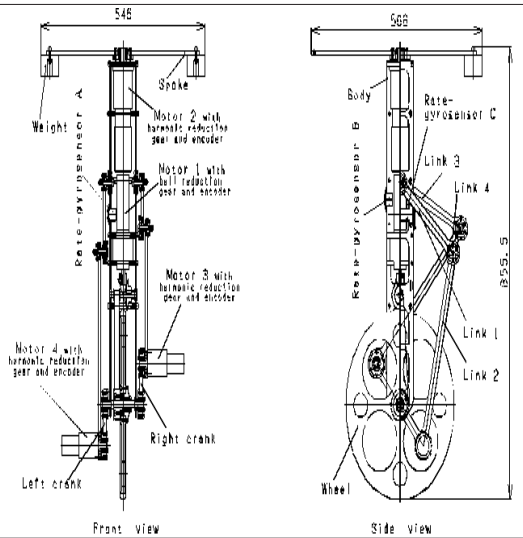

Yamafuji et all model
1995 [3-5]

DOI: https://doi.org/10.30564/aia.v2i1.1556

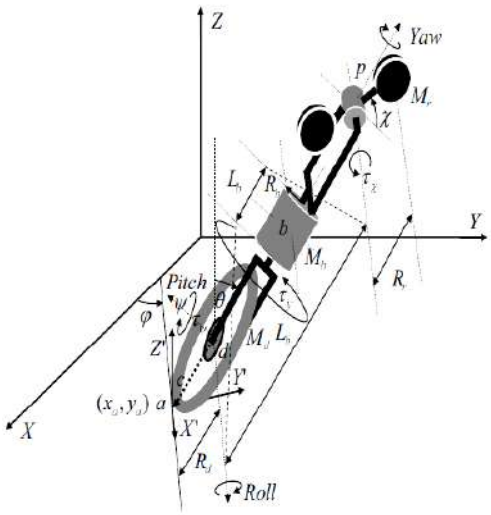

Kim et all model
2010 [18]

Murata Seiko Girl model 2011 [15]

Eric Wieser model
2017 [16]

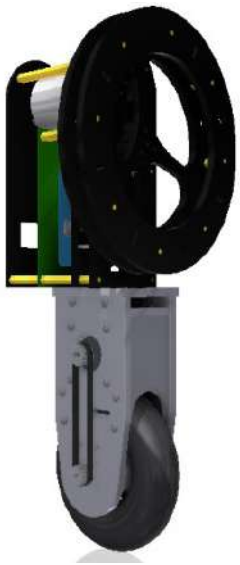

J.F. De Vries model 2018 [17]

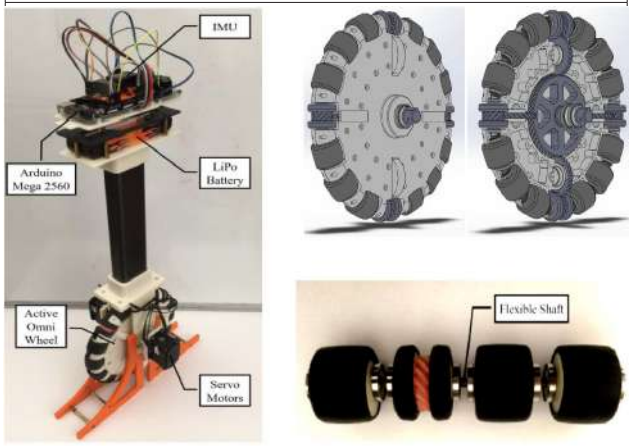

Shen J. model [27]

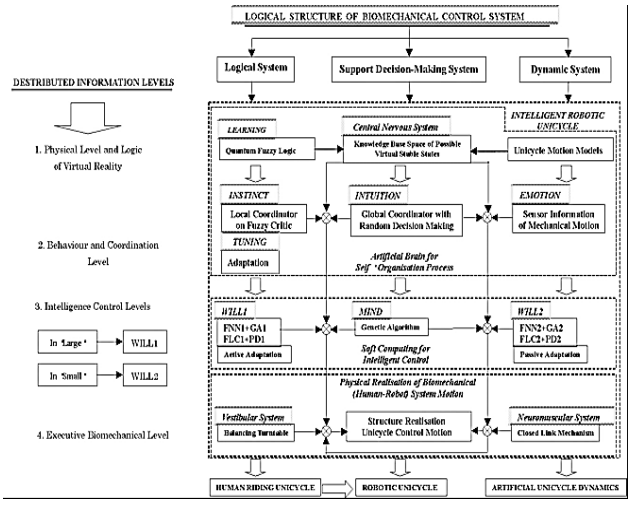

Figure 1(a). Conceptual Logical Structure of Distributed Knowledge Representation (on Information Levels) in Artificial Life of the Robotic Unicycle

 DOI: https://doi.org/10.30564/aia.v2i1.1556

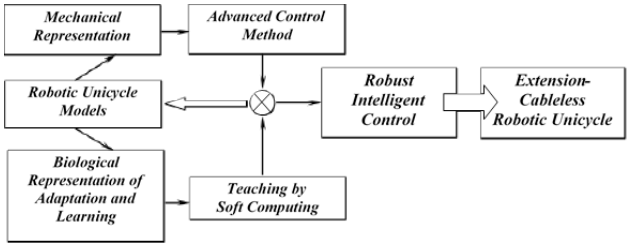

Figure 1(b). The conceptual scheme of the Robotic Unicycle R&D

This approach ensures the global stability of the dynamic control object and robustness it's of the control system. Based on this approach the "Self-organizing structure of an artificial intelligence (AI), robust control system design with a new physical measure of control quality" (see below Figure 3) with a new type of intelligent feedback based on the principles of computational intelligence, as well as "Fuzzy Simulation structure of an intelligent control system design with soft computing algorithms "(see Figure 5 below) has been developed. In previous studies, the problem of external and internal excitations on the mechanical and control system was not considered, see [1-4]. As a result, the global dynamic stability in object's control was not achieved.

In this article the modelling and optimization of intelligent control system with stochastic external / internal excitations simulation in the mechanical and control systems (floor roughness's, mechanical vibrations, zero sensors drift etc.) using the structure of the forming filters [5] is represented. The results of the simulation and experiment confirming the efficiency of the model robotic unicycle control system.

2. Problem Statement and Research Purpose: Creation of the Robotic Unicycle Mathematical Model with Essentially Nonlinear Intersection between Generalized Coordinates

As mentioned above, the objective of this research is development the intelligent control system for non-holonomic, essentially nonlinear, global spatially unstable with high amount of linking constraints model of the robotic unicycle. For this purpose, a new unicycle mathematical model was created for the "Real" unicycle's coordinate system (see, Figure 2).

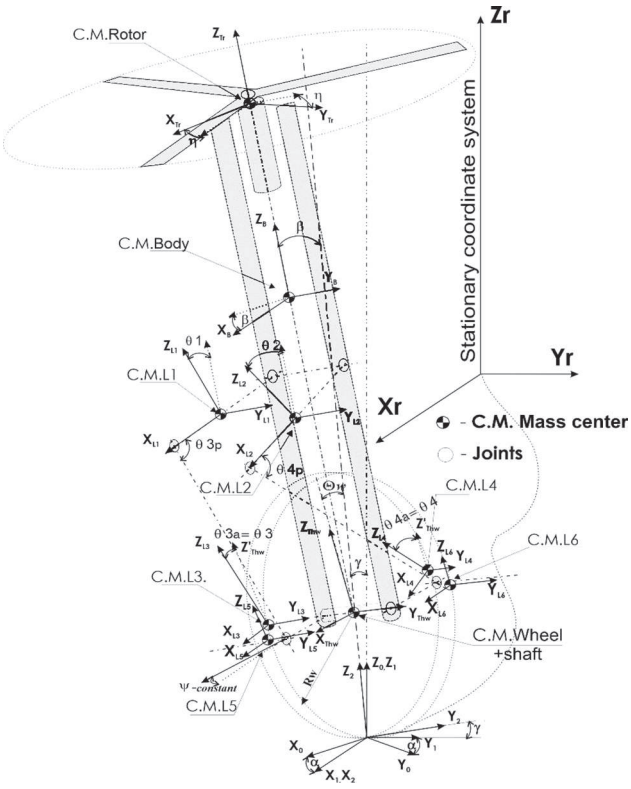

Figure 2. Coordinates description of the robotic unicycle model

For this coordinate system model derived the following explanations for basic and generalized coordinates, generalized velocities, accelerations:

Elemental Coordinates -q_j (t)=[$x0$,$y0$,α,γ,β,θw,Ψ,$\theta 1$, $\theta 2$,$\theta 3$,$\theta 4$,η]; where j = 1,…,12, $\Psi(t)=\theta w(t)+\psi(const)$, $\psi(const)$ - initial position of pedals Figure 2. (link 5,6). Hereinafter, the indices (i, j) denotes the serial numbers of elements in the corresponding vectors, matrices, and in the system equations

The *equation of non-holonomic constraints* in case of unslipping rolling between wheel and ground:

$$\frac{dx0(t)}{dt} = Rw \cdot \frac{d\theta w(t)}{dt} \cdot \cos(\alpha(t)); \quad \frac{dy0(t)}{dt} = Rw \cdot \frac{d\theta w(t)}{dt} \cdot \sin(\alpha(t)) \tag{1.1}$$

where Rw - wheel radius, $\frac{d\theta w(t)}{dt}$ - velocity of wheel rotation, $\alpha(t)$ - yaw angle. The coordinates x0, y0 are eliminated by substituting of Eq. (1.1) to kinematic Lagrangean part.

Generalized Coordinates -

$$q_j(t) = [\alpha, \gamma, \beta, \theta w, \theta 1, \theta 2, \theta 3, \theta 4, \eta]\text{, j} = 1,\ldots,9.$$

DOI: https://doi.org/10.30564/aia.v2i1.1556

In Figure 2 notation: α - yaw angle; γ - roll angle; β - pitch angle; C.M. - center of mass; L 1,…,6 - links 1-6; θ1, …,4 - links rotation angles; Ψ - initial position of pedals and the current angle of pedal rotation (link 5,6) is included in equations as summa - $\Psi(t)=\theta w(t)+\psi(const)$.

Thus, Lagrangian solving including represented above equations of nonholonomic/holonomic constraints and external forces of stochastic excitations, gives the following generalized stochastic equation of the robotic unicycle system motion with control:

$$\begin{cases} ME_{i,j}(q)\cdot \overset{\cdot T}{q_j}(t) = \tau^T{}_i + C^T{}_i(q,\lambda) + \xi^T{}_i(t) - (BT_{i,j}(q,\dot{q})\cdot \dot{q}_j^T(t) + G^T{}_i(q) + D^T{}_i(\dot{q})) \quad (a), \\ A_{i,n}(q)\cdot\lambda_n = Mc_{i,j}(q)\cdot \overset{\cdot T}{q_j}(t) + Bc_{i,j}(q,\dot{q})\cdot \dot{q}_j^T(t) + Gc^T{}_i(q) + Dc^T{}_i(\dot{q}) - \tau c^T{}_i - \xi c^T{}_i(t) \quad (b), \end{cases} \tag{1.2}$$

where - i,j=1..9; vector of generalized accelerations $\ddot{q}_j(t)=[\ddot{a},\ddot{\gamma},\ddot{\beta},\ddot{\theta}w,\ddot{\theta}1,\ddot{\theta}2,\ddot{\theta}3,\ddot{\theta}4,\ddot{\eta}]$; vector of generalized velocities $\dot{q}_j(t)=[\dot{\alpha},\dot{\gamma},\dot{\beta},\dot{\theta}w,\dot{\theta}1,\dot{\theta}2,\dot{\theta}3,\dot{\theta}4,\dot{\eta}]$. In the system of equations Eq (1.2), equation (a) is the dynamical equation of motion for the whole unicycle model with stochastic excitations, and equation (b) is the description of Lagrangian multipliers λ_n, where n=1…4. Matrices, vectors and another terms of equations (1.2) described in detail in the following sections of this article.

Stochastic excitation appears in case of $\xi c_i(t)$ & $\xi_i(t) \neq 0$ and described via differential equation *of Forming Filter* as Gaussian (as in our case) random process with autocorrelation function $R(\tau_{\xi}^{'}) = \sigma_{\xi}^2 \cdot \exp(-\alpha_{\xi} \cdot |\tau_{\xi}^{'}|)$. This disturbance is included into equation of motion for some generalized coordinates, and it is modelling possible roughness of flow, jamming in closed-links mechanism, and inaccuracy of angular acceleration measuring (sensors zero drift).

Under these conditions obtained ***stochastic equation of motion*** with parametric excitations. All of this gives a possibility to simulate behavior of dynamic controlled system more realistically and to determine real parameters of intelligent controllers for error estimation and control robustness. Stochastic modelling via Forming Filters is described below in [5].

3. Stability Estimation of Robotic Unicycle System

For definition of (un)stability is used a *Salvadory* theorem about equilibrium of mechanical systems with dissipative forces of a $Q_i(q,\dot{q})$ type along with full energy of system $E(q,\dot{q})$ as Lyapunov function $V(q,\dot{q}) \equiv E(q,\dot{q}) = T(q,\dot{q}) + U(q)$; where $T(q,\dot{q})$ is kinetic energy of system, $U(q)$ - potential energy of system. Under Lyapunov's theorem conditions, if the function $V(q,\dot{q})$ is: 1) positively determined about any $q,\dot{q}$ and have 0 at $(q,\dot{q})$=0, i.e. $V(q,\dot{q}) \geq a(q,\dot{q})$ & $V(0)=0$, where a is a some continuous, strictly increasing function, satisfying to a condition a(0)=0; 2) Derivative of function V by time t is negative, i.e. $\dot{V}(q,\dot{q}) \leq 0$; when origin is stable [6]:

Let's considering conditions of Salvadori's theorem that determine the dynamical systems stability.

Assume iff:

(1) U(q) have minimum at q=0;

(1a) U(q) don't have minimum at q=0;

(2) equilibrium statement q=0 is insulated;

(3) absolute dissipation $(Q \mid \dot{q}) \leq -a(\dot{q})$, where a is a strictly positive definite function.

Then with conditions 1) equilibrium state $(q,\dot{q})$ = 0 is stable; in the case 2), with condition 1a), equilibrium state $(q,\dot{q})$ = 0 - unstable.

Basing on the both theorems lets define a stability condition of robotic unicycle system.

The equation for expression of robotic unicycle potential energy for q_j = (0,0,0,0,θ1,θ2,θ3,θ4, 0) has following form:

$$\sum_n U_n(0) = g\cdot[Rw\cdot\sum_n \mathrm{M}_n + \mathrm{M}_3\cdot(2\cdot e1 - e2\cdot(\sin(\theta 1) + \sin(\theta 2))) + \Delta z\cdot \mathrm{M}_5\cdot(\cos(\theta 3)+\cos(\theta 4)) + \mathrm{M}_7\cdot e6] \tag{1.3}$$

where: coordinates - $\theta 1,\theta 2,\theta 3,\theta 4$ cannot be equal to 0 at $\gamma,\beta,\theta w$ =0 by mechanical constraints of closed-links mechanism; M_i - masses of robotic unicycle parts; *Rw, e1,e2,e6,* Δz - sizes in Figure 2. From Eq. (1.3) follows, that U(0) has ***maximum*** value in the equilibrium statement. The Eq. (1.3) satisfies to a condition 1a) of *Salvadory* theorem, that describes instability of robotic unicycle system at equilibrium statement. This enables to assert about global instability of the robotic unicycle autonomous dynamic system. However, as discussed in [6], in case the U(0) has maximum value it might happen that equilibrium will be stable owing to occurrence of external forces, such as gyroscopic or similar that in our case is controlled torques.

This research proclaims that it is possible to create such intelligent control system, which can continuously stabilize dynamic motion of nonlinear robotic unicycle and the simulation results are shown below.

4. Methods for Task Solving - Conceptual Model of Biomechanical Robotic Unicycle Control System

To provide computational intelligence methods that can

 DOI: https://doi.org/10.30564/aia.v2i1.1556

coordinating the complex motion components, it is necessary to use qualitatively new control algorithms that can operate with linguistic variables [8]. Soft computing methods fully satisfy to requirements, and that is determines their use. Based on the physical and sophisticated description of the biomechanical model, and using soft computing methods, the following structure of modeling the intelligent control system is represented.

Biomechanical Model of Intelligent Control System. The human riding control of the unicycle as logic-dynamic hierarchical process may be formed by:

(1) mechanical dynamic system "*human-rider - unicycle*";

(2) decision-making process of unicycle intelligent control with different levels of "*riding skills*";

(3) logical behavior for human body motorists (legs, hands and torso coordination) based on intuition, instinct, and emotion mechanisms;

(4) distributed information system for cooperative coordinating of sub-systems in biomechanical model [8].

In accordance with this representation of dynamic control process a hierarchical logic structure of distributed knowledge representation of the robotic unicycle artificial life is shown in Figure 1. For description of artificial life of robotic unicycle, the methods of qualitative physics for internal world representation based on mathematical model of unicycle motion used.

Logic structure of biomechanical control system for description a human riding of unicycle includes four levels:

(1) distributed information levels with sub-levels;

(2) logical system;

(3) support decision-making system;

(4) dynamic mechanical system.

Further the proposals of this structure are described in details. *Distributed information levels* include *four* sub-levels:

(1) physical level and logic of virtual reality;

(2) behavior and coordination level;

(3) intelligent control levels with two sub-levels;

(4) executive biomechanical level.

Intersections between the horizontal lines of distributed information levels and vertical lines of *logical system, support decision-making system, and dynamic system* (of unicycle motion and a human-rider behavior as biomechanical control model) realize the particular for human unicycle riding models with different skill levels of smart control tools using. Let's consider here this approach with examples.

Example 1: *Physical and logical level of virtual reality*. The intersection of the first horizontal level (Physical and logical level of virtual reality) with the first vertical level (Logical system) gives the structure of the human learning process to ride (control) a unicycle. The intersection with the second vertical level (support decision making system) corresponds to the level of the central nervous system (CNS) as a biological control system. The intersection with the third level (Dynamic (mechanical) system) is introduced mechanical model of the of a unicycle movement as a dynamic system. The logical sum of these sublevels implements the physical level of the unicycle movement description and the physical interpretation of the experimental data (attempts). The mathematical background for describing the learning process is the *quantum fuzzy logic*. The functions of the CNS are realized as the knowledge base (KB) domain of possible stable states. But, to create a control system of such a high intelligent level is not currently possible.

Example 2: *Behavior and coordination level.* This structure includes the mechanisms of instinct, intuition and emotion. The mechanism of instinct is described in the logical structure as a *local coordinator* with fuzzy rules and corresponds to a control structure with *active and passive adaptation* based on a fuzzy neural network (FNN). The mechanism of intuition is represented as a *global coordinator* and realized in the control process as a decision-making process based on a genetic algorithm (GA). The mechanism of emotions is described basing on the information from motion sensors and represented in the form of lookup tables with different semantic expression of the linguistic description of the desired dynamic motion behavior (as examples, "smoothly", "quickly" and so on). Thus, the intersection of two distributed information levels with logical systems is realizing the artificial brain unit for the process of unicycle control system self-organization.

Example 3: The Intelligent control level - an artificial intelligent control system with a distributed knowledge representation, includes "will" and "mind" (desires and opportunities) concepts, just like a human being [9,10]. For the mechanisms of instinct and emotion, new lookup tables are determined using an FNN. The mechanism of intuition is realized on the GA basis and directs the two fuzzy controllers' actions. Thus, the fuzzy simulation based on mathematical GA and FNN tools implements the soft computing algorithm in the robot's intelligent control system.

From a qualitative physical description and movement simulation the domain of possible virtual stable states described by a strange attractor is obtained, as it was shown in [3,4]. This suggests that the human postural control system is a highly organized complex system and the position

DOI: https://doi.org/10.30564/aia.v2i1.1556

of the human body changes (sways) stochastically. This fully corresponds to the results described in [11].

Example 4: *Executive biomechanical level - the physical process of the robotic unicycle system realization.* In this case, the *vestibular system* as a logical control system is realized by the *balancing turntable* (torso, shoulder girdle and arms), and the *neuro-muscular* system is formed by the *closed-links mechanism of the legs*.

Thus, the dynamic process of human unicycle riding control with different intelligent behavior levels should be described as the intersection of logical systems with distributed information levels.

The intelligent robust control system structuring. The development of complex dynamic systems robust motion control has two ways of research: 1) the study of stable motion processes; and 2) the study of unstable motion processes of complex dynamic systems.

As mentioned above, our attention has been focused on the study of the robotic unicycle as a dynamic, global-spatially unstable controlled object. Such a global-spatially unstable dynamic object requires a new intelligent robust control algorithm based on knowledge description of an essentially nonlinear, unstable dynamic system movements [3,8]. The structure of the intelligent robust control algorithm in the conceptual form for the entire class of unstable dynamic control objects, was described in [2-4,8], here we apply it to the problem of controlling the robotic unicycle.

The control structure with a new intelligent feedback type is represented in Figure 3. It is based on the *scheme of a conventional control system with linear feedback P(I)D*, intelligent soft computing tools (fuzzy set theory, fuzzy neural networks (FNN), genetic algorithms (GA)); nonlinear model of the control object; entropy production rate calculating; stochastic simulation of random external/internal excitations.

In the structure Figure 3 the following designations are used: GA - Genetic Algorithm; f - Fitness Function of GA; S- Entropy of System; S_c - Entropy of Controller; S_i - Entropy of Controlled Plant; - Error; u*- Optimal Control Signal; m(t) - Disturbances (random external/internal excitations); FC - Fuzzy Controller; FNN - Fuzzy Neural Network; FLCS - Fuzzy Logic Classifier System; SSCQ - Simulation System of Control Quality; K - Global Optimum Solution of Coefficient Gain Schedule (Teaching Signal); LPTR - Look-up Table of Fuzzy Rules; CGS - Coefficient Gain Schedule (in case of 2 PD controllers - $K = (k_1, k_2, k_3, k_4)$).

The control self-organization in this system, at the first stage, is provided by optimizing the control parameters of the P(I)D controller by selecting the best solutions with a genetic algorithm, in which the selection criterion is the best fitted solution, calculated using the fines function. To determine solution fitness's a new physical measure of control quality is used - ***a entropy production minimum rate.*** This measure is the difference between entropy production by the control object itself and the control system included in it. This allows you to adapt the parameters of the linear control system to a nonlinear control object [7,12].

The next adaptation stage is training the control system to ensure its robustness. This step is based on a fuzzy logic classifier that defines fuzzy rules for logical relationships of linear controller parameters. The classifier is the FNN for which the training signal is optimized control parameters obtained from the genetic algorithm output. This stage generates fuzzy lookup tables, adapted control parameters of the low-level controller P(I)D.

In this approach, solving the problem of a nonlinear object controlling, the criterion of the control quality (controllability) is the entropy production function, which is directly related to the Lyapunov function i.e. to a dynamic system stability, as it shown in [7,12,13]. The interrelation between these functions in an intelligent control system ensures its robustness, as shown in Figure 4. Further, the obtained lookup tables are used by a fuzzy controller (FC) to control the linear controller parameters.

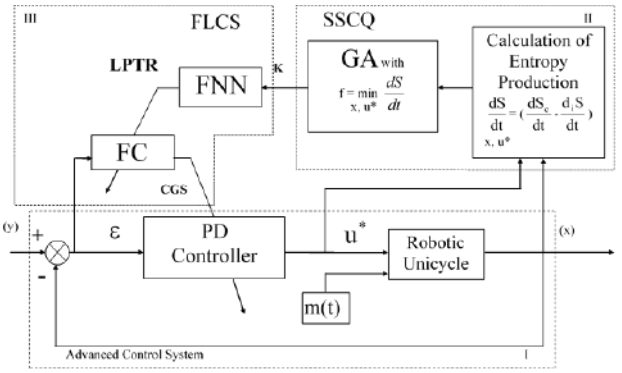

Figure 3. Self-organizing structure of an artificial intelligent (AI), robust control system design with a new physical measure of control quality

Description:

1. GA - Genetic Algorithm;	**10. FNN - Fuzzy Neural Network;**
2. f - Fitness Function of GA;	**11. FLCS - Fuzzy Logic Classifier System;**
3. S- Entropy of System;	**12. SSCQ - Simulation System of Control Quality;**
4. S_c - Entropy of Controller;	**13. K - Global Optimum Solution of Coefficient Gain Schedule (Teaching Signal);**
5. S_i - Entropy of Controlled Plant;	**14. LPTR - Look-up Table of Fuzzy Rules;**
6. e - Error;	**15. CGS - Coefficient Gain Schedule $K=(k_1,k_2,k_3,k_4)$.**
7. u*- Optimal Control Signal;	
8. m(t) - Disturbance;	
9. FC - Fuzzy Controller;	

 DOI: https://doi.org/10.30564/aia.v2i1.1556

Figure 4. Interrelation structure between a Stability, Robustness and Controllability of the system

Based on the intelligent control structure and interrelationship in Figure 4, the *Fuzzy Simulation structure of an intelligent control system design* was developed in Figure 5.

Simulation is decomposed into two main stages: **Off-Line** and **On-Line**. At the first stage a controlled object mathematical model is creating and the thermodynamic equations of its states are founding to calculate the entropy. Further, the equations for entropy production forming the GA fitness function. GA in computer stochastic simulation mode optimizes the P(I)D controller parameters. The next step is the training of the control system based on the optimized controller parameters obtained from the GA and obtaining lookup tables (FC Knowledge Base) using the FNN.

In **On-Line** mode basing on the obtained lookup tables the P(I)D controller parameters of the robotic unicycle are changes by a fuzzy controller in real time. The structure of the robot control system is described below.

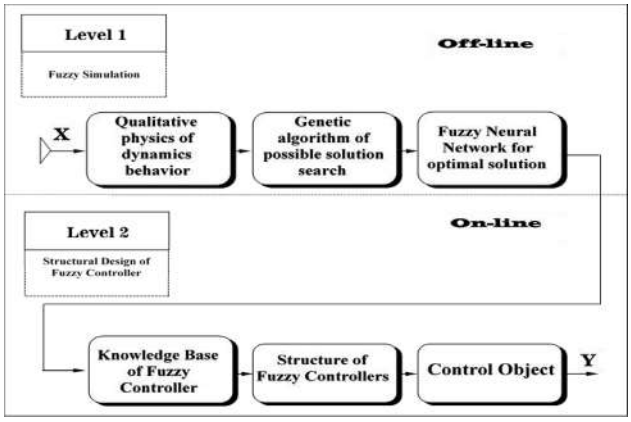

Figure 5. Fuzzy Simulation structure of an intelligent control system design

5. Mathematical System Modeling Using Soft Computing Methods

The simulation basis is a mathematical description of the control object motion represented in (1.2). Let us dwell on the equations (1.2) description.

For the mathematical simulation of a robotic unicycle movement the following parameters of the model (1.2) are adopted and graphically represented in Figure 2: where - $i,j = 1 \ldots 9$; $\ddot{q}_j(t) = [\ddot{\alpha}, \ddot{\gamma}, \ddot{\beta}, \ddot{\theta}w, \ddot{\theta}1, \ddot{\theta}2, \ddot{\theta}3, \ddot{\theta}4, \ddot{\eta}]$ - vector of generalized accelerations;

- vector of generalized velocities; In the system of equations Eq(1.2), equation (a) is the dynamic equation of motion for the whole unicycle model, and equation (b) is the description of Lagrangian multipliers λ_n, where $n = 1 \ldots 4$.

In Eq.(1.2,a), $ME_{i,j}(q)$ is a 9×9 block matrix that consists of inertial acceleration's terms $M(q)$, derived from Lagrange equations, and geometrical acceleration's terms derived from equations of closed-links mechanism constraints $E(q)$; $BT_{i,j}(q,\dot{q})$ is a 9×9 block matrix that consists of Coriolis and centrifugal $B(q,\dot{q})$ & $T(q,\dot{q})$ terms, derived from Lagrange equations, and equations of closed-links mechanism constraints, respectively; $G_i(q)$ is a 9-dimensional vector of gravity terms $G_i(q) = [0, G_2(q), G_3(q), G_4(q), 0, 0, 0, 0, 0]$; $D_i(q,\dot{q})$ is a 9-dimensional vector of viscous friction forces terms $D_i(\dot{q}) = [D_1(\dot{q}), D_2(\dot{q}), D_3(\dot{q}), D_4(\dot{q}), 0, 0, 0, 0, D_9(\dot{q})]$; τ_i is a 9-dimensional vector of torque $\tau_i = [0, 0, 0, 0, 0, 0, 0, 0, \tau_{(\eta)3}]$; $C_i(q,\lambda)$ is 9-dimensional vector of Lagrangian multipliers with respected coefficients of constraint equations $C_i(q,\lambda) = [0, 0, C_{(\beta)1}, C_{(\theta w)2}, 0, 0, 0, 0, 0]$; $\xi_i(t)$ is 9-dimensional vector of given stochastic excitation.

$$ME_{i,j}(q) = \begin{bmatrix} M_{11}(q) & .. & .. & .. & .. & M_{19}(q) \\ .. & .. & .. & .. & .. & .. \\ M_{41}(q) & .. & .. & .. & .. & M_{49}(q) \\ 0 & 0 & E_{53}(q) & .. & E_{58}(q) & 0 \\ .. & .. & .. & .. & .. & 0 \\ 0 & 0 & E_{83}(q) & .. & E_{83}(q) & 0 \\ M_{91}(q) & .. & .. & .. & .. & M_{99}(q) \end{bmatrix};$$

$$BT_{i,j}(q,\dot{q}) = \begin{bmatrix} B_{11}(q,\dot{q}) & .. & .. & .. & .. & B_{19}(q,\dot{q}) \\ .. & .. & .. & .. & .. & .. \\ B_{41}(q,\dot{q}) & .. & .. & .. & .. & B_{49}(q,\dot{q}) \\ 0 & 0 & T_{53}(q,\dot{q}) & .. & T_{58}(q,\dot{q}) & 0 \\ .. & .. & .. & .. & .. & 0 \\ 0 & 0 & T_{83}(q,\dot{q}) & .. & T_{83}(q,\dot{q}) & 0 \\ B_{91}(q,\dot{q}) & .. & .. & .. & .. & B_{99}(q,\dot{q}) \end{bmatrix};$$

In Eq.(2,b), $Mc_{i,j}(q)$ is a 9×9 matrix of inertial acceleration's terms M(q) derived from Lagrange equations; $Bc_{i,j}(q,\dot{q})$ is a 9×9 matrix of Coriolis and centrifugal $B(q,\dot{q})$ terms, derived from Lagrange equations; Gc_i(q) is a 9-dimensional vector $Gc_i(q) = [0, 0, 0, 0, G_5(q), G_6(q), G_7(q), G_8(q), 0]$ of gravity terms; $Dc_i(q,\dot{q})$ is a 9-dimensional vector $Dc_i(\dot{q}) = [0, 0, 0, 0, D_5(\dot{q}), D_6(\dot{q}), D_7(\dot{q}), D_8(\dot{q}), 0]$ of viscous friction forces terms; τc_i is a 9-dimensional vector of torque $\tau c_i = [0, 0, 0, 0, 0, 0, 0, \tau_{(\theta 3)1}, \tau_{(\theta 4)2}, 0]$; $\xi c_i(t)$ is given stochastic excitation; $A_{i,n}(q)$ is a 9×4 matrix of

DOI: https://doi.org/10.30564/aia.v2i1.1556

geometrical terms derived from constraints equations of closed-links mechanism, correspond to motion equation by i index; λ_n- 4-dimensional vector of Lagrangian multipliers:

$$Mc_{i,j}(q)=\begin{bmatrix} 0 & .. & 0 \\ .. & .. & .. \\ M_{51}(q) & .. & M_{59}(q) \\ .. & .. & .. \\ M_{81}(q) & .. & M_{89}(q) \\ 0 & .. & 0 \end{bmatrix};$$

$$Bc_{i,j}(q,\dot{q})=\begin{bmatrix} 0 & .. & 0 \\ .. & .. & .. \\ B_{51}(q,\dot{q}) & .. & B_{59}(q,\dot{q}) \\ .. & .. & .. \\ B_{81}(q,\dot{q}) & .. & B_{89}(q,\dot{q}) \\ 0 & .. & 0 \end{bmatrix};$$

$$A_{i,n}(q)=\begin{bmatrix} 0 & 0 & 0 & 0 \\ .. & .. & .. & .. \\ A_{51}(q) & A_{52}(q) & 0 & 0 \\ 0 & 0 & A_{63}(q) & A_{64}(q) \\ A_{71}(q) & A_{72}(q) & 0 & 0 \\ 0 & 0 & A_{83}(q) & A_{84}(q) \\ 0 & 0 & 0 & 0 \end{bmatrix}$$

The equations of the Robotic Unicycle system's controlled torques. In the case of PD controller for the Links mechanism, the controlled torque is given as:

$$\tau_{(\theta 3)1}=-\tau_{(\theta 4)2}=-kp1(T)\cdot\beta(t)-kd1(T)\cdot\dot{\beta}(t) \quad (4.1)$$

and for the Rotor mechanism - as:

$$\tau_{(\eta)3}=kp2(T)\cdot\gamma(t)+kd2(T)\cdot\dot{\gamma}(t) \quad (4.2)$$

GA generates P(I)D controller's parameters $kp1(T), kp2(T), kd1(T), kd2(T)$, selecting them basing on the results of the fitness function calculations, each sampling time T = 0.05sec. This sampling time is defined from real controller scheme of Robotic Unicycle.

Information-thermodynamic criterion of the control qualities distribution. The thermodynamic ratio of the robust intelligent control quality to the optimization criterion, used in the quantum algorithm (QA) of a knowledge bases (KB) self-organization [8], are shown in Table 2. In Table 2 the following notations are introduced: V- Lyapunov function; S_O, S_C entropy production in the Control Object & Controller, respectively; $V=\frac{1}{2}\sum_{i=1}^{n}q_i^2+\frac{1}{2}S^2; S=S_O-S_C; \dot{q}_i=\phi(q_i,u,t)$ - the CO equation of motion; q_i - generalized coordinates; u - the desired control.

In the Table. 2, the equation of a dynamic system control qualities distribution connects in an analytical form, on the basis of the phenomenological thermodynamics entropy concept, such a qualitative notions of control theory as - stability, controllability and robustness. As a result, the necessary distribution between the stability, controllability and robustness levels allows achieving the control goals in emergency situations with a minimum of useful resource consumption by using as a GA's fitness function the criterion of minimum generalized entropy production. The thermodynamic definition of the S and information H entropies are interrelated by the von Neumann relation in the form: $S=kH=-k\sum_i p_i \ln p_i$, where $k\approx 1.38\times 10^{-23}$ J/K is the Boltzmann constant. As a result (after substitution of this ratio), obtained an equation that also relates stability, controllability and robustness, but on the basis of the Shannon's information entropy, which allows to determine the control to guaranteed achievement of the control goal in emergency situations with the requirement of a minimum information quantity about the external environment and CO states.

As mentioned above, to assess the quality of control, a new physical principle: the minimum entropy production rate in the object's movement and in the control system [4-13]. The physical measure of entropy production rate is applied as a fitness function in the genetic algorithm (GA).

Closed system	Open system
$\dot{q}_i=\varphi(q_i,t)$ Control Object Lyapunov Function $\frac{dV}{dt}=-\frac{1}{T}\frac{dS_O}{dt}$	Thermodynamic correlation between stability, controllability and robustness $0>\underbrace{\frac{dV}{dt}}_{\text{Stability Condition}}=\underbrace{\sum_i q_i\cdot\varphi(q_i,u,t)}_{\text{CO Dynamics Controllability}}+\underbrace{(S_O-S_C)\cdot\left(\frac{dS_O}{dt}-\frac{dS_C}{dt}\right)}_{\text{Thermodynamic CO Behavior Robustness}}$
Generalized Entropy Production Rate $S_G=(S_O-S_C)\cdot\left(\frac{dS_O}{dt}-\frac{dS_C}{dt}\right)$ Control Object Controller	Robustness Criteria $\min_{q,u}\int S_G\,dt$

Table 2. Thermodynamic ratio of a robust intelligent control quality distribution

Therefore, these ratios are forming an equations system of control defining which guarantees the control goal achievement in emergency situations with a minimum useful resource consumption and the minimum required initial information [8-13].

Information and thermodynamic distribution of

 DOI: https://doi.org/10.30564/aia.v2i1.1556

control quality rates. Assume that the control object is described in general form by the equation $\dot{q}_i = \varphi\left(q,t,S\left(t\right),u\right)$, where the generalized coordinate q_i describes the control object movement, u is the desired control and $S\left(t\right) = S_O\left(t\right) - S_C\left(t\right)$ is the generalized entropy of the system represented as the difference between the control object's entropy production $S_{\mathrm{O}}\left(t\right)$ and the controller's entropy production . $S_{\mathrm{C}}\left(t\right)$ Consider the following equation:

$$\underbrace{\frac{dV}{dt}}_{Stability} = \underbrace{\sum_{i=1}^{n} q_i \cdot \varphi\left(q,t,S\left(t\right),u\right)}_{Controllability} + \underbrace{\left(S_{\mathrm{O}} - S_{\mathrm{C}}\right)\cdot\left(\dot{S}_{\mathrm{O}} - \dot{S}_{\mathrm{C}}\right)}_{Robustness} \le 0 \tag{4.3}$$

Equation (4.3) in analytical form interrelates such qualitative notations of control theory as stability V (Lyapunov function), controllability and robustness basing on the concept of phenomenological thermodynamics entropy [8,9,19-22].

This approach allows, as noted earlier, to find the necessary distribution between the levels of stability, controllability and robustness, which permitting to achieve the control goal in emergency situations with a minimum useful resource consumption by using the minimum generalized entropy production as a fitness function in the genetic algorithm, which is included in the right part Eq. (4.3).

Consider now the (4.3) regarding to the interrelation of thermodynamic entropy to Shannon information entropy. The thermodynamic definition of S and H entropies are interrelated by the von Neumann' relation in the: $S = kH = -k\sum_i p_i \ln p_i$, where $k \approx 1.38\times10^{-23}$ J/K is the Boltzmann constant. Substitution the Shannon information entropy - H instead of $S\left(t\right)$ in equation (4.3) give as a result:

$$\underbrace{\frac{dV}{dt}}_{Stability} = \underbrace{\sum_{i=1}^{n} q_i \cdot \varphi\left(q,t,k\left(H_O - H_C\right),u\right)}_{Controllability} + \underbrace{k\left(H_O - H_C\right)\cdot\left(\dot{H}_O - \dot{H}_C\right)}_{Robustness} \le 0 \tag{4.4}$$

Thus, equation (4.4) also interrelates stability, controllability and robustness, but already on the Shannon's information entropy basis, which also allows defining controlling approaches for guaranteed achievement of the control goal in emergency situations with the requirements of a minimum information about the external environment and the control object state. Consequently the (4.3) and (4.4) forming an equations system, which solution are determining the controlling approaches that guarantees the achievement of the control goal in emergency situations with a minimum useful resource consumption and the minimum initial information requirements.

6. The Cognitive Intelligent Control System Information-Thermodynamic Analysis

Result of equations (4.3) and (4.4) generalization is the following equations system:

$$\begin{aligned}\underbrace{\frac{\mathrm{dV}}{\mathrm{dt}}}_{Stability} &= \underbrace{\sum_{\mathrm{i}=1}^{\mathrm{n}} \mathrm{q_i}\cdot\varphi\left(\mathrm{q,t,k}\left(\mathrm{S_O} - \left(\mathrm{S_{Tc}} + \mathrm{S_{Cc}}\right)\right),\mathrm{u}\right)}_{Controllability} \\ &+ \underbrace{\left(\mathrm{S_O} - \left(\mathrm{S_{Tc}} + \mathrm{S_{Cc}}\right)\right)\cdot\left(\dot{\mathrm{S}}_{\mathrm{O}} - \left(\dot{\mathrm{S}}_{\mathrm{Tc}} + \dot{\mathrm{S}}_{\mathrm{Cc}}\right)\right)}_{Robustness} \le 0\end{aligned} \tag{5.1}$$

$$\begin{aligned}\underbrace{\frac{dV}{dt}}_{Stability} &= \underbrace{\sum_{i=1}^{n} q_i \cdot \varphi\left(q,t,k\left(H_O - \left(H_{\mathrm{Tc}} + H_{\mathrm{Cc}}\right)\right),u\right)}_{Controllability} \\ &+ \underbrace{\left(H_O - \left(H_{\mathrm{Tc}} + H_{\mathrm{Cc}}\right)\right)\cdot\left(\dot{H}_O - \left(\dot{H}_{Tc} + \dot{H}_{Cc}\right)\right)}_{Robustness} \le 0\end{aligned} \tag{5.2}$$

where $\left(S_{\mathrm{Tc}} + S_{\mathrm{Cc}}\right)$ and $\left(H_{\mathrm{Tc}} + H_{\mathrm{Cc}}\right)$ means the total thermodynamic and information entropies of the Technical intelligent (Tc) and Cognitive (Cc) controllers, respectively.

From equation (5.1) follows that the robustness of the intelligent control system can be increased by the cognitive regulator entropy producing, which reduces the useful resource consumption, and equation (5.2) shows that the negentropy of the cognitive controller reduces the minimum requirements for the initial information to achieve robustness. Moreover, information based on knowledge in the cognitive controller's KB allows to obtain an additional resource for effective capacity, which is equivalent to the appearance of a targeted action on the control object to ensure the achievement of the control goal.

One of the key tasks of modern robotics is the development of technologies for the cognitive interaction of robotic systems, which allow solving the tasks of intelligent hierarchical control by redistributing knowledge and control functions, for example, traditional "master - slave" system. Modern approaches to solving this issue are based on the theory of multi-agent systems, theory of a swarm

DOI: https://doi.org/10.30564/aia.v2i1.1556

artificial intelligence, and many others [8,9,23-25].

According to [24-26], in a multi-agent system there is a new synergetic information effect of knowledge bases self-organization and formation of an additional information resource arising from the information and knowledge exchanges between active agents (swarm synergetic information effect). Extraction of an additional resource in the form of quantum information, which hidden in classical states, is realized on the basis of quantum fuzzy inference, which in turn, is a new quantum search algorithm and a special case of a quantum self-organization algorithm.

Due to the synergistic effect, an additional information resource is created and the multi-agent system is able to solve complex dynamic tasks for the joint work implementation. The assigned task may not be performed by each element (agent) of the system individually in environments variety without external control, monitoring or coordination, but the exchange of knowledge and information allows to perform joint effective work to achieve the control goal in the conditions of initial information uncertainty and limitations on the useful resource consumption [14]. In particular, it is well known that for feedback control systems, the amount of recoverable useful work W satisfies the inequality $W_{max}(t) = k\int_0^t T_{min}\dot{I}dt' \le kTI_c$, where k is the Boltzmann constant, $T_{min}(t)$ is interpreted as the lowest achievable by the system temperature in time t under feedback control, assuming $T_{min}(0) = T$, and I_c determines the Shannon information quantity (entropy transfer) extracted by the system from the measurement process [23].

The synergetic effect physically means the self-organization of knowledge and creation of an additional information quantity that allows to the multi-agent system making the most useful work with a minimum useful resource consumption and with a minimum initial information requirement, nondestructive the lower executive control system level [22-25]. Together with the information-thermodynamic intelligent control law (optimal distribution of control qualities "stability -controllability - robustness"), an intelligent control system (ICS) for multi-agent systems is designed, which guarantees the achievement of the control goal in the conditions of initial information uncertainty and limited useful resource [14,19,25].

Let's consider these statements in more detail on the basis of the interrelationship analysis between the information quantity and extracted on its basis useful work and free energy.

As noted above, if microscopic degrees of freedom are available to the Maxwell demon observer form, then the second thermodynamics law can be violated. Szilárd showed from the Maxwell demon model analysis that the work in the form - $kT\ln 2$ is extracted from the thermodynamic cycle. Moreover, it was shown that the extracted work W_{ext}^S from the system is determined by the information quantity (or quantum-classical mutual information) I that determine the knowledge about the system during measurement. At the same time, a similar ratio in the form of a lower bound exists for the total measurement cost W_{cost}^M and information erasing $W_{ext}^S \le -\Delta F^S + kTI$ and $W_{cost}^M \ge kTI$, where ΔF^S determines the free energy of the system. Then it is easy to notice that the speed of the extracted work $\dot{W}_{ext}$ is limited by the value $\dot{W}_{ext} \le kT\dot{I}$, i.e. it is limited by the speed of the extracted information.

The proposed quantum algorithm model of ICS self-organization, based on the minimum information entropy principles (in the "intelligent" state of control signals) and on a generalized thermodynamic measure of entropy production (in the system "control object + controller"). The main result of the self-organization process application is the acquisition of the robustness necessary level and the reproducible structure flexibility (adaptability). It is noted that the robustness property (by its physical nature) is an integral part of self-organization, and the required level of ICS robustness is achieved by fulfilling the minimum generalized entropy production principle, described above. The minimum entropy production principle in the CO and control system [14] acting as the physical principle of optimal functioning with minimal useful work consumption and underlies the development of robust ICS. This statement is based on the fact that, for the general case of dynamic objects controlling, the optimal solution to the finite variational problem of the maximum useful work W determining is equivalent, according to [14], to the solution of the finite variational problem of finding the minimum entropy production S. Thus, the study of the conditions of the maximum functionality $\max_{q_i,u}(W)$ (where q_i, u a CO's generalized coordinates and the control signal respectively) are equivalent, accordingly to [25], to study the associated problem of the minimum entropy production, i.e. $\min_{q_i,u}(S)$.Therefore, in the developed quantum algorithm model, the applied principle of minimum informational entropy guarantees the necessary condition for self-organization - the minimum of the required initial information in the learning signals; the thermodynamic criterion of a new measure the generalized entropy production minimum provides a sufficient condition for self-organization - the control processes robustness with a minimum consumption of a useful resource.

More significant is the fact that the averaged val-

 DOI: https://doi.org/10.30564/aia.v2i1.1556

ue of the produced work by the dissipation forces - $\frac{W_{diss}}{kT} = S_{KL}\left(P_F P_B\right)$, i.e. the dissipation forces work is determined by the Kulbak-Leibler divergence for the probability distributions P_F, P_B. Note that the left part of this ratio represents the physically a thermal energy, and the right part determines a purely system's information.

Information entropy is a measure of the information quantity about a system and the Kulbak-Leibler divergence, as well as the Fisher's information quantity determination. The similar interrelation exists between the work produced by the dissipation forces and the Renyi divergence.

Thus, substituting into (5.1) and (5.2) represented relationship between information - the extracted free energy and the work obtaining the conclusion noted above - the intelligent control systems robustness may increase by the cognitive controller entropy production, which reduces the useful resource consumption of the control object, and same time, the negentropy of cognitive control reduces the minimum initial information requirements to achieve robustness. Therefore, the extracted information, based on knowledge in the cognitive controller's KB allows obtaining an additional resource for useful work, which is equivalent to appearance of a targeted action on the control object to guarantee the achievement of the control goal.

General mathematical simulation structure. The structure of *Fuzzy Simulation structure of an intelligent control system design* represented in Figure 5, and decomposed into two main stages: Off-Line and On-Line as mentioned earlier.

In the Off-Line a controlled object mathematical model is creating and the thermodynamic equations of its states are founding to calculate the entropy which forming the GA's fitness function and computer stochastic simulation with GA optimizes the P(I)D controller parameters.

In the next step GA randomly selects an optimized PD's controller parameters in the all possible solutions domain, using the minimum entropy production in the intelligent control system and in the complex nonlinear model dynamic behavior as a criterion for the solution suitability (fitness function). The fitness function of the GA is represented as:

$$Eval = \min((S^O - S^C)(\frac{dS^O}{dt} - \frac{dS^P}{dt})) \tag{5.3}$$

where $\frac{dS^C}{dt}$ - is the control system's entropy production rate; $\frac{dS^O}{dt}$ - is entropy production rate in the motion of the robotic unicycle (Object) with following condition: $\frac{dS^C}{dt} > \frac{dS^O}{dt}$. Description of entropy production rate calculation is presented in [8,9].

Thermodynamic equation of motion. The equations for calculation of the entropy production rate for intelligent control system and dynamic motion of robotic Unicycle are derived from approach as described in [8]. These equations are described in the following form:

$$\begin{bmatrix} \frac{dS^P}{dt} \\ \frac{dS^C}{dt} \end{bmatrix} = \begin{bmatrix} M_{i=j}(q) & 0 \\ 0 & 1 \end{bmatrix}^{-1} \cdot \begin{bmatrix} B_{i=j}(q,\dot{q}) \cdot \dot{q}^T(t) + D^T(\dot{q}) \\ \tau_d^T \end{bmatrix} \cdot \dot{q}^T(t) \tag{5.4}$$

where: i,j=1..9; $M_{i=j}(q)$ is a 9×9 diagonal matrix of inertial acceleration's terms $M(q)$ derived from Lagrange equations; $B_{i=j}(q,\dot{q})$ is a 9×9 diagonal matrix of Coriolis and centrifugal terms, derived from Lagrange equations; $D(\dot{q})$ is a 9-dimensional vector of viscous friction forces terms $D_i(\dot{q}) = [D_1(\dot{q}), D_2(\dot{q}), D_3(\dot{q}), D_4(\dot{q}), D_5(\dot{q}), D_6(\dot{q}),\ D_7(\dot{q}), D_8(\dot{q}), D_9(\dot{q})]$; τ_d is a 9-dimensional vector of torque's dissipative parts $kd_i \cdot [\dot{\beta}, \dot{\gamma}]$, $\tau_d = [0, \tau_3, \tau_{1,2}, 0, 0, 0, 0, 0, 0]$.

Following the Figure 5, the next step is the training of the control system based on the optimized controller parameters obtained from the GA and obtaining lookup tables (FC Knowledge Base) using the FNN.

In On-Line mode basing on the obtained lookup tables the P(I)D controller parameters of the robotic unicycle are changes by a fuzzy controller in real time.

7. Mathematical Simulation and Experimental Results

Soft Computing Simulation structure in MathLab Simulink® system is shown in Scheme 1. It consists from following parts:

(1) Block of main equations;

(2) Block of random excitation;

(3) Blocks of equation's coefficients;

(4) Blocks of Lagrangian multipliers calculation;

(5) Block of Intelligent control system based on Soft Computing - GA or FNN.

In all simulation cases, the real parameters of the robotic unicycle model were used see the Figure 6, and the corresponding stochastic effects: disturbing from the floor to the yaw rotation angle and jamming in the closed-links

DOI: https://doi.org/10.30564/aia.v2i1.1556

mechanism. (see Figure 7).

The method of algebraic loops expulsion, described in detail in the patent [19], was applied to accelerate the simulation processes. This method allowed to accelerate the computer simulation process - integration is about 190 times down with the difference in integration result less than 1%, as shown in Figure 8 and Figure 9.

Simulation results discussion. In Figure 4 shown the comparison of three types of control approaches:

(1) Conventional PD controller with fixed gain coefficients - temporal mechanical and thermodynamic controlled system behavior;

(2) The GA with fitness function as minimum of entropy production rate for conventional PD controller.

(3) The Fuzzy PD controller with lookup tables obtained after learning process by FNN with pattern from GA.

Such structure is the most applicable because of its flexibility, it has an opportunity to change only necessary separated blocks, such as control, main equations, excitation etc., without changing the whole structure.

From presented results it is visible, that: (1) usage of the approach described above, with application of a minimum entropy production rate as fitness function in GA and learning process by FNN, is completely justified; (2) dynamic motion occurs more smoothly even the control signal's discretization time is use in PD-GA and Fuzzy PD controllers with sampling time = 0.05 sec.

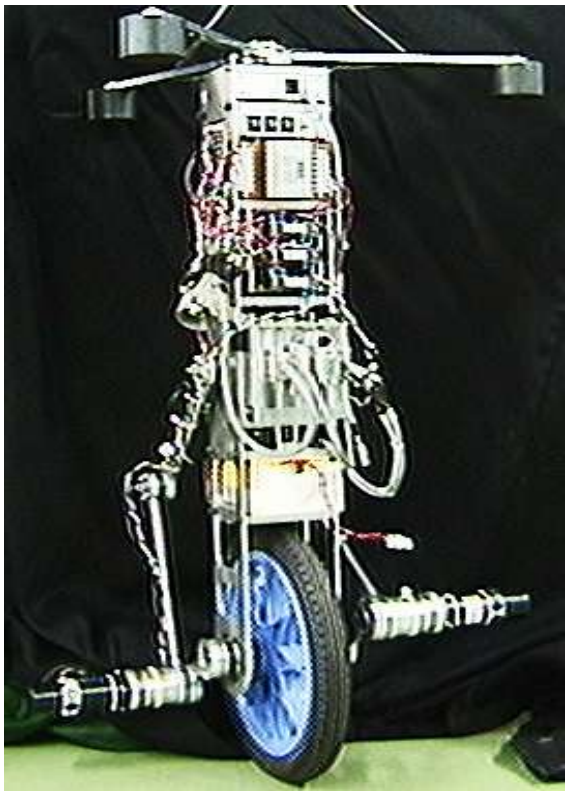

Figure 6. Robotic Unicycle model

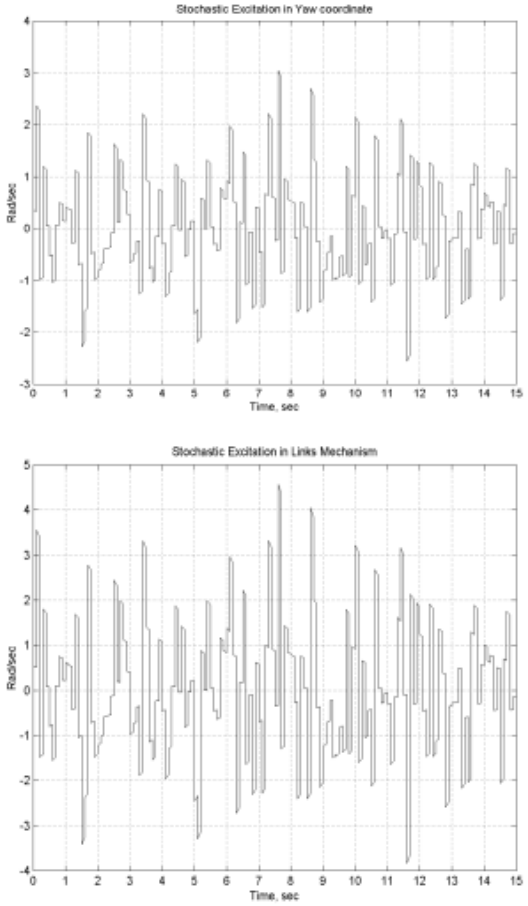

Figure 7. Simulated stochastic excitations - from a floor roughness's and jamming in closed-links mechanisms

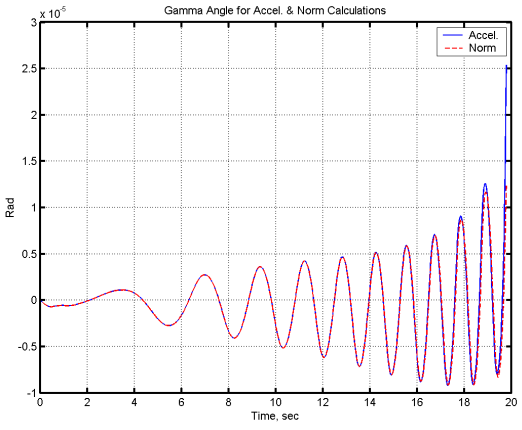

Figure 8. The accelerated and standard model's an integrating accuracy example (with & without algebraic loops)

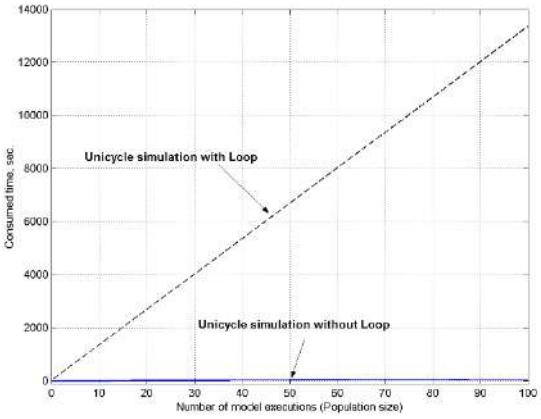

Figure 9. Integration time comparison for accelerated & standard models

Entropy production rate for the Pitch angle after the learning by FNN is decreased to 10 times. For the Yaw and Roll angles Entropy production rate is 10 times less for PD-GA and 1000 times less for the Fuzzy PD than for cconventional PD controller.

However, such energy transmitting increases amplitude of Pitch angle in case of PD-GA controller that conducts to increase torque in Links control system. But, after learning by FNN the motion in the pitch direction becomes smooth with small amplitude. It confirms about learnability and intellectualization of the Robotic Unicycle control system.

As can be seen from Figure 11 a, the movement of the model is smoother, which leads to a saving of the resource of the system as a whole. Also shown are the changes in the gain kp1, kd1, kp2, kd2 of the control equations (4.1) and (4.2). From the Figure 11a its visible that the model movement is going

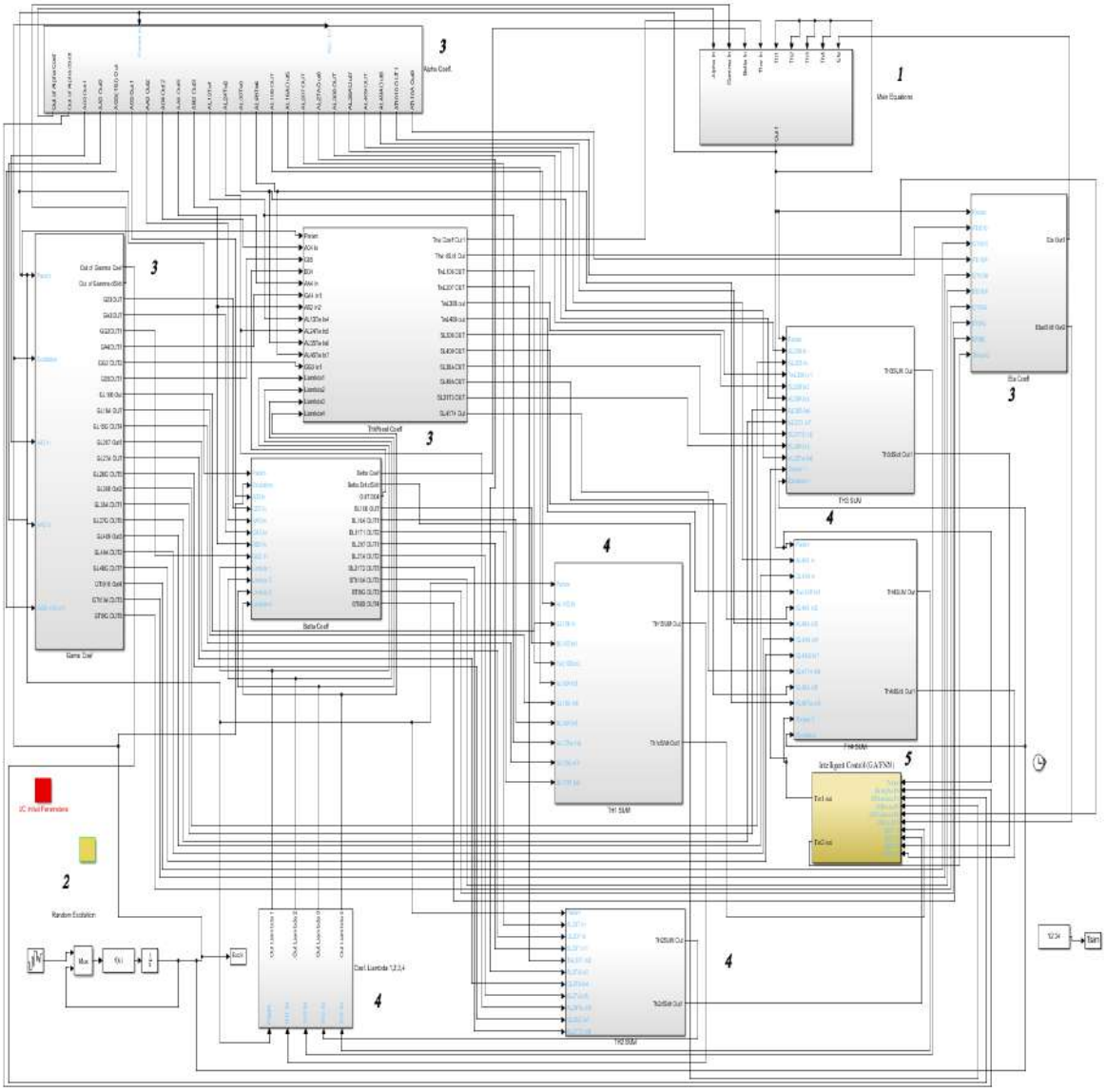

Scheme 1. MathLab Simulink® diagram of the Robotic Unicycle computer simulation - main part

DOI: https://doi.org/10.30564/aia.v2i1.1556

smoother, which leads to the system resource saving at whole. There are also shown the gain coefficients $kp1, kd1, kp2, kd2$ changes in the control equation (4.1) and (4.2).

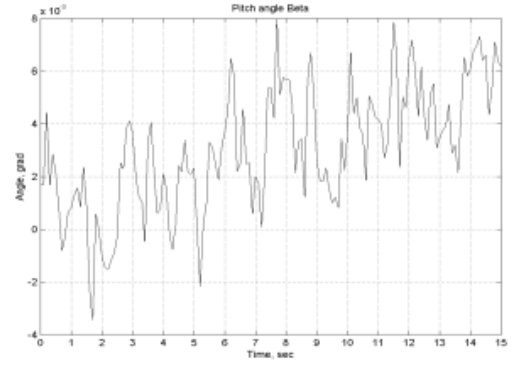

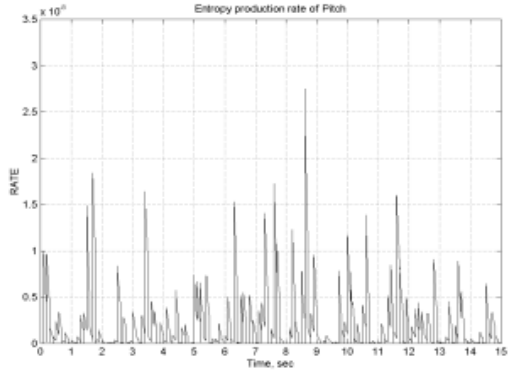

a

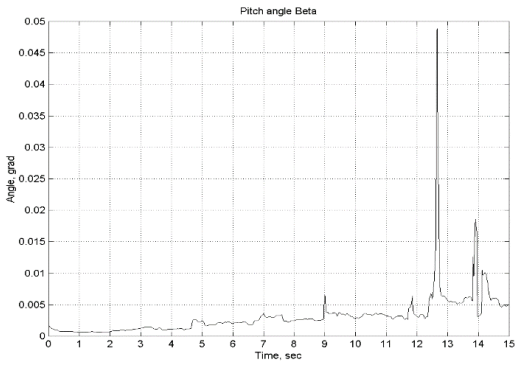

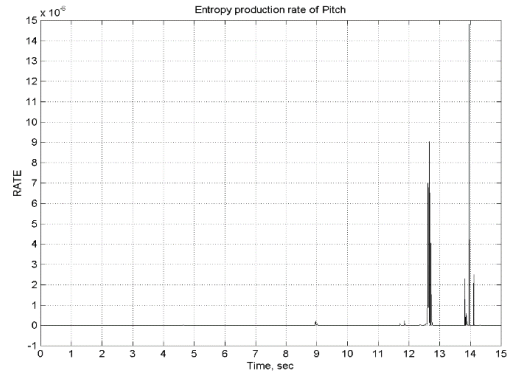

b

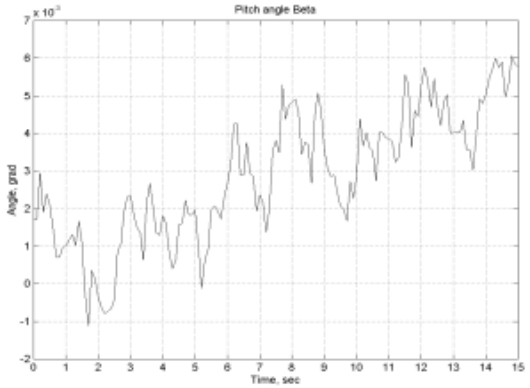

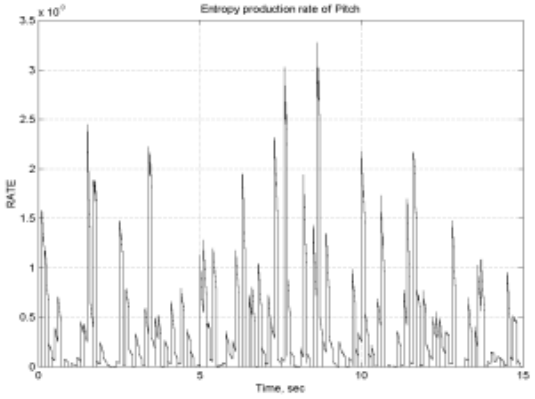

c

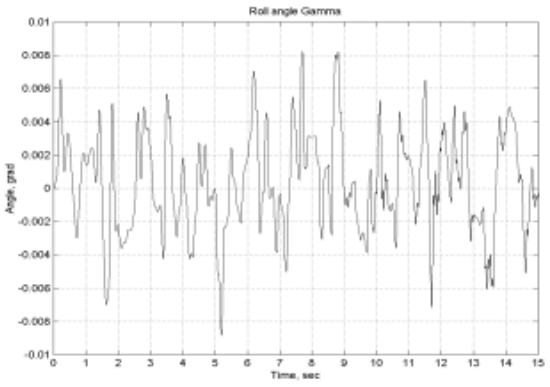

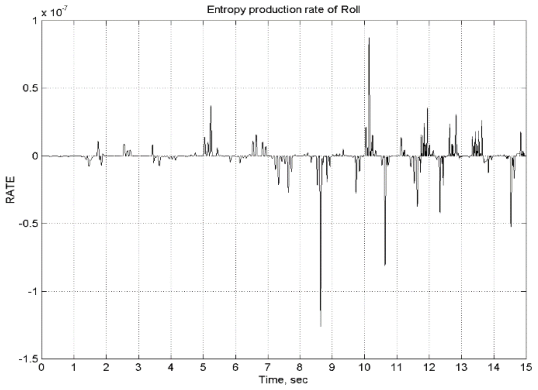

a

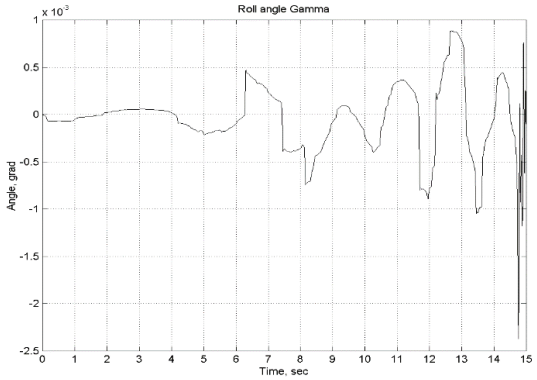

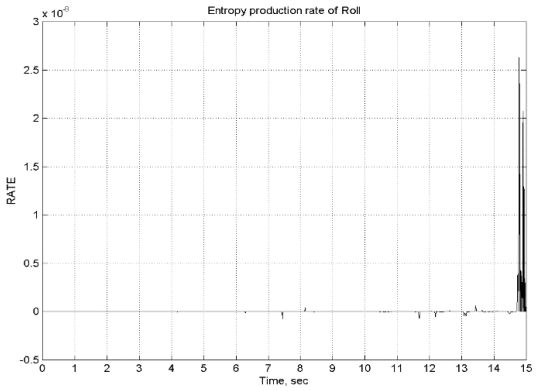

b

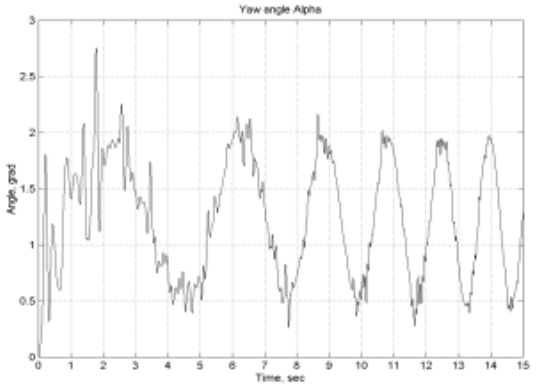

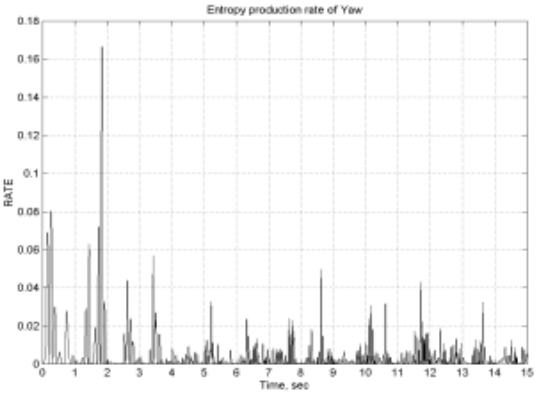

a

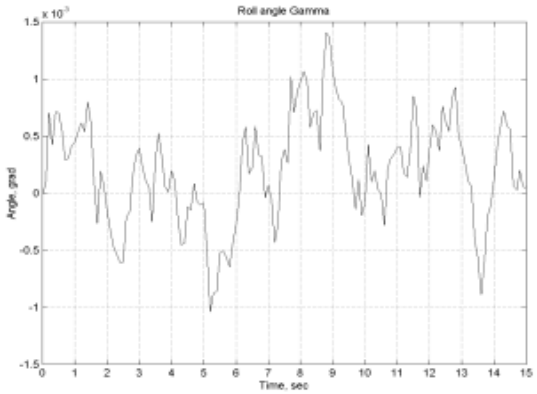

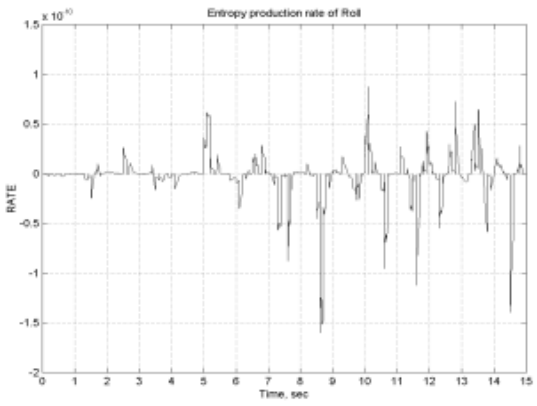

c

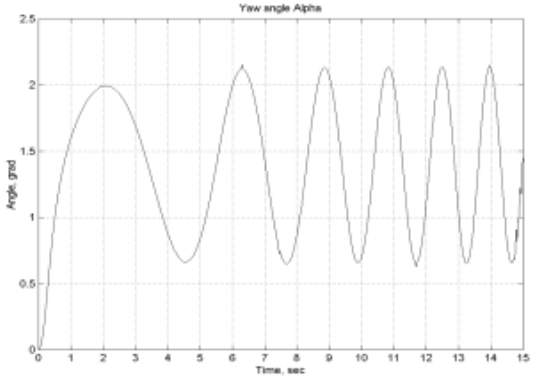

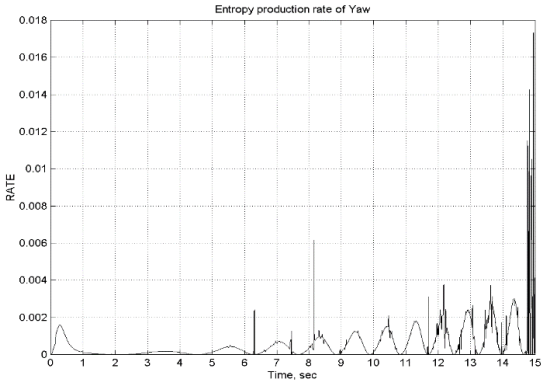

b

DOI: https://doi.org/10.30564/aia.v2i1.1556

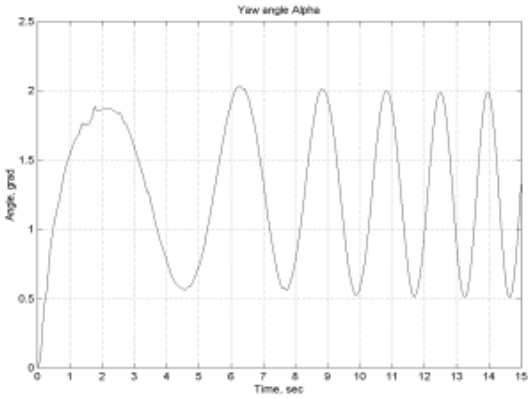

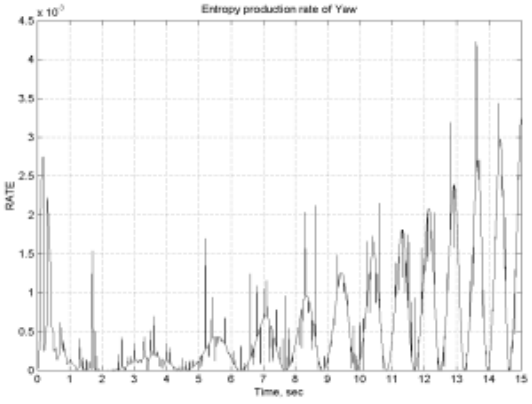

c

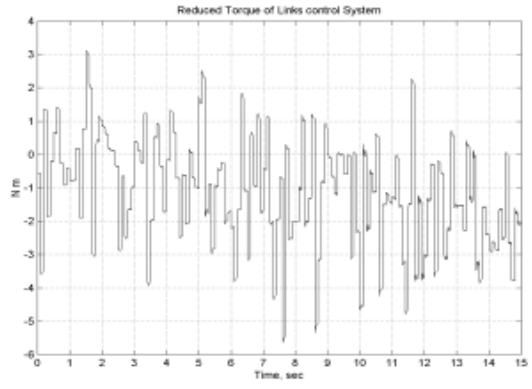

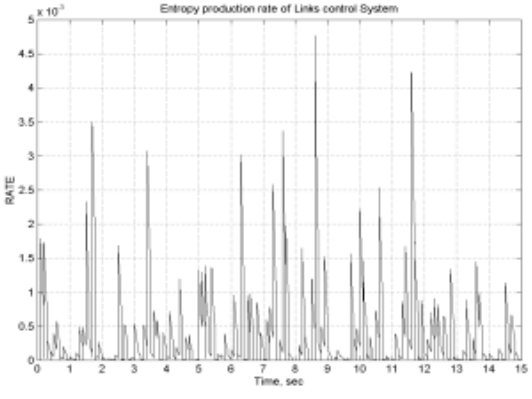

d

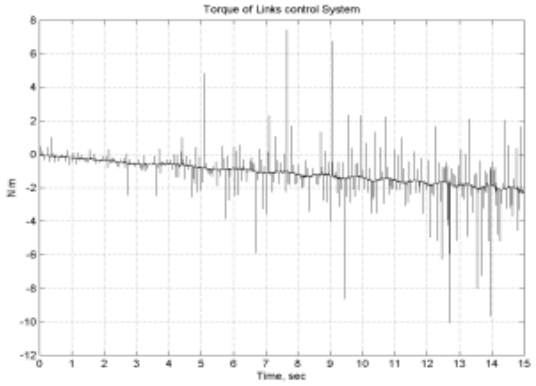

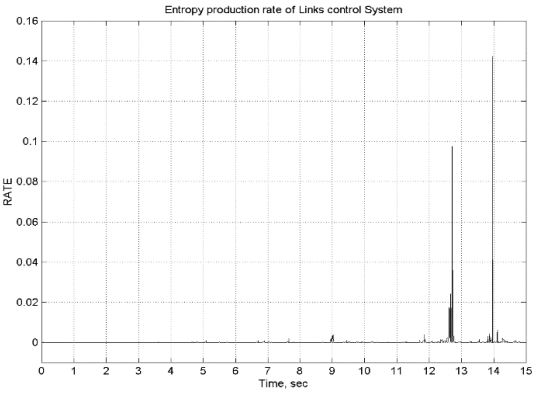

e

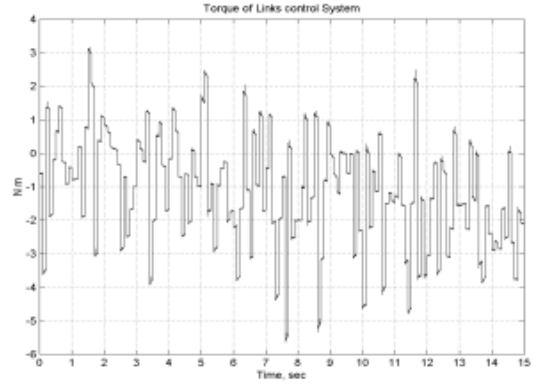

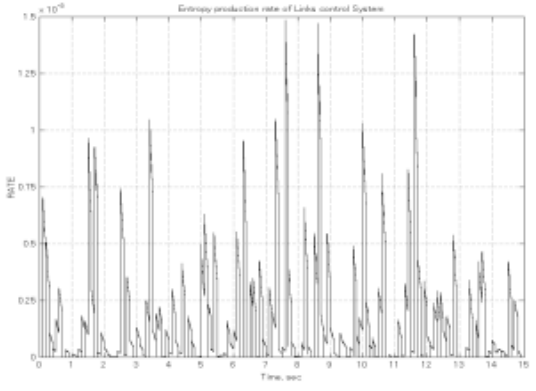

f

 DOI: https://doi.org/10.30564/aia.v2i1.1556

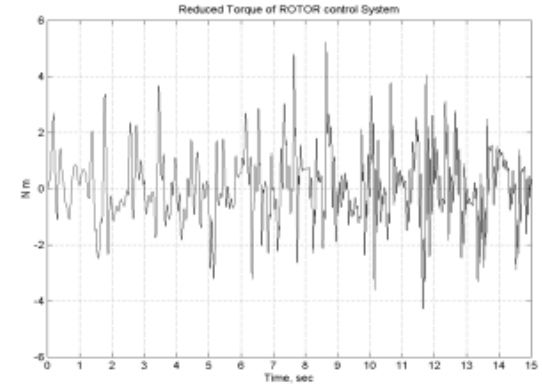

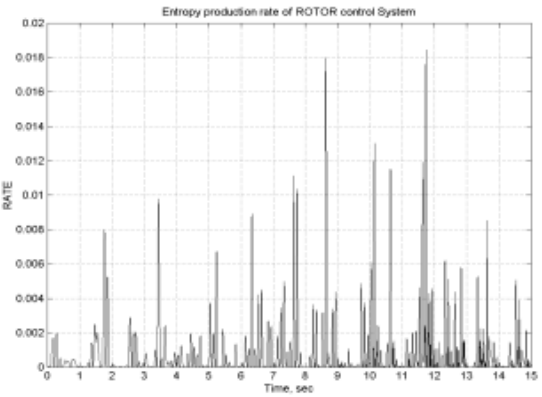

d

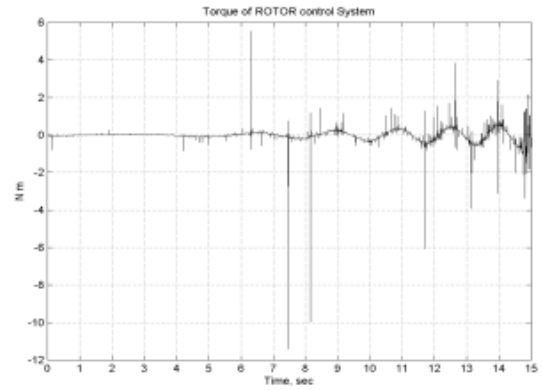

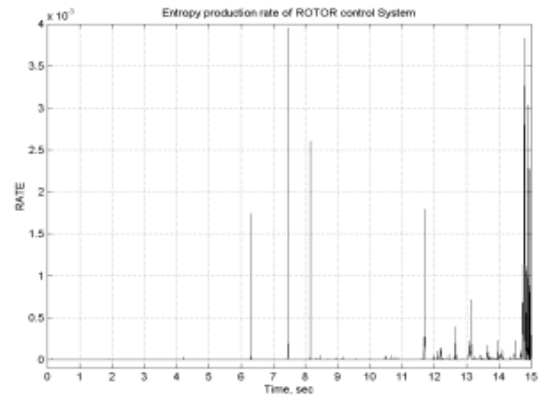

e

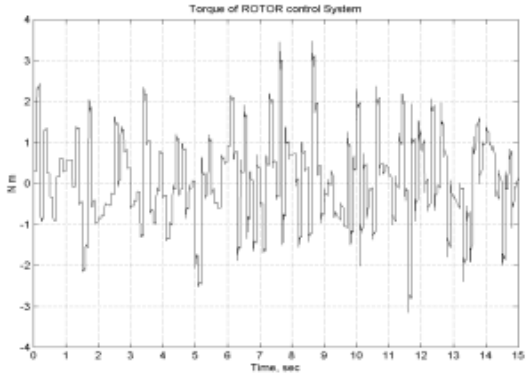

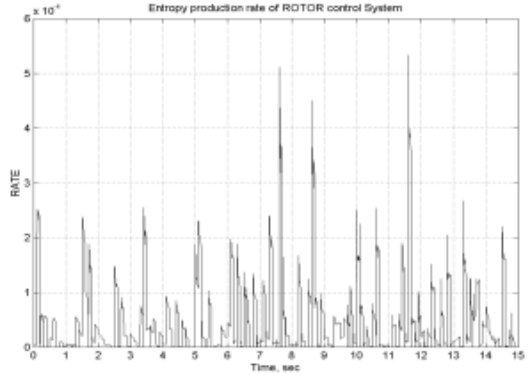

f

Figure 10. Stochastic simulation results of Robotic Unicycle Model: Temporal mechanical and thermodynamic behavior of Robotic Unicycle with: (a) conventional PD controller; (b) PD-GA controllers; (c) Fuzzy PD controllers; Temporal mechanical and thermodynamic behavior; (d) conventional PD control system torques; (e) PD-GA control system torques; (f) Fuzzy PD control system torques

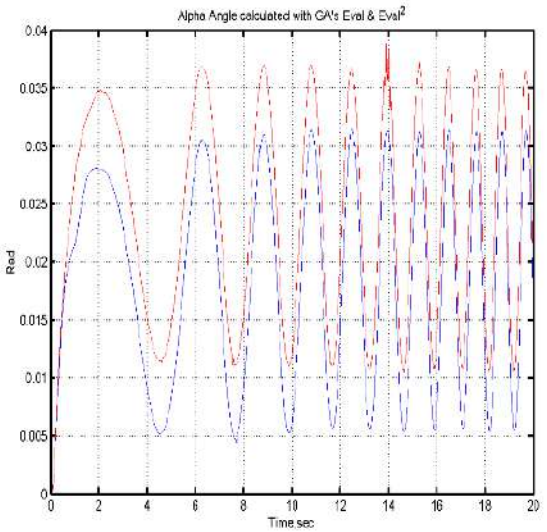

DOI: https://doi.org/10.30564/aia.v2i1.1556

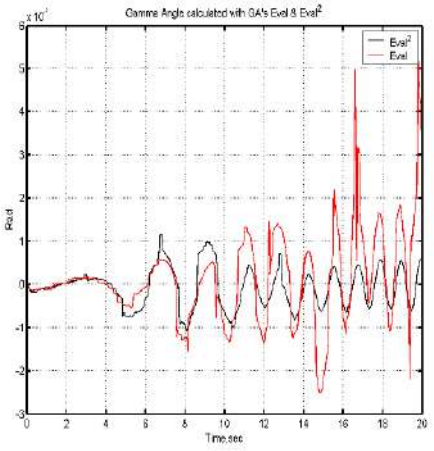

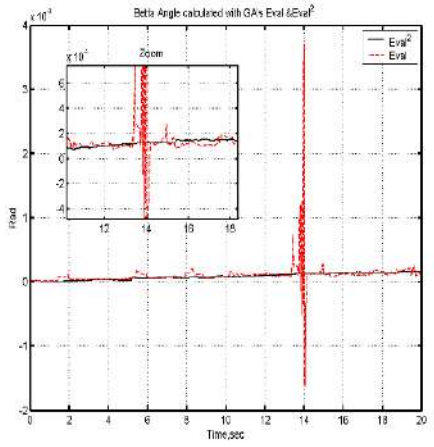

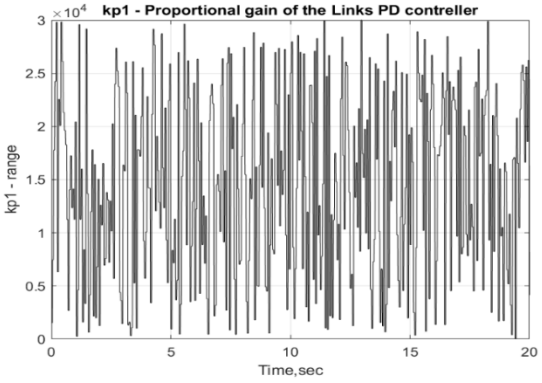

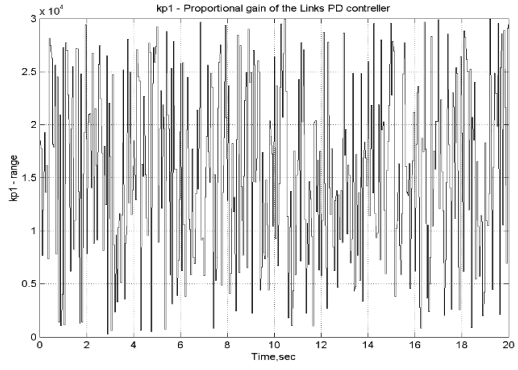

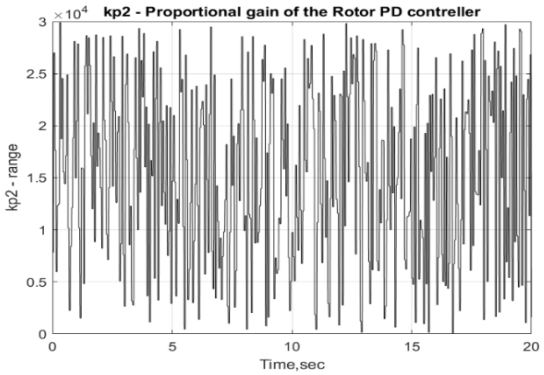

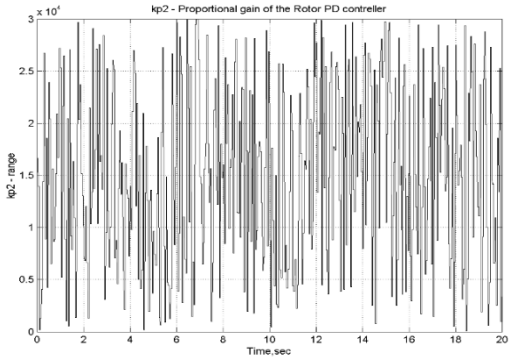

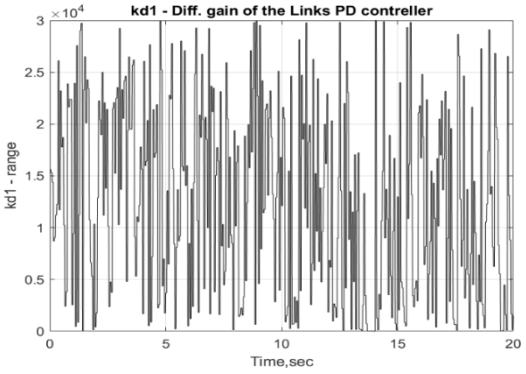

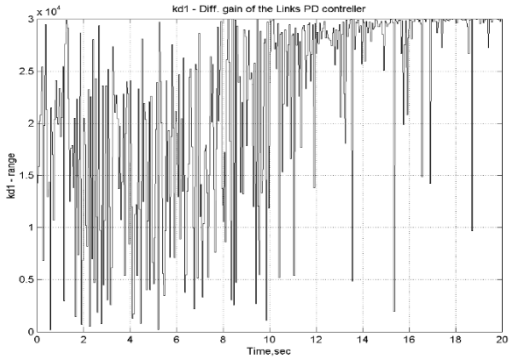

 DOI: https://doi.org/10.30564/aia.v2i1.1556

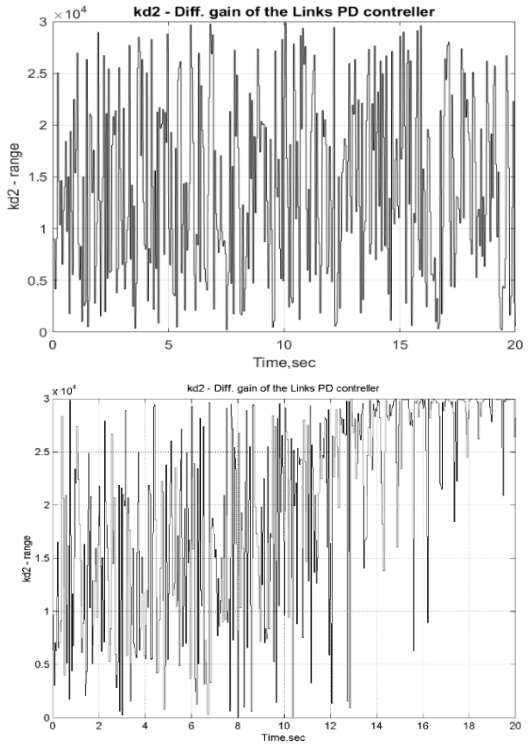

Figure 11. Stochastic simulation results of Robotic Unicycle Model with different GA's fitness functions - Eval и Eval2

The introduction of the GA fitness function in the quadratic form of a generalized function excludes the controls leading to local instability (negative value of the generalized entropy). As a consequence, it gives improved characteristics of control quality (minimum complexity in the implementation of the gain coefficients change laws time, minimum driving mechanisms efforts and useful resource consumption). In this case, the information-thermodynamic law of the compromise distribution of the conflicting control qualities (stability, controllability and robustness) is fully satisfied.

Experimental Results Discussion. Created in 1997-2000, the robotic unicycle is shown in Figure 6. The experimental results are presented in Figure 12-13. The time of the full-scale experiment was limited to 8 seconds due to the adverse effect of the gyroscopic sensors drift signal.

Though, it should be noted that sampling (more than 0.001 sec) of control signal from conventional PD, as it is present in real model, offers the Unicycle simulation system to "falling" after 8-10 sec.

In Figure 12 shows the experimental results for the cableless unicycle model. As it shown, the robot's lateral stability - in the roll direction γ, and posture in the pitch direction β is obtained.

In Figure13 shown the temporal behavior of the fuzzy gains kp1, kd2, kp2, kd2 for 2 PD controllers (Eq. 4.1, 4.2).

From the result in Figure 11c absorbed that the robot's posture in the yaw direction a is changed rapidly during the experiment, which indicates a satisfactory redistribution of control energy that provides lateral stability of

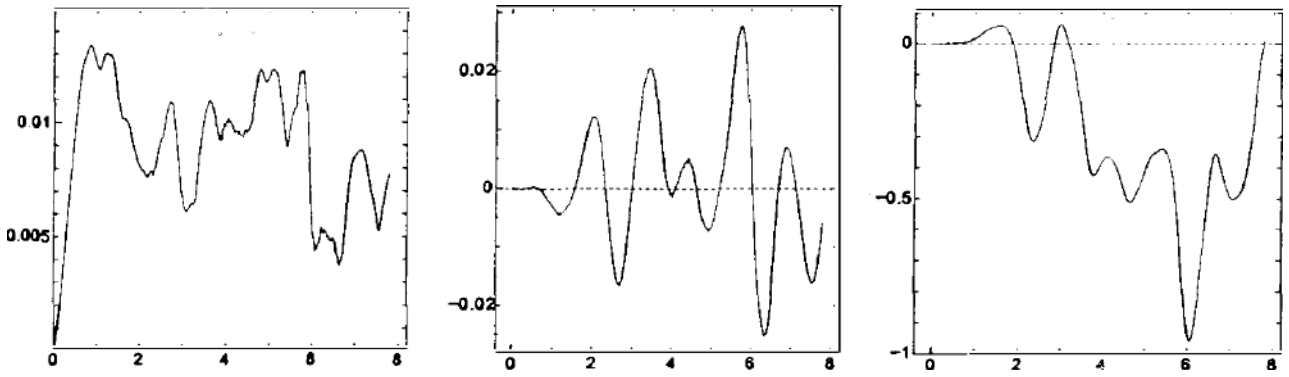

Figure 12. Experimental results, angles - pitch β, roll γ and yaw α angles

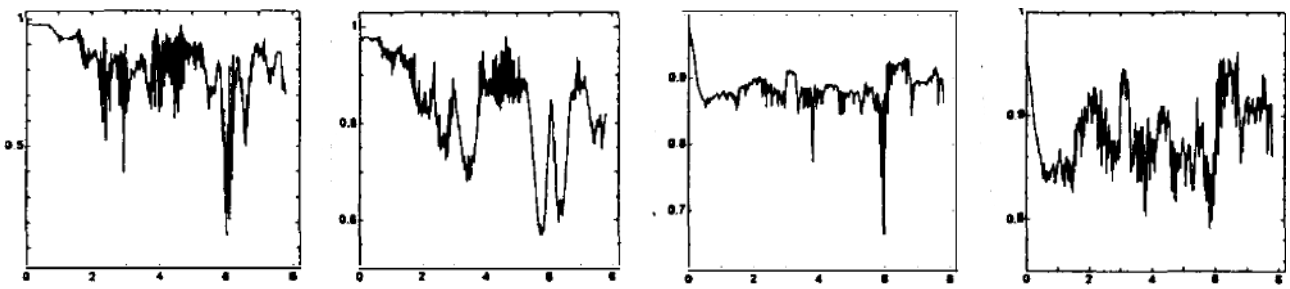

Figure 13. Experimental results of the fuzzy gains temporal behavior kp1, kd2, kp2, kd2 for 2 PD controllers

DOI: https://doi.org/10.30564/aia.v2i1.1556

the robot (roll γ) and tracking stochastic excitations on the model (*floor roughness's and jamming in closed-links mechanisms*) by controlling the yaw angle α and pitch angle b.

Remark 1. The obtained experimental results were achieved using empirically generated fuzzification and defuzzification functions for the gain coefficients *kp1, kd2, kp2, kd2* of two fuzzy PD controllers, which were generated on the basis of preliminary results of GA simulation with the fitness function - reduction only the entropy production rate of the control system, i.e. incomplete simulation process of soft computing technology. The simulation results presented above were obtained later, upon completion of the of a robotic unicycle mathematical model development (Figure 2, Eq. (1.2)), formation the soft computing process technology (Figure 3), and most importantly, the occurrence of this approach calculating possibility - appropriate computational capabilities, without which this process was extremely difficult.

Remark 2. Despite of this, the obtained result at this time and with those computational capabilities, leads to confirmation of quite satisfactory operation of the represented structure of the intelligent control system. The represented structure of the process, as well as the new developments in this direction, is planned to be fully applied in the new prototype - an Autonomous Flexible Robotic Unicycle.

8. Conclusions

(1) In this work represents the basic idea of intelligent control of dynamical, globally unstable, nonlinear objects on the robotic unicycle example. The basis of this approach is a qualitative physical analysis of the robot dynamic movement with the introduction of intelligent feedback in the control system and the implementation of instinct and intuition mechanisms based on the FNN and GA.

(2) The main components of an intelligent control system based on soft computing and robustness determination are also presented. Thus, there is an adaptation of the two fuzzy PD controllers' parameters to achieve a stable motion of the robotic unicycle over a long(finite) time interval, without changing the structure of the control system executive level, is achieved.

(3) The introduction of these two new mechanisms to an intelligent control system is based on the principle of minimum entropy production in the robot unicycle's motion and the control system itself. The fuzzy stochastic simulation of thermodynamic equations of motion and the intelligent control system confirm the effectiveness of the robot's postural stability control to handle the system's nonlinearity [20-22].

(4) In this case the unicycle robot model is a new benchmark for intelligent fuzzy controlled motion of a nonlinear dynamic system with two (local and global) 3D unstable states.

(5) The use of a fuzzy gain schedule PD controller with look-up tables calculated by FNN, offers the ability to use instinct and intuition mechanisms in on line to intellectualize the intelligent control system levels.

(6) Quantum soft computational intelligence toolkit [23-26] applied to design of self-organized conventional PD controllers can increase the robustness of robotic unicycle.

References

[1] Schoonwinkel A. Design and test of a computer stabilized unicycle. Ph. D. dissertation of Stanford Univ., USA, 1987.

[2] David William Vos. Nonlinear control of an autonomous unicycle robot: practical issues. Ph. D. dissertation of Massachusetts Institute of Technology, 1992.

[3] Ulyanov S.V., Sheng Z.Q., Yamafuji K. Fuzzy Intelligent control of robotic unicycle: A New benchmark in nonlinear mechanics. Proc. Intern. Conf. on Recent Advanced Mechatronics, Istanbul, Turkey, 1995, 2: 704-709.

[4] Ulyanov S.V., Sheng Z.Q., Yamafuji K., Watanabe S., Ohkura T. Self-organization fuzzy chaos intelligent controller for a robotic unicycle: A New benchmark in AI control. Proc. of 5th Intelligent System Symposium: Fuzzy, AI and Neural Network Applications Technologies (FAN Symp,'95), Tokyo., 1995: 41-46.

[5] Sheng Z.Q., Yamafuji K., Ulyanov S.V. Study on the stability and motion control of a unicycle. Pts 3,4,5. JSME International Journal, 1996, 39(3): 560-568; 569-576; Journal of Robotics & Mechatronics, 1996, 8(6): 571-579.

[6] Panfilov S.A., Ulyanov V.S., Litvintseva L.V., Ulyanov S.V., Kurawaki I. Robust Fuzzy Control of Non-Linear Dynamic Systems Based on Soft Computing with Minimum of Entropy Production Rate. Proc. Int. Conf. ICAFS 2000, Siegen, Germany, 2000: 59-75.

[7] Rouch N., Habets P. Laloy M. Stability Theory by Lyapunov's Direct Method. Berlin, Springer, 1977.

[8] Ulyanov V.S., Panfilov S.A., Ulyanov S.V. etc. Principle of minimum entropy production in applied soft computing for advanced intelligent robotics and mechatronics. Soft Computing, 2000, 2: 141-146.

[9] Ulyanov V.S., Yamafuji K., Ulyanov S.V., Tanaka K. Computational intelligence with new physical controllability measure for robust control algorithms

 DOI: https://doi.org/10.30564/aia.v2i1.1556

of extension-cableless robotic unicycle, Journal of Advanced Computational Intelligence. 1999, 3(2): 82 - 98.

[10] Ulyanov S.V., Yamafuji K. Fuzzy Intelligent emotion and instinct control of a robotic unicycle, Proc. 4th Intern. Workshop on Advanced Motion Control. Mie, Japan, 1996, 1: 127-132.

[11] Ulyanov S.V., Watanabe S., Yamafuji K., Ohkura T. A new physical measure for mechanical controllability and intelligent control of a robotic unicycle on basis of intuition, instinct and emotion computing. Proc. 2nd Intern. Conf. on Application on Fuzzy Systems and Soft Computing (ICAF'96), Siegen, Germany, 1996: 49-58.

[12] Ulyanov S.V., Watanabe S., Ulyanov V.S., Yamafuji K., Litvintseva L.V., Rizzotto G.G. Soft computing for the intelligent control of a robot unicycle based on a new physical measure for mechanical controllability. Soft Computing, 1998, 2(2): 73-88.

[13] Lauk M., Chow C.C., Pavlik A.E., Colloins J.J. Human balance out of equilibrium: Non-equilibrium statistical mechanics of posture control. Physical Review Letters, 1998, Vol. 80(2): 413-416.

[14] Ulyanov S.V., Yamafuji K., Ulyanov V.S., et.al. Computational intelligence for robust control algorithms of complex dynamic systems with minimum entropy production. Part1: simulation of entropy-like dynamic behavior and Lyapunov stability. Journal of Advanced Computational Intelligence, 1999, 3(2): 82-98.

[15] Murata Manufacturing Company, Ltd. MURATA GIRL, Japan, 2011. https://www.murata.com/en-sg/about/mboymgirl/mgirl

[16] Wieser E. Machine learning for a miniature robotic unicycle. Master of science thesis of Cambridge University, 2017, UK.

[17] De Vries J.F. Redesign & implementation of a moment exchange unicycle robot. Master of science thesis of Twente University, Netherlands, 2018.

[18] Kim S., Lee J., Hwang J. et al. Dynamic modeling and performance improvement of a unicycle robot. J. Inst. of Control, Robotics and Systems, 2010, 16(11): 1074-1081.

[19] Ulyanov S.V. et al. System and method for stochastic simulation of nonlinear dynamic systems with a high degree of freedom for soft computing applications. USA Patent Application Publication - US 2004/0039555 Al., 2004.

[20] Ulyanov S.V. et al. Soft computing optimizer of intelligent control system structures. Patent No.: US 2005/0119986 A1, Fil.: Jul. 23, 2004, Pub. Date: Jun. 2, 2005.

[21] Ulyanov S.V. et al. System for soft computing simulation. Patent No.: US 2006/0218108 A1, Fil.: Oct. 4, 2005, Pub. Date: Sep. 28, 2006.

[22] Ulyanov S.V. et al. Soft computing optimizer of intelligent control system structures. Patent No.: WO 2005/013019 A2, Priority data: 25 July 2002, Pub. Date: 10.02. 2005.

[23] Ulyanov S.V. System and method for control using quantum soft computing)[P]. US Patent No 7,383,235 B1, 2003; EP PCT 1 083 520 A2, 2001; Efficient simulation system of quantum algorithm gates on classical computer based on fast algorithm[P]. US Patent No 883 2006/0224547 A1, 2006.

[24] Litvintseva L.V., Ulyanov S.V. Quantum fuzzy inference for knowledge base design in robust intelligent controllers[J]. Journal of Computer and Systems Sciences Intern, 2007, 46(6): 908 - 961.

[25] Ulyanov S.V. Self-organizing quantum robust control methods and systems for situations with uncertainty and risk[P]. Patent US 8788450 B2, 2014.

[26] Ulyanov S.V. Quantum fast algorithm computational intelligence PT I: SW / HW smart toolkit[J]. Artificial Intelligence Advances, 2019, 1(1): 18-43. DOI: https://doi.org/10.30564/aia.v1i1.619

[27] Shen J., Hong D. OmBURo: A novel unicycle robot with active omnidirectional wheel. arxiv.org/abs/2020.07856v1.

DOI: https://doi.org/10.30564/aia.v2i1.1556

Author Guidelines

This document provides some guidelines to authors for submission in order to work towards a seamless submission process. While complete adherence to the following guidelines is not enforced, authors should note that following through with the guidelines will be helpful in expediting the copyediting and proofreading processes, and allow for improved readability during the review process.

Ⅰ. Format

- Program: Microsoft Word (preferred)
- Font: Times New Roman
- Size: 12
- Style: Normal
- Paragraph: Justified
- Required Documents

Ⅱ. Cover Letter

All articles should include a cover letter as a separate document.

The cover letter should include:

- Names and affiliation of author(s)

The corresponding author should be identified.

Eg. Department, University, Province/City/State, Postal Code, Country

- A brief description of the novelty and importance of the findings detailed in the paper

Declaration

v Conflict of Interest

Examples of conflicts of interest include (but are not limited to):

- Research grants
- Honoria
- Employment or consultation
- Project sponsors
- Author’s position on advisory boards or board of directors/management relationships
- Multiple affiliation
- Other financial relationships/support
- Informed Consent

This section confirms that written consent was obtained from all participants prior to the study.

- Ethical Approval

Eg. The paper received the ethical approval of XXX Ethics Committee.

- Trial Registration

Eg. Name of Trial Registry: Trial Registration Number

- Contributorship

The role(s) that each author undertook should be reflected in this section. This section affirms that each credited author has had a significant contribution to the article.

1. Main Manuscript
2. Reference List
3. Supplementary Data/Information

Supplementary figures, small tables, text etc.

As supplementary data/information is not copyedited/proofread, kindly ensure that the section is free from errors, and is presented clearly.

Ⅲ. Abstract

A general introduction to the research topic of the paper should be provided, along with a brief summary of its main results and implications. Kindly ensure the abstract is self-contained and remains readable to a wider audience. The abstract should also be kept to a maximum of 200 words.

Authors should also include 5-8 keywords after the abstract, separated by a semi-colon, avoiding the words already used in the title of the article.

Abstract and keywords should be reflected as font size 14.

Ⅳ. Title

The title should not exceed 50 words. Authors are encouraged to keep their titles succinct and relevant.

Titles should be reflected as font size 26, and in bold type.

Ⅳ. Section Headings

Section headings, sub-headings, and sub-subheadings should be differentiated by font size.

Section Headings: Font size 22, bold type

Sub-Headings: Font size 16, bold type

Sub-Subheadings: Font size 14, bold type

Main Manuscript Outline

Ⅴ. Introduction

The introduction should highlight the significance of the research conducted, in particular, in relation to current state of research in the field. A clear research objective should be conveyed within a single sentence.

Ⅵ. Methodology/Methods

In this section, the methods used to obtain the results in the paper should be clearly elucidated. This allows readers to be able to replicate the study in the future. Authors should ensure that any references made to other research or experiments should be clearly cited.

Ⅶ. Results

In this section, the results of experiments conducted should be detailed. The results should not be discussed at length in

this section. Alternatively, Results and Discussion can also be combined to a single section.

Ⅷ. Discussion

In this section, the results of the experiments conducted can be discussed in detail. Authors should discuss the direct and indirect implications of their findings, and also discuss if the results obtain reflect the current state of research in the field. Applications for the research should be discussed in this section. Suggestions for future research can also be discussed in this section.

Ⅸ. Conclusion

This section offers closure for the paper. An effective conclusion will need to sum up the principal findings of the papers, and its implications for further research.

Ⅹ. References

References should be included as a separate page from the main manuscript. For parts of the manuscript that have referenced a particular source, a superscript (ie. [x]) should be included next to the referenced text.

[x] refers to the allocated number of the source under the Reference List (eg. [1], [2], [3])

In the References section, the corresponding source should be referenced as:

[x] Author(s). Article Title [Publication Type]. Journal Name, Vol. No., Issue No.: Page numbers. (DOI number)

Ⅺ. Glossary of Publication Type

J = Journal/Magazine

M = Monograph/Book

C = (Article) Collection

D = Dissertation/Thesis

P = Patent

S = Standards

N = Newspapers

R = Reports

Kindly note that the order of appearance of the referenced source should follow its order of appearance in the main manuscript.

Graphs, Figures, Tables, and Equations

Graphs, figures and tables should be labelled closely below it and aligned to the center. Each data presentation type should be labelled as Graph, Figure, or Table, and its sequence should be in running order, separate from each other.

Equations should be aligned to the left, and numbered with in running order with its number in parenthesis (aligned right).

Ⅻ. Others

Conflicts of interest, acknowledgements, and publication ethics should also be declared in the final version of the manuscript. Instructions have been provided as its counterpart under Cover Letter.

BILINGUAL PUBLISHING CO.
Pioneer of Global Academics Since 1984

Artificial Intelligence Advances

Aims and Scope

Artificial Intelligence Advances publishes original research papers that offers professional review and publication to freely disseminate research findings in all areas of Basic and Applied Computational Intelligence including Cognitive Aspects of Artificial Intelligence (AI), Constraint Processing, High–Level Computer Vision, Common Sense Reasoning and more. The Journal focuses on innovations of research methods at all stages and is committed to providing theoretical and practical experience for all those who are involved in these fields.

Artificial Intelligence Advances aims to discover innovative methods, theories and studies in its field by publishing original articles, case studies and comprehensive reviews.

The scope of the papers in this journal includes, but is not limited to:

- Planning and Theories of Action
- Heuristic Search
- High-Level Computer Vision
- Multiagent Systems
- Machine Learning
- Intelligent Robotics
- Knowledge Representation
- Intelligent Interfaces
- Cognitive Aspects of AI
- Common Sense Reasoning
- AI and Philosophy
- Automated Reasoning and Interface
- Reasoning Under Uncertainty

Bilingual Publishing Co. (BPC)

Tel:+65 65881289

E-mail:contact@bilpublishing.com

Website:www.bilpublishing.com

About the Publisher

Bilingual Publishing Co. (BPC) is an international publisher of online, open access and scholarly peer-reviewed journals covering a wide range of academic disciplines including science, technology, medicine, engineering, education and social science. Reflecting the latest research from a broad sweep of subjects, our content is accessible world-wide——both in print and online.

BPC aims to provide an analytics as well as platform for information exchange and discussion that help organizations and professionals in advancing society for the betterment of mankind. BPC hopes to be indexed by well-known databases in order to expand its reach to the science community, and eventually grow to be a reputable publisher recognized by scholars and researchers around the world.

BPC adopts the Open Journal Systems, see on ojs.bilpublishing.com

Database Inclusion

Asia & Pacific Science Citation Index

Creative Commons

China National Knowledge Infrastructure

Google Scholar

Crossref

MyScienceWork

Bilingual Publishing Co. is a company registered in Singapore in 1984, whose office is at 12 Eu Tong Sen Street, #07-169, Singapore 059819, enjoying a high reputation in Southeast Asian countries, even around the world.

BILINGUAL PUBLISHING CO.
Pioneer of Global Academics Since 1984

Tel:+65 65881289
E-mail:contact@blipublishing.Com
Website:www.Blipublishing.Com

ISSN 2661-3220 01
9 772661 322203